NITROGEN MONOXIDE REDUCTION OVER ZSM-5 ZEOLITE-SUPPORTED CATALYSTS

by

Fakhry Seyedeyn-Azad

B.E. (Sharif University of Technology) 1975

M.E. (Sharif University of Technology) 1978

Thesis submitted for the degree of

Doctor of Philosophy

in

Department of Chemical Engineering

Faculty of Engineering

The University of Adelaide

1999

DECLARATION

This work contains no material which has been accepted for the award of any other degree or diploma in any university or any other tertiary institution, and to the best of my knowledge and belief, contains no material previously published or written by another person, except where due reference has been made in the text.

I give consent for this copy of my thesis to be available for photocopying and loan, when deposited in the Library of the University of Adelaide.

SIGNED: .

DATE: 12/7/99

To My Beloved Children, Pouya and Pardis

ACKNOWLEDGMENTS

First of all, I would like to thank my supervisor, Professor Dong-ke Zhang for his continued guidance, support, and encouragement throughout the course of this work. I also wish to thank him for always being available when I needed his assistance.

I am indebted to my country, Iran and her people, for sponsoring my research in Australia with a scholarship. I am so grateful, and I know that my debt can never be repaid. I wish all the best for my country and people.

Special thanks go to Andrew Wright, Bruce Ide, Peter Kay, Brian Mulcahy and Jason Peak for their excellent technical support throughout the project. I sincerely thank Mrs. Mary Barrow, Mrs. Elaine Minerds and Mrs. Lynette Kelly for the administrative support and their friendship.

I would like to thank the staff of the Department of Chemical Engineering and fellow postgraduate students, especially Kylie Headon and Ben Daughtry, for their support and assistance.

Last, but not least, I would like to thank my mother. Without her never ending love and support I could not have continued my studies. Also, I would like to thank my husband Mohammad for his encouragement and very valuable input during discussions in the process of this project.

SUMMARY

The emission of nitrogen oxides (NO_x) from combustion sources has been known to cause serious environmental problems. Increasingly stringent regulations require new technologies to control or eliminate this emission from combustion systems. ZSM-5 zeolite has reemerged as a potential catalyst for reducing nitrogen monoxide (NO) emissions from combustion exhausts containing excess oxygen. This study aims at understanding the effect of zeolite properties on the activity of zeolite-supported catalysts for direct decomposition and selective catalytic reduction (SCR) of NO. The effect of catalyst preparation on the catalytic activity, kinetics and mechanism of direct decomposition are also investigated.

The starting materials for preparing the catalysts are ZSM-5 zeolites, either synthesised in the present study or obtained from commercial sources. ZSM-5 zeolites with 100% crystallinity with a silica to alumina molar ratio (SiO_2/Al_2O_3) of 40 and with SiO_2/Al_2O_3 ratios of 70 to 176 are synthesised without using any template and using tetrapropylammonium bromide (TPABr) as a template, respectively. The zeolites are characterised by XRD. Some zeolites are also provided by commercial sources (Zeolyst International Corporation). They are ion-exchanged and then subjected to activity tests for the direct decomposition and selective catalytic reduction (SCR) of NO using a fixed bed tubular reactor.

The effect of ion-exchange temperature and time (repetition) of ion-exchange on copper ion-exchange level and the activity of copper ion-exchanged ZSM-5 zeolites (Cu-ZSM-5) are investigated. Increasing the temperature of the ion-exchange solution from 25 to 45 °C leads to an increasing ion-exchange level. Increasing the temperature from 45 to 80 °C increases the ion-exchange level if the catalyst is ion-

exchanged only for a period of 24 hours. This level decreases considerably by repetition of the ion-exchange procedure.

The kinetic study of the direct decomposition of NO over Cu-ZSM-5 with a SiO_2/Al_2O_3 ratio of 40 reveals that the reaction rate equation is dependent on the reaction temperature. A new reaction rate equation supported with a proposed reaction mechanism for temperatures lower than the most effective temperature is suggested. In this equation, the order in O_2 concentration in the denominator term is 1 instead of 1/2 at high temperatures.

SCR of NO by methane or propene over a sample of Cu-ZSM-5 zeolite leads to 15% and 82% NO conversion into N_2, whereas Co-ZSM-5 catalyst shows similar activities (50% NO conversion) when either methane or propane is used. Accordingly, the effect of SiO_2/Al_2O_3 ratio, copper loading and ion-exchange level on the activity of over-exchanged Cu-ZSM-5 catalysts for SCR of NO by propene is investigated. The results indicate that NO conversion increases slightly by increasing the SiO_2/Al_2O_3 ratio, and decreases by increasing copper loading. Comparing catalysts with the same copper ion-exchange level but different SiO_2/Al_2O_3 ratios reveals that a catalyst with a higher SiO_2/Al_2O_3 ratio is more active.

The effects of catalyst preparation, SiO_2/Al_2O_3 ratio, cobalt loading and ion-exchange level on the activity of Co-ZSM-5 catalysts for SCR of NO using methane are also investigated. The most effective temperature is 450 °C and is not dependent on SiO_2/Al_2O_3 ratio or cobalt loading. A semi-continuous process is more effective than a batch system for catalyst preparation, and results in 17% more NO conversion. NO conversion decreases by 25% by increasing the SiO_2/Al_2O_3 ratio from 40 to 80, and decreases by 8-10% for a catalyst with SiO_2/Al_2O_3 ratio of 80 when the ion-exchanged level of the catalyst is 428%.

Catalysts including combinations of ZSM-5, metal oxides, MCM-41, and Pillared Clays from the University of Queensland are also examined for direct decomposition and SCR. The maximum NO_x conversion achieves over either Cu-ZSM-5 zeolite or a

mixture of copper ion-exchanged ZSM-5 zeolite and MCM-41 molecular sieve. The latter catalyst exhibits a higher activity than Cu-ZSM-5 alone for NO decomposition over the temperature range between 250 and 650 °C. This catalyst is also very active for SCR of NO by propene, but not by methane. Pillared Clays are not active for SCR of NO using methane.

This study shows how ZSM-5 zeolites can be synthesised under different conditions, and highlights the effect of zeolite properties especially the SiO_2/Al_2O_3 ratio on the activity of Cu-ZSM-5 and Co-ZSM-5 catalysts for SCR of NO. It also introduces a systematic approach to catalyst preparation via ion-exchange and deduces a reaction rate equation and reaction mechanism involved for the direct decomposition at temperatures lower than the most effective temperature. Finally, it compares the activity of Cu-ZSM-5 zeolites with a wide range of catalysts, and reveals that Cu-ZSM-5 is the most active, and also that the addition of MCM-41 to ZSM-5 zeolite-support results in a wider NO conversion profile.

TABLE OF CONTENTS

Content	Page
Declaration	i
Acknowledgments	ii
Summary	iv
Table of Contents	vii
List of Figures	xii
List of Tables	xxiii
1 INTRODUCTION	1
2 LITERATURE REVIEW	
2.1 Introduction	5
2.2 Sources of Nitrogen Oxides	6
2.3 Environmental Effects of Nitrogen Oxides	8
2.4 Chemistry of Nitrogen Monoxide	8
2.5 Nitrogen Oxides Control Technologies	12
2.5.1 Combustion Control Technologies	12
2.5.2 Post-Combustion Technologies for Stationary Sources	14
2.5.3 Post-Combustion Technologies for Mobile Sources	15
2.5.4 Technologies under Investigation	17
2.5.4.1 Direct Decomposition of NO over ZSM-5 Zeolites	20
2.5.4.1.1 Effect of Operating Temperature	21
2.5.4.1.2 Effect of Oxygen	23
2.5.4.1.3 Effect of Contact Time	25
2.5.4.1.4 Effect of Ion-Exchange Level	25
2.5.4.1.5 Effect of Cocations	27
2.5.4.1.6 Effect of Catalyst Preparation Methods	29
2.5.4.1.7 Decay of Catalytic Activity	32

2.5.4.1.8 Proposed Mechanisms of Direct Decomposition of NO 32
2.5.4.2 Selective Catalytic Reduction (SCR) of NO 35
2.5.4.2.1 Catalytic Reduction of NO using N-containing Reductants 36
2.5.4.2.2 Catalytic Reduction of NO using N-free Reductants 37
2.5.4.2.3 Effect of Silica to Alumina Ratio 39
2.5.4.2.4 Mechanisms of SCR 40
2.5.4.3 Experimental Techniques 43
2.5.4.4 Theoretical Analysis and Modelling 45
2.5.4.4.1 Kinetic Analysis and Rate Law 46
2.5.4.4.2 Mathematical Modelling 47
2.6 Conclusions from Literature Review 49
2.7 Objectives of the Present Research 51

3 ZSM-5 ZEOLITE SYNTHESIS

3.1 Introduction 54
3.2 Background 55
3.3 The Structures of the Zeolites 56
3.4 Zeolite Synthesising Methods 58
3.4.1 Equipment 59
3.4.2 Experimental Procedures 61
3.4.2.1 Method I 63
3.4.2.2 Method II 63
3.4.2.3 Method III 64
3.4.2.4 Method IV 65
3.5 Results And Discussion 66
3.5.1 A Comparison of the Synthesis Methods 77
3.6 Summary 81

4 EXPERIMENTAL TECHNIQUE

4-1 Introduction 82
4.2 Catalysts Sources and Preparation Methods 82

4.2.1 Hydrogen Ion-Exchange 83
4.2.2 Copper Ion-Exchange 84
4.2.3 Cobalt Ion-Exchange 85
4.3 Catalyst Pre-Treatment 87
4.4 Flow Sheet Diagram of the Experimental System 88
4.5 Gas Supply System 90
4.6 Reactor and Temperature Controller 90
4.7 Gas Analysis Instruments 92
4.7.1 NO_x Analyser 92
4.7.2 Gas Chromatograph (GC) 93
4.8 Experimental Procedures 99
4.8.1 Start-up 99
4.8.2 Operation 100
4.8.3 Shut-down 103
4.9 Data Analysis 103
4.10 Experimental Errors Analysis 106

5 THE DIRECT DECOMPOSITION OF NITROGEN MONOXIDE

5.1 Introduction 109
5.2 The Effect of Preparation Method on Cu ion-exchange Level 110
5.2.1 Preparation of Catalysts from ZSM-5 Support 110
5.2.2 Catalyst Preparation and Specification 111
5.2.3 The Direct Decomposition of NO 113
5.3 Kinetic Studies of the Direct Decomposition of NO 121
5.3.1 Theory and Background 122
5.3.2 Catalyst Preparation 123
5.3.3 Dependence of NO Conversion on Temperature 123
5.3.4 Dependence of NO Conversion on Contact Time 124
5.3.5 Determination of the Reaction Rate 126
5.3.6 Reaction Mechanism at Temperatures Lower Than the Most Effective Temperature 132
5.4 Summary 137

6 SELECTIVE CATALYTIC REDUCTION OF NITROGEN MONOXIDE

6.1 Introduction 139

6.2 SCR of NO by Propene or Methane over Cu-ZSM-5 or Co-ZSM-5 Zeolites 140

6.3 SCR of NO by Propene over Cu-ZSM-5 Zeolites 144

6.3.1 The Effect of SiO_2/Al_2O_3 Ratio 146

6.3.2 The Effect of Copper Loading 149

6.3.3 The Effect of Copper Ion-Exchange Level 153

6.4 SCR of NO by Methane over Co-ZSM-5 Zeolites 156

6.4.1 The Effect of Catalyst Preparation Method 157

6.4.2 The Effect of SiO_2/Al_2O_3 Ratio 158

6.4.3 The Effect of Cobalt Loading 159

6.5 Summary 162

7 NO CONVERSION STUDIES USING OTHER CATALYSTS

7.1 Introduction 164

7.2 Catalyst Synthesis and Preparation Methods 165

7.2.1 ZSM-5 Zeolite and MCM-41 Molecular Sieve 166

7.2.2 Pillared Clays (PILCs) 166

7.3 Experimental Technique 169

7.4 Results and Discussion for the First Group of Catalysts 172

7.4.1 NO_x Conversion Without the Presence of Oxygen 172

7.4.2 NO_x Conversion in the Presence of Oxygen 175

7.4.3 NO_x conversion in the Presence of Methane 177

7.4.4 A Mixture of ZSM-5 and MCM-41 Molecular Sieve 180

7.5 Results and Discussion for the Second Group of Catalysts 186

7.6 Summary 187

8 AN EVALUATION OF THE PRESENT STUDIES

8.1 Introduction 189

8.2 Comparison of Present Results with Literature Data 189
8.3 Validity of the Data Presented in This Project 194
8.4 Practical Implication of the Present Studies 198

9 CONCLUSIONS AND RECOMMENDATIONS

9.1 Conclusions 203
9.2 Recommendations for Future Work 206

ABBREVIATIONS AND NOMENCLATURES

Abbreviations 208
Nomenclature 208
Greek Symbols 209
Subscripts 209

REFERENCES 210

APPENDICES 223
Appendix A Drawings of Three Autoclaves Used in This Study 224
Appendix B XRD Patterns of ZSM-5 Zeolites Synthesised in This Study 228
Appendix C Detailed Analysis of The Catalysts Used in This Study 240
List of Publications 243

LIST OF FIGURES

Figure 2.1. Sources of nitrogen oxide emissions (adapted from Mason and Herther, 1982). 7

Figure 2.2. The principle of 3-way catalyst for exhaust emission control. Catalyst efficiencies measured in the laboratory with a steady feed stream composition at various simulated air/fuel ratios. Catalyst: 0.042 wt% Pt, 0.0.18 wt% Rh, alumina (reproduced from Schalatter et al., 1983). 16

Figure 2.3. The dependence of NO_x level on air-to fuel ratio and temperature (reproduced from Lambert and McGowan, 1996). 17

Figure 2.4. The dependence of NO conversion (O) into N_2 (Δ) O_2 (□) and N_2O (●) on temperature over Cu-ZSM-5-23.3-143 at 4.0 g s ml^{-1} and P_{NO} = 1.0% (reproduced from Iwamoto et al., 1989). 22

Figure 2.5. Influence of oxygen on the decomposition activities of Cu-ZSM-5-23.3-122 (●,O) and 89 (▲,Δ) catalysts at 1.0 g s ml^{-1} (●) P_{O2} = 8%, P_{NO} = 0.47% (▲) P_{O2} = 3%, P_{NO} = 0.50% (O, Δ) P_{O2} = 0%, P_{NO} = 0.51% (reproduced from Iwamoto et al., 1991a). 24

Figure 2.6. Conversions (%) of NO decomposition and NO into N_2 and O_2 as a function of exchange level obtained over Cu-ZSM-5-23.3 at 723 K, W/F = 4.0 g s ml^{-1} and P_{NO} = 1.0% (reproduced from Iwamoto et al., 1989). 26

Figure 2.7. Conversions of NO decomposition as a function of time over Cu-ZSM-5-26-166 at 773 K using a mixture of 4% NO in helium and a contact time of 2 second (reproduced from Li and Hall, 1990). Li and Hall used the lines to compare their results with Iwamoto et al. results. The lines were obtained on the Cu-ZSM-5-25-54 at the same temperature and a contact time of 8 seconds by Iwamoto et al. (1986b). 32

Figure 3.1. A cross section of ZSM-5. Shaded units show the chain as the building unites (reproduced from Szostak, 1989). 57

Figure 3.2. The "hollow tube" provides easy visualisation of the straight and zigzag channels in ZSM-5 zeolite framework (reproduced from Szostak, 1989).

Figure 3.3. XRD pattern of the reference sample. 62

Figure 3.4. X-ray diffraction profile of a sample of Na-ZSM-5 zeolite prepared using TPABr from Method I. 66

Figure 3.5. X-ray diffraction profile of a sample of Na-ZSM-5 zeolite prepared without template from method III. 69

Figure 3.6. Scanning electron micrographs of various Na-ZSM-5 zeolites. (a) synthesised using TPABr with the following ratios in the initial gel, $SiO_2/ Al_2O_3 = 176$, $OH^-/SiO_2 = 0.1$ and 90% crystallinity; (b) the same as (a) but with 96% of crystallinity. 73

Figure 3.7. Scanning electron micrographs of various Na-ZSM-5 zeolites. (a) synthesised using TPABr with the following ratios in the initial gel, $SiO_2/Al_2O_3 = 100$, $OH^-/SiO_2 = 0.2$ 74

	and 94% crystallinity; (b) synthesised using TPABr with the in following ratios in the initial gel, SiO_2/Al_2O_3 = 70, OH^-/SiO_2 = 0.2 and 100% crystallinity.	
Figure 3.8.	Scanning electron micrographs of various Na-ZSM-5 zeolites synthesised without template with the following ratios in the initial gel, SiO_2/Al_2O_3 = 40, OH^-/SiO_2 = 0.22 and 100% crystallinity.	75
Figure 3.9.	Scanning electron micrographs of various Na-ZSM-5 zeolites. (a) same as 3.6(b) but smaller magnitude, (b) same as 3.6(b) but with larger magnitude (c) same as 3.7(a) with larger magnitude.	76
Figure 4.1.	Experimental Set-up.	89
Figure 4.2.	A schematic of Catalyst location in the reactor; a) The reactor with the catalyst bed and welded cross, b) Cross section of welded cross.	91
Figure 4.3.	Schematic diagram of the inlet and the outlet gas streams of the reactor, showing where O_2 is added into the stream.	92
Figure 4.4.	Schematic diagram of GC columns and detectors.	94
Figure 4.5.	A typical print-out of results of a calibration run for O_2, N_2, CO, CH_4 and CO_2.	95
Figure 4.6.	A Typical chromatogram of a calibration run. Peaks monitored in these chromatograms belong to O_2, N_2, CO, CH_4 and CO_2, respectively.	96

Figure 4.7. A typical calibration curve for N_2. 96

Figure 4.8. A typical chromatogram showing N_2, O_2, CO_2 peaks. 98

Figure 4.9. A typical print-out of results reported by GC, belonged to the chromatogram represented in Figure 4.8. 98

Figure 4.10. The dependence of NO conversion into N_2 on operation time at 300 °C over H-Cu-ZSM-5-32.2-101.7 catalyst. Reaction conditions: 2000 ppm NO, 2000 ppm C_3H_6, 2% O_2, balance He, 1 g catalyst weight, and 100 ml min^{-1} total flow rate. 101

Figure 4.11. The dependence of NO conversion into N_2 on operation time at 350 °C over H-Cu-ZSM-5-32.2-101.7 catalyst. Reaction conditions: 2000 ppm NO, 2000 ppm C_3H_6, 2% O_2, balance He, 1 g catalyst weight, and 100 ml min^{-1} total flow rate. 102

Figure 5.1. The dependence of copper ion-exchange level on ion-exchange temperature and the number of repetition of ion-exchange. 114

Figure 5.2. The dependence of NO conversion into N_2 on operation temperature and ion-exchange temperature for H-Cu-ZSM-5-50 zeolites. Reaction conditions: 2000 ppm NO, balance He, catalyst weight 1.0 g, and total flow rate 150 ml min^{-1}. 116

Figure 5.3. The dependence of NO conversion into N_2 on operation temperature and repetition of ion-exchange at 45 °C for H-Cu-ZSM-5-50 zeolites. Reaction conditions: 2000 ppm NO, balance He, 1.0 g catalyst weight, and 150 ml min^{-1} total flow rate. 117

Figure 5.4. The dependence of NO conversion into N_2 on ion-exchange 118

level and catalyst preparation for H-Cu-ZSM-5-50 zeolites. (Δ) Ion-exchange level changed by repeating ion-exchange temperature, ( ) ion-exchange level changed by changing ion-exchange temperature. Reaction conditions: 2000 ppm NO, balance He, 1.0 g catalyst weight, and total flow rate 150 ml min^{-1}.

Figure 5.5. The dependence of NO conversion on temperature with and without the presence of O_2 over: (a) H-Cu-ZSM-5-50-58, ion-exchanged at 25 °C once for 24 h, (b) H-Cu-ZSM-5-50-62.3, ion-exchanged at 45 °C once for 24 h, (c) H-Cu-ZSM-5-50-132, ion-exchanged at 80 °C once for 24 h. Reaction condition: 2000 ppm NO, balance He, 1.0 g catalyst weight, and 150 ml min^{-1} total flow rate. 119

Figure 5.6. The dependence of NO conversion on temperature with and without the presence of O_2 over: (a) H-Cu-ZSM-5-50-62.3, ion-exchanged at 45 °C once for 24 h (b) H-Cu-ZSM-5-50-106.7, ion-exchanged at 45 °C twice for 24 h, (c) H-Cu-ZSM-5-50-139.3, ion-exchanged at 45 °C three times for 24 h. Reaction condition: 2000 ppm NO, balance He, 1.0 g catalyst weight, 150 ml min^{-1} total flow rate. 120

Figure 5.7. The dependence of NO conversion into N_2 on temperature over 1 g of H-Cu-ZSM-5-32.2-101.7. Reaction conditions: 2000 ppm NO, balance He, 1.0 g catalyst weight, and 100 ml min^{-1} total flow rate. 124

Figure 5.8. The dependence of NO conversion on contact time at 450 °C. Reaction conditions: 2000 ppm NO, balance He, 0.25 to 1.0 g catalyst weight, and 100 ml min^{-1} total flow rate. 125

Figure 5.9. The dependence of NO conversion on contact time at 500 °C. Reaction conditions: 2000 ppm NO, balance He, 0.25 to 125

1.0 g catalyst, and 100 ml min^{-1} total flow rate.

Figure 5.10. The dependence of turnover frequency (TOF) on NO concentration for H-Cu-ZSM-5-32.2-101.7 catalyst at 350 and 450 °C. Reaction conditions: 1000 to 10000 ppm NO, 0.5 g catalyst weight, and 100 ml min^{-1} total flow rate. 127

Figure 5.11. The dependence of turnover frequency (TOF) on NO concentration for H-Cu-ZSM-5-32.2-101.7 catalyst at 550 °C. Reaction conditions: 1000 to 10000 ppm NO, 0.5 g catalyst weight, and 100 ml min^{-1} total flow rate. 127

Figure 5.12. The dependence of turnover frequency (TOF) on O_2 concentration for H-Cu-ZSM-5-32.2-101.7 catalyst. Reaction conditions: 2000 ppm NO, 2000 to 20000 ppm O_2, 0.5 g catalyst weight, and 100 ml min^{-1} total flow rate. 129

Figure 5.13. The dependence of $\ln\left[\frac{k[NO]^n}{r} - 1\right]$ on $\ln[O_2]$ at 450 °C. Reaction conditions: 2000 ppm NO, 5000 to 20000 ppm O_2, 0.5 g catalyst weight, and 100 ml min^{-1} total flow rate. 130

Figure 5.14. The dependence of $\ln\left[\frac{k[NO]^n}{r} - 1\right]$ on $\ln[O_2]$ at 550 °C. Reaction conditions: 2000 ppm NO, 1000 to 10000 ppm O_2, 0.5 g catalyst weight, and 100 ml min^{-1} total flow rate. 130

Figure 5.15. The dependence of $\ln\left[\frac{k[NO]^n}{r} - 1\right] + \ln[NO]$ on $\ln[O_2]$ at 450 °C. Reaction conditions: 2000 ppm NO, 5000 to 20000 ppm O_2, 0.5 g catalyst weight, and 100 ml min^{-1} total flow rate. 136

Figure 6.1. Comparison of methane and propene as reducing agents in the SCR of NO over H-Cu-ZSM-5-40-101.7 and H-Co-ZSM-5-40-45. Reaction conditions: 2000 ppm NO, 2000 ppm CH_4 or C_3H_6, and 2% O_2, balance He, 1.0 g catalyst, and 100 ml min^{-1} total flow rate. 141

Figure 6.2. The dependence of NO conversion on temperature for SCR of NO over Co-ZSM-5 using CH_4 or C_3H_6 in this study (solid-lines) and using CH_4 or i-C_4H_{10} reported by Witzel et al. in 1994 (dashed-lines). Reaction conditions of this study: 2000 ppm NO, 2000 ppm CH_4 or C_3H_6, and 2% O_2, balance He, 1.0 g catalyst, 100 ml min^{-1} total flow rate. Reaction conditions of Witzel et al. study: 2000 ppm NO, 8000 ppm CH_4 or 2000 i-C_4H_{10} and 10% O_2, balance He, 0.25 g catalyst, and 75 ml min^{-1} total flow rate. 143

Figure 6.3. The dependence of NO conversion (a) and C_3H_6 conversion (b) on temperature and SiO_2/Al_2O_3 ratio. All catalysts have a 1.3% copper loading. Reaction conditions: 2000 ppm NO, 2000 ppm C_3H_6, 2% O_2, balance He, 1.0 g catalyst weight, and 150 ml min^{-1} total flow rate. 147

Figure 6.4. The dependence of NO conversion on Cu/Al and temperature over Cu-ZSM-5-100 catalysts. Reaction conditions: 2000 ppm NO, 2000 ppm C_3H_6, 2% O_2, balance He, 1.0 g catalyst weight, and 150 ml min^{-1} total flow rate. 150

Figure 6.5. The dependence of NO conversion on temperature and copper loading for SCR of NO. All the catalysts have SiO_2/Al_2O_3 ratio of 100. Reaction conditions: 2000 ppm NO, 2000 ppm C_3H_6, 2% O_2, balance helium, 1.0 g catalyst weight, and 150 ml min^{-1} total flow rate. 151

Figure 6.6. The dependence of NO conversion on temperature and copper loading of the catalysts prepared from H-ZSM-5 zeolites with SiO_2/Al_2O_3 ratios of 50 for SCR of NO. Reaction conditions: 2000 ppm NO, 2000 ppm C_3H_6, 2% O_2, balance helium, 1.0 g catalyst weight, and 150 ml min^{-1} total flow rate. 153

Figure 6.7. The dependence of NO conversion on temperature for two samples of Cu-ZSM-5 with almost the same copper ion-exchange level but different SiO_2/Al_2O_3 ratios. Reaction conditions: 2000 ppm NO, 2000 ppm C_3H_6, 2% O_2, balance helium, 1.0 g catalyst weight, and 150 ml min^{-1} total flow rate. 154

Figure 6.8. The effect of catalyst preparation on SCR of NO over Co-ZSM-5. The catalysts had the same SiO_2/Al_2O_3 ratio. Co-ZSM-5 catalyst prepared using batch (Δ) or semi-continuous system (◊).Reaction conditions: 2000 ppm NO, 2000 ppm CH_4, 2% O_2, balance He, 1.0 g catalyst weight, 150 ml min^{-1} total flow rate. 158

Figure 6.9. The dependence of NO conversion (a) and CH_4 conversion (b) on temperature and SiO_2/Al_2O_3 ratio for SCR of NO and oxidation of methane over Co-ZSM-5. Both catalysts included 1% copper loading. Reaction conditions: 2000 ppm NO , 2000 ppm CH_4 , 2% O_2, balance He, 1.0 g catalyst weight, and 150 ml min^{-1} total flow rate. 160

Figure 6.10. The dependence of NO conversion on temperature and cobalt loading for SCR of NO over Co-ZSM-5 with SiO_2/Al_2O_3 Ratio of 80. Reaction conditions: 2000 ppm 161

NO, 2000 ppm CH_4 , 2% O_2, balance helium, 1.0 g catalyst weight, and 150 ml min^{-1} total flow rate.

Figure 7.1. XRD patterns of silicalite-1 and MCM-41 molecular sieves as a typical example. Surface area, pore size, and pore volume of these two materials are also shown in this Figure. 171

Figure 7.2. The dependence of NO_x conversion on temperature for 5 synthesised samples. Reaction conditions: 2000 ppm NO, balance He, 1.5g catalyst weight, and 100 ml min^{-1} total flow rate. 173

Figure 7.3. The dependence of NO_x conversion on temperature in the presence of O_2. Reaction conditions: 2000 ppm NO, 1.6% O_2, balance He, 1.5g catalyst weight, and 100 ml min^{-1} total flow rate. 175

Figure 7.4. The dependence of NO_x conversion on temperature in the presence of O_2. Reaction conditions: 2000 ppm NO, 1.6% O_2, balance He, 1.5g catalyst weight, and 100 ml min^{-1} total flow rate. 176

Figure 7.5. The dependence of NO_x Decomposition in the presence of CH_4 on temperature. Reaction conditions: 2000 ppm NO, 0.52% CH_4, balance He, 1.5g catalyst weight, and 100 ml min^{-1} total flow rate. 177

Figure 7.6. The dependence of NO_x Decomposition on temperature for sample 7. Reaction conditions: 2000 ppm NO, 0.0% or 0.52% CH_4, 0.0% or 1.6% O_2, balance He, 1.5g catalyst weight, and 100 ml min^{-1} total flow rate. 180

Figure 7.7. The dependence of NO/NO_x decomposition on temperature for Sample 3 with and without pre-treatment of the catalyst. Reaction conditions: 2000 ppm NO, balance He, 1.5g catalyst weight, and 100 ml min^{-1} total flow rate. The catalyst was exposed to a helium stream with a flow rate of 100 ml min^{-1} for one hour at 500 °C before the use. 182

Figure 7.8. The dependence of NO conversion on temperature with and without the presence of oxygen and SCR of NO using methane or propene for Sample 3. Reaction conditions: 1.5g catalyst weight, and 100 ml min^{-1} total flow rate. The catalyst was exposed to a helium stream with a flow rate of 100 ml min^{-1} for one hour at 500 °C before the use. 183

Figure 7.9. A comparison among the results obtained from this study for the dependence of NO conversion into N_2 on temperature for a mixture of MCM-41 and ZSM-5, Sample 3, (the solid lines) and the results reported by Iwamoto and Mizuno (1993) for Cu-ZSM-5-23.3-152 (the dashed-lines). The contact time was 0.9 g s ml^{-1} for the solid lines whereas it was 0.3 g s ml^{-1} for the dashed-lines. 184

Figure 7.10. The dependence of NO Conversion on contact time for Sample 3 at 450 °C. Reaction conditions: 2000 ppm NO, 0.0% or 2% O_2, balance He, 1.5g catalyst weight, and 50 to 150 ml min^{-1} total flow rate. The catalyst was exposed to a helium stream with a flow rate of 100 ml min^{-1} for one hour at 500 °C prior to use. 185

Figure 7.11. The dependence of NO conversion on NO concentration for Sample 3 at 450 °C. Reaction conditions: 0.1 to 1.2 ppm NO, 2% O_2, balance He, 1.5g catalyst weight, and 100 ml 185

min^{-1} total flow rate. The catalyst was exposed to a helium stream with a flow rate of 100 ml min^{-1} for one hour at 500 ^{o}C prior to use.

Figure 7.12. The dependence of NO conversion on O_2 concentration for Sample 3 at 450 ^{o}C. Reaction conditions: 2000 ppm NO, 0.5 to 5% O_2, balance He, 1.5g catalyst weight, and 100 ml min^{-1} total flow rate. The catalyst was exposed to a helium stream with a flow rate of 100 ml min^{-1} for one hour at 500 ^{o}C prior to use. 186

LIST OF TABLES

Table 2.1.	The results reported by Iwamoto et al. (1991a) on the effect of oxygen on the direct decomposition of NO.	24
Table 2.2.	Ion-exchange details used by different researchers.	30
Table 2.3.	The specifications of facilities used by different researcher.	44
Table 2.4.	Reaction rate constants reported by Li and Hall (1991) used in Equation 2-10.	47
Table 3.1.	Specifications of the three autoclaves (all values are in mm).	60
Table 3.2.	The specifications of the synthesised ZSM-5 zeolites using Method I.	68
Table 3.3.	The specifications of the products using Method III with the composition ratios of $90SiO_2$: Al_2O_3: $7.7N_2O$: $3000H_2O$.	70
Table 3.4.	Surface areas and pore diameters of typical synthesised ZSM-5 zeolites.	71
Table 3.5.	Synthesis data of various ZSM-5 zeolites using four different methods.	78
Table 3.6.	A comparison among the specifications of the synthesised	79

ZSM-5 zeolites from the four different methods.

Table 3.7. SiO_2/Al_2O_3 ratios of starting gels and ZSM-5 products for three samples synthesised using Method I and one sample using Method II. 80

Table 4.1. Copper ion-exchanged ZSM-5 zeolites prepared for this study. 85

Table 4.2. Cobalt ion-exchanged ZSM-5 zeolites prepared for this study. 87

Table 4.3. The specifications of the GC columns. 94

Table 4.4. The types and the concentrations of the gases existing in the six gas cylinders used for GC calibration. 95

Table 4.5. Typical analytical results of SA-C5, STM-C5 and Cu-H-NT catalysts. 104

Table 4.6. Typical analytical results of SA-C5, STM-C5 and Cu-H-NT catalysts. 104

Table 4.7. The last five data reported by GC for N_2 concentrations over H-Cu-ZSM-5-32.2-101.7. Reaction condition: 2000 ppm NO, 2000 ppm C_3H_6, 2% O_2, balance helium, 1 g catalyst weight, and 100 ml min^{-1} total flow rate. 108

Table 4.8. Standard deviation, standard deviation of the mean, and uncertainty for the last five data used in Figures 4-10 and 4-11 at 300 °C and 350 °C respectively. 108

Table 5.1.	Specifications of preparation of Cu-ZSM-5 catalysts prepared from H-ZSM-5.	112
Table 5.2.	The detailed analysis of the catalyst used for kinetic studies (weight %).	123
Table 5.3.	The orders of NO in reaction rate and rate constants.	128
Table 5.4.	The reaction orders in O_2 concentration in the reaction rate and the K values in Equation(5-3).	129
Table 5.5.	The reaction orders in NO (n) and in O_2 (m) concentrations in the reaction rate.	131
Table 5.6.	The rates and adsorption equilibrium constants.	132
Table 6.1.	Specifications of the three copper ion-exchanged ZSM-5 catalysts with the same copper loading but different SiO_2/Al_2O_3 ratios.	146
Table 6.2.	Specifications of two groups of copper ion-exchanged ZSM-5 catalysts with the same SiO_2/Al_2O_3 ratios but different copper loadings.	149
Table 6.3.	Specifications of two copper ion-exchanged ZSM-5 catalysts prepared from H-ZSM-5 zeolite with the same SiO_2/Al_2O_3 ratio.	152
Table 6.4.	Specifications of two copper ion-exchanged ZSM-5 catalysts with almost the same copper ion-exchange level but different SiO_2/Al_2O_3 ratios.	154

Table 6.5.	Specifications of the two cobalt ion-exchanged ZSM-5 catalysts prepared using different preparation methods.	157
Table 6.6.	Specifications of the two cobalt ion-exchanged ZSM-5 catalysts with different SiO_2/Al_2O_3 ratios.	159
Table 6.7.	Specifications of the three cobalt ion-exchanged ZSM-5 catalysts with same SiO_2/Al_2O_3 ratio but different cobalt loadings.	161
Table 7.1.	Preparation conditions of the first group of samples and their specifications.	167
Table 7.2.	The type and the pH values of the solutions used to restore the cation exchange capacity of the pillared clays.	169
Table 8.1.	A Comparison between the maximum NO conversions obtained using different Cu-ZSM-5 catalysts in this study and the literature for the direct decomposition.	190
Table 8.2.	A Comparison between the maximum NO conversions achieved for SCR of NO over several Cu-ZSM-5 catalysts in this study and literature data.	192
Table 8.3.	A Comparison between the maximum NO conversions achieved for SCR of NO over Co-ZSM-5 catalysts in this study and literature data.	193
Table 8.4.	Full-scale flow rates and uncertainties of the mass flow controllers used in this study.	195
Table 8.5.	NO conversions and the uncertainties involved for the	197

direct decomposition of NO over H-Cu-ZSM-5-32.2-101.7 catalyst.

Table 8.6. NO conversions and the errors involved for SCR of NO using propene over H-Cu-ZSM-5-40-101.7 catalyst. 197

Table 8.7. NO conversions and the errors involved for SCR of NO using methane over H-Co-ZSM-5-40-45 catalyst. 197

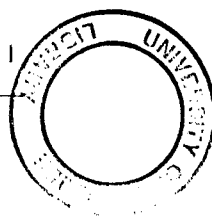

CHAPTER ONE

INTRODUCTION

Nitrogen oxides (NO_x: NO, NO_2) are by-products of high-temperature combustion processes. Their emissions from stationary installations and the exhaust of motor vehicles pollute the atmosphere. The primary component of these nitrogen oxides produced in these processes is nitrogen monoxide (NO). Nitrogen monoxide reacts with oxygen at low temperatures to form nitrogen dioxide (NO_2) which is released to the atmosphere. NO_2 contributes to acid rain, urban smog and ozone layer depletion. It has also been linked to many diseases such as bronchitis and pneumonia (Armor, 1994). Therefore, the removal of nitrogen monoxide from the exhaust gases is required before it is released into the atmosphere to control NO_x pollution.

Two main post-combustion technologies are currently used to control NO_x emissions. The first technology is Selective Catalytic Reduction (SCR) of nitrogen monoxide using ammonia as the reducing agent which is utilised to control NO emissions from stationary combustion processes. Ammonia has high selectivity towards reaction with NO in the presence of high excess oxygen (Bosch and Janssen, 1988) but this technology is not practical for application in mobile systems due to the difficulties associated with on-board ammonia storage. Therefore, the second technology, Three-Way Catalysts (TWC) are utilised to control NO emissions from automotive engine exhausts.

TWC is currently employed to meet the most stringent emission standards for passenger cars with gasoline engines which operate with a stoichiometric air-to-fuel ratio of 14.7:1. However, working under the stoichiometric air-to-fuel ratio results in low fuel efficiency. On the other hand, lean-burn gasoline or diesel engines which work under fuel-lean conditions, provide higher efficiencies, but TWC is not

applicable for these engines due to oxygen poisoning. The TWC constituents include platinum (Pt), palladium (Pd), and rhodium (Rh) or include only Pt or Pd with Rh. Lack of Rh in TWC results in much lower NO conversion (Shelef and Graham, 1994). Rhodium deposits are limited, and this metal is also very expensive. It is desirable to use the lean-burn engines which operate with a higher air-to-fuel ratio of 21:1 so that the efficiency of the combustion process is increased (Shelef, 1995). Hence, a catalyst which is able to remove NO from exhaust gases in an oxidising atmosphere is required.

To reduce NO emissions by converting NO to N_2, the following two catalytic technologies have been suggested: direct decomposition, and selective catalytic reduction (SCR). In the first of these technologies NO can be directly decomposed into nitrogen (N_2) and oxygen (O_2). In the second, NO is reduced to N_2 by a N-containing reductant such as ammonia or a N-free reductant, such as a hydrocarbon.

Much research has been carried out to find active and stable catalysts for direct decomposition and SCR of NO in an oxidising atmosphere. Noble metals and metal oxides have been examined for direct decomposition, but their activities were not high enough for practical use (Li and Hall, 1990). SCR of NO by hydrocarbons and oxygenated hydrocarbons over metal oxide catalysts was summarised by Hamada (1994) where it was concluded that various metal oxides can catalyse the reaction. Different zeolites were also tested. Copper ion-exchanged ZSM-5 (Cu-ZSM-5) zeolite was found to have high catalytic activity for NO decomposition (Iwamoto et al., 1986a). However, the reaction rate over this catalyst is too slow to be used in practical situations.

It is believed that in direct decomposition processes, oxygen available in exhaust gas or generated through the decomposition of NO, poisons the catalyst. In addition, the presence of water and sulfur dioxide inhibit the reaction. In SCR processes, the common reductants introduced to the system for NO conversion are usually oxidised with excess oxygen on a heterogenous catalyst first, and then react with nitrogen oxides. Therefore, in direct decomposition, the catalyst must be stable and resistant to

oxygen poisoning. In a SCR process, the reductant also has to be selectively oxidised by NO_x but not to react initially with oxygen. Ammonia is well known as a selective reductant and it has been used in Japan and Europe to clean power plant effluents to reduce NO_x emissions (Shelef, 1995).

Many parameters such as reaction temperature, copper ion-exchange level, SiO_2/Al_2O_3 ratio, cocation/Al ratio, NO concentration, O_2 concentration, water vapour, sulfur oxides and catalyst preparation technique affect the conversion of NO to nitrogen. As a result, conversion of NO is a complex reaction whether by direct decomposition or SCR.

For direct decomposition and SCR of NO, ZSM-5 zeolites are usually supplied by commercial sources e.g. Tosoh Corporation (Iwamoto et al., 1989; Sato et al., 1992; Nishizaka and Misono, 1993). In this study, in order to control the zeolite properties, ZSM-5 zeolites are synthesised in our laboratory. The zeolites with 100% crystallinity are synthesised using two different methods, with and without a template. Tetrapropylammonium bromide (TPABr) is used as a template and Na-ZSM-5 zeolites with different silica alumina ratios (SiO_2/ Al_2O_3) of 70, 80, 100, 140 and 176 are synthesised. Na-ZSM-5 zeolite with SiO_2/Al_2O_3 of 40 is synthesised in a system without any template. To confirm the zeolite structure and crystallinity, the synthesised zeolites are characterised by the X-Ray Diffraction (XRD) technique.

In general, this research is aimed at recognising direct decomposition and SCR of NO and the problems involved in order to control environmental pollution using the synthesised zeolites as well as zeolites from commercial sources. The overall aim of the current project is to generate knowledge that may lead to the development of a catalyst potentially capable of practical use.

This thesis includes nine chapters. The following chapters are detailed as follows:

Chapter 2 presents a literature review on direct decomposition and SCR of NO. Particular attention is given to copper ion-exchanged ZSM-5 zeolites for direct

decomposition and the investigation of the effect of various factors affecting the decomposition of NO. SCR of NO using propene over copper ion-exchanged ZSM-5 zeolites and using methane over cobalt ion-exchanged ZSM-5 zeolites are also reviewed.

In Chapter 3, four different methods for ZSM-5 zeolite synthesis are described. The methods are compared and the properties of the zeolites synthesised are discussed. The two best methods are selected to synthesise ZSM-5 zeolite for subsequent studies in NO decomposition and SCR of NO after converting to a catalyst form.

In Chapter 4, catalyst preparation and experimental techniques for NO conversion studies are described. The instruments used in this work, i.e. a NO_x analyser and a gas chromatograph (GC), and the data analysis are also introduced.

Chapter 5 discusses the effect of preparation method on copper ion-exchange levels and catalytic activity of Cu-ZSM-5 zeolites for the direct decomposition of NO. Kinetic studies of the direct decomposition of NO over copper ion-exchanged ZSM-5 synthesised with template-free method are also presented and discussed.

In Chapter 6, the results obtained for the effect of SiO_2/Al_2O_3 ratio, copper loading and ion-exchange level on NO reduction, using propene over Cu-ZSM-5 and methane over Co-ZSM-5 zeolites, are presented and discussed. Catalytic activity of the copper-exchanged zeolites prepared from Na-form and H-form ZSM-5 zeolites are also compared.

In Chapter 7, the experimental results achieved using two different groups of catalysts prepared by Queensland University are presented and discussed.

In Chapter 8, an evaluation of the current study as well as justification of the data presented are made. Practical implications of the current work are also discussed.

Finally, Chapter 9 presents general conclusions over the whole study and suggestions for future work.

CHAPTER TWO

LITERATURE REVIEW

2.1 Introduction

There has been a vast amount of information in the literature regarding direct decomposition and selective reduction of nitrogen oxides (NO_x) using catalysts. It is necessary to establish a solid knowledge base for the current research by examining the information available on this subject.

The influence of variables related to copper ion-exchanged ZSM-5 zeolites catalytic activity for direct decomposition and some aspects of SCR of NO are discussed. The experimental techniques used by other researchers are also reviewed in order to utilise their experiences. To overview the reactions involved, an understanding of the mechanisms is required. Therefore, publications about the mechanisms of direct decomposition in the absence and presence of oxygen, and selective catalytic reduction of NO over copper ion-exchanged ZSM-5 zeolites, are reviewed.

Attention is also paid to preparation methods for copper or cobalt ion-exchanged ZSM-5 zeolite. This is employed to prepare ZSM-5 with different copper or cobalt loading. To concentrate on those aspects that are related to the objectives of this study, the effect of silica alumina molar ratio on the catalytic activity of the copper and cobalt ion-exchanged zeolites for selective catalytic reduction of NO is presented. Special focus is given to the effect of this on the catalytic activity of Cu-ZSM-5 and Co-ZSM-5, using propene in the case of Cu-ZSM-5 and methane in the case of Co-ZSM-5 catalyst.

From this review, gaps in the present state of knowledge in the field of catalytic decomposition of NO are identified. Those form the major objectives of the current project, as presented at the end of this chapter.

2.2 Sources of Nitrogen Oxides

NO is produced naturally by microbial decomposition of proteins in soil, volcanic activity, meteor trails and lightning flashes. NO is also generated through human activities including most combustion processes and some chemical processes such as nitric acid plants. NO can be further oxidised to NO_2 in the atmosphere. NO and NO_2 are collectively called NO_x. Various NO sources are summarised in Figure 2.1. This Figure shows a modified view of what was reported by Mason and Herther (1982). From anthropogenic sources, 23.2 million metric tonnes NO_x was emitted in the USA alone in 1992 (Bell et al., 1995). This example indicates the large extent of NO_x emissions worldwide from all sources.

Combustion processes such as power stations and industrial boilers, cement kilns and other high temperature manufacturing processes, as well as automobile engines, are the major sources of human-generated NO_x. Temperature has a very important role in the formation of NO in combustion processes. The equilibrium concentration of NO increases sharply at temperatures above 1770 K. In 1967 Danielson (cited in Harrison et al., 1981) reported that for formation of 500 ppm NO, it takes 1370 seconds at 1590 K whereas this time reduces to 16.2 seconds at 1810 K. Unfortunately, this temperature is in the range of rich and lean flammability limits (1620 - 2470 K). NO concentration also depends on the quantity of N_2 and O_2 entered into the process and the heat of combustion (Harrison et al., 1981).

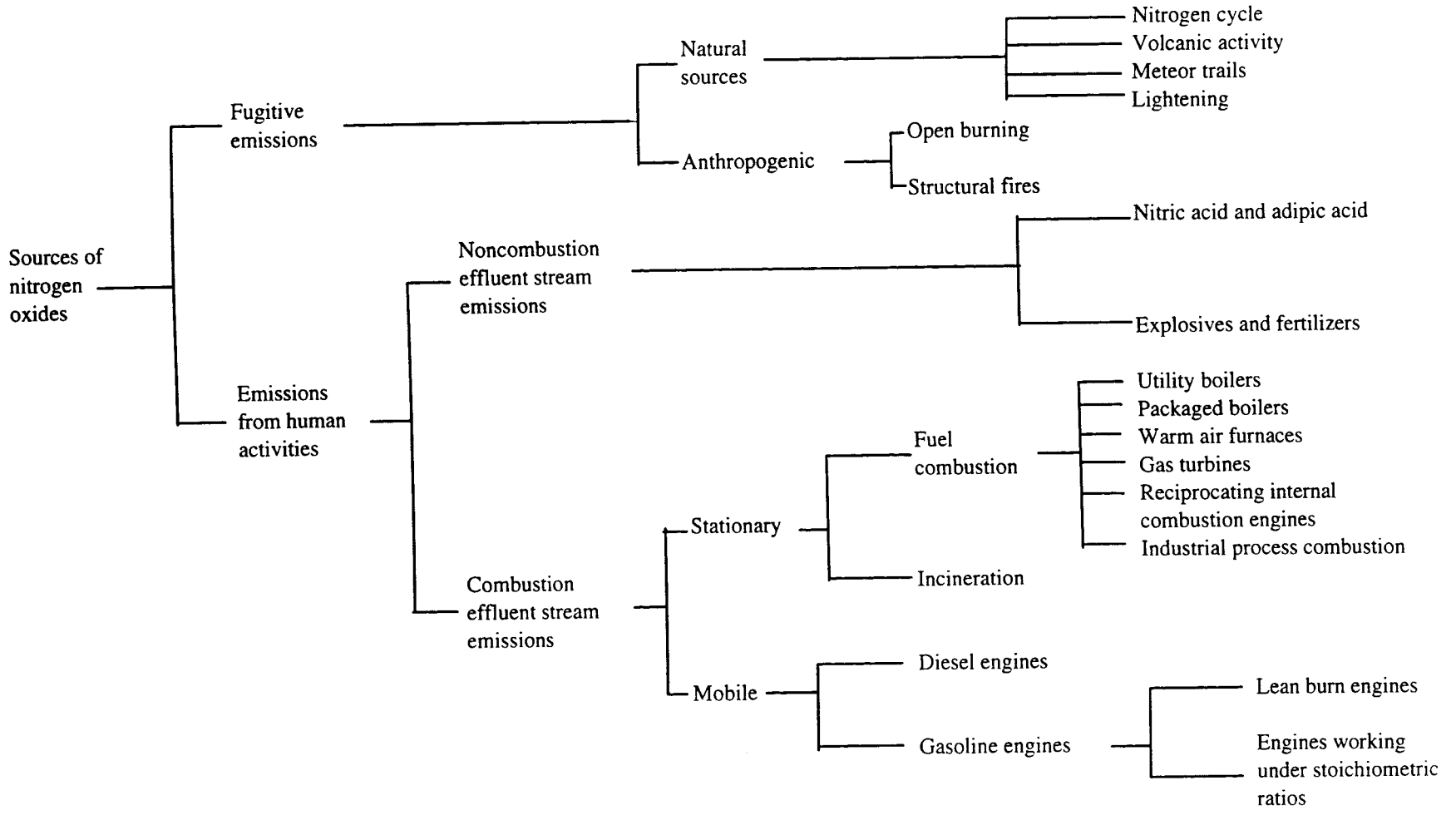

Figure 2.1. Sources of nitrogen oxide emissions (adapted from Mason and Herther 1982)

2.3 Environmental Effects of Nitrogen Oxides

NO_x emissions from the exhausts of car engines and stationary combustion processes have a major role in the formation of acid rain and photochemical smog. Many diseases such as pneumonia can also be caused by NO_2. It also contributes to ozone layer depletion (Armor, 1994). One of the consequences of NO_x emissions is acid rain (Elvins et al., 1991). NO_2 in the atmosphere is dissolved in clouds and rain drops to form nitrous and/or nitric acid:

$$2NO_2\,(g) + H_2O\,(l) \longrightarrow \underset{\text{Nitric Acid}}{H^+(aq) + NO_3^-(aq)} + \underset{\text{Nitrous Acid}}{HNO_2\,(aq)} \qquad \text{(R2-1)}$$

A significant component of acid rain in many industrial countries such as the USA and European countries is nitric oxide. 30-35% and 30% of the acid precipitation was reported to be nitric acid in north eastern parts of the USA (Gibson and Linthurst, 1982) and central parts of Sweden (Lindau, 1982), respectively.

NO_x play also an important role in the initiation of formation of photochemical smog which is a mixture of chemical pollutants (Elvins et al., 1991). Photochemical smog, which is so called because ultra violet (UV) light is usually required for initiation of the reactions, is visible as a brown haze, especially on sunny days. Photochemical smog is produced by interaction between nitrogen oxides, unburnt hydrocarbons and oxygen, which are usually available in the exhaust gases of combustion processes (Zumdahl, 1986). NO emitted from exhaust gases into the atmosphere is oxidised to NO_2. It then breaks into NO and a free oxygen atom in the presence of sunlight. In the next step, the oxygen atom combines with an oxygen molecule to form ozone, according to the following reactions:

$$NO_2(g) + h\nu \longrightarrow NO(g) + O(g) \qquad \text{(R2-2)}$$

$$O(g) + O_2(g) \longrightarrow O_3(g) \qquad \text{(R2-3)}$$

Ozone is also a pollutant gas. Irritation of the eyes can occur in the atmosphere with only 0.3 ppm ozone present, and it can cause respiratory problems at higher concentrations (Elvins et al., 1991). Ozone is extremely reactive. It reacts with unburnt hydrocarbons to produce other pollutants. Many problems such as decreased visibility, eye and lung irritation, and crop damage can be caused by ozone.

Exposure to NO_x can also cause several diseases such as bronchitis and pneumonia. These poisonous gases allow human bodies to be more susceptible to some infections (Armor, 1994). The type and extent of these health effects depend on NO_x concentration, time of exposure, presence of additional pollutants, pre-existing disease in the host and the mode of exposure. Most studies carried out by researchers on the influence of NO_2 on the human body have been conducted in combination with other pollutants. In addition, most studies have only considered the health effects associated with NO_x in animals. The evaluation and extrapolation of the hazard from animal to human depend on the type of animals exposed to NO_x. Therefore, it is difficult to make a judgment about the exact diseases which are associated with nitrogen oxides in humans (Esch and Menzel, 1982). Due to the hazards caused by NO_x emissions, tight regulations have been established in most industrialised countries e.g. European countries, the USA, Japan, and Korea. For example, it was recently agreed in some parts of the USA that NO_x emissions have to be reduced to 65% or no more than 0.2 lb/million BTU by May 1, 1999, and 75% or not more than 0.15 lb/million BTU by 2003 (Lambert and McGowan, 1996).

2.4 Chemistry of Nitrogen Monoxide

Nitrogen monoxide is a key starting point of other oxides of nitrogen. It is formed during and after combustion processes. Three mechanisms are believed to contribute to NO formation during a combustion process: thermal NO_x, prompt NO_x and fuel NO_x. Thermal NO_x is formed in high temperature zones under fuel-lean conditions by reactions between oxygen and atmospheric nitrogen. This can occur anywhere if the temperature, concentrations, and residence times are favourable. The mechanism

of thermal NO_x formation was first proposed by Zeldovich (1946). The Zeldovich chain mechanism is believed to be the predominant mechanism for NO formation. It consists of the following two reactions:

$$O + N_2 \rightleftharpoons NO + N \quad \text{(R2-4)}$$

$$N + O_2 \rightleftharpoons NO + O \quad \text{(R2-5)}$$

Only one oxygen atom is required to combine with an available N_2 molecule from the air to initiate the above mechanism. The first oxygen radical can be produced from available oxygen molecules from the air at such high temperatures in a combustion process. In the first reaction, a NO molecule and a nitrogen atom are formed. In the second, the produced nitrogen atom reacts rapidly with an oxygen molecule to form another NO molecule and an oxygen atom. Therefore the formation of one NO molecule leads to the formation of a second NO molecule, and so the chain continues.

Prompt NO_x is formed rapidly when a combustion process starts (Baggley, 1993). This has been identified as the mechanism involved in the formation of NO_x from atmospheric nitrogen by hydrocarbon radicals in fuel rich zones of the flame. The reaction can be initiated by a hydrocarbon radical such as the following reaction:

$$\text{-CH-} + N_2 \longrightarrow HCN + H \quad \text{(R2-6)}$$

This is followed by

$$\text{-CH}_2\text{-} + X \longrightarrow \text{-CH-} + HX \quad \text{(R2-7)}$$

where X is either H or OH. HCN is thus a precursor of the formation of nitric oxide. A weak dependence exists between the formation of prompt NO_x and temperature. In most cases, the amount of prompt NO_x is relatively low in comparison with thermal NO_x. In low-NO_x burners, however, prompt NO_x is the main source of NO formation (Wojtowicz et al., 1993).

Fuel NO_x is generated by oxidation of fuel bound nitrogen compounds. Most fossil fuels, other than natural gas, contain nitrogen bound as an organic compound in their structures. 15-30% of the nitrogen present in the fuel is converted into NO_x (Bell et al., 1995). It is first converted into a range of cyanide and amine species which are then further oxidised to NO_x. This mechanism is more dependent on the availability of oxygen than on the temperature. The significance of this is limited to the combustion of coal and some nitrogen rich fuel oils.

Nitrogen monoxide properties define the interaction of NO with other chemicals. NO is a paramagnetic molecule. The magnetic nature of the molecule is predicted using the molecular orbital theory (Zumdahl, 1986). There are 11 valance shell electrons (5 electrons belonging to nitrogen and 6 electrons to oxygen) in NO which are arranged according to molecular orbital energy-level as follows:

NO: $(\sigma_{2s})^2(\sigma_{2s}{}^*)^2\,(\pi_{2p})^4(\sigma_{2p})^2(\pi_{2p}{}^*)^1$

According to the molecular orbital theory, the bond order in NO is: (8-3)/2 = 2.5 which is the difference between 8 bonding and 3 antibonding electrons divided by 2. This indicates that the bond between oxygen and nitrogen in NO is stronger than double, and weaker than triple bond. The odd electron located in a π antibonding orbital makes the molecule paramagnetic. This electron can be readily removed to produce the nitrosonium ion, NO^+. In addition, NO is also a powerful π-acceptor and can form complexes with transitional metals such as Rh, Ir, Ni, Pd, Pt, Cu, Fe, Ru, Co (Griffith, 1973). The interactions between NO and transitional metals have led researchers to use different types of catalysts using these metals in their structures for decomposition or reduction of NO. Different techniques such as dispersion, incorporation, impregnation and ion-exchange have been employed to use these metals through supported materials.

2.5 Nitrogen Oxides Control Technologies

Many techniques have been developed to control NO_x emissions. They are generally divided into two groups: combustion control technologies that limit NO formation in combustion processes, and post-combustion control technologies that decompose or reduce NO to N_2 after its formation during combustion. The most common post-combustion technologies are; reduction of NO using ammonia in stationary sources, and three-way catalysis (TWC) systems in spark ignited gasoline engines.

2.5.1 Combustion Control Technologies

The most common techniques used to limit NO formations during combustion processes include flue gas recirculation, air staging and fuel staging (Syska, 1993). Flue gas recirculation techniques can be utilised in both stationary and mobile combustion processes, whereas air staging and fuel staging are applied only in stationary plants. These techniques are based on the NO formation mechanisms. For example, to reduce the amount of thermal NO_x the flame temperature is reduced by recirculation of the flue gas.

In the first technique, the flue gas recirculation, combustion air is diluted by introducing inert substances e.g. oxygen-deficient combustion products (De Jong, 1993). These substances consume some part of produced energy from combustion process to be heated from their initial temperature. As a result of the gas recirculation, a reduction occurs in flame temperature, resulting in lower thermal NO_x formation. In addition, some of the NO present in the recirculated gas can be reburned and reduced to molecular nitrogen. For this purpose, 10-20 % of the combustion air is usually recirculated. Around 70% reduction in NO_x formation can be achieved in natural gas burners using the flue gas recirculation technique. This technique is not sufficient when oil or coal is used as the fuel. The reason is that a significant amount of NO_x is formed from the fuel-bound nitrogen available in those fuels. There are two advantages of this technique: 1) it can be utilised with the other

NO_x reduction techniques simultaneously and 2) the burner requires minor modifications. The disadvantages are the flame instability and the delay of the fuel and air mixing which usually occurs during the use of this technique (Lambert and McGowan, 1996).

In the second technique, air staging, fuel is introduced into the combustion zone at one mixing location, whereas air is added in two or more locations (Lahaye and Prado, 1986). This means that the burner is operated with less air than the theoretical amount required for the combustion process. The remainder of the combustion air is subsequently added further at later positions. In the gas burners, using this technique results in a decrease in the peak flame temperature and consequently less thermal NO_x formation. In the case of firing liquid fuels containing organically bound nitrogen compounds, these compounds are released in the fuel- rich zone, where they are converted to molecular nitrogen, rather than oxidised to NO.

In the third technique, fuel staging, all of the air is mixed with a portion of the fuel in one location, and the remainder of the fuel is added in one or more stages (Lahaye and Prado, 1986). As a result of splitting the fuel into two or more fuel streams, more than one combustion stage is created. The second combustion stage can be assumed to be the NO reduction stage. The sub-stoichiometric operation of this second stage is of great importance. Stoichiometric composition, reduction zone temperature and residence time in the first stage (between both fuel additions) are important factors that affect the NO_x reduction.

Improved combustion process technology can be taken into consideration for reducing NO_x emissions. NO_x gases from diesel engine exhaust can be decreased by using exhaust gas recirculation. However, the strict regulations for NO_x emissions cannot be met by using this technique only. Consequently, worldwide research is being carried out in the field of post-combustion techniques.

2.5.2 Post-Combustion Technologies for Stationary Sources

Selective reduction of nitric oxide using ammonia as a reducing agent is commercially used for removal of NO from stationary sources. For this purpose, two processes, one homogeneous and one heterogeneous, are available (Wallman and Carlsson, 1993). These two processes are called thermal NO_x reduction or selective non-catalytic reduction (SNCR), and selective catalytic reduction (SCR), respectively. In the first process, the operating temperature is between 1250-1350 K which is very high in comparison with that of selective catalytic reduction (less than 800 K). It has been shown that 90% of NO_x reduction is achievable with SCR, while only 30-70% is achievable with SNCR technology (Lambert and McGrown, 1996). In both processes, ammonia reacts selectively with nitric oxide in the presence of large excess oxygen (Wallman and Carlsson, 1993).

The most accepted method for removing NO from flue gases of stationary sources is selective catalytic reduction. Ammonia is used as a reductant in stationary installations, e.g. power plants and factories where a combustion process is carried out in the presence of large amounts of excess air (Bosch and Janssen, 1988). Ammonia is able to reduce the oxides of nitrogen selectively, according to the following reactions:

$$4NO + 4NH_3 + O_2 \rightarrow 4N_2 + 6H_2O \qquad \text{(R2-8)}$$

$$2NO_2 + 4NH_3 + O_2 \rightarrow 3N_2 + 6H_2O \qquad \text{(R2-9)}$$

In reference to Reaction (R2-8) which is the main reaction, the number of moles of ammonia should be kept equal to that of NO. Although increasing the amount of ammonia shift both reactions towards the right which is favourable for NO and NO_2 reduction but, some unfavourable reactions may take place with the emission of excess ammonia.

The basis of the SCR technology is the pairing of two nitrogen atoms, one from nitric oxide and the other from ammonia on a catalyst. Noble metal catalysts are used for

SCR with NH_3 at a low temperature (<570 K) and vanadia/titania catalysts at temperatures up to 720 K (Shelef, 1995). High selectivity of ammonia towards NO in the presence of O_2 and the promoting effect of oxygen on the rate of the reaction between NH_3 and NO are the most important advantages of this method. However, ammonia is a poisonous material. Therefore, storage, transportation and emission during the reaction have to be handled with extreme care. The stoichiometric amount of ammonia needs to be maintained during the reaction to avoid any emission of unreacted ammonia. This introduces high facility and maintenance costs. The toxicity of the catalyst is also a potential problem. For example, vanadium is a toxic material in V_2O_5-WO_3-TiO_2, which is a typical catalyst for the NH_3-NO reaction (Amiridis et al., 1996).

Selective catalytic reduction of NH_3 is not practical for transportation in mobile systems due to the difficulties of carrying ammonia, and the probability of ammonia leakage. Therefore, three-way catalysis technology is utilised for NO emission control for mobile sources.

2.5.3 Post-Combustion Technologies for Mobile Sources

Three-way catalysis (TWC) technology has been utilised on most passenger cars in the USA since 1982 (Taylor, 1993). Three-way catalysts usually consist of noble metals including rhodium (Rh), platinum (Pt) and palladium (Pd) supported on metal oxides attached to ceramic monoliths. They are so called because they deal with three pollutant gases: uncombusted hydrocarbons, carbon monoxide, and nitrogen oxides, simultaneously. This technology is able to meet the most stringent emission standards in gasoline engines which work under a stoichiometric air-to-fuel ratio (14.7:1) using only unleaded gasoline (Shelef, 1995). However, this is not applicable for lean-burn gasoline or diesel engines which work under lean-fuel conditions. Figure 2.2 shows the dependence of NO, CO and HC conversions on air-to-fuel ratio using TWC (Schlatter et al., 1983). Rh plays the most important role in the TWC technology for NO removal. Some compositions include the three metals, but others include only Pt

or Pd with Rh. It has been reported that over a typical Rh-free catalyst, all other parameters being the same, much lower NO conversion was achieved at the left side of the control point where excess oxygen was not available, and no NO conversion could be achieved at the right side where the excess oxygen was present (Shelef and Graham, 1994).

In lean-burn applications, the air-to-fuel ratio is made lean in order to achieve high fuel efficiency. In this case, exhaust gases contain a large amount of oxygen which is not suitable for TWC technology. On the other hand, the maximum NO_x is generated at very near to stoichiometric air-to-fuel ratios in the lean-fuel side. Figure 2.3 shows that the major problems involved in the NO_x emission control is the contradiction between high fuel efficiency and low NO_x emissions (Lambert and McGowan, 1996). On the fuel lean side, high fuel efficiency can be achieved but it results in high NO_x emissions. The only exception is a narrow region which is at the low excess air (LEA) zone. Operating in this region requires very tight control on the combustion system. Operating in the fuel-rich region, on the other hand, creates another problem: the production of large amounts of carbon monoxide and unburnt hydrocarbons.

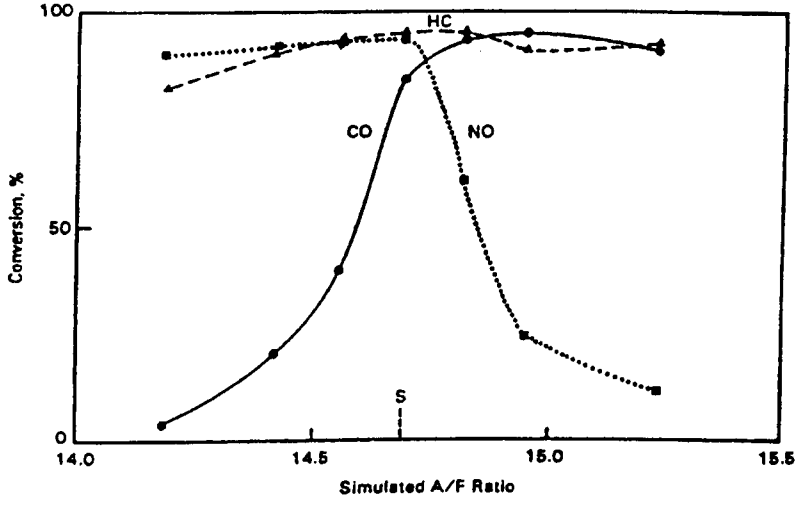

Figure 2.2. The principle of 3-way catalyst for exhaust emission control. Catalyst efficiencies measured in the laboratory with a steady feed stream composition at various simulated air/fuel ratios. Catalyst: 0.042 wt% Pt, 0.018 wt% Rh, alumina (reproduced from Schlatter et al., 1983).

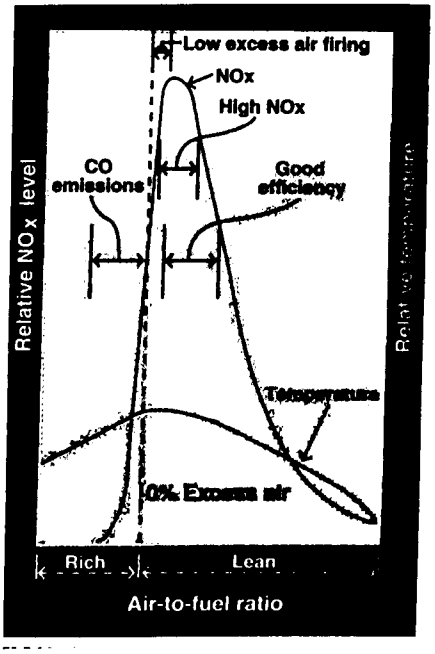

Figure 2.3. The dependence of NO_x level on air-to fuel ratio and temperature (reproduced from Lambert and McGowan, 1996).

Considering the above problems, a new technology is required to remove NO_x in exhaust gases from diesel and lean-burn gasoline engines which operate under fuel-lean conditions. A suitable catalyst is required to decompose and/or reduce NO in an oxidising atmosphere. Three main problems which need to be taken into account for the catalyst are selectivity towards NO decomposition, thermal stability, and high activity in a wide range of temperatures.

2.5.4 Technologies under Investigation

There are two exciting research developments associated with the removal of NO_x from the exhaust of newly developed engines which work under an oxidising atmosphere. The first of these is direct decomposition of NO to N_2 and O_2, a reaction which is thermodynamically favoured but proceeds slowly in the absence of a catalyst. The second research development relates to the selective catalytic reduction of NO by using various reductants. This technique can be employed for reduction of

NO using hydrocarbons as reductants over Cu-ZSM-5, and other cation exchanged zeolites. This was reported in 1990 independently by Held et al. (1990) and Iwamoto (1990) for the first time.

Noble metals, metal oxides, and especially zeolites are candidates for removal of NO. Noble metals because of their activity at low temperatures, some metal oxide catalysts for their high selectivity and their durability at high temperatures, and zeolites for their high activity, have been investigated for the removal of NO (Hamada, 1994).

Among several metal oxides which were reported by Hamada (1994) to be active and selective for the reduction of NO, alumina was reported as the most active catalyst. 44% and 38% NO conversions were achieved using propene or propane, respectively. Adding water had no inhibition effect on NO conversion when propene was the reducing agent whereas NO conversion reduced from 38% to 5% when propane was used. The reduction of NO over alumina was also reported using methanol as a reducing agent under diesel exhaust gas. Therefore, alumina is a potential candidate for NO reduction in diesel engine exhausts.

Considerable research has been carried out for decomposition and/or reduction of NO using different zeolites. Cu-ZSM-5 zeolite is considered to be an active catalyst for NO decomposition (Iwamoto et al., 1986a). However, the presence of oxygen inhibits the reaction, and SO_2 and H_2O have serious inhibiting effects so that the practical applications of this catalyst under oxygen-rich atmosphere depend on being able to solve these problems. The direct decomposition of NO over these catalysts continues to be investigated because it seems to be the most economical and simplest method.

Activity of a catalyst for direct decomposition or SCR of NO is usually evaluated by conversion of NO into N_2 specifically, conversion of NO or conversion of NO_x. The first definition, which is the most accurate, was used by most researchers (Teraoka et al., 1990; Vassallo et al., 1995). This is expressed by the following equation:

$$X_{NO} = 2\left(\frac{[N_2]_{out}}{[NO]_{in}}\right)\times 100 \qquad (2\text{-}1)$$

Where:

X_{NO} = percentage conversion of NO into N_2,

$[N_2]_{out}$ = N_2 concentration in the exit stream of reactor, and

$[NO]_{in}$ = NO concentration in the supplied stream to reactor.

The second definition is defined by calculation of NO conversion using the following equation:

$$X'_{NO} = \left(1-\frac{[NO]_{out}}{[NO]_{in}}\right)\times 100 = \frac{[NO]_{in}-[NO]_{out}}{[NO]_{in}}\times 100 \qquad (2\text{-}2)$$

Where:

X'_{NO} = percentage conversion of NO, and

$[NO]_{out}$ = NO concentration in the exit stream of reactor.

.

This definition, however is not a true indication of NO conversion to N_2. X'_{NO} shows total conversion of NO to different components such as N_2, NO_2 and N_2O.

The third definition is:

$$X_{NO_x} = \left(\frac{[NO_x]_{in}-[NO_x]_{out}}{[NO_x]_{in}}\right)\times 100 \qquad (2\text{-}3)$$

$[NO]$ and $[NO_2]$ are usually measured by a NO_x analyser (Tanaka, 1997). Therefore, Equation (2-3) can be written as:

$$\left(\frac{[NO_x]_{in} - [NO_x]_{out}}{[NO_x]_{in}}\right) = \frac{([NO]_{in} + [NO_2]_{in}) - ([NO]_{out} + [NO_2]_{out})}{[NO_x]_{in}} \quad (2\text{-}4)$$

An atomic balance for nitrogen can be written as:

$$[NO]_{in} + [NO_2]_{in} = [NO]_{out} + [NO_2]_{out} + 2[N_2O]_{out} + 2[N_2]_{out} \quad (2\text{-}5)$$

or

$$([NO]_{in} + [NO_2]_{in}) - ([NO]_{out} + [NO_2]_{out}) = 2[N_2]_{out} + 2[N_2O]_{out} \quad (2\text{-}6)$$

Therefore,

$$\left(\frac{[NO_x]_{in} - [NO_x]_{out}}{[NO_x]_{in}}\right) = \left(\frac{2[N_2]_{out} + 2[N_2O]_{out}}{[NO]_{in} + [NO_2]_{in}}\right) \quad (2\text{-}7)$$

As a result, in the above definition a part of NO which is converted to N_2O is also considered in NO_x conversion. In addition, some of the NO converts to NO_2 as a result of a secondary oxidation of undecomposed NO down stream of the reactor at room temperatures (Li and Hall 1991). Therefore, this is not also a true indication of the degree of the NO decomposition to N_2.

Among all conversion measurements described, the only true indication of NO decomposition into N_2 is X_{NO} calculated by Equation (2-1).

2.5.4.1. Direct Decomposition of NO over ZSM-5 Zeolites

Direct decomposition of NO into molecular nitrogen and oxygen over many catalysts has been studied extensively. However, the reaction rate over the catalysts is very slow. After Iwamoto's discovery (1986a), many researchers have focused on the

decomposition of NO using zeolites, especially Cu-ZSM-5 zeolites. Since then, the most active catalyst has remained to be Cu-ZSM-5. However, the reaction over this catalyst is too slow for practical use. It is believed that the activity of the catalyst can be improved by 1-2 orders of magnitude (Shelef, 1995).

The dependence of catalytic activity on variables such as reaction temperature, oxygen partial pressure, contact time, exchange level of copper ions, coexistence of different ions with copper, and the effect of operating time has been investigated for the direct decomposition of NO.

2.5.4.1.1 Effect of Reaction Temperature

Reaction temperature is one of the important factors affecting the catalytic activity of the catalysts. The temperature dependency of NO decomposition over copper exchanged ZSM-5 zeolites was investigated by Iwamoto et al. (1986a, 1989, 1991a) and Zhang and Flytzani-Stephanopoulos (1994) over different samples and under different conditions. Hereafter, the catalysts are identified using the following method: cation-type of zeolite-silica to alumina molar ratio- Cu exchange level (%). For example, Cu-ZSM-5-50-73 can be interpreted as Cu ion-exchanged ZSM-5 with SiO_2/Al_2O_3 ratio of 50 and Cu ion-exchange level of 73%. The existence of a cocation such as Mg is shown as Mg(a)-Cu(b)-ZSM-5-50 which indicates that Mg ion-exchange level is (a) and Cu ion-exchange level is (b).

Experiments examining the temperature dependence of catalytic activity were carried out by Iwamoto et al. (1986a, 1989) over Cu-ZSM-5-50-73 and Cu-ZSM-5-23.3-143 respectively, and by Zhang and Flytzani-Stephanopoulos (1994) over Cu-ZSM-5-40-72. All experiments were performed in fixed-bed reactors. The contact times (the amount of catalyst per total gas flow rate) and the NO concentrations in the inlet gas were 4 g s ml^{-1} and 4.0% NO in helium; 4 g s ml^{-1} and 1% NO; and 1 g s ml^{-1} and 2% NO over the three above mentioned catalysts respectively. Under these conditions, the maximum NO conversions into N_2 achieved over the three catalysts were 80%, 90%, and 65% respectively.

Figure 2.4 shows the conversion of NO and the conversion of NO into N_2 and into O_2 over Cu-ZSM-5-23.3-143 as a function of temperature. The conversion of NO was very low at low temperatures and started to increase at 350 °C. The maximum activity was observed at 450-550 °C and then decreased with a further increase in the temperature. A similar trend for NO conversion as a function of temperature was reported by Zhang and Flytzani-Stephanopoulos (1994) and the maximum NO conversion was obtained at 450 °C. According to Iwamoto et al. (1989), the percentage conversions of NO and NO into N_2 were not equal but the difference between the NO conversion and the NO conversion to N_2 were equal to the difference between the NO conversion to N_2 and the NO conversion into O_2. This revealed that after the following reaction:

$$2NO \rightleftharpoons N_2 + O_2 \qquad \text{(R2-10)}$$

some part of O_2 produced reacted with unreacted NO to produce NO_2.

$$2NO + O_2 \rightleftharpoons NO_2 \qquad \text{(R2-11)}$$

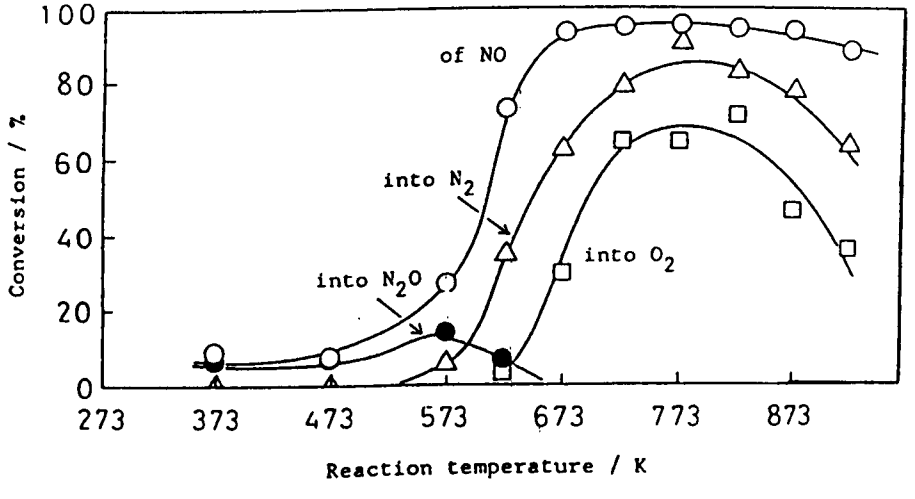

Figure 2.4. The dependence of NO conversion (O) into N_2 (Δ) O_2 (□) and N_2O (●) on temperature over Cu-ZSM-5-23.3-143 with a contact time of 4.0 g s ml^{-1} and P_{NO} = 1.0% (reproduced from Iwamoto et al., 1989).

The percentage conversion of NO into N_2O was also measured at various temperatures by Iwamoto et al. (1989). At low temperatures, a small amount of N_2O was produced and the maximum amount was observed at 300 °C (~15%) and then decreased. It seems that N_2O is one of the intermediate products during the NO decomposition. The decomposition of N_2O might be faster than that of NO at higher temperatures because at temperatures above 400 °C no N_2O was detected.

2.5.4.1.2 Effect of Oxygen

The effect of the addition of oxygen was investigated by Iwamoto et al. (1991a), who reported that conversion of NO over Cu-ZSM-5 decreased by adding oxygen into the feed. They used Cu-ZSM-5-23.3-89 and Cu-ZSM-5-23.3-122 catalysts with and without the presence of oxygen for the direct decomposition of NO. Figure 2.5 shows the result of this investigation. It seems that the conversion of NO has been considered, which is different from conversion of NO into N_2 as some parts of NO may convert to NO_2.

According to Figure 2.5, the activity of the catalyst was slightly reduced by the presence of oxygen in the feed when the copper exchange level was higher than 100%, and significantly decreased when the copper exchange-level was less than 100%. It seems that in addition to ion-exchange level, the partial pressure of O_2 to that of NO also affects NO conversion. However, there is no data available for NO conversion over ZSM-5 zeolite samples with the same ion-exchange level but different P_{O2}/P_{NO} to judge the trend of this effect.

To compare the effect of the presence of O_2, the results reported by Iwamoto et al. (1991a) are shown in Table 2.1. The first and the second rows of the table were taken from Figure 2.5, and the third was expressed to explain that the conversion level was also a function of O_2 partial pressure to NO partial pressure (P_{O2}/P_{NO}). It seems that the higher P_{O2}/P_{NO} ratio, the less inhibition effect on the activity of the catalyst. However, a more reliable comparison could be made if different NO conversions

were achieved over two samples with the same ion-exchange level but different P_{O2}/P_{NO} ratios.

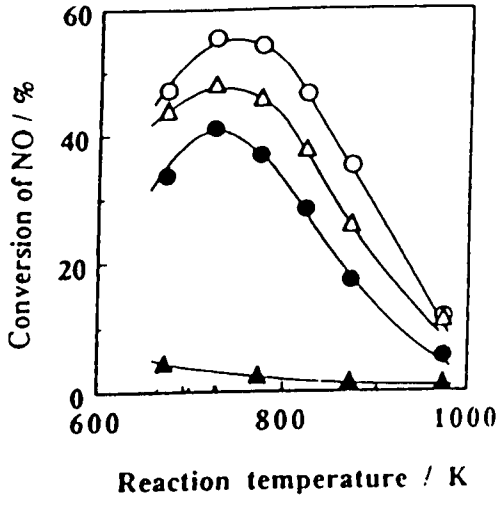

Figure 2.5. Influence of oxygen on the decomposition activities of Cu-ZSM-5-23.3-122 (●,O) and 89 (▲,Δ) catalysts at 1.0 g s ml^{-1} (●) P_{O2} = 8%, P_{NO} = 0.47% (▲) P_{O2} = 3%, P_{NO} = 0.50% (O, Δ) P_{O2} = 0%, P_{NO} = 0.51% (Iwamoto et al., 1991a).

Table 2.1. The results reported by Iwamoto et al. (1991a) on the effect of oxygen on the direct decomposition of NO.

Temp. °C	Ion-Exchange level	P_{O2}/P_{NO}	NO Conversion, % in the Absence of O_2	NO Conversion, % in the Presence of O_2
480	89	3/ 0.5=6	47	5
480	122	8/ 0.47=20	55	40
500	152	0.5/ 0.1=5	23	5

Li and Hall (1990) also reported that adding oxygen decreased NO conversion. They achieved 97% NO conversion at 500 °C without adding oxygen to the feed over Cu-

ZSM-5-12-140. This conversion is reduced to 80% after adding 10% O_2 into the feed for 1 hour at the same temperature. The catalyst was not poisoned because the conversion reached to 97% again 30 minutes after elimination of oxygen in the feed.

More research is still required to investigate the effect of oxygen on NO conversion, especially for low concentrations of NO. This is because, for practical operation, a very high conversion of NO should be achieved over a catalyst in the presence of a high percentage of O_2 for very low concentrations of NO, as low as a few hundred parts per million (Shelef, 1995).

2.5.4.1.3 Effect of Contact Time

Contact time is defined as the ratio of catalyst weight (W) to total flow rate of the gas (F) which passes through the rector. The effect of contact time on NO conversion was investigated at 480 °C by Iwamoto and Hamada (1991). The conversion of NO was reported to be 40-60% at 0.2 g s ml^{-1} and 13-25% at 0.025 g s ml^{-1}. These results indicate that the catalytic activity decreases when contact time decreases. In addition, this experiment confirmed that at a contact time as low as 0.025 g s ml^{-1}, Cu-ZM-5 zeolites are active for catalytic decomposition of NO. Li and Hall (1991) also showed that the catalytic activity is directly proportional to the contact time. In the experiments they conducted for this purpose, the conversion was kept at less than 10% to ensure that the reaction rate was not controlled by diffusion.

2.5.3.1.4 Effect of Ion-Exchange Level

Iwamoto et al. (1989) investigated the dependence of the catalytic activity of Cu-ZSM-5 on the copper ion-exchange level. They reported that the catalytic activity of the Cu-ZSM-5 zeolites increased with increasing copper ion-exchange level. 100% ion-exchange occurs when one copper (II) ion is exchanged with every two sodium ions. Excess copper loading (above 100%) on the ZSM-5 zeolite was achieved by

repetition of the ion exchange procedure using new copper (II) acetate solutions. The catalytic activities of the resulting Cu-ZSM-5 zeolites were very high for direct decomposition of NO, and increased with the increasing ion-exchange level.

Figure 2.6 shows the correlation between copper ion-exchange level and the conversion of NO and into N_2 and O_2. Catalysts with different ion-exchange levels were prepared from ZSM-5 zeolites with silica to alumina ratio of 23.3. In each run of the experiment, one gram of each catalyst was used in a fixed-bed flow reactor and the reactant gas used contained 1.0 %vol of NO and 99.0% of helium with a flow rate of 15 ml min^{-1}.

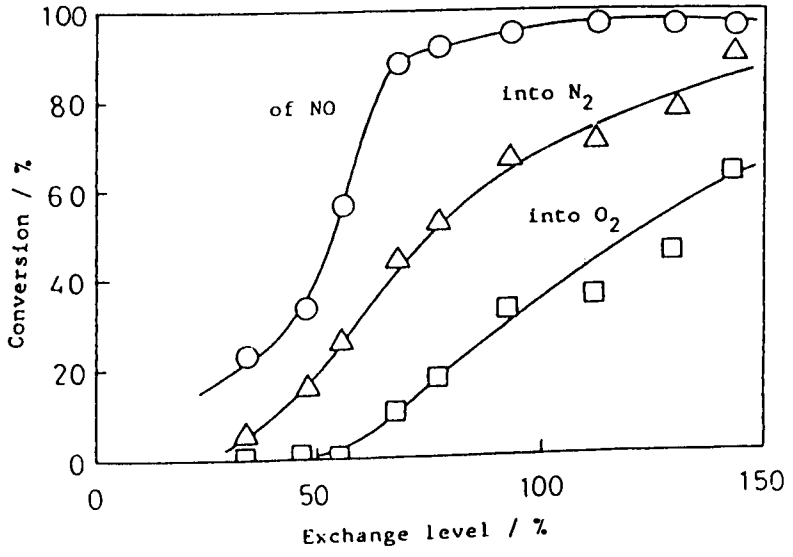

Figure 2.6. Conversions (%) of NO decomposition and NO into N_2 and O_2 as a function of exchange level obtained over Cu-ZSM-5-23.3 at 723 K, W/F = 4.0 g s ml^{-1} and P_{NO} = 1.0% (reproduced from Iwamoto et al., 1989).

The results obtained showed that the total conversion of NO as a function of ion exchange level was S-shaped. Also, the decomposition rate was very small at low copper ion-exchange level, but increased rapidly above 50% copper ion-exchange level. The maximum NO conversion was more than 95%. The N_2 formed was less than the expected amount from the decomposed NO, and O_2 was even less than N_2. It

was an interesting point that the difference between the amount of NO consumed and N_2 generated was approximately equal to that between N_2 and O_2 formed. This suggested that the NO is mainly converted to N_2 and O_2 but a small amount of NO and O_2 could be consumed in the formation of NO_2. The next interesting phenomenon was that no deterioration of the catalytic activity was observed after 30 hours.

Iwamoto et al. (1989) considered two interpretations for explaining the interaction between catalytic activity and the exchange level of copper ions. In the first interpretation, the possibility of the existence of two or more kinds of copper sites in ZSM-5 involved in NO decomposition reaction was considered. These copper sites could be Cu^+, Cu^{2+} and Cu_2O that each of which could play different roles in the chemical reaction. In the second, it was postulated that the reaction may take place over two adjacent active sites and therefore two nitrogen atoms can join together to make N_2. However, there is no convincing evidence for either possibilities at this stage.

2.5.4.1.5 Effects of Cocations

Incorporation of a cocation with Cu ion in ZSM-5 zeolites affects the catalytic activity for direct decomposition of NO in O_2-free or O_2-containing gas streams. Kagawa et al. (1991) reported that the coexistence of alkaline earth and transitional metal cocations with Cu ions promoted the catalytic activity of Cu-ZSM-5 zeolites at temperatures above 450 °C. At 550 °C and at a constant ion-exchange level of Cu, a strong cocation effect was observed, and the catalytic activity of the catalyst was enhanced by many different cocations. The only exceptions were Fe, Cr and alkali metals which did not show any effect.

Zhang and Flytzani-Stephanopoulos (1994) also investigated the effect of alkaline earth and transition metals ions on the catalytic activity of Cu ions in ZSM-5 in the presence of oxygen and rare earth metals in both oxygen-free and oxygen-containing

gases. They reported that the coexistence of Mg ions with copper promoted the catalytic activity of the ZSM-5 in the absence of O_2. For example, higher conversions of NO were obtained by using Mg(52)-Cu(66)-ZSM-5-39 than using Cu-ZSM-5-40-72 at temperatures above 450 °C. This effect was more pronounced for coexistence of Mg with Cu exchange levels less than 110%. The results indicated that the effect of cocation was not sensitive to the type of cocation chosen, and was almost independent of the type of cocation. They also used Sr, Pd and Ni as cocations with Cu to investigate the effect of these cocations on the catalytic activity of Cu-ZSM-5 zeolite. For example, Mg(34)-Cu(86)-ZSM-5-34, Sr(39)-Cu(105)-ZSM-5-42, Pd(88)-Cu(90)-ZSM-5-42 and Ni(-)-Cu(96)-ZSM-5-42 showed roughly equal catalytic activity in O_2-free gas streams. Cerium (Ce) and lanthanum (La) were also reported to promote the performance of the copper ion activity.

Zhang and Flytzani-Stephanopoulos (1994) also showed that the mode of ion-exchange and preparation method play important roles in the activity of ZSM-5 zeolite-supported catalysts. Their results showed that a high exchange level of Mg^{2+} could not be obtained when Na^+ in ZSM-5 was first ion-exchanged with copper ions and then by magnesium ions, or even when Na^+ was exchanged with copper and magnesium ions simultaneously. Therefore, the zeolite should be ion-exchange with cocation first and then with copper ions. In addition, some loss of Mg^{2+} in the solution was detected during Cu^{2+} ion-exchange which could be due to more favourable exchange equilibrium between Cu^{2+} and Na^+ ions. Furthermore, a higher exchange level and better stability was obtained when Mg^{2+} solution was heated during the Mg ion-exchange.

Zhang and Flytzani-Stephanopoulos (1994) also reported that air calcination of the Mg ion-exchanged ZSM-5 zeolites was effective in keeping the magnesium ions in the zeolite framework even after the copper ion-exchange. For example, 10% more conversion of NO into N_2 was achieved over calcined Mg(34)-Cu(86)-ZSM-5-34 (at 500 °C for two hours after ion-exchange with Mg ions) than non-calcined Mg(40.4)-Cu(91.2)-ZSM-5-38 over the whole range of temperatures investigated (350-600 °C).

Further studies are required to understand the effect of the coexistence of rare earth ions with copper in ZSM-5 zeolites. These studies may lead to distinguishing a catalyst with a high performance for the direct decomposition of NO to N_2.

2.5.4.1.6 Effect of Catalyst Preparation Methods

Very similar techniques have been utilised by different authors to prepare catalysts. The Na^+ or H^+ form of ZSM-5 zeolites with different Si/Al ratios are the predominant starting materials for preparation of catalysts. Copper acetate or copper nitrate solutions with different (low) concentrations are used in Cu^{2+} ion-exchange. The solutions are usually stirred during the ion-exchange procedures to improve ion-exchange levels. Then the slurries are filtered, and washed with water or deionised water. Resulting cakes are dried at different temperatures for various times.

Table 2.2 shows some of the ion-exchange details used by different researchers. It may be noted that, apart from Si/Al ratios and concentrations of ion-exchange solution, temperature and exchange time as well as the subsequent drying method can also influence the ion-exchange level and catalytic activity.

The effect of the concentrations of copper acetate solution on copper ion-exchange level is shown in Table 2.2 using the data presented by Li and Hall (1990). In the first and the second row of their data, the concentration of copper acetate was varied while the other parameters were kept constant. It is shown that an increase in the concentration of copper acetate from 25 to 50 mmol l^{-1} resulted in an increase in the ion-exchange level from 76% to 166%. A comparison between the second and third rows of the same data indicates that, in spite of increasing ion-exchange time and repetition of ion-exchange procedure, the ion-exchange level decreased with decreasing the Si/Al ratio. This is true if it is assumed that the difference between the drying temperatures (80 and 25 °C) did not affect the ion-exchange level.

Table 2.2. Ion-exchange details used by different researchers

Author	Si/Al Ratio	Conc. of Cu.Ac. mmol l^{-1}	Exchange Temperature °C	Exchange time hours	No. of ion-exchange	Drying temperature °C	Drying time hours	Cu ion-exchange level	Cocation	Cocation ion-exchange level
Iwamoto et al. (1989)*	23.3 "	10-11 "	25 "	" "	Several "	110 "	Over night "	143 112	- -	- -
Li and Hall (1990)**	24.2 26.4 12.3	25 50 50	25 25 25	16 16 123	1 1 2	80 80 25	not available	76 166 140	- - -	- - -
Zhang Flytzani-Stephanopoulos (1994)***	20.5 19.9 18.0 17.1 19.5 20.8 20.8 20.7 19.5 19.4	7 " " " " " " " " "	85 or room " " " " " " " " "	2 or 10 " " " " " " " " "	thrice once twice " " " " " " "	100 " " " " " " " " "	10 " " " " " " " " "	141 72 91 86 66 96 105 90 119 123	- - Mg Mg Mg Ni Sr Pd Ce La	- - 40 34 52 - 39 88 11 18

* The Zeolite was washed with dilute $NaNO_3$ solution and then ion-exchanged. It was then washed with water and dried.
** After the ion-exchanges the catalysts were washed twice, with stirring, in water for two hours.
*** After drying the catalysts were calcined at 500 °C for two hours.

The type of copper salt used for the ion-exchange also has a significant effect on catalytic activity of a catalyst, because each type of copper salt solution has a specific pH. In a typical experiment, Wichterlova et al., (1995) examined the activity of two ZSM-5 zeolite samples ion-exchanged with copper acetate and copper chloride solutions. They pointed out that the Cu sites characterised by the Cu^{+} luminescence at 540 nm were active in NO decomposition and a higher number of these sites were identified of the sample ion-exchanged using copper acetate solution than the one ion-exchanged using copper chloride solution. The reason for this observation is that higher pH of the copper acetate solutions result in the formation of $(Cu^{2+}\text{-}OH)^{+}$ species, which are then converted to Cu^{+}. Although these two samples contained nearly equal amounts of Cu, the NO conversion achieved over the first sample was much higher than the second, indicating that different Cu sites had different activities for NO decomposition.

In catalysts containing copper and a cocation, the ZSM-5 zeolites are usually first exchanged with a dilute cocation solution in nitrate form and then ion-exchanged with dilute copper acetate solution. This may be repeated several times, depending on the desired amount of ion-exchange levels.

Ion-exchange levels greater than 100% have been reported in the ion-exchange system of $CuCl_2$ + acetic acid solution and a Y-type zeolite by Schoonheydt et al. (1976). Iwamoto et al. (1989) then prepared copper ion-exchanged ZSM-5 zeolites with ion-exchange level greater than 100%. They reported that it was impossible to prepare excessive copper ion-exchanged ZSM-5 zeolite with copper (II) nitrate or sulfate solutions. They repeated the ion exchange procedure three or more times and obtained excess loading of copper ions on ZSM-5 but only when copper acetate solution was used.

To avoid repetition of ion-exchange procedure, Iwamoto et al. (1990) on the other hand suggested that a catalyst with a high exchange level could be prepared in one step by adding a basic compound such as NH_4OH or $Mg(OH)_2$ into the mother copper solution. They reported that about 15 grams of ZSM-5 with Si/Al ratio of 23.3 was washed in 2 litres of dilute $NaNO_3$ solution, and stirred for 24 hours in 1 litre of

aqueous $Cu(NO_3)_2$ solution with concentration of 12 mmol l^{-1}. Then an aqueous basic solution was progressively added to the solution until the pH value of the solution increased to a desired value. After filtration, the resulting cake was dried for 24 hours at room temperature in vacuo. The best results were obtained using ammonia solution (0.3 mol l^{-1}) as a basic additive until the pH of the solution increased to 7.5. The maximum NO conversion of 48.45% which was achieved at the maximum ion-exchange level (148%).

2.5.4.1.7 Decay of Catalytic Activity

The conversion of NO as a function of operation time at 500 °C over Cu-ZSM-5-26-166 catalyst was presented by Li and Hall (1990). As Figure 2.7 shows, initially the activity increased slightly with operation time. The conversion of NO was about 90%, and the conversions into N_2 and O_2 were about 60% and 20%, respectively. They confirmed the results presented by Iwamoto et al. (1986b) shown as lines in Figure 2.7. The results indicate that the performance of the catalysts remained constant after 24 hours of operation.

The effect of addition of sulfur dioxide on the direct decomposition and SCR of NO by hydrocarbons was investigated by Iwamoto et al. (1991b). The decomposition of NO into N_2 was completely diminished when sulfur dioxide was introduced into the inlet gas stream. This deactivation was reversible and could be restored upon exposing the catalyst to a helium stream at 973 K.

2.5.4.1.8 Proposed Mechanisms of Direct Decomposition of NO

Iwamoto and Hamada (1991) proposed the following mechanism for NO decomposition:

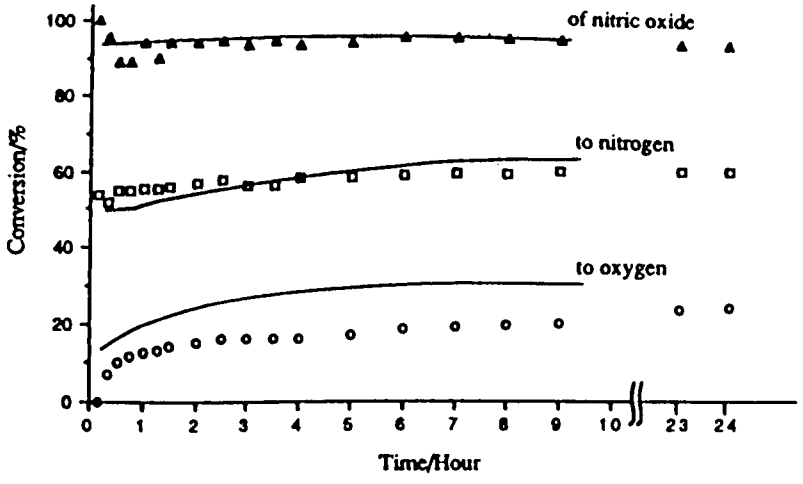

Figure 2.7. Conversions of NO decomposition as a function of time over Cu-ZSM-5-26-166 at 773 K using a mixture of 4% NO in helium and a contact time of 2 second (reproduced from Li and Hall, 1990). Li and Hall used the lines to compare their results with Iwamoto et al. results. The lines were obtained on the Cu-ZSM-5-25-54 at the same temperature and a contact time of 8 seconds by Iwamoto et al. (1986b). [According to a private communication with W. K. Hall, they assumed that the bulk density was 0.5 g ml^{-1} and the contact time was defined as a ratio of catalyst volume to the gas flow rate (catalyst volume, ml/gas flow rate, ml s^{-1})].

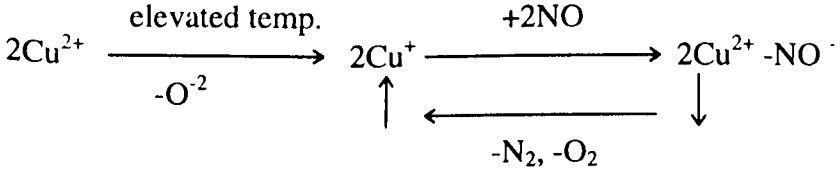

In the first step of this mechanism, a pair of cubic ions are reduced to supply a pair of cuprous ions due to the electrons the O^{2-} had left behind. Then a pair of NO is adsorbed on the two cuprous ions to produce an adsorbed pair of anions on copper sites. The pair of anions decomposes into oxygen and nitrogen molecules, regenerating the cuprous ions site.

The evidence given for this mechanism relies on spectroscopic studies such as infra red (IR) spectra of NO chemisorption on Cu-ZSM-5 at room temperature. However, there are a number of questions about the above mechanism, e.g. how do two oxygen atoms come together to make an oxygen molecule? The same question can be posed for nitrogen. As far as the mechanism tells us, two active sites are required for chemisorption of NO. These active sites have to be close to each other, which is unlikely in the case of high silica zeolites.

Shelef (1992) proposed another mechanism for NO decomposition over Cu-ZSM-5 zeolites. He believed that the active sites consist of coordinatively unsaturated cupric ions in square planar configurations. The chemisorption of NO molecules occurs in the gem-dinitrosyl form, $(NO)_2^-$. It is necessary to mention that two types of Cu cations are known, a four-coordinated square planar and a five coordinated. Shelef believes that only the square planar sites are adequate for the gem-dinitrosyl adsorption. Then, the complex on one active site decomposes and desorbs an oxygen and a nitrogen molecule. As Shelef postulates, this mechanism is not involved in any redox cycle on the surface of the zeolite. This is unlikely that a redox cycle is being involved especially when there is no reducing species in the gas phase.

The kinetics of the catalytic decomposition of NO over Cu-ZSM-5 zeolite was also studied by Li and Hall (1991). This study reported that a redox mechanism is involved. They assume that a small fraction of reduced sites is available in the steady state. NO reacts with reduced form of the active sites and converts them to the oxidised form by chemisorption. These sites are then reduced by releasing O_2 produced by NO decomposition. The following reaction rate proposed by Li and Hall was consistent with their experimental results:

$$r = \frac{d[N_2]}{dt} = \frac{k[NO]}{1 + K[O_2]^{1/2}} \qquad (2\text{-}8)$$

where:

r = reaction rate, [s^{-1} site $^{-1}$],

k = the rate constant, [l s^{-1} site $^{-1}$ mol^{-1}],

K = the equilibrium constant for O_2 adsorption on the catalytic sites, [$l^{+1/2}$ $mol^{-1/2}$],

[NO] = NO concentrations in terms of [mol lit^{-1}], and

[O_2] = O_2 concentrations in terms of [mol lit^{-1}].

On the other hand, Hall and Valyon (1992) published a paper opposing Shelef's idea but supporting the mechanism proposed by Li and Hall (1991). They also deduced that NO decomposition is a redox process. They believe that the most abundant surface intermediates are O atoms which are not desorbed easily below approximately 623 K. The desorption of O_2 at higher temperatures provide a small fraction of reduced active sites. The limiting step of the reaction mechanism is supposed to be the rate of reoxidation of the oxygen vacancies by NO and by the O_2 desorption. A gem-dinitrosyl species is suggested to be the intermediate for the formation of N-N bound.

2.5.4.2 Selective Catalytic Reduction (SCR) of NO

Another approach to the control of the exhaust emission of NO is selective catalytic reduction (Iwamoto and Hamada, 1991; Jen and Gandhi, 1994; Kharas et al., 1994; Nishizaka and Misono, 1993; Yogo et al., 1993). In this case, NO reacts with a reductant over a catalyst. The reductants may be classified in two groups, N-free reductants such as CO and hydrocarbons, and N-containing reductants such as NH_3.

In SCR, the selectivity of a catalyst which is defined as the ratio of the amount of hydrocarbon participated in a useful reaction (the reduction of NO) to the total hydrocarbon consumption is extremely important. It is obvious that several selectivities are involved in the SCR processes. A hydrocarbon reductant can have a positive role, to react with NO, or a parasitic role, to combust with oxygen. Therefore, a hydrocarbon as a reductant is involved in two major selectivities between the two reactions. In a complete reduction, N_2 is only N-containing product

whereas in an incomplete reduction, N_2O is also produced. In a complete oxidation, CO_2 is formed whereas in an incomplete oxidation CO is also produced.

2.5.4.2.1 Catalytic Reduction of NO using N-Containing Reductants

One of the major catalytic technologies for NO_x removal is selective catalytic reduction process by using a N-containing reductant such as ammonia (NH_3). This technology can be used to remove NO_x from exhaust gases containing a high oxygen concentration according to Reactions (R2-8) and (R2-9).

In a stationary installation, NH_3 is usually utilised as a reductant. According to Shelef (1995), noble metals are used as catalysts at temperatures lower than 300 °C and vanadia/titania catalysts for medium temperature range (< 425 °C). The selectivity of NH_3 has a major role because, a large amount of excess air is used for the combustion. In addition, the amount of available oxygen is much higher than the amount of NO_x. Several percent of oxygen is available in the effluent of a combustion chamber whereas only a few hundred parts per million (ppm), NO_x is produced. Therefore, a suitable reductant has to have a high selectivity for nitrogen oxides than oxygen. For this purpose, NH_3 which has its own nitrogen atom, can be used as a selective reductant for NO_x decomposition in order to pair nitrogen atoms of the reductant and of NO_x.

The availability and cost are two important factors for selection of a desired reductant in stationary sources application. Among N-containing reductants such as urea or cyanic acid, NH_3 is more readily available and easier to use however, there is a considerable price for this reductant. The cost aside, probable leakage and incomplete reaction of ammonia creates secondary environmental pollution. NH_3 has been used in stationary plants but not in motor vehicles, as carrying an ammonia tank can cause serious problems. Therefore the use of N-free reductants have been noticed for several decades and are still under investigation.

2.5.4.2.2 Catalytic Reduction of NO using N-Free Reductants

Various reductants, from methane to cetane which are present in diesel fuels, have been studied since Iwamoto's discovery. Several reductants were used to compare the activity of Cu-ZSM-5 or Co-ZSM-5 by Witzel et al. (1994). They reported that only molecules with cross sections smaller than 5.5 Å are suitable reductants, because they can diffuse into the intersectional cavities of the ZSM-5 framework.

Methane can be a desirable reductant. In the case of gas powered engines, methane is the main part of natural gas which is readily available and widely used as a fuel in many combustion engines. Therefore, methane is usually available in the effluent of these systems. A catalyst having a very high activity is required for the activation of methane because it is one of the least reactive hydrocarbons, but very active catalysts tend to combust methane, consuming oxygen rapidly thus leaving NO unreacted. Methane was classified into the non-selective reducing agents group for reduction of NO over Cu-ZSM-5 catalysts (Iwamoto and Hamada, 1991). On the other hand, effective reduction of NO_x using methane was reported by Li and Armor (1992) over cobalt ion-exchanged ZSM-5 zeolite. They published many papers on selective catalytic reduction of NO_x with methane over metal exchanged zeolites (Li and Armor, 1993) and other supports ion-exchanged with cobalt such as Co-Ferrierites (Li and Armor, 1994). They reported that Co^{2+}, Mn^{2+} and Ni^{2+} exchanged ZSM-5 and mordenite were active in an oxidising atmosphere. The NO reduction was increased with increasing temperatures up to 400-500 °C and then decreased. The reduction of NO over Co-ZSM-5 was also increased with the ion-exchange level of Co^{2+}, but excess exchange of Co^{2+} did not have effect on NO conversion.

Kinetic inhibition of NO reduction over Cu-ZSM-5 by adding water to the reactants was reported by Martinez et al. (1997). The activity of the catalyst could be slowly recovered after H_2O removal from the feed depending on the operating conditions. Irreversible deactivation was also observed after more than 15 hours water in the stream. The authors believed that neither structural changes or dealumination of the zeolite were responsible for the catalyst deactivation. Deactivation of Cu-ZSM-5 was

also reported at high temperatures (600-800 °C) after one hour of reaction of NO with hydrocarbons in the presence of 10% H_2O and under oxidising conditions by Kharas et al., (1993). Sintering of copper species to CuO and perhaps Cu_2O, were observed by XRD. A decrease in micropore volume and degradation of the crystalline zeolite were not considered as the main reason for catalyst deactivation. Sintering of the active component (Cu^{2+} or Cu^{+}) was reported to be responsible for this deactivation.

The effect of addition of sulfur dioxide on SCR of NO by propene was investigated by Iwamoto et al. (1991b). The extent of NO reduction was only slightly decreased when sulfur dioxide was added into the reaction system of NO, O_2, and C_3H_6. After 20 minutes the conversion had reached a steady-state. It is worth noting that even after 220 minutes, no deterioration of the catalytic activity of the catalyst was observed. For example, the conversion of NO into N_2 was decreased from 100% to 85% when sulfur dioxide was introduced to the inlet gas. The catalytic activity could be restored to the initial amount after ceasing the addition of sulfur dioxide to the gas stream.

Ga ion-exchanged zeolites were also reported to show very high selectivity using several hydrocarbons such as CH_4, C_2H_4, C_2H_6 or C_3H_6. CH_4 and C_2H_6 were reported by Yogo et al. (1993) to be very active and selective reductants of NO over Ga-ZSM-5-23-92 . They used either methane or ethane as a reducing agent in the presence of oxygen. The NO, O_2, CH_4 or C_2H_4 concentrations in the feed were 1000 ppm, 10% and 1000 ppm, respectively. 90% and 100% NO conversions were obtained at 500 °C using methane and ethane respectively. The catalyst weight was 0.5 g and the total flow rate was 100 ml min^{-1} (W/F = 0.3 g s ml^{-1}). They also reported that the molar ratios of reacted NO to consumed carbon in CH_4 and C_2H_6 were 2 and 1.5, respectively.

Similar research was carried out using methane as a reductant in the presence of oxygen by Nishizaka and Misono (1993). The NO, O_2 and CH_4 concentrations were 1000 ppm, 2% and 1000 ppm, respectively. The maximum conversion of NO to N_2 over Pd-Ce-H-ZSM-5 and Pd-H-ZSM-5 were approximately the same (70% at 480

°C). The catalyst weight and the total flow rate were 0.5 g and 150 ml min^{-1}, respectively (W/F = 0.2 g s ml^{-1}). This flow rate was 1.5 times of the flow rate used by Yogo et al. (1993). A comparison between these two researchers confirms a proportional relationship between contact time and catalytic activity. The lower the contact time, the lower the conversion of NO to N_2.

Yogo et al. (1992) investigated selective catalytic reduction of NO with propane using various ion-exchanged ZSM-5 zeolites in the presence of excess oxygen. They reported that Ga-ZSM-5-23.3-79 prepared by the ion-exchange of the ammonia form zeolite showed a high activity and selectivity for reduction of NO to N_2 in a wide range of temperature (300 -600 °C). The maximum conversion was 91.1% which occurred at 400 °C over 0.5 g catalyst using a gas mixture with a rate of 100 ml min^{-1}. The inlet gas contained 1000 ppm NO, 1000 ppm propane and 10% O_2. It seems that gallium exchanged-ZSM-5 zeolite is a candidate for practical applications. However, this research was carried out under laboratory conditions with a synthetic gas mixture. More practical investigation is required with real exhaust gases.

2.5.4.2.3 Effect of Silica to Alumina Ratio

The effect of Si/Al ratio and copper loading on SCR of NO with propene over Cu-ZSM-5 and copper ion-exchanged mordenite was investigated by Torre-Abreu et al. (1997a and 1997b respectively). The acid form of ZSM-5 zeolite was used to prepare Cu-ZSM-5 catalysts. The authors concluded that the influence of silica to alumina ratio on catalytic activity of Cu-ZSM-5 as well as Cu-mordenites for SCR of NO using propene depends on the copper content of the catalyst. Their experiment was conducted over 0.5 g of catalyst using a gas mixture consisting of 800 ppm NO, 800 ppm C_3H_6, 4% O_2, and balance helium at 15 l h^{-1} (250 ml min^{-1}) total flow rate.

In order to analyse the effect of Si/Al atomic ratio on SCR of NO, the authors tested a group of copper ion-exchanged ZSM-5 with the same copper loading, i.e. 1.4 wt. %, but with different Si/Al atomic ratios, i.e. 11, 27, 45 and 100. They observed that

maximum conversion was achieved over the zeolite with Si/Al atomic ratio of 27. Another group of catalysts with the same Si/Al ratios but different copper loading and copper exchange level were also tested. They reported that the catalytic activity of ZSM-5 catalysts increased sharply when the copper was introduced to the zeolite and increased up to 80% of ion-exchange level. However, no sample with ion-exchange level between 80 and 127 was tested. Therefore, it is not clear within ion-exchange levels of 80 to 127, what the trend would be.

They also tested two samples with different Si/Al ratios and copper loading, but the same copper ion-exchange level. It was shown that the catalysts had similar activity profiles for SCR of NO. However, this comparison was made only between two samples with Si/Al ratios of 11, 27 and therefore, more research is required to ensure the reliability of the conclusion.

2.5.4.2.4 Mechanisms of SCR

There is a great deal of debate on the mechanisms of SCR of nitric oxide by reducing agents in an oxidising atmosphere. A unique idea about the reduction mechanisms of NO has not been yet accepted by various researchers.

The mechanisms and the role of oxygen in the selective catalytic reduction of NO using propane over H-ZSM-5 and Cu-ZSM-5 were investigated by Sasaki et al. (1992). Two different mechanisms were considered. For H-ZSM-5, they proposed that NO is probably converted to NO_2 in the first step, followed by oxidation of propane by NO_2 to form a partially oxidised hydrocarbon intermediate which can reduce NO_x to N_2.

$$NO \xrightarrow{+O_2} NO_2 \xrightarrow{+C_3H_8} (C_xH_yO_z) \xrightarrow{+NO_x} N_2 + CO_x + H_2O \qquad \text{(R2-15)}$$

This catalyst has a high selectivity for NO reduction as confirmed by experiments. Low activity of H-ZSM-5 for propane oxidation in the absence of NO_x (1.5% conversion to CO and CO_2 at 573 K) and high activity in the presence of a small amount of NO_x justified this mechanism.

A different mechanism was proposed for reduction of NO over Cu-ZSM-5 (Sasaki et al., 1992). The activity of this catalyst was very high for propane oxidation in the absence of NO_x. Therefore, it was proposed that in the first step, the propane was to be partially oxidised over Cu-ZSM-5. The intermediate then reacts with NO (or NO_2) to form N_2.

$$C_3H_8 \longrightarrow (C_pH_qO_r) \xrightarrow{+NO\ (or\ NO_2)} N_2 + CO_x + H_2O \qquad \text{(R2-16)}$$

$$(C_pH_qO_r) \xrightarrow{+O^*} CO_x + H_2O$$

where O^* is an activated oxygen atom. According to this mechanism, a side reaction occurs over the transitional metal catalysts by the activated oxygen. Therefore, the selectivity of NO reduction is reduced.

Montreuil and Shelef (1992) investigated the reduction of NO using oxygen containing organic compounds. They deduced that oxygenated hydrocarbons as intermediates in the reduction of NO are responsible for high efficiency of the reaction. They also concluded that oxygenated hydrocarbons are intermediates in the case of $C_3H_8/NO/O_2$ reaction. Ansell et al. (1993) rejected the idea of the initial conversion of propene into an oxygenated hydrocarbons due to the activity of the catalyst in an oxygenate-NO-O_2 feed, has been always lower than that in a propene-NO-O_2 feed. They speculated that the oxygenated species, introduced by Montreuil and Shelef as reaction intermediates, may crack to form coke on the acidic zeolite sites.

Ansell et al. (1993) then proposed a different mechanism for the lean NO_x reaction over Cu-ZSM-5 using propene. They used temporal analysis of products (TAP) to

find reducing species involved in the formation of nitrogen. They concluded that two processes: nitric oxide activation and coke deposition are involved in the reaction mechanism. Cu-NO_2 species are formed on the exchanged copper sites by activation of NO_x with oxygen. The propene is converted to coke and the coke species are deposited on the catalyst surface whether oxygen is present or not. Then Cu-NO_2 species are reduced by the adjacent coke sites. It is relevant to note that the presence of oxygen increases the reduction. The reason for this is that oxygen promotes the formation of Cu-NO_2 species by activation of NO_x, which is a major step in the reaction mechanism.

However, Burch and Millington (1993) employed gas switching experiments, examining the first few minutes of reaction, to show that carbon deposition is not responsible for the conversion of NO into N_2. For this purpose, a mixture of NO, propene and oxygen in argon was flown through a packed bed tubular reactor. After flowing this mixture of gas in three runs of experiments (10 seconds, 10 minutes and 1 hour) propene was switched off. It was observed that the rate of NO conversion decreased to almost zero within a few seconds. In another set of experiments, propene was switched on to NO + O_2 inlet gas. The conversion of NO within two minutes reached to the steady state and within 30 seconds reached to 80% of conversion at steady state amount. From these observations, the authors concluded that the carbon deposition is not responsible for NO reduction on copper-based zeolites. If it was, NO conversion would have continued after propene was switched off, at least for a while. Furthermore, exposure of catalyst to the mixture of NO, O_2 and C_3H_6 at different times would have resulted in different amount of carbon deposition. Therefore, the reduction of NO would continue for different times to consume the deposited carbon. They suggested that a partially oxidised hydrocarbon intermediate is formed to reduce NO in the presence of a large amount of oxygen. The precise nature of the partially oxidised hydrocarbon intermediate however remains unanswered.

2.5.4.3 Experimental Techniques

Experimental techniques including facilities and instrumentation used by different researchers are reviewed in this section. Various facilities have been used to evaluate catalytic activities for NO decomposition. Table 2.3 shows some specifications of the experimental facilities which have been used by different researchers.

Zhang and Flytzani-Stephanopoulos (1994) used two different reactors for conversion measurements and kinetic studies. It is clear that overall reaction rate can be controlled by one of the following three steps: diffusion of reactants, reaction on the surface of the catalyst and diffusion of the products. They wanted to be sure that the overall reaction rates were not limited by the diffusion steps so they used a very small reactor for kinetic studies. The reason being, less amount of catalyst can be used in a smaller reactor and this leads to shorter contact time. Less contact time causes less conversion, so in the gas stream the concentration of the reactant is high and the concentration of the product is low. In this case the diffusion of the reactants and the products is fast and overall reaction rate is controlled by the reaction rate on the catalyst surface.

Li and Hall (1990) used a packed bed reactor with an expansion section as a catalyst bed. It seems that they used the expansion section to prevent the gas velocity increment. The gas flow velocity increases through a catalyst bed because of two reasons. The first reason is increasing the gas volume which is caused by the temperature increment. The second reason is catalyst void fraction which provides less cross section for the gas so that the velocity increases. However the disadvantage of this kind of reactor is that some part of catalyst may not be in contact with the gas.

There is not much information given about the analytical equipment which was used to analyse product gases because only some researchers described their instrumentation. Some researchers utilised only a NO_x analyser (Zhang and Agnew, 1995; Tanaka, 1997). It is worth noting that the only gases which can be analysed by this instruments are NO and NO_2. Therefore, the available information leads to obtain only NO or NO_x conversion. These do not indicate the NO conversion into N_2.

Table 2.3. Specification of facilities used by different researchers

Researcher	Reactor type	reactor diameter	reactor material	Catalyst weight g	Temp. measurement instrument
Iwamoto et al. (1991a)	flow reactor	-	stainless	1.0	-
Li and Hall (1991)	microcatalytic reactor with an expanded section 0.8-1.3 cm i.d. as a catalyst bed	0.4 cm i.d.	glass tube (pyrex)	few tenth of g to 1 g	Chromel-alumel thermocouple temp.controller
Zhang and Flytzani-Stephanopoulos+ (1994)	conversion measurement reactor microcatalytic reactor for kinetic studies	1.1 cm 0.4 cm	quartz tube "	0.5 to 1 g 30 to 35 mg	temperature-programmed furnace with temperature controller (Tetrahedron: model Wizard)
Zhang and Flytzani-Stephanopoulos (1995)	" " " "	1 .1 cm 0.4 cm	quartz tube "	0.5 to 1.5 g 20 to 50 mg	electricity furnace

+ Two reactors were used for conversion measurement and kinetic studies by Zhang and et al. (1994). Total gas pressure was 1.5 atm during conversion measurement and 2 atm in kinetic studies.

As it was discussed in section 2.4.4.1, in the case of using only NO_x analyser, it is preferred to calculate NO_x conversion rather than NO conversion because, the former is closer to NO conversion to N_2.

Most researchers employed gas chromatography techniques to determine the concentration of flue gases. The concentrations of O_2, N_2, N_2O, CO, CO_2 and hydrocarbons are usually measured by Gas Chromatographs. The concentration of NO was also reported to be measured by GC (Iwamoto et al., 1991a). They used a Gas Chromatograph equipped with two columns, a Porapak Q for N_2O and a 5A molecular sieve for N_2, O_2 and NO.

Some researchers employed NO-NO_x analyser as well as GC to measure the concentrations of NO and NO_2 (Zhang and Flytzani-Stephanopoulos, 1994). Gopalakrishnan et al. (1994) besides the GC and NO-NO_x analyser, employed a NH_3 gas analyser and an Allen CO/HC infra-red analyser to measure NO, NH_3, CO, CO_2, N_2O and N_2 concentrations. Li and Hall (1991) used a mass spectrometer to measure NO_2 quantity.

2.5.4.4 Theoretical Analysis and Modelling

A few papers have been published on the theoretical analysis and modelling of the reaction rate of NO decomposition. In a heterogenous reaction, turnover frequency is usually calculated and considered as a value for reaction rate. The turnover frequency of NO decomposition is expressed as twice the number of N_2 molecules produce from NO decomposition per Cu ion per second. In this definition, the total NO conversion can not be used because some part of NO may be oxidised to NO_2 instead of decomposition to N_2.

For kinetic studies, the conversion of NO to N_2 has to be kept low to ensure that the reaction rate is controlled by chemical reaction but not by diffusion steps.

2.5.4.4.1 Kinetic Analysis and Rate Law

Turnover frequency is an indication of the activity of each site involved in a heterogenous reaction. Li and Hall (1991) investigated the dependence of the NO decomposition rate on the partial pressure of NO and O_2 over Cu-ZSM-5-26-166 over a temperature range of 350-550 °C. They kept the NO conversion below 10% to make sure that the reaction rate is controlled by reaction step but not by diffusion. The power rate law was assumed to determine the reaction order.

$$r = k\,[NO]^n\,[O_2]^m \qquad (2\text{-}9)$$

Where: [NO] is the concentration of NO in feed, $[O_2]$ is the concentration of O_2 in feed (when O_2 is added), n is the reaction order in NO and m is the reaction order in O_2.

Li and Hall (1991) reported that the NO decomposition was close to the first order in NO concentration (between 0.9 to 1.1) over the above range of temperature when NO concentrations varied from 1 to 4%. The reaction order for O_2 was reported to be negative and its values were different depending on temperatures at which the catalyst was tested. This dependency was less sensitive at higher temperatures. The O_2 concentration range was between 0.5 to 1 % in the test. The rate equation for NO decomposition reaction over Cu-ZSM-5-26-166 was deduced as expressed in Equation (2-8).

The rate constants (k) and the equilibrium constants (K) resulted from their experiments are detailed in Table 2.4.

2.5.4.4.2 Mathematical Modelling

Two types of mathematical models have been used to simulate a chemical reactor performance for reduction of NO (Lionta et al., 1996):

Table 2.4. Rate and equilibrium constants reported by Li and Hall (1991) used in Equation 2-10.

T, K	k, [l s^{-1} $site^{-1}$ mol^{-1}]	K, [$l^{1/2}$ $mol^{-1/2}$]
623	0.95	-
673	1.91	-
723	5.03	157.5
773	7.58	84.2
823	7.43	53.0

- Developing an analytical expression for NO concentration along the reactor,
- using Numerical techniques to find the reaction rate.

In the first model, usually a first order reaction rate is assumed for use in the mass and energy balance equations. Then the equations can be solved analytically.

Lionta et al. (1996) considered a pseudohomogeneous model in the development of their mathematical modeling of a fixed-bed reactor. They solved the problem using numerical techniques for isothermal and non-isothermal operation of the reactor. Two partial differential equations, the mass and the energy balance, were considered for the reactive gases: The only independent variable considered in both equations was the axial distance. Besides of experimental data achieved over Pt/alumina, they also utilised the experimental data of Li and Armor (1993) over Co-ZSM-5 and Mn-ZSM-5 to validate their model. NO reduction rate by using propene was independent of propene concentration and was expressed as follows:

$$r = \rho_b k[NO]^{0.375} \qquad (2\text{-}10)$$

where ρ_b is the apparent density of the catalyst (0.5 g ml^{-1}) and k is the reaction rate constant. They also predicted the following expression for propene oxidation rate:

$$r_{ox} = \rho_b k_{ox} \exp(-E_{ox} / RT)[HC][NO] \quad (2\text{-}11)$$

where, r_{ox} is the propene oxidation rate, k_{ox} is the frequency factor, E_{ox} is the apparent activation energy, T is the reaction temperature, [HC] is the propene concentration and [NO] is the NO concentration. The apparent activation energy was also estimated to be 13740, 10500 and 10500 cal $mole^{-1}$ for Pt/alumina, Co-ZSM-5 and Mn-ZSM-5, respectively. The experimental data and simulation data were in agreement.

The authors referred to another paper, (Buzanowski and Yang, 1990) who used this approach to simulate catalytic reduction of NO with NH_3. Buzanowski and Yang (1990) developed a model to derive analytic solution for a monolithic honeycomb reactor with two different types of catalyst. They obtained the overall NO conversion as a function of space velocity and other parameters. NO concentration profile within the honeycomb walls and the effectiveness factor were also expressed, which is useful for optimum catalyst design.

If the reaction rate is complex, the second model is more feasible to simulate the reactor performance. Tronconi et al. (1992) used this approach to simulate the performance of the reactor by employing numerical approximations. The reaction rate expression was considered in a radial coordinate system.

2.6 Conclusions from Literature Review

NO_x emission from combustion engines is one of the major worldwide environmental concerns. Two major techniques are currently employed to control this emission:

- Catalytic reduction of NO_x with ammonia, applicable only in stationary sources, but not in automotive engines because of ammonia "slip" and the problems in transportation of ammonia within residential areas.

- TWC technology which is currently employed to control the NO_x emission from mobile sources. This technology can not meet requirements of lean-burn gasoline engines and diesel engines which work under oxidising atmospheres.

Therefore, the decomposition or reduction of NO in the presence of oxygen over a solid catalyst is a dominant target. Various catalysts were examined and finally led to transitional metals ion-exchanged ZSM-5 zeolite supported-catalysts, especially Cu-ZSM-5 which shows high and stable steady-state activity for direct decomposition of NO to N_2 and selective catalytic reduction of NO by hydrocarbons.

It is generally accepted that the nature of a catalyst and conditions of the reaction influence the reaction rate. Many researchers examined different combinations of cations with ZSM-5 zeolites and under different conditions. Therefore, a large body of literature is available however, many problems remain to be solved.

1. Reaction temperature plays a major role in NO decomposition over ZSM-5 zeolite-supported catalysts. The reaction rate of the decomposition of NO into N_2 and O_2 and also the reduction of NO into N_2 increase with increasing temperature, passing through a maximum. The maximum NO conversion usually occurs at temperatures ranging 400-600 °C, depending on the reaction conditions and the nature of catalyst (e.g. type and level of cation ion-exchanged). This also depends on the type and concentration of reductant in the case of SCR. Cu-ZSM-5 zeolite is a stable and an active catalyst for NO decomposition. It is also stable and active for reduction of NO but, the selectivity of the reductant plays a key role in catalytic reduction of NO. The temperature window for decomposition and the reduction of NO is relatively narrow for practical use. Different cations and also various combinations of cations have been tried in order to find a stable catalyst with high activity working in a wide range of temperatures. In both cases, the direct decomposition and SCR of NO, modification of the catalyst is required in order to obtain an active catalyst in a wider range of temperature.

2. It is believed that the role of catalyst selectivity in SCR of NO is crucial. Therefore, a significant effort has been made to introduce a selective catalyst for reduction of NO. Cu-ZSM-5 has been introduced as a selective catalyst for NO reduction using reductants such as C_2H_4, C_3H_6 and C_3H_8 but not as a selective catalyst in the presence of other reductants such as H_2, CO, CH_4 and C_2H_6. On the other hand, the reductants with no selectivity over Cu-ZSM-5 may show selectivity over another catalyst. For example, CH_4 reacts with NO selectively over Co-ZSM-5 and Ga-ZSM-5 whereas methane has been known as non-selective reductant for NO conversion into N_2 over Cu-ZSM-5 zeolites.

3. The presence of O_2 inhibits the NO decomposition over cation exchanged ZSM-5 zeolite-supported catalysts but the inhibition decreases with increasing of temperature. The extent depends on the ion-exchange level of the catalyst used. For example, this effect is more pronounced at copper exchange level less than 100% for Cu-ZSM-5 than over exchanged ones. In contrast, the presence of oxygen usually increases the reduction of NO into N_2 for SCR.

4. Sulfur dioxide which is usually present in the exhaust gas of combustion processes, completely destroys the catalytic activity of Cu-ZSM-5 for direct decomposition of NO. SO_2 also reduces the catalytic activity of the catalyst slightly in selective catalytic reduction of NO by propene. It is evident that the deactivation of the catalyst is reversible and the catalytic activity of the catalyst could be restored in both technologies by exposing the catalyst to helium at high temperatures or eliminating sulfur dioxide from the gas stream respectively.

5. The activity of Cu-ZSM-5 zeolite for NO decomposition is reversibly suppressed by water vapour. The catalyst is deactivated by adding water in gas stream for SCR of NO. This phenomenon is also reversible. There have been very few studies in the literature on the effect of H_2O on Co-ZSM-5 expressing that H_2O suppresses the SCR over this catalyst as well.

6. Reaction mechanisms both for direct decomposition and SCR are still under investigation. More research is required to clarify the real mechanisms in both cases.

2.7 Objectives of the Present Research

Based on the literature review and conclusions drawn from the review, several areas were identified for further investigation with the following objectives for the present research:

1. Due to the effect of zeolite properties on the reaction rate, ZSM-5 zeolite is synthesised in our own laboratory in order to control the properties of the catalyst. The synthesis of ZSM-5 zeolites with different SiO_2/Al_2O_3 ratios are essential to investigate the effect of the silica alumina ratio of the catalyst on the reaction rate. This is because the zeolite with different SiO_2/Al_2O_3 ratios can be provided from commercial sources, but they could be synthesised with different ratios of other reactants (e.g. OH^-/SiO_2 ratios). Therefore, to control all aspects of the catalyst synthesis, it is important to synthesise zeolite in our own laboratory.

2. It is clear that catalyst preparation has an effect on catalytic activity of a catalyst. The effect of catalyst preparation has not been examined in detail. The preliminary objective of the current project is to find out the effect of catalyst preparation on the catalytic activity of Cu-ZSM-5. This is carried out using nine H-Cu-ZSM-5 samples. The samples are classified in three groups to ion-exchange at three different temperatures (25, 45 and 80). Each group is ion-exchanged for 24, 48 and 72 hours. All the samples are tested for direct decomposition of NO with and without the presence of oxygen. The preparation of these catalysts also establishes a systematic method in order to employ for preparation of the catalysts with a desirable copper loading or copper ion-exchange level, which is required for the next sections of this study.

3. Kinetic of the direct decomposition of NO has been rarely reported in the literature. Therefore, a sample of Cu-ZSM-5 zeolite with initial SiO_2/Al_2O_3 ratio of 40 in template free system is prepared. This sample is used for kinetic study of direct decomposition of NO in the presence of oxygen.

4. Cu-ZSM-5 is believed to be active and selective for reduction of NO by propene. Co-ZSM-5 is also known as an active and selective catalyst in the presence of methane. The activity of these two catalysts, Cu-ZSM-5 and Co-ZSM-5 zeolites, for SCR of NO using propene and methane has not been compared in the literature. In order to perform this, copper and cobalt ion-exchanged ZSM-5 samples are prepared from Na-ZSM-5 synthesised without using a template. The zeolite (i.e. Na-ZSM-5) is ion-exchanged with ammonium nitrate in order to prepare the H-form of ZSM-5. Then, the sample is divided into two parts. One part is ion-exchanged with copper acetate and the second part is ion-exchanged with cobalt acetate. The two catalysts are examined for SCR of NO using methane and propene.

5. It is accepted in the literature that Cu-ZSM-5 zeolite is active and selective catalyst for SCR of NO using propene as a reducing agent but not methane. On the other hand, Co-ZSM-5 is a selective catalyst for SCR of NO using methane while it is not if propene used. Several samples of Cu-ZSM-5 with different SiO_2/Al_2O_3 ratios are prepared from home-made Na-ZSM-5 zeolites and also H-ZSM-5 zeolite provided from commercial sources. The samples are tested for SCR of NO using propene in order to investigate the effect of SiO_2/Al_2O_3 ratio on the catalytic activity of copper ion-exchanged of both Na and also H-form of ZSM-5. The effect of SiO_2/Al_2O_3 ratio on SCR of NO using methane is investigated as well. This is done by preparation of a group of samples of cobalt ion-exchanged ZSM-5. Both Na and H-form of the zeolite are used to prepare cobalt ion-exchanged ZSM-5 zeolites.

6. More experiments are carried out over different catalyst for decomposition and SCR of NO. Two groups of catalysts prepared at the University of Queensland are examined. The first group includes ten samples of ZSM-5 zeolites prepared using different preparation methods such as ion-exchange, impregnation and incorporation of copper in ZSM-5 zeolite framework as well as MCM-41 molecular sieve, a combination of ZSM-5 and MCM-41, ZSM-5+TiO_2, SiO_2+Al_2O_3 and MCM-41+MoO_3+TiO_2. The second group includes twenty one samples of Pillared Clays (PILC). The first group of samples are examined for direct decomposition with and without the presence of O_2. Several samples are selected to investigate SCR of NO

using methane or propene. The second group of samples are tested for SCR of NO using methane.

CHAPTER THREE

ZSM-5 ZEOLITE SYNTHESIS

3.1 Introduction

ZSM-5 zeolites, after proper ion-exchange, have been reported as catalysts with high activities and stabilities for decomposition of nitrogen monoxide (NO) by many researchers such as Iwamoto et al. (1986a) and Li and Hall (1990). However, more research is needed in order to improve the catalytic activity for practical applications. ZSM-5 zeolite synthesis has been identified as a starting point in this present project regarding direct decomposition and selective catalytic reduction of NO. The advantage of synthesising zeolites in our own laboratory is that the zeolite compositions, and thus their properties which to a great extent determine the final catalyst activity could be controlled.

ZSM-5 zeolites were synthesised using four different methods in order to obtain zeolites with different compositions and properties. The aim was to investigate the effect of the zeolite properties on their ion-exchange and catalytic activity towards decomposition and reduction of NO. In two of the four methods, zeolites with 100% crystallinity and with different silica alumina molar ratios (SiO_2/Al_2O_3) ranging from 40 to 176 were synthesised. For each SiO_2/Al_2O_3 ratio, zeolites with different amounts of alkaline inclusion were also synthesised. The synthesised zeolites were used for further investigation of the decomposition and reduction of NO.

As the zeolite was synthesised for use as a catalyst support, physical properties which affect the catalytic activity of the catalyst were of interest. Surface area of a series of synthesised zeolites were measured using BET and Langmuir Methods and the results were compared with the literature. Direct examinations of typical samples

synthesised using different methods and conditions were made by scanning electron microscopy (SEM). It was observed that many variables such as ratios of the starting materials and the conditions of the process affect the crystal topology i.e. the shape of the crystals but not the shape of the zeolite framework.

In this chapter, following a review of general information about zeolites and the structure of the ZSM-5 zeolites, the details of the methods used for ZSM-5 zeolite synthesis are introduced. The influence of the synthesis procedures and initial composition on the structure and property of the final products are discussed. Comparisons with literature data are also made where possible.

3.2 Background

The discovery of a new class of inorganic material, zeolite molecular sieves, resulted in wide scientific interest and development of applications. The first industrial research in this area was carried out at Union Carbide Corporation in 1948. From that time until the end of 1973, over 7000 papers and 2000 USA patents were published on zeolite science and technology (Breck, 1974). Further literature searches from that date indicate that unlimited numbers of papers are available.

Zeolite properties are unique due to the uniformly sized pores incorporated in their structures. The zeolites are able to select and organise molecules with cross sections smaller than their pore sizes. They are used in catalytic reactions because of a wide range of acidic active sites which contribute to acid-catalysed reactions.

ZSM-5 zeolites have been synthesised from two different hydrothermal systems, i.e., with (Argauer and Landolt, 1972) and without an organic template (Shiralkar and Clearfield, 1989). In both systems, a silica source, an alumina source and an alkaline source such as sodium hydroxide are used. In the first system, an organic material, e.g. Tetrapropylammonium Bromide, is used as a template. It is later removed from the zeolite structure by calcination in air at 500 - 550 ^{o}C.

3.3 The Structures of the Zeolites

In general, crystalline aluminosilicate materials including zeolites have a unit cell formula, $M_{(x/n)}[(AlO_2)_x(SiO_2)_y].z(H_2O)$, where M is a metal cation with n positive charges that is exchangeable with other cations. The crystalline structure of the aluminosilicates are usually determined by X-Ray Diffraction (XRD).

Zeolites, both natural and synthetic, have three-dimensional framework structures. Each silicon or aluminium atom is joined to four oxygen atoms to make a $(SiO_4)^{4-}$ or $(AlO_4)^{-5}$ unit. The zeolite frameworks are constructed by joining together $(SiO_4)^{4-}$ and $(AlO_4)^{5-}$ tetra hedra. In these aluminosilicates, the tetra hedra are cross-linked by shared oxygen atoms so that the ratio of total aluminium and silicon atoms to oxygen atoms is 1:2.

In the zeolite structure, a large number of small cavities are interconnected by a number of smaller channels. These cavities and channels are uniform in size. A number of water molecules are also incorporated into the zeolite structures. The extent and the location of these H_2O molecules depend on the architecture of the zeolite (the size and the shape of the cavities and channels) and the number of cations. Zeolites are identified by their Si/Al atomic ratio (i.e. y/x in the formula) or, more commonly, in terms of molar ratio of their oxides, SiO_2/Al_2O_3. As this ratio increases, ion exchange capacity and hydrophilic character of the zeolite decrease, but the thermal stability increases (Shelef, 1995).

A family of crystalline aluminosilicate zeolites, named the Pentasil Group, including ZSM-5 and ZSM-11 has the compositions of $Na_n(Al_n Si_{96-n} O_{192}) \sim 16H_2O$ (Barrer, 1982). They are named after the laboratory name where they were discovered, namely, Zeolite Socony Mobil. In the Pentasil group, the oxygen tetra hedra join together to form five member rings. These rings then link together to form 10-member oxygen rings (Figure 3.1) and therefore create two systems of intersecting channels. In ZSM-5, the created channels are straight and zigzag (Figure 3.2) which

have elliptical mouths of $5.4 \times 5.6 \overset{\circ}{A}$ and $5.1 \times 5.5 \overset{\circ}{A}$ respectively. From the connection of the channels, large room-like cavities are created.

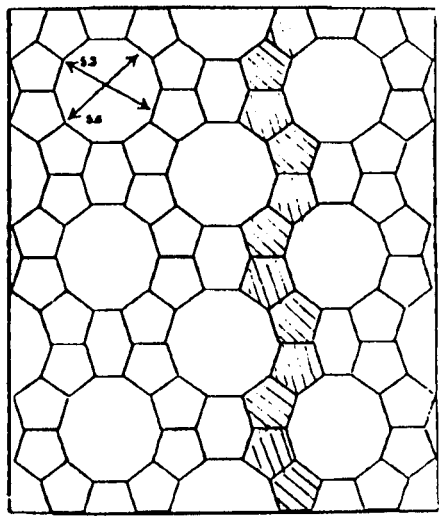

Figure 3.1. A cross section of ZSM-5. Shaded units show the chain as the building unites (reproduced from Szostak, 1989).

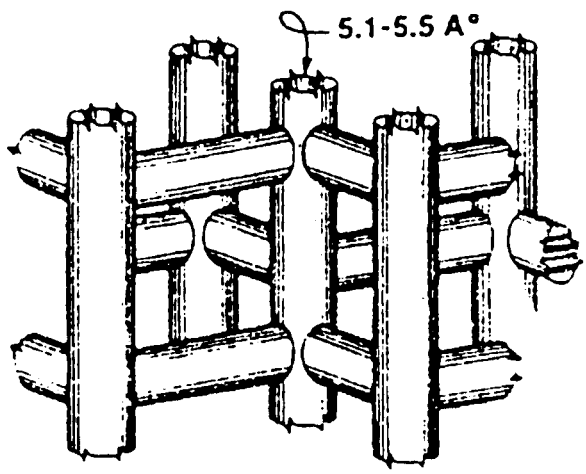

Figure 3.2. The "hollow tube" provides easy visualisation of the straight and zigzag channels in ZSM-5 zeolite framework (reproduced from Szostak, 1989).

In high silica molecular sieves such as ZSM-5 zeolites, which some of $(SiO_4)^{4-}$ tetra hedra are replaced by $(AlO_4)^{5-}$ tetra hedra, an acid site occurs whenever an Al substitutes for a Si in the zeolite framework. Accordingly, each of the four oxygen

atoms attached to the aluminium atom exhibits an acidic property. It is worth noting that aluminium is not an essential component in each ring and in the formation of the zeolite lattice. The amount of aluminium, contributing to a given ZSM-5 structure, can be as little as trace quantities. In ZSM-5 with very high Si/Al ratios, some cells may not contain any aluminium. Therefore, aluminium inhomogeneity exists among cells. According to calculations by Haag et al. (1984), in ZSM-5 with a Si/Al ratios of 190, the amount of aluminium per unit cell in the zeolite structure is equivalent to one. In this case, 36% of all unit cells contain no aluminium whereas the other cells have more than one aluminium ion if the aluminium ions distribute randomly.

3.4 Zeolite Synthesising Methods

The first publication on synthesising ZSM-5 zeolite was a USA patent published in 1972 by Argauer and Landolt (1972) from Mobil Oil Corporation. The ZSM-5 zeolites were synthesised from SiO_2-Al_2O_3 gels containing an organic template of either tetrapropylammonium Bromide (TPABr) or tetrapropylammonium hydroxide (TPAOH). The templates which act as structure directing agents control the kinetics of the complex nucleation and crystallisation processes during the zeolite synthesis.

There are many patents and considerable literature on the synthesis of ZSM-5 zeolites using a wide range of organic compounds as templates. Besides quaternary ammonium compounds, other organic materials such as amines (Wilkosz et al., 1993; Kulkarni et al., 1982; Forbes and Rees, 1995; Valyocsik and Rollmann, 1985), ethanol (Uguina et al., 1995), acetone (Narita et al., 1985), and seed crystals (Narita et al., 1984) have also been used as templates. Nevertheless, TPA-bromide, iodide or hydroxide are still the most popular options. Attempts have also been made and the zeolites were synthesised without using any templating agents (Shiralkar and Clearfield 1989).

Although many organic compounds have been used as templates, TPA compounds are still the most efficient templates for ZSM-5 zeolites synthesis. For example, the

zeolites were synthesised by Wilkosz et al. (1993) using ethylendiamine (ED) as the template. Besides ED, crystalline seeds of pure ZSM-5 zeolites synthesised using TPABr, were also added. In addition, the ZSM-5 zeolite obtained in this way was contaminated with quartz, mordenite and amorphous phase. Diethanolamine (DEA) was also used by Forbes and Rees (1995). However, the maximum purities of the ZSM-5 zeolite reported were 96% with the use of ED, and 95% with DEA.

According to several patents, under certain conditions, ZSM-5 zeolites can be synthesised in aluminosilicate systems without any organic compound. Dai et al. (1986) and then Shiralkar and Clearfield (1989) reported synthesis of ZSM-5 zeolites without the aid of a template. Shiralkar and Clearfield produced different gels with general composition of $aSiO_2$: Al_2O_3: bNa_2O: $1500H_2O$. The pure ZSM-5 zeolite was synthesised only when a and b were 40 and 4.5 respectively.

The main advantage of using organic templates in ZSM-5 zeolite synthesis is that these zeolites have a higher structural stability than those without any template. However, using templates for synthesising zeolites has the following disadvantages (Shiralkar and Clearfield, 1989):

- Most of the templates for synthesising zeolites are corrosive and poisonous.
- The templates are generally expensive and constitute approximately 50% of the total production cost.
- The zeolites require thermal decomposition to remove the template residuals to make them active before being used as catalysts.

3.4.1 Equipment

Equipment used for zeolite synthesis in the present project included three stainless-steel autoclaves with teflon sleeves, an air oven and a furnace connected to a

compressed air source by a flow rate meter. The temperature indicator of the oven was calibrated as the zeolite synthesis was very sensitive to any temperature changes.

The stainless-steel cylindrical autoclaves with teflon beakers used as internal lining were designed and constructed in three different sizes, 60, 120 and 300 ml. The thickness of the beaker wall was important because teflon was not a good heat conductor. The wall thickness of the autoclave bomb depended on the bomb diameter and the type of stainless steel. A teflon lid was required for the beaker as well as a stainless-steel cover for the bomb. These materials were selected to prevent corrosion due to the high pH of the gel for zeolite synthesis. The specifications of the three autoclaves are detailed in Table 3.1.

Table 3.1. Specifications of the three autoclaves (all values are in mm).

specification	Bomb I	Beaker I	Bomb II	Beaker II	Bomb III	Beaker III
internal diameter	35	30	41	36	50	45
thickness	6.5	2.0	7.0	2.0	7.5	2.0
internal height	84.8	76.3	128.5	120	198.5	190
overall height	99.5	84.8	145.6	128.5	215.1	198.5

The smallest autoclave with capacity of 60 ml was used in the preliminary experiments to reduce the risk of wasting materials. After synthesising some zeolites and accumulating enough experience to prepare pure ZSM-5, the larger autoclaves were then used for synthesis of the zeolites. Schematic designs of three autoclaves are presented in Appendix A.

3.4.2 Experimental Procedures

Four different methods were chosen from the literature and used to synthesise ZSM-5 zeolites. In the first and second methods, Method I and Method II, TPABr was used as the template. In the third method no template was used. In the fourth method n-propylamine as well as TPABr were used. The ingredients and the procedures used for the four methods were different. In each method, the ingredients were mainly from both, silica and alumina sources. Water and a cation source were also used. In the first, second and fourth methods, a binary mixture of cations, i.e. Na^+ and TPA^+, was available in the system whereas in the third method, the only cation was Na^+.

In each method, the composition of the reactants, time, temperature and other factors such as stirring, nature of the mixture and order of mixing were different. Since the concentrations and the purities of the starting materials differed from different companies, the amount of each starting material was calculated from the hydrogel compositions reported by the researchers (Shiralkar and Clearfield, 1989; Sano et al., 1991; Gabelica et al., 1983; Whittingham, 1995).

After mixing ingredients, an unclear gel was formed. After stirring for a specified time, the gel was transferred into the autoclave and sealed. The autoclave was then placed into the oven set at a specified temperature. When the temperature reached the required level, the time was recorded. As the crystallisation progressed two separate phases, a solid and a liquid, were formed. The solid settled to the bottom of the autoclave with a clear liquid phase on the top.

The liquid phase was decanted. The solid phase was filtered out, washed with deionised water several times and dried in an air oven at a specified temperature. The formed crystals were very light. If the product was like a suspension or a sticky mixture or very dense, the product was unlikely to be a pure zeolite. In the first, second and the fourth methods, calcination of the obtained zeolites was necessary in order to remove the template residuals. Therefore after drying, the zeolites were calcined. During calcination, air with a flow rate of 25 l min^{-1} was passed through the

furnace and each sample was spread out on a crucible so that the decomposed template could diffuse through the zeolite layers and be removed easily. It was unnecessary to calcine the product from the third method.

The zeolite samples synthesised were characterised using a X-ray diffraction (XRD) as this can be used for identification purposes by comparing the resultant patterns of a sample with the standard patterns for known zeolites. The XRD patterns were recorded with a Philips PW1800 microprocessor-controlled diffractometer using CoKα radiation, a variable divergence slit, and graphite monochromator. The diffraction patterns were recorded in steps of 0.05° 2θ with a 1.0 second counting time per step, and logged to permanent data files on an IBM-compatible PC for analysis. The zeolite structures were confirmed by XRD patterns. The XRD patterns of the synthesised zeolites are exhibited in Appendix B. They were compared with a ZSM-5 zeolite sample donated by Hamada, National Institute of Materials and Chemical Research, Ibaraki, Japan. The percentage of crystallisation of the synthesised zeolites was calculated from the area under the peaks in the range of 2θ = 26-29, divided by the area under the peaks of the reference sample. The XRD pattern of the reference sample is shown in Figure 3.3.

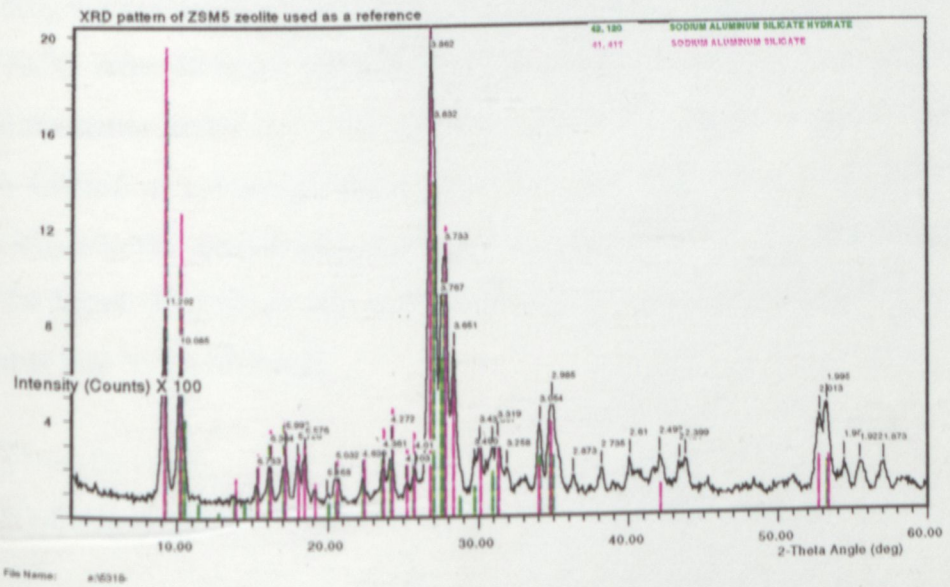

Figure 3.3. XRD pattern of the reference sample.

3.4.2.1 Method I

This method has been reported by Sano et al. (1991). In this work, the same procedure as outlined by Sano et al., but different sources of the ingredients were used. Aluminium nitrate $Al(NO_3)_3.9H2O$, (Prolabo, EEC) and Ludox colloidal silica (Ludox, HS-40 silica sol, Dupont, USA) which was an aqueous colloidal dispersion of very small silica particles with 40% SiO_2 were used. Sodium hydroxide (Merck, Germany) was used to provide both Na cations and alkalinity in the zeolite structure. Tetrapropylammonium bromide (TPABr) with 98% purity supplied by Acros, Belgium, was used as the template. Deionised water was used to prepare all solutions.

In a typical run of zeolite synthesis, 1.33 g TPABr and 0.117 g sodium hydroxide were dissolved in 15 ml of deionised water and stirred. Then, 0.25 g aluminium nitrate was added to this solution. In the next step, 7.507 gr colloidal silica was added and the solution was mixed. Finally, remaining water (e.g. 16.333 g) was added and the solution mixed to form a hydrogel with a composition of $100SiO_2$: Al_2O_3: 10TPABr: 5.0 Na_2O: $4000H_2O$. In different runs, the SiO_2/Al_2O_3 molar ratio was changed from 70 - 180 depending on desirable SiO_2/Al_2O_3 ratios.

The hydrogel was transferred to the autoclave and placed in the oven which had been set at 170 °C. After 40 hours, the autoclave was removed from the oven and cooled to room temperature under tap water. The top liquid was decanted and the rest was vacuum filtered in a Buchner funnel with two fine filter papers (42 grade). The sample was washed with deionised water. The collected solid was then dried at 120 °C for 24 hours. To remove the organic base within the zeolite framework, it was calcined at 500 °C for 16 hours.

3.4.2.2 Method II

In this method, reported by Gabelica et al., (1983), the ingredients used were sodium metasilicate ($Na_2SiO_3.5H_2O$, from BDH laboratory supplies, Poole, BH15, England)

and hydrated aluminium sulfate as silicon and aluminium sources, respectively. Tetrapropylammonium bromide (98% pure, Acros, Ceel, Belgium) was used as the templating agent. Na cations were provided in the zeolite structure by sodium chloride (BDH Chemicals, AnalaR, Victoria). Sulfuric acid 98% (Merk, Germany) and deionised water were used to adjust the pH and to make all solutions.

100 g sodium silicate was dissolved in 50 ml deionised water (Solution A). 3.26 g of $Al_2(SO_4)_3.18H_2O$ (hydrated aluminium sulfate) was dissolved in a dilute sulfuric acid solution (8.5 g H_2SO_4 98% and 50 ml distilled water). It was cooled to room temperature and added slowly to 12 g TPABr. This mixture was stirred until a homogeneous solution was achieved (Solution B). 3.58 g NaCl was dissolved in 50 ml deionised water (Solution C). One third to one quarter of both Solution A and Solution B were simultaneously added to Solution C and blended together under vigorous mixing. The pH had to be between 2 and 4 and was usually around 2.6. The mixture was stirred continuously for a minimum of two hours. Then the remainder of Solution A was added to this and the pH checked to ensure it was between 8 and 10 (usually around 8.86). The stirring of the mixture was continued for a further 2 hours. The gel composition was $96.5SiO_2$: Al_2O_3: $28.8Na_2O$: $17.3H_2SO_4$: 8.9TPABr: 47.1NaCl: $1888H_2O$. The final gel was transferred into the 300 ml teflon-lined autoclave. The autoclave was placed in an oven set at 140 °C for 6-7 days. The autoclave was shaken three times in a day (excluding the nights). At the end of this process, the autoclave was removed from the oven and quenched under cold tap water. The clear top liquid was decanted and ZSM-5 crystals were continuously washed with deionised water and filtered until the pH of the washing water did not change during washing. The solid was dried at 100 °C in an oven overnight and once dried was calcined at 550 °C for 10 hours.

3.4.2.3 Method III

In this method, as reported by Shiralkar and Clearfield (1989), the ingredients used were Ludox colloidal silica with 40% SiO_2 (Ludox, HS-40 silica sol, Du Pont, USA) as a silica source and aluminium hydroxide as the alumina source. Sodium hydroxide

(Merck, Germany) was also used to provide Na cations and alkalinity. Deionised water was used to make the solutions.

7. 507 g Ludox was diluted with 10 ml of deionised water (Solution A). To make the next solution, Solution B, 0.409 g Sodium hydroxide was dissolved in 10 ml of deionised water. In the next step, 0.195 g Aluminium hydroxide was added slowly to Solution B while being stirred and boiled until the most of the aluminium hydroxide was dissolved to provide a colloidal suspension (Solution C). Solution C was cooled to room temperature and added slowly to Solution A with constant vigorous stirring. After the addition of 60% of Solution C, a thick gel formed. The gel was homogenised by mechanical stirring. The remaining Solution C, as well as 9.05 ml of water, were both added slowly with constant stirring, so that a hydrogel with a composition of 40 SiO_2: Al_2O_3: $4.5N_2O$: $1500H_2O$ was made. After the addition was completed, the gel was stirred for at least 30 minutes to obtain a homogeneous gel-mix with pH 12.9 ± 0.1. This mixture was transferred to the autoclave and sealed before being placed in an air oven. The temperature of the oven was set to 190 °C. After attaining this temperature, the time was recorded and after 40 hours the autoclave was quenched under tap water and cooled to the room temperature. The white crystalline solid that settled to the bottom was separated from the supernatant liquid (pH = 11.6 ± 0.1) by filtration. The product was washed several times with deionised water and dried at 120 °C for 4 hours in an air oven.

3.4.2.4 Method IV

In this method, introduced by Whittingham (1995), the ingredients used were: colloidal silica with 40% SiO_2 (Ludox, HS-40 silica sol, Dupont, USA), hydrated aluminium sulfate, tetrapropylammonium Bromide (98% pure, Acros, Ceel, Belgium), sulfuric acid (98%, Merk, Germany), n-propylamine and sodium hydroxide. In the first step, 1.071 g sodium hydroxide pellets were finely grinded with a mortar and pestle, and 9.67 g Ludox and 2.525 g tetrapropylammonium bromide were added. 20 ml deionised water, and 2.5 ml n-propylamine were added

(Solution A). 2.5 ml aluminium sulfate solution (1.0 molar) and 0.125 ml sulfuric acid were mixed in a separate beaker (Solution B). Solution A was then added to Solution B. Enough deionised water was added to raise the volume to 75 ml. This resultant solution was stirred for ten minutes, and then transferred to an autoclave and sealed. It was shaken gently before being placed in the oven. The oven was heated to 160 °C and the solution was held for 44 hours in the oven at this temperature. Then, the autoclave was removed from the oven, cooled under tap water and the product was filtered using a Buchner funnel. The sample was washed with deionised water several times, dried at room temperature for 20 minutes and then calcined at 500 °C for 2 hours.

3.5 Results and Discussion

By using Method 1, ZSM-5 zeolites were synthesised with 100% crystallinity. More than 10 samples were produced. The results were consistent and a XRD pattern of a sample typically synthesised using the first method is shown in Figure 3.4.

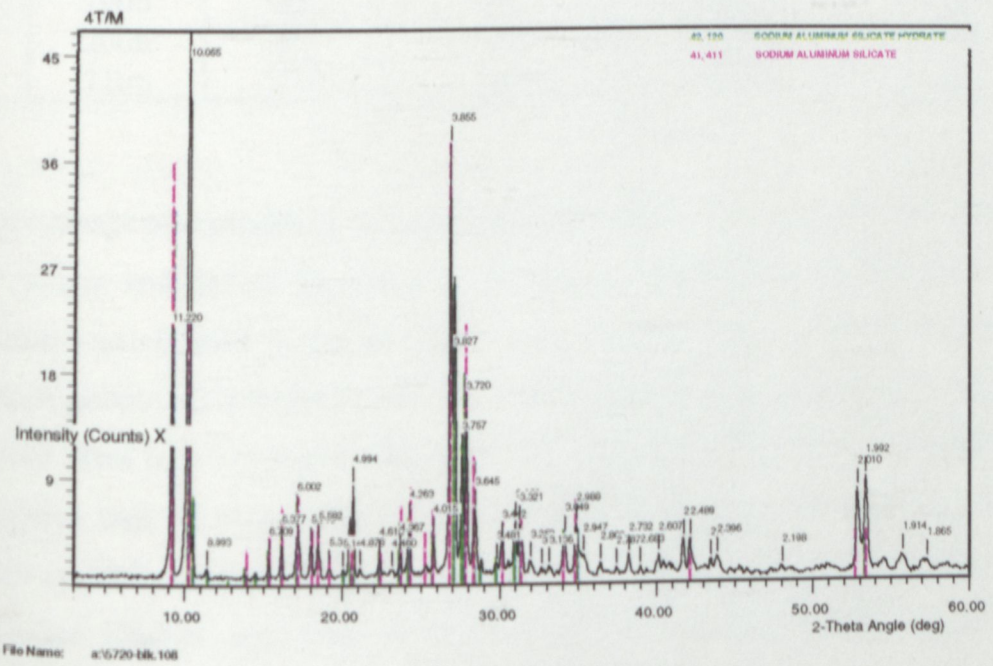

Figure 3.4. X-ray diffraction profile of a sample of Na-ZSM-5 zeolite prepared using TPABr from Method I.

The initial amount of alumina source was changed in different runs in order to produce zeolites with different SiO_2/Al_2O_3 ratios. The SiO_2/Al_2O_3 ratios in the initial ingredients were 70, 100, 140 and 176. Three different amounts of inorganic alkali substances were also used in order to compare the effect of alkalinity on the properties of the zeolites. The H_2O/SiO_2 ratio can be varied from 40 to 100. In this study, the ratio was 40 for all samples synthesised by this method. The XRD patterns of the samples confirmed that all samples produced by this method consisted of only two solid phases, sodium aluminosilicate and sodium aluminosilicate hydrated. Table 3.2 shows the specifications of typical ZSM-5 zeolites synthesised using Method I.

Table 3.2. The specifications of the synthesised ZSM-5 zeolites using Method I.

Run	Sample code	XRD Pattern Figure No.	Initial SiO_2/Al_2O_3 molar ratio	initial OH^-/SiO_2 molar ratio	% of crystallinity
1	4tm	B1	176	0.1	90
2	6tm	B2	176	0.1	106
3	7tm	B3	176	0.1	94
4	8tm	B4	176	0.1	105
5	9tm	B5	176	0.1	96
6	18tm	B7	70	0.2	94
7	19tm	B8	100	0.2	94
8	20tm	B9	70	0.15	100
9	21tm	B10	100	0.15	101

The percentage of crystallinity of each sample was calculated using the area under its XRD pattern and that of the reference sample as described in section 3.4.2. The measured crystallinities of the samples were sometimes different from that of the reference sample. This could be due to different crystal sizes in the samples and the reference. This is in agreement with what was reported by Shiralkar et al. (1996) in that crystal size, or distribution of sizes, determines the shape and breadth of the profiles in XRD patterns. More than 100% of crystallinities were achieved for some synthesised samples, indicating that the samples were better crystallised than the reference sample.

One of the important factors influencing zeolite crystallisation is the alkalinity of the mixture that affects the size of the produced crystalline materials. At low concentrations of hydroxide ions, larger crystals form whereas in high hydroxide concentrations, smaller crystals result. Increasing pH up to a point also results in shorter crystallisation times. Above that point, the yield will very sharply reduce with further increasing pH.

The effect of alkalinity on the crystallinity of ZSM-5 zeolites was discussed by Kulkarni et al. (1982). They interpreted that OH^- ions accelerate the dissolving of the formed amorphous aluminosilicate gel into smaller hydroxylated Al, Si and aluminosilicate species in the first stage of zeolite synthesis. In the next stage, the presence of excess OH^- ions inhibit the condensation of these species which suppose to form the nuclei which are the starting point of crystallisation. Therefore, a narrow range of OH^- concentrations can be utilised for zeolite synthesis. This amount of OH^- ions is essential for dissolving hydroxy species, but not so high that it inhibits the nucleation in the next stage. Sano (personal communication) believed that the range of OH^-/SiO_2 for ZSM-5 zeolite synthesis using the first method should be 0.1-0.2. As shown in Table 3.2, the percentage of crystallinities for the zeolite synthesised from Method I was ~100% +/- 5%.

Table 3.2 also shows that lower percentages of crystallinities were synthesised by increasing the alkalinity. The reason for this is that an increase in alkalinity increases the induction period for nucleation and the rate of crystallisation. This is in agreement with the results presented in Table 3.2 for runs 6 to 9.

From Method II, ZSM-5 zeolites with low crystallinity were produced. The experiments were carried out only for three runs because of the complicated procedure.

ZSM-5 zeolites with 100% of crystallinity were synthesised using Method III. The experiments were performed for more than ten runs and the results were consistent. A typical XRD pattern of a ZSM-5 zeolite synthesised using Method III is shown in Figure 3-5.

The pH of the gel in this method, has been reported to be 12.9± 0.1 by Shiralkar and Clearfield whereas the pH of our gel was between 12.4 and 12.7. To increase the pH of the gel, the pH of the Ludox colloidal silica was adjusted to 10.5 by adding around 6-8 drops of ammonia (25%). The initial pH of the Ludox HS-40 silica sol was around 9.7. The final pH of the gel-mix was between 12.5-13.0. By adjusting the pH of the Ludox, ZSM-5 Zeolite with 100% crystallinity was finally synthesised.

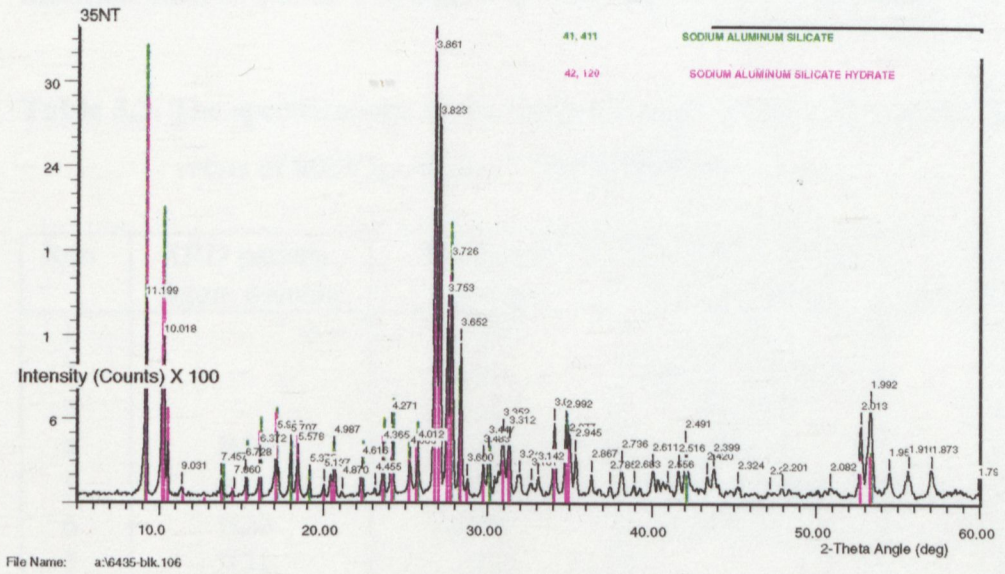

Figure 3.5. X-ray diffraction profile of a sample of Na-ZSM-5 zeolite prepared without template from method III.

Organic ions are generally considered to play a structure-guiding role and form the architecture of frameworks consisting of zeolite crystals. It was reported that ~ 3.2-3.7 moles TPA cations are required per unit cell in ZSM-5 crystals. This means that one organic cation is required to incorporate to the zeolite structure per each channel intersection (Szostak 1989). Although, ZSM-5 zeolite can be synthesised without the aid of any template, the question on how the zeolite structure forms without any directing crystallisation agent still remains unanswered.

Shiralkar and Clearfield (1989) carried out synthesis runs with different ratios of SiO_2/ Al_2O_3 and Na_2O/Al_2O_3 in order to determine the composition range of the gel that would result in ZSM-5 zeolite. They reported that the pure ZSM-5 was only

obtained with a $SiO_2/Al_2O_3 = 40$ and $Na_2O/Al_2O_3 = 4.5$. To investigate the possibility of ZSM-5 zeolite synthesis with higher SiO_2/Al_2O_3 ratio using this method, beyond the compositions they had tested, several synthesis runs were carried out from a hydrogel system whose oxide mole composition was $90SiO_2$: Al_2O_3: $7.7N_2O$: $3000H_2O$. The oven temperature was fixed at 190 °C and the crystallisation time was 40 h. The specifications of the products are summarised in Table 3-3. This table shows that the products were mainly SiO_2 and ZSM-5, contaminated with some other materials such as quartz. The highest percentage of zeolite crystallinity was only 54.

Table 3.3. The specifications of the products using Method III with the composition ratios of $90SiO_2$: Al_2O_3: $7.7N_2O$: $3000H_2O$.

Run	XRD pattern figure number	Dominant phase	Existed traces in the products	% of crystallisation
1	-	ZSM-5	SiO_2	54
2	-	SiO_2	ZSM-5, Quartz	-
3	-	SiO_2	ZSM-5	10
4	B18	SiO_2	ZSM-5	27
5	B19	ZSM-5	SiO_2, Quartz	45
6	B20	ZSM-5	Quartz	40
7	B21	SiO_2	-	16
8	B22	SiO_2	-	5

Several runs were carried out to synthesise ZSM-5 zeolites from Method IV. Zeolites with up to 60% crystallinity were achieved. The remainder were amorphous materials. More investigation is required to improve the crystallinity of the zeolite using Method IV.

Surface areas of some samples were measured by Huazong University of Science and Technology, Wuhau, China. Before testing, the samples were dried for 8 hours to remove water and impurities. Liquid N_2 (-196 °C) was used for absorption on the surface of the samples. The results are presented in Table 3.4. Surface areas were measured using two methods, Langmuir and BET methods. BET is after the names of the researchers (Stephen Brunauer, Paul Emmett, and Edward Teller) who employed this method to measure surface areas of porous materials.

Langmuir isotherm is based on two assumptions: 1) every adsorption site is equivalent 2) the ability of a particle to bind is independent of whether or not nearby sites are occupied. This isotherm also ignores the possibility that the initial monolayer may act as a substrate for further adsorption while BET isotherm deals with multilayer adsorption. BET is the most common method for measuring surface area in catalyst studies and was developed by Brunauer et al. (1938). More descriptions and evaluations were given by Emmett (1948 and 1954) as cited in Satterfield (1991).

Table 3.4. Surface areas and pore diameters of typical synthesised ZSM-5 zeolites.

Sample code (SiO_2/Al_2O_3)	Surface area, ($m^2\ g^{-1}$)	
	Langmuir	BET
4tm (176)	357.4	265.3
8tm (176)	523.3	386.8
9tm (176)	365.9	272.7
18tm (70)	394.9	291.1
19tm (100)	332.0	246.1
20tm (70)	353.4	262.3
21tm (100)	502.8	372.0
23tm (70)	335.1	247.5
35NT (40)	151.2	110.6

The BET surface area of ZSM-5 zeolites synthesised using Method I were reported by Sano et al. (1991) to be between 347-378 $m^2\ g^{-1}$ for five runs of their experiment. Some of the results in Table 3.4. are different from the data reported in the literature due to many variables which affect zeolite synthesis. According to Table 3.4, it is evident that there is no relationship between silica alumina ratio and surface area of the synthesised ZSM-5 zeolites. A similar outcome regarding zeolite pore diameters was reported by Sano et al. (1997) who concluded that microporosity does not depend upon the SiO_2/Al_2O_3 ratio.

The scanning electron micrographs of various synthesised ZSM-5 zeolite samples are presented in Figures 3.6, 3.7, 3.8 and 3.9. The name of the samples and the scale of the images are shown on the micrographs. All micrographs belong to the samples synthesised using Method I, except Figure 3.8 which is for a sample synthesised using Method III. The micrographs show that different crystal sizes and morphologies are achieved even for the samples produced using the same method. Therefore, the difference between the crystal size and morphology may be related to process conditions.

Figure 3.6 shows the images of two different samples with the same amounts of ingredients in the initial gel (SiO_2/Al_2O_3 ratio of 176 and OH^-/SiO_2 of 100) but different crystallinities. Figures 3.6a and 3.6b belong to two samples (4tm and 9tm) with crystallinities of 90% and 96% respectively. The impurities are clearly shown in Figure 3.6a. The morphology of the two samples seems to be similar but the crystal sizes are different, indicating that other parameters rather than the silica alumina ratio and alkalinity have effects on the crystal sizes. The shape of the crystals in 3.6a and 3.6b consist of interpenetrating twinned crystals. In some cases more than two crystals appear to be linked together and this could be a characteristic of the ZSM-5 zeolites with high SiO_2/Al_2O_3 ratios.

Figures 3.7(a) and 3.7(b) are images of two zeolite samples synthesised with the same alkalinity but different silica alumina ratios, 100 and 70 respectively. The crystallinities of the samples were 94 and 100 respectively, and the construction of the crystals were similar. The latter sample crystallised very well. These two samples are different in topology with the first two samples which are shown in Figures 3.6(a) and 3.6(b). This is because changing the pH of the initial gel can change crystal topology i.e. change the shape of the crystals but not the shape of the framework. Figures 3.7(a) and 3.9(c) are related to the same sample but with different magnifications. The construction of the sample is more clearly evident at the larger magnification as shown in Figure 3.9(c).

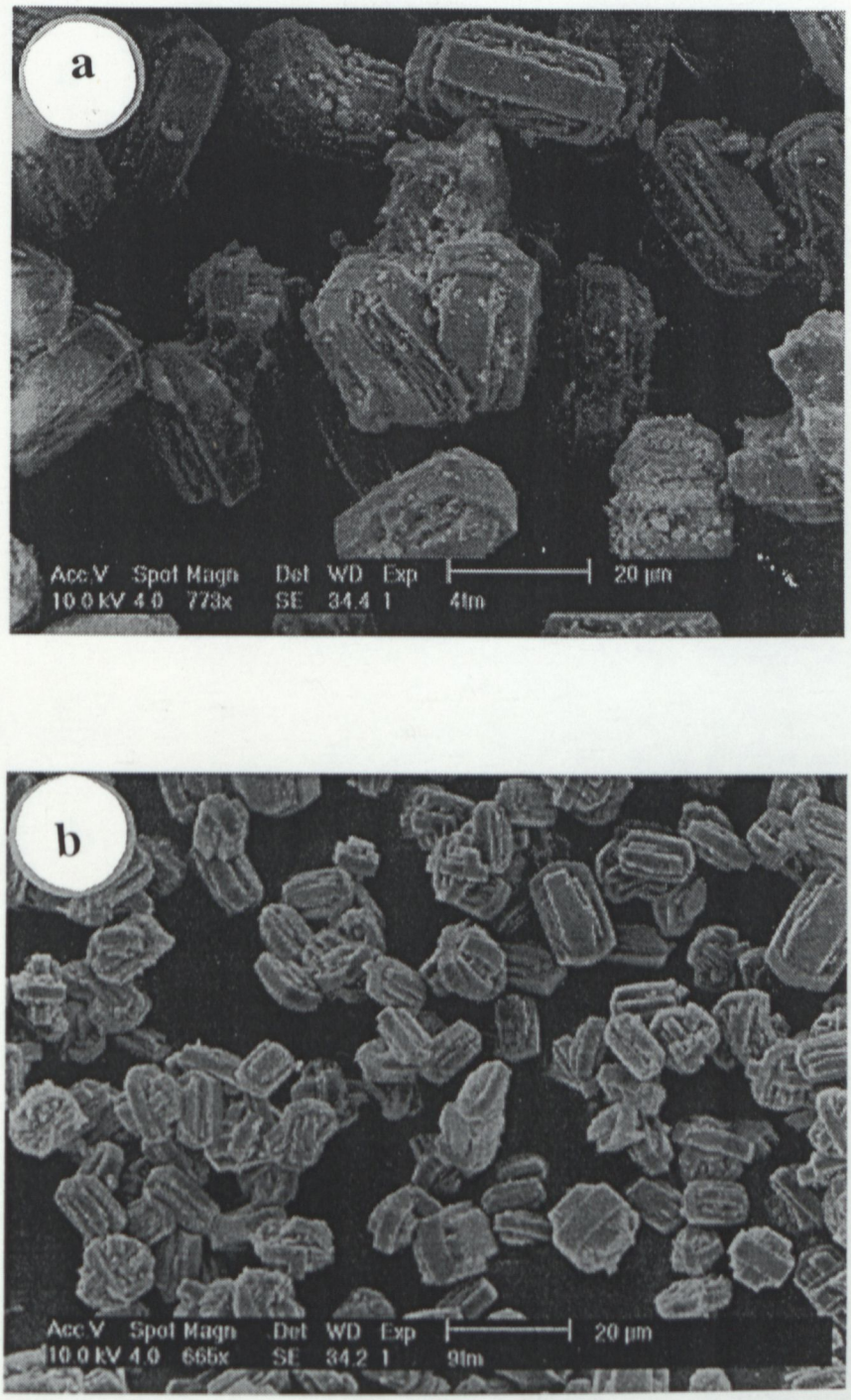

Figure 3.6. Scanning electron micrographs of various Na-ZSM-5 zeolites. (a) synthesised using TPABr with the following ratios in the initial gel, $SiO_2/Al_2O_3 = 176$, $OH^-/SiO_2 = 0.1$ and 90% crystallinity; (b) the same as (a) but with 96% of crystallinity.

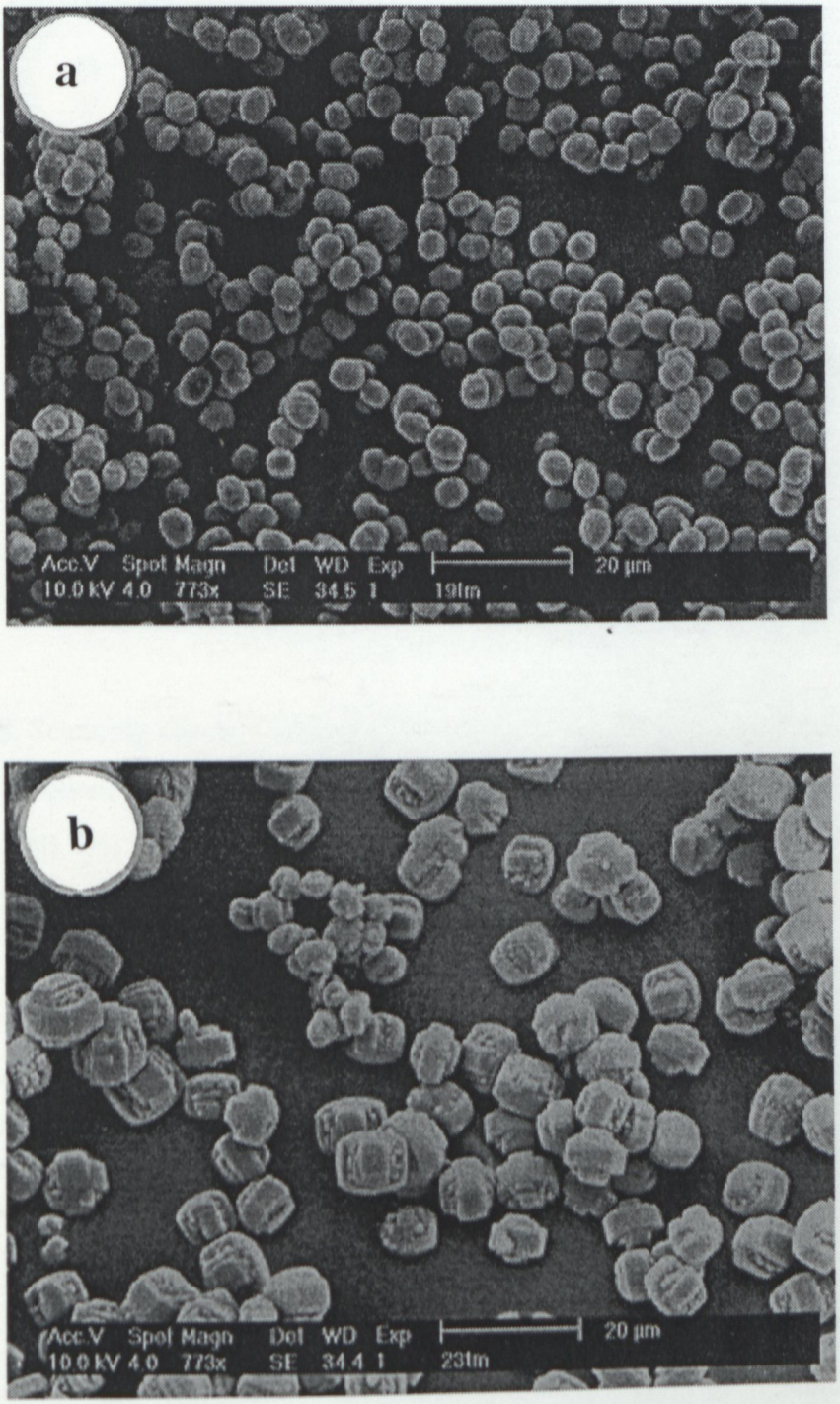

Figure 3.7. Scanning electron micrographs of various Na-ZSM-5 zeolites. (a) synthesised using TPABr with the following ratios in the initial gel, $SiO_2/Al_2O_3 = 100$, $OH^-/SiO_2 = 0.2$ and 94% crystallinity; (b) synthesised using TPABr with the in following ratios in the initial gel, $SiO_2/Al_2O_3 = 70$, $OH^-/SiO_2 = 0.2$ and 100% crystallinity.

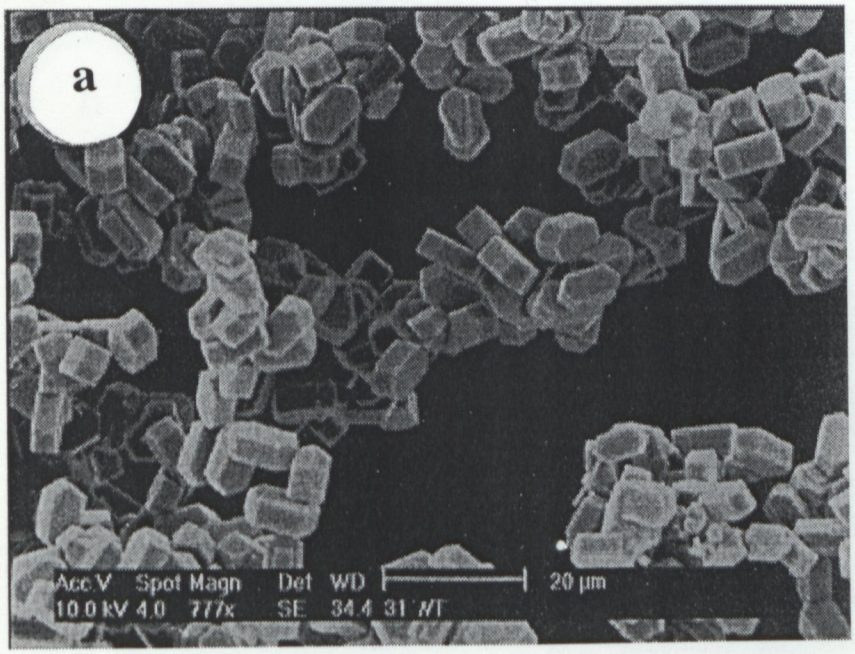

Figure 3.8. Scanning electron micrographs of various Na-ZSM-5 zeolites synthesised without template with the following ratios in the initial gel, SiO_2/Al_2O_3 = 40, OH^-/SiO_2 = 0.22 and 100% crystallinity.

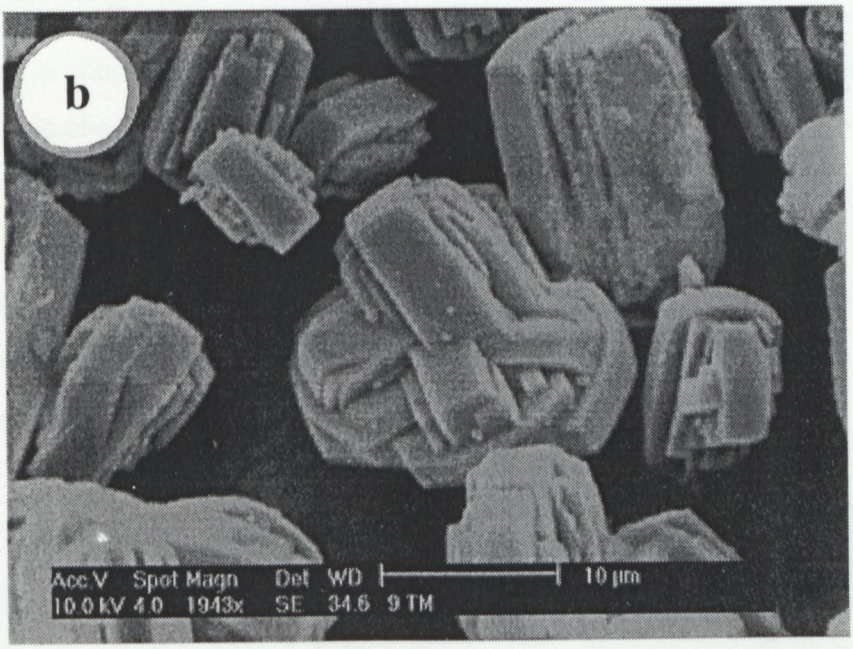

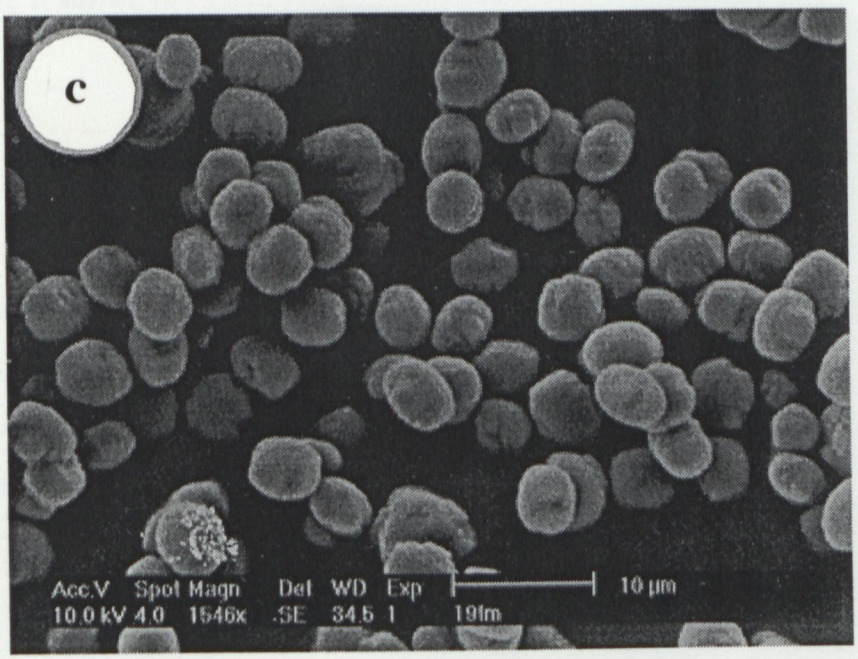

Figure 3.9. Scanning electron micrographs of various Na-ZSM-5 zeolites. (a) same as 3.6(b) but smaller magnitude, (b) same as 3.6(b) but with larger magnitude (c) same as 3.7(a) with larger magnitude.

Figure 3.8 is the SEM image of a sample synthesised without using a template. The morphology of this sample is completely different from the other samples. The construction is more rectangular and similar to a hexagonal prism and this may be due to the lack of a template in the synthesis of the sample.

Figures 3.6(b), 3.9(a) and 3.9(b) are for the same sample but at different magnifications. Figure 3.9(b) with the largest degree of magnification shows that some crystals have a complicated construction resulting from interpenetration of several crystals.

A comparison between all images reveals that the crystal sizes are completely different in different samples. The greatest differences are seen in Figures 3.6(a) and 3.7(a) with the relatively large and small crystal sizes respectively. In addition, different crystal sizes of the zeolites are even seen in a sample. The variety of the crystal sizes is shown in Figure 3.9(a).

3.5.1 A Comparison of the Synthesis Methods

A great deal of research has been undertaken to synthesise ZSM-5 zeolites using different methods with different procedures, compositions and initial sources of substances by many researchers. The procedures of some methods are very easy to follow while others are relatively complicated. To compare the procedures of the four synthesis methods used in this project, synthesis data of the methods are presented in Table 3.5.

Among the four methods, Method III is the safest and the easiest method to use because in this method, no template is used and the procedure is also not complicated. The only disadvantage of this method is that the zeolite cannot be synthesised with different silica alumina ratios. A comparison among the other methods (Method I, Method II and method IV) reveals that the procedure of Method I is the easiest procedure. In method I and Method IV, 48 and 44 hours are required to

complete a zeolite crystallisation procedure respectively whereas in the Method II, at least 5 days is required (Table 3.5). In addition, in Method II the reactants are stirred twice and each time for two hours. Furthermore, the autoclave has to be shaken several times within each day while the process is in progress. The second advantage for Method I is that it is not necessary to work with hazardous materials i.e. sulfuric acid or n-propylamine which are required in zeolite synthesis using Method II and Method IV respectively. The third advantage is that ZSM-5 zeolites can be synthesised in a wide range of SiO_2/Al_2O_3 ratios (i.e. from 70 to ∞).

Table 3.5. Synthesis data of various ZSM-5 zeolites using four different methods.

Method	Stirring	Autoclavation		Drying		Calcination	
		Time	Temperature	Time	Temperature	Time	Temperature
	hr	hr	°C	hr	°C	hr	°C
I	-	48	170	24	120	16	500
II	2×2	120	140	14	120	10	550
III	0.5	40	190	4	120	-	-
IV	0.1-0.2	44	160	0.3	25	2	500

A comparison of the molar compositions of the ingredients of the initial gels in the four methods are as follows:

Method I: $100SiO_2$: Al_2O_3: 5.0 Na_2O: 10TPABr: 4000-10000 H_2O,

Method II: $96.5SiO_2$: Al_2O_3: $28.8Na_2O$: 8.9TPABr: $17.3H_2SO_4$: 47.1NaCl: $1888H_2O$,

Method III: 40 SiO_2: Al_2O_3: $4.5N_2O$: $1500H_2O$,

Method IV: 25.7 SiO_2: Al_2O_3: 6.35 Na_2O: 3.8TPABr: $0.94H_2SO_4$: $1388H_2O$.

In the fourth method, in addition to the above ingredients, 1000 ml of n-propylamine per mole of Al_2O_3 is used. When comparing the ingredients and the ratios of the ingredients used, it is observed that the compositions of the initial gels are different therefore making it difficult to compare the synthesis mixtures.

A comparison amongst the ratios of the ingredients used for zeolite synthesis using the four methods and the maximum crystallinities achieved for the products are shown in Table 3.6.

Table 3.6. A comparison among the specifications of the synthesised ZSM-5 zeolites from the four different methods.

Method	Initial SiO_2/Al_2O_3 ratio	OH^-/SiO_2 ratio	Crystallinity, %
I	70	0.15	100
I	70	0.2	94
I	100	0.15	100
I	100	0.2	94
I	176	0.1	105
II	96.5	0.2	70
III	40	0.2	100
IV	26	9.0	59

In this work, from Methods I and III, ZSM-5 zeolites with 100% crystallinities were synthesised. A comparison between the results obtained from Method I and Method III shows that the synthesised zeolites in the presence of binary cations, sodium hydroxide and TPABr, have a wider range of SiO_2/Al_2O_3 ratios than those synthesised solely in the presence of sodium hydroxide.

When comparing SiO_2/Al_2O_3 ratios, it was evident that ZSM-5 zeolites with different SiO_2/Al_2O_3 ratios were only synthesised from Method I by using different amounts of aluminium nitrate in the initial gels. However, all synthesised zeolites have to be analysed to measure the real amount of SiO_2/Al_2O_3 ratio because the starting synthesis mixtures are not necessarily consistent with that of the products. A comparison of the SiO_2/Al_2O_3 ratios of the starting gels and ZSM-5 products is typically presented in Table 3.7. As it is shown, the SiO_2/Al_2O_3 ratio of the products are less than that of starting gels no matter how the sample was synthesised, with or without a template.

Table 3.7. SiO_2/Al_2O_3 ratios of starting gels and ZSM-5 products for three samples synthesised using Method I and one sample using Method II.

Sample specification	SiO_2/Al_2O_3 ratio of starting gel for ZSM-5 zeolite synthesis	SiO_2/Al_2O_3 ratio of ZSM-5 zeolite product
Method I (Run 4)	176	163
Method I (Run 8)	70	67
Method I (Run 9)	100	97
Method III	40	34

The only detected phases in the products obtained using Method I and Method III were sodium aluminium silicate and sodium aluminium silicate hydrated. From Methods II and IV, zeolites with lower crystallinities were produced. In these cases, besides the mentioned phases, silica and in some samples quartz were detected in the products. The impurities were more likely to be amorphous SiO_2 in high silica zeolites such as ZSM-5. Amorphous SiO_2 is deposited from the top hot liquid of the crystallisation products as silicon oxide is not soluble in either cold or hot water and it is very slightly soluble in alkali solutions (Weast et al., 1983-1984).

3.6 Summary

In this work, ZSM-5 zeolites were synthesised using four different methods including different procedures and initial sources of required materials. From the first method, the zeolites were synthesised with different SiO_2/Al_2O_3 ratios with 100% crystallinity. This method was the easiest method among the four methods used. The zeolites synthesised using this method were pure but with different crystal sizes. However, ZSM-5 zeolites can only be synthesised with SiO_2/Al_2O_3 ratios greater than 70. An attempt has been made to use this method for synthesis of the zeolite with the silica to alumina ratios less than 70, but a pure zeolite has not yet been synthesised.

The second method is found to be complicated. Synthesising ZSM-5 zeolites from this method takes more time. The results are less consistent. Safety precautions are needed because 98% sulfuric acid is used.

ZSM-5 zeolite with 100% of crystallinity was synthesised using the third method. This method is easy to follow and consistent results can be achieved. It seems that the procedure is very sensitive due to the lack of a template. However, ZSM-5 zeolites with different SiO_2/Al_2O_3 ratios cannot be synthesised using Method III. The only option would be SiO_2/Al_2O_3 of 40.

The fourth method is also easy to follow but for the use of n-propylamine and sulfuric acid, some safety precautions are required. An advantage of this method is, ZSM-5 zeolite with lower SiO_2/Al_2O_3 ratio can be synthesised (SiO_2/Al_2O_3 = 25).

Synthesising ZSM-5 zeolites from different methods results in different crystal topology. The shape of the crystals changes when different methods are used to synthesise the zeolite while the shape of the framework remains the same. The size of the crystals is different in the zeolites produced in different batches even when the same method is used. In addition, sometimes even the size of the crystals obtained from one batch is different. This indicates that not only the ingredients of the initial gel affect the crystal size but also the conditions of the process.

CHAPTER FOUR

EXPERIMENTAL TECHNIQUE

4.1 Introduction

Direct decomposition and selective catalytic reduction of NO over ZSM-5 zeolite-supported catalysts have been investigated extensively under different conditions in the literature. However, the zeolites used have been usually provided by commercial sources. The effect of zeolite properties, e.g. silica alumina ratio, on the catalytic activity of the catalysts has rarely been addressed. In this study, the starting materials were ZSM-5 zeolites in the Na^+ form synthesised in our laboratory, as reported in Chapter 3, or the H^+ form zeolites provided by Zeolyst International Corporation. The zeolites samples were ion-exchanged with copper or cobalt ions using conventional ion-exchange methods (Larsen et al., 1994; Beutel et al., 1996; Li and Armor 1994). In some cases, the Na^+ ions were ion-exchanged with H^+ ions prior to the ion-exchange with copper or cobalt ions. The catalysts were used for the direct decomposition or SCR of NO in a packed bed tubular reactor. The feed and effluent of the reactor were analysed by a NO_x analyser and a gas chromatograph. This chapter contains detailed descriptions of the catalyst preparations, experimental technique and the procedure involved, as well as the data analysis procedures.

4.2 Catalyst Sources and Preparation Methods

The zeolite samples used in this study were obtained from three different sources:

1. In an early stage of this study, a comprehensive study was performed to synthesise Na-ZSM-5 zeolites with different properties. The zeolites were synthesised with two different methods, with and without a template as described in Chapter 3. The zeolites synthesised had a wide range of silica to alumina ratios. The H-ZSM-5 zeolites were then obtained by ion-exchanging the Na-form of the zeolite with NH_4NO_3 solution followed by calcination of the catalysts.

2. H-ZSM-5 zeolites was also obtained from Zeolyst International Ltd.

3. Some samples including different catalysts such as pillared clays as well as Cu-ZSM-5 zeolites were provided by our collaborative partner at The University of Queensland (Lu and Zhao, 1996).

The catalysts prepared from the zeolites synthesised in our laboratory or provided by Zeolyst International Ltd. are introduced further in Tables 4.1 and 4,2. All the catalysts used in this study were prepared using ion-exchange technique, excepting some of the samples received from The University of Queensland. The details of the preparation methods used for these samples are described in Chapter 7.

4.2.1 Hydrogen Ion-Exchange

To prepare the H-form of ZSM-5 zeolite from the Na-form, Na- ZSM-5 zeolite was ion-exchanged with 0.1 M ammonium nitrate solution at 50 ^{o}C. Similar methods were used by Nishizaka and Minsono (1993) and Sass and Kevan (1988). However, they did not mention the temperature at which the ion-exchange was carried out. Tynjala and Pakkanen (1996) and Wendlandt et al. (1987) also prepared H-ZSM-5 zeolite using a similar method but the ion-exchange was performed at 80 and 70 ^{o}C, respectively. In this study, 10 g of synthesised Na-ZSM-5 zeolite was suspended in 100 ml of NH_4NO_3 solution with a constant, vigorous stirring using a magnetic stirrer for 24 hours. Then solution was filtered and the obtained cake was stirred in deionised water for two hours using a magnetic stirrer, and then filtered. The ion-

exchange process was repeated three times. After the third ion-exchange, the obtained cake was dried at 105-110 °C overnight and then the sample was calcined at 500 °C for 3 hours to remove ammonia from zeolite lattice. The calcination was carried out in an furnace under a stream of air with a flow rate of 2.5 l min^{-1}. The resulting solids are called H-form ZSM-5 zeolites.

4.2.2 Copper Ion-Exchange

Copper ion-exchanged zeolite samples were prepared using the conventional method reported in the literature (Li and Hall, 1990). The starting materials were Na-ZSM-5 synthesised or H-ZSM-5 zeolites either provided by Zeolyst International Corporation or using hydrogen ion-exchanged synthesised Na-ZSM-5. The zeolite was ion-exchanged in 0.01 M copper acetate aqueous solution with constant, vigorous stirring. The ion-exchange processes were performed at room temperature or 45 °C, repeated several times depending on the desirable ion-exchange level and each time lasting 24 hours. The samples were then dried at 105-110 °C overnight.

In order to provide a systematic approach for preparation of Cu-ZSM-5 catalysts with a desired copper ion-exchange level, nine samples classified in three groups were ion-exchanged at three different temperatures (25, 45 and 80 °C). The ion-exchange processes took 24, 48 and 72 hours, respectively. The preparation procedures are further discussed in Chapter 5 where the effect of ion-exchange temperature and repetition of ion-exchange procedure are studied.

The obtained catalysts were analysed and the SiO_2/Al_2O_3 ratios and the copper ion-exchange levels of the catalysts were calculated. More descriptions and the results of the analyses are given in Section 4.9 and Appendix C, respectively. The copper ion-exchanged ZSM-5 catalysts for this study are summarised in Table 4.1.

Table 4.1. Copper ion-exchanged ZSM-5 zeolites prepared for this study.

Sample code	Sample name	SiO_2/Al_2O_3 ratio	Zeolite source
Cu-25-1	H-Cu-ZSM-5-50-58.0	50	Zeolyst
Cu-25-2	H-Cu-ZSM-5-50-77.3	50	"
Cu-25-3	H-Cu-ZSM-5-50-99.3	50	"
Cu-45-1	H-Cu-ZSM-5-50-62.3	50	"
Cu-45-2	H-Cu-ZSM-5-50-106.7	50	"
Cu-45-3	H-Cu-ZSM-5-50-139.3	50	"
Cu-80-1	H-Cu-ZSM-5-50-132.6	50	"
Cu-80-2	H-Cu-ZSM-5-50-111.1	50	"
Cu-H-NT	H-Cu-ZSM-5-40-101.7	40	Our laboratory
Sample 5	Cu-ZSM-5-176-199.2	176	"
Sample 9b	Cu-ZSM-5-140-160.7	140	"
3Cu24-100	Cu-ZSM-5-100-127.5	100	"
Sample 7b	Cu-ZSM-5-100-168.6	100	"
3Cu 8-100	Cu-ZSM-5-100-108.3	100	"
Sample 7a	Cu-ZSM-5-100-99	100	"
Cu-25-2	H-Cu-ZSM-5-50-77.3	50	Zeolyst
Cu-25-3	H-Cu-ZSM-5-50-99.3	50	"

4.2.3 Cobalt Ion-Exchange

Different preparation methods are addressed in the literature for preparation of cobalt ion-exchanged ZSM-5 zeolites. The methods reported in the literature can be classified in two groups, batch (Sun et al, 1996), and semi-continuous system (Beutel et al., 1996). In the first method, an aqueous solution of cobalt acetate or cobalt nitrate (0.001-0.02 M) is added to a certain amount of a Na-form or H-form ZSM-5 zeolite. The cobalt exchange is typically carried out at 80 °C. The ion-exchange time

is dependent on the desired ion-exchange level. The resultant slurry is filtered, washed with deionised water and dried at 110 °C overnight.

The first method was easier to use, however, it has some limitations. The water available in the solution is evaporated at 80 °C which leads to increasing concentration of the ion-exchange solution. Therefore, the ion-exchange between Na^+ or H^+ ions in the zeolite and Co^{2+} ions in the solution may not be performed well. Preparation of a small amount of catalyst is more difficult using this method as a smaller volume of the solution is used to ion-exchange less zeolite.

In this study, one sample was prepared using this method to compare the effect of catalyst preparation on the activity of Co-ZSM-5 zeolites. For this purpose, 500 ml of acetate solution (0.01 M) was added to 10 g of ZSM-5 zeolite. The ion-exchange was carried out at 80 °C for 24 hours. The obtained slurry was filtered, washed with deionised water and dried at 110 °C for 24 hours.

In the semi-continuous system, a refluxing system is employed to return the evaporated water into the zeolite slurry. Therefore, the solution would not be concentrated due to evaporation of the water. Cobalt salt solution is added drop-wise to a mixture of the zeolite and water. For example, 10 g of zeolite is mixed with 500 ml of deionised water. 500 ml of cobalt acetate (0.01 M) is added drop-wise during the ion-exchange to the mixture of the zeolite and water. After a certain time, for example 24 hours, the slurry is filtered and washed with a great deal of deionised water. To achieve more cobalt loading, this procedure can be repeated for several times. The obtained cake is dried overnight at 110 °C.

In this project the semi-continuous system was used to prepare most of the Co-ZSM-5 zeolite catalysts. In a typical cobalt ion-exchanged preparation, the catalyst was prepared using the same sources of zeolites as used for preparation of Cu-ZSM-5. The zeolite was ion-exchanged using cobalt acetate solution (0.03 M) at 80 °C. To obtain cobalt acetate solution, 3.71 g of cobalt acetate tetrahydrate, $Co(CH_3COO)_2.4H_2O$, was dissolved in 500 ml of deionised water. To prepare cobalt ion-exchanged ZSM-5, for instance, 9 g of H-ZSM-5 was suspended in 450 ml of

deionised water and 150 ml cobalt acetate solution was slowly added into the zeolite slurry using a refluxing system. The solution was vigorously stirred using a magnetic stirrer. The sample was ion-exchanged with cobalt acetate three times, each time for 24 hours. After each ion-exchange, the slurry was filtered, and the obtained cake was washed with deionised water. This procedure was repeated after the last ion-exchange, followed by drying at 105 °C for 24 hours. More descriptions on calculation of SiO_2/Al_2O_3 ratio, cobalt ion-exchange level, and the results of the analysis are given in Section 4.9 and Appendix C, respectively. The cobalt ion-exchanged ZSM-5 catalysts for this study are summarised in Table 4.2.

Table 4.2. Cobalt ion-exchanged ZSM-5 zeolites prepared for this study.

Sample code	Sample name	SiO_2/Al_2O_3 ratio	Zeolite source
6a	H-Co-ZSM-5-80-71	80	Zeolyst
Co-H80	H-Co-ZSM-5-80-77.9	80	"
6b	H-Co-ZSM-5-80-96.6	80	"
CoH-NTB	H-Co-ZSM-5-40-45	40	Our laboratory
HCo-80	H-Co-ZSM-5-80-428	80	Zeolyst

4.3 Catalyst Pre-treatment

In all experiments where the GC was used for analyses of the reactor effluents, the catalysts were flushed with pure helium with a flow rate of 100 ml min^{-1} for one hour at 500 °C. In some experiments carried out using the catalysts received from The University of Queensland, only a NO_x analyser was used. In these cases, the catalysts were used without any pre-treatment. The effect of the pre-treatment, flushing with helium at 500 °C for one hour, on the activity of the most active catalyst of this group was also investigated. After flushing the catalyst with helium for one hour, the

furnace was set at the required temperature for experiments and the samples were continuously flushed with helium until the reactor reached the required temperature.

4.4 Flow Sheet Diagram of the Experimental System

The flow sheet diagram of the experimental system for investigation of the activities of the catalysts for decomposition and selective catalytic reduction (SCR) of NO is shown in Figure 4.1. The equipment consists of the following three sections: 1. gas supply system including gas cylinders and mass flow controllers, 2. a reactor equipped with a temperature controller, and 3. gas analysis system. The gas flow could be switched to either pass through the reactor or by-pass it. A 4-way valve, three 3-way valves, and also two by-pass tubes were employed to send the reactor inlet or outlet gases to the GC or NO_x analyser. In all parts of this research, the GC was used to measure the concentrations of N_2, O_2, CO, CO_2, N_2O and hydrocarbons before and after the reactor. The only exception was for the experiments using a group of catalysts including the ten samples received from The University of Queensland. From the data obtained using the GC, NO conversion into N_2 and into N_2O, and also the conversion of hydrocarbons into CO and CO_2 were calculated. For the first group of the samples received from the University of Queensland, NO, NO_2, and NO_x concentrations in the inlet and outlet gas streams of the reactor were measured by the NO_x analyser to calculate NO_x conversions. Then, more experiments over the most active catalyst were carried out using the GC.

Except for the NO_x analyser and the GC, all facilities shown in Figure 4.1 and the NO source gas cylinder were placed in a fume cupboard to ensure safety. A ventilator worked permanently to remove any NO from the fume cupboard. The outlet gases of the system were passed through a series of gas washers, containing high concentrations of NaOH solutions, before releasing them into the atmosphere. To indicate the strength of the alkalinity of the NaOH solutions, a small amount of phenolphthalein was added in the solutions as a visual indicator. When the indicator solution changed colour, the NaOH solutions were renewed.

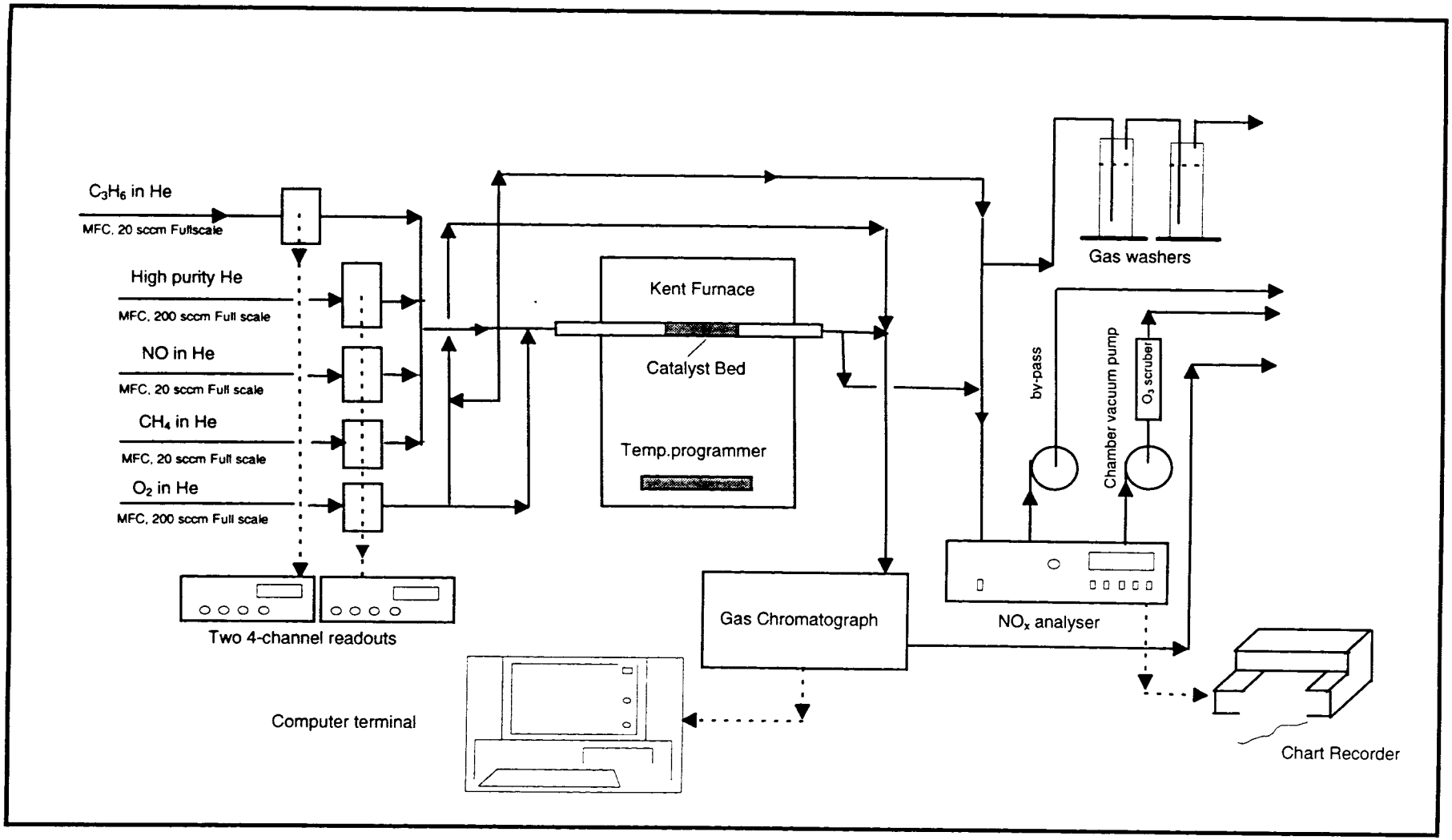

Figure 4.1. Experimental Set-up

4.5 Gas Supply System

The gas supply section consists of six gas containers and five mass flow controllers used with two 4-channel readout units (MKS Instrument Inc., Massachusetts, USA). The gas concentrations in the six cylinders, on the volumetric basis, were:

- 4000 ppm NO and 70 ppm NO_2 in nitrogen (when using the NO_x analyser) or 12% NO in helium (for GC studies), as the NO sources;
- pure helium, as the balance gas;
- 5.24% methane in helium, as a hydrocarbon source;
- 5.32% oxygen in helium, as an oxygen sources;
- and 5.22% propene in helium, as a hydrocarbon source.

Each gas cylinder was connected to one mass flow controller to control the flow rate of the gas. The output signals of mass flow controllers were received on the two 4-channel readout units. The full scales of mass flow controllers were different, depending on the required concentrations (and hence flow rate) of the gases. The types of gases and the full scales of the mass flow controllers are shown in Figure 4.1.

4.6 Reactor and Temperature Controller

A fixed bed tubular reactor containing a catalyst for NO conversion studies was located in a temperature-controlled, electrically heated furnace. The furnace temperature was controlled by a temperature control system. Three different reactors were used in this research: a quartz tube (I.D. 10 mm) and two stainless steel tubes (I.D. 5 and 10 mm). Two thin porous ceramic fibre disks were placed inside the reactor on both sides of the packed catalyst. This prevented the gas flow causing any movement of the catalyst. The furnace was equipped with a temperature indicator.

The temperature of the reactor was also monitored using a thermocouple located inside the catalyst bed.

The difference between the two temperatures was more pronounced at lower rather than at higher temperatures. Furthermore, the temperature in the reactor fluctuated in a range of 6 °C, due to the temperature controlling system which was trying to adjust the temperature. It was observed that the fluctuation of the temperature had a similar effect on the NO conversion. Therefore the reported results on NO conversions are the average NO conversion values during the test. The reported temperatures in this study are based on those measured by the thermocouple because it was located in the catalyst bed. This was regularly checked to ensure that the thermocouple did not touch the reactor wall.

Inside each stainless steel reactor, a cross-shaped steel structure was welded behind the catalyst bed to prevent any catalyst movement due to gas flow as shown in Figure 4.2. Otherwise, the catalyst location might change and therefore the temperature of the catalyst bed would differ from with the specified temperature.

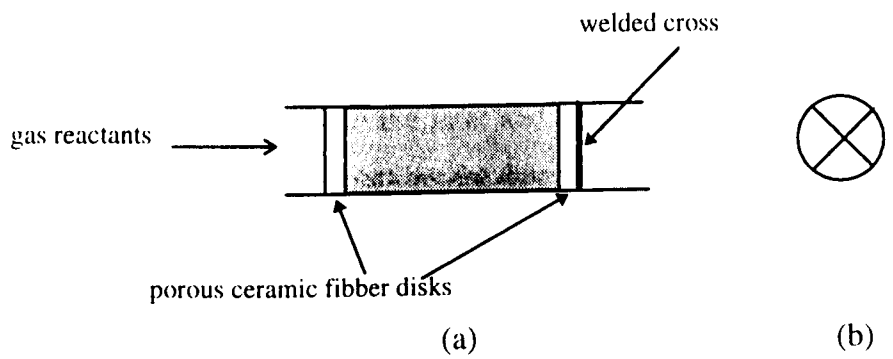

Figure 4.2. A schematic of Catalyst location in the reactor;
a) the reactor with the catalyst bed and welded cross,
b) cross section of welded cross.

Oxygen was added to the other inlet gases (NO, helium, and hydrocarbon in the case of SCR studies) inside the reactor exactly before the furnace. This prevents NO_2

formation upstream of the reactor as NO can react with O_2 to form NO_2 in a homogeneous reaction at ambient temperature. The schematic diagram of this system is given in Figure 4.3.

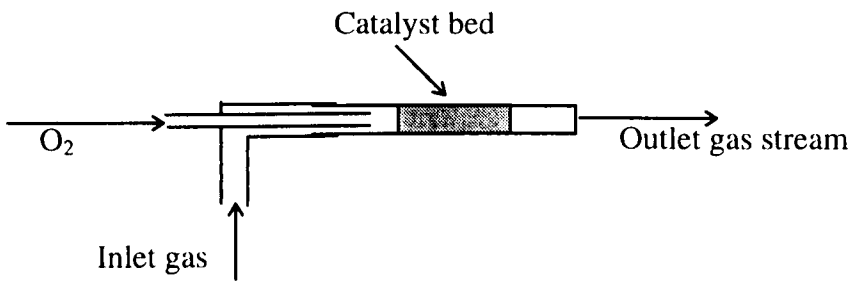

Figure 4.3. Schematic diagram of the inlet and the outlet gas streams of the reactor, showing where O_2 is added into the stream.

4.7 Gas Analysis Instruments

A chemiluminescence NO_x analyser and/or a gas chromatograph equipped with a thermal conductivity detector (TCD) and a flame ionisation detector (FID) connected in series, were used to analyse the inlet and outlet gases. The NO_x analyser and the GC, their calibrations and operations are described below.

4.7.1 NO_x Analyser

The chemiluminescence NO_x analyser (Thermo Environmental Model 42H) equipped with a by-pass pump was utilised to determine the concentrations of NO, NO_2 and NO_x of the inlet and outlet gases. A gas cylinder containing 4000 ppm of NO and 70 ppm NO_2 in N_2 was used as the NO source gas to calibrate the NO_x analyser. A gas stream at a rate of 25 ml min^{-1} passed continuously through the NO_x analyser to detect NO and NO_2.

This instrument was calibrated before being used for each run of the experiment. For this purpose, a calibration by-pass line was designed using a four-way valve to connect NO_x gas cylinder to the NO_x analyser. The same gas used for NO_x analyser studies was also used for NO_x analyser calibration. Since the sample gas flow to the NO_x analyser was required to be at atmospheric pressure, an atmospheric pressure dumping tube was used. The by-pass pump was not used in this research, because the gas flow rates were 100 or 150 ml min^{-1} and the use of the by-pass pump is only necessary in large gas flow rates (minimum 500 ml min^{-1}). A two-pen chart-recorder was connected to the NO_x analyser to record the concentrations of NO and NO_2.

The NO_x conversion, X_{NO_x}, was calculated using NO_x analyser results based on the difference in NO_x concentrations between outlet and inlet gases of the reactor divided by NO_x concentration in the inlet gas as shown in Equation (2-3).

$$X_{NO_x} = \left(\frac{[NO_x]_{in} - [NO_x]_{out}}{[NO_x]_{in}} \right) \times 100 \qquad (2\text{-}3)$$

where $[NO_x]_{out}$ is NO_x concentration in the effluent gas stream and $[NO_x]_{in}$ is NO_x concentration in the inlet gas stream.

This calculation was justified as the influence of changing gas volume over the reactions was very minimal with the very small concentrations of NO and NO_2.

4.7.2 Gas Chromatograph (GC)

A gas chromatograph (Varian, Star 3400CX series) fitted with a thermal conductivity detector (TCD) and a flame ionisation detector (FID) was utilised to analyse the gas streams received from the inlet or outlet of the reactor. The analytical system included two packed columns in series, a Haysep N and a Molecular Sieve Columns, and a combination of the thermal conductivity and the flame ionisation detectors. Molecular sieve (MS 13X) column is used for separation of oxygen, nitrogen, carbon

monoxide and methane, and the Haysep N Column for separation of carbon dioxide, nitrous oxide, ethene and propene. This two-column system operates in series so that the sample enters the Haysep N column and then flows either to the molecular sieve column or by-passes it using a 6-port valve and then enters the detectors. A schematic diagram of the columns and detectors is shown in Figure 4.4 and the specifications of the GC columns are presented in Table 4.3.

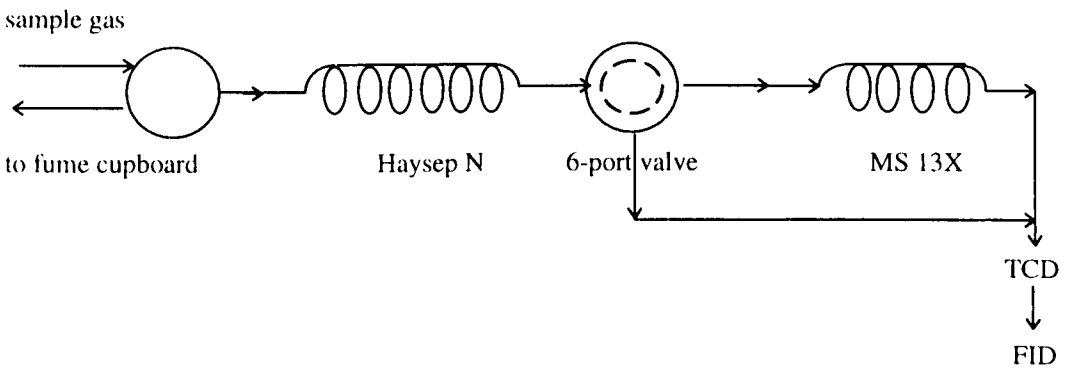

Figure 4.4. Schematic diagram of the GC columns and detectors.

Table 4.3. The specifications of the GC columns.

GC Columns	Column Support	Column Material	Length [ft]	Inside Diameter	Mesh Range
1	Haysep N	Stainless steel	12	1/8 inch	80-100
2	MS 13X	Stainless steel	4	1/8 inch	80-100

The GC required calibration to generate quantitative results. For GC calibration, six gas cylinders containing known amounts of one or more compounds of gases balanced with helium were used. The specifications of the calibration gases are shown in Table 4.4. To calibrate the GC, several runs of each gas cylinder were injected. As a result of each calibration run, a table of results and a chromatogram including peaks related to the gases available in the injected flow were generated. In the table of results, for example in Figure 4.5, the area under each peak and the retention time for each gas were given. The amount of each gas was evaluated by

calculating the area under the peak corresponding to that gas. The system automatically generated a calibration curve for each compound by plotting the concentrations of the gas injected against the detectors response, i.e. peak area. Figures 4.5, 4.6 and 4.7 show typical calibration results, chromatograms and the calibration curves, for N_2, respectively. Once the GC was calibrated, the system used the resulting calibration curves to determine the amount of a calibrated compound in an analytical sample.

Table 4.4. The types and the concentrations of the gases existing in the six gas cylinders used for GC calibration.

Gas Cylinder	O_2 %	N_2 %	CO_2 %	CH_4 %	CO %	N_2O %	C_3H_6 %	C_2H_4 %
1	1.17	0.586	0.560	0.373	0.305			
2	3.21	1.76	1.12	1.52	0.726	-	-	-
3	5.14	3.49	3.21	3.24	1.48	-	-	-
4	-	-	-	-	-	0.481	-	-
5	-	-	-	-	-	-	5.22	-
6	-	-	-	-	-	-	-	5.34

Peak No.	Peak Name	Result (%)	Ret. Time (min)	Time Offset (min)	Area (counts)	Sep. Code	Width 1/2 (sec)
1		31.0018	1.814	0.000	2464076	BV	3.4
2		20.7496	2.164	0.000	1649212	VP	3.8
3		17.5859	3.104	0.000	1397759	PP	5.4
4		7.5041	3.651	0.000	596439	PB	8.1
5		0.0470	3.990	0.000	3732	VP	0.4
6		23.1116	4.143	0.000	1836952	PB	9.6
	Totals:	100.0000		0.000	7948170		

Figure 4.5. A typical print-out of results of a calibration run for O_2, N_2, CO, CH_4 and CO_2.

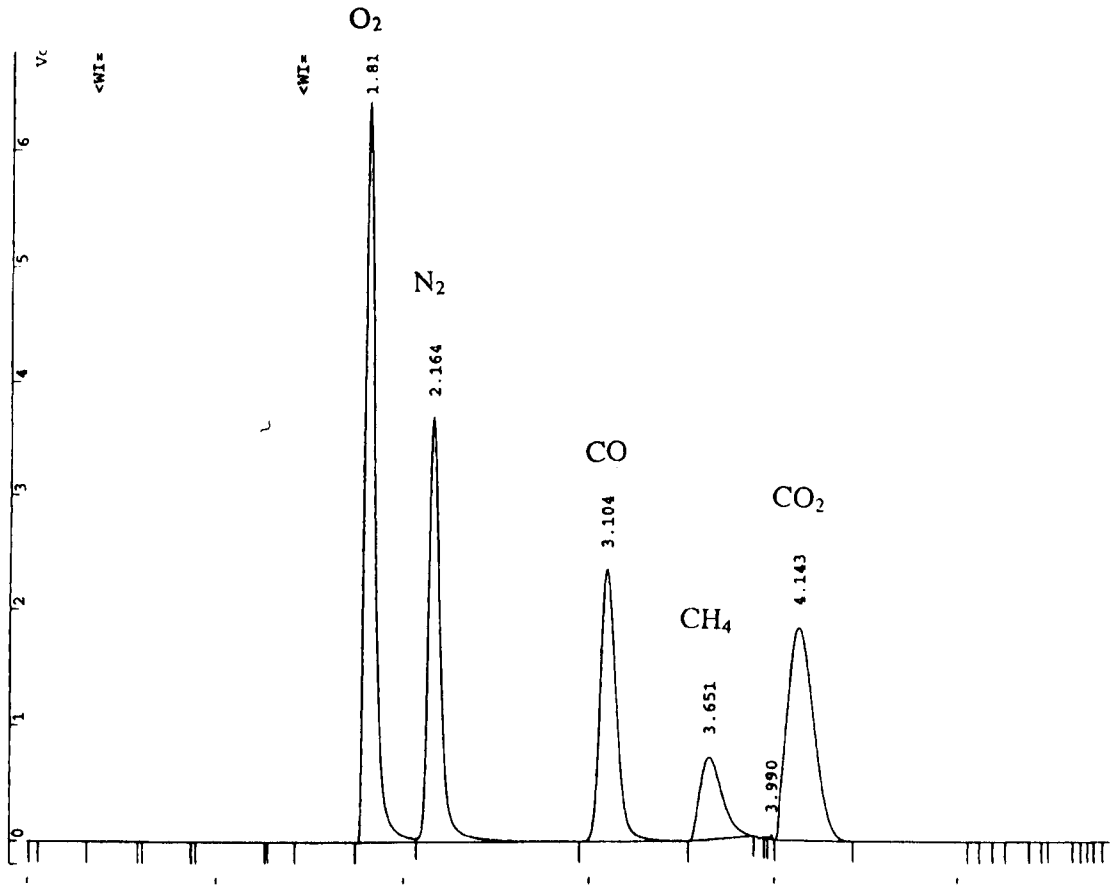

Figure 4.6. A typical chromatogram of a calibration run. Peaks monitored in these chromatograms belong to O_2, N_2, CO, CH_4 and CO_2, respectively.

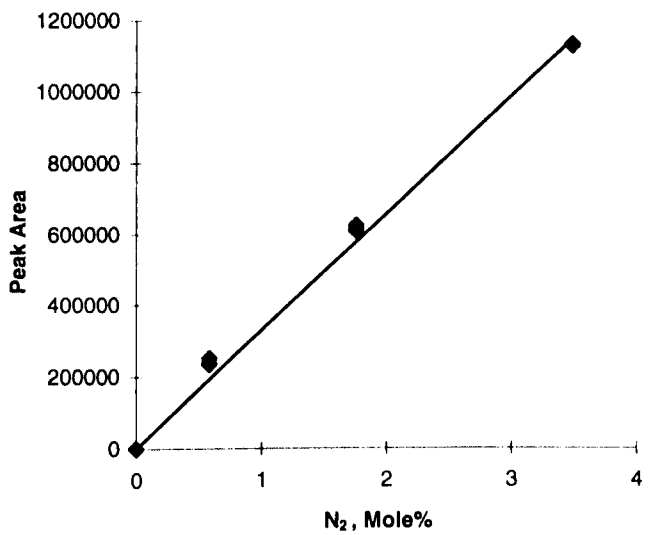

Figure 4.7. A typical calibration curve for N_2.

In general, each chromatogram produced by TCD could have six peaks related to O_2, N_2, CO, CH_4, CO_2 and N_2O, respectively. The first four gases are adsorbed by the molecular sieve column before the 6-port valve switches and detected by the TCD detector. Therefore, the first four peaks to appear belong to O_2, N_2, CO and CH_4, respectively. The valve then switches and sends the sample to detectors through the by-pass line. This is because the other two gases (CO_2 and N_2O) are adsorbed by Haysep N column. If they are allowed to pass the MS column, it would take a greater length of time for the two peaks to appear. These two peaks belong to CO_2 and N_2O, are also detected by TCD. Methane as well as any other hydrocarbons such as C_2H_4 and C_3H_6 are detected by FID, if required.

To record the results of gas analysis, the GC was connected to a computer. Generation of a report and chromatogram are achieved using Varian star 4.0 software. The software was set in such a way that it records the mole percentage of all detected gases (e.g. N_2, O_2, CO, CH_4, CO_2, N_2O and C_3H_6).

Typical chromatograms and the results obtained from the GC analysis of the outlet gas of the reactor are shown in Figures 4.8 and 4.9. The chromatograms show three peaks, two peaks before the valve switched at 3.7 minutes and one after. The first two peaks correspond to O_2 and N_2 and the third peak to CO_2.

Column regeneration was required periodically to achieve better gas separation and remove any possible impurities from the GC columns. The GC had to be re-calibrated after regeneration of the columns and any changes in the flow rate of the GC carrier gas, as each of them changes the retention times. To ensure that the GC calibration had not been changed, several verification runs were performed using calibration gas cylinders containing gases with known concentrations. If the results indicated the concentration measured by the GC differed from the gas concentrations used, the GC would be re-calibrated.

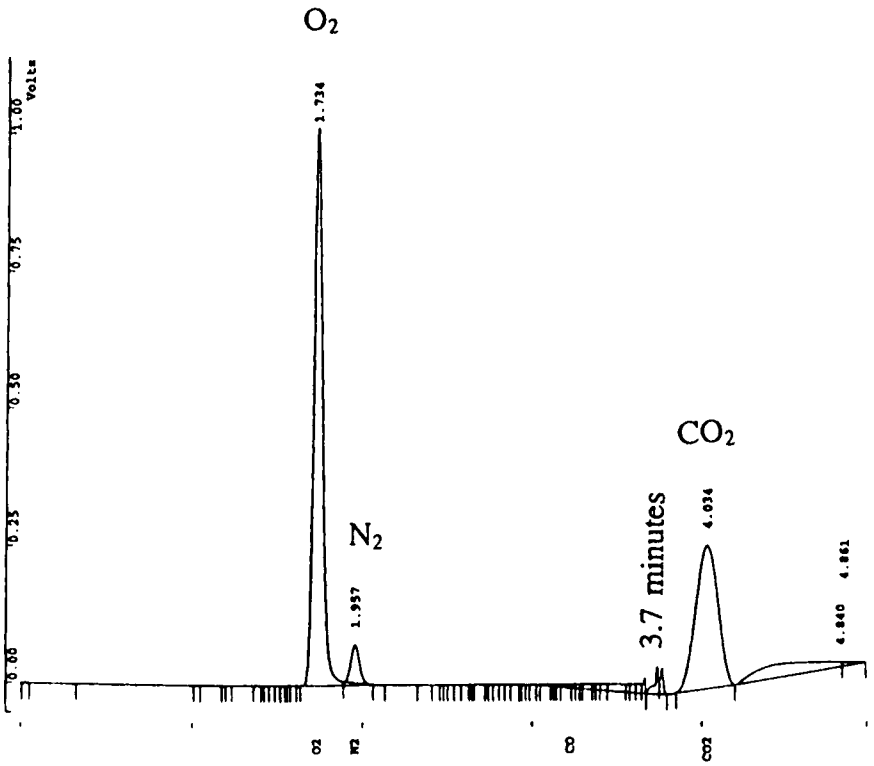

Figure 4.8. A typical chromatogram showing N_2, O_2, CO_2 peaks.

Run Mode : Analysis
Peak Measurement: Peak Area
Calculation Type: External Standard

Peak No.	Peak Name	Result (%)	Ret. Time (min)	Time Offset (min)	Area (counts)	Sep. Code	Width 1/2 (sec)
1	O2	1.0191	1.734	-0.046	356903	PB	3.1
2	N2	0.0694	1.957	-0.050	24103	TS	0.0
3	CO	0.0056	3.226	0.043	2145	VV	2.0
4		0.0000	3.269	0.000	1029	VV	1.4
5		0.0000	3.345	0.000	2962	VV	4.7
6		0.0000	3.367	0.000	1154	VV	0.0
7		0.0000	3.384	0.000	1619	VV	0.0
8		0.0000	3.401	0.000	2822	VV	3.9
9		0.0000	3.531	0.000	8483	VV	4.0
10		0.0000	3.561	0.000	2100	VV	0.0
11		0.0000	3.594	0.000	3312	VV	0.0
12		0.0000	3.619	0.000	3466	VV	0.0
13		0.0000	3.661	0.000	2805	VP	0.1
14		0.0000	3.738	0.000	8483	PV	0.6
15		0.0000	3.769	0.000	5826	VB	0.7
16	CO2	0.5864	4.034	-0.016	237480	BP	8.9
17		0.0000	4.840	0.000	64835	PV	0.0
18		0.0000	4.861	0.000	3558	VB	0.0
	Totals:	1.6805		-0.069	733085		

Figure 4.9. A typical print-out of results reported by the GC, belonged to the chromatogram represented in Figure 4.8.

Finally, the percentage of NO conversion into N_2, X_{NO}, was calculated using Equation (2-1).

$$X_{NO} = 2\left(\frac{[N_2]_{out}}{[NO]_{in}}\right)\times 100 \qquad (2\text{-}1)$$

where $[N_2]_{out}$ is N_2 concentration in the outlet reported by the GC, and $[NO]_{in}$ is NO concentration in the inlet gas stream which is calculated from the folowing equation.

$$[NO]_{in} = \frac{F_{NO}[NO]_{cyl.}}{(F_{NO} + F_{He} + F_{C_nH_m} + F_{O_2})} \qquad (4\text{-}1)$$

where:

$[NO]_{cyl.}$ = concentration of NO in the NO cylinder

F_{NO} = inlet volumetric flow rate of the gas stream containing NO

F_{He} = inlet volumetric flow rate of He

$F_{C_nH_m}$ = inlet volumetric flow rate of the gas stream containing methane or propene

F_{O_2} = inlet volumetric flow rate of the gas stream containing O_2.

4.8 Experimental Procedures

4.8.1 Start-up

At beginning of each experiment, a new catalyst was weighted, and placed into the reactor between two ceramic fibre disks. The reactor was placed inside the furnace and the system was assembled. The reactor was isolated from the atmosphere using two circular bricks on both sides of the reactor.

To perform pre-treatment of the catalyst, the electric furnace was turned on, and set at 500 °C. The helium flow was set at 100 ml min^{-1}, and the helium cylinder valve

was opened. Previously disconnected joints were checked for any possible leakage using soapy water. The catalyst was left at 500 °C under helium gas for one hour. The electric furnace was then set at the required temperature for the experiment. The helium gas was let to pass over the catalyst while the system was approaching the required temperature.

The Gas Chromatograph and the computer were switched on after the valve of the helium gas cylinder supplying carrier gas to the GC was opened. The required method for gas analysis was activated to make GC columns ready for sample injections. This was necessary as different analytical methods were defined depending on the type of the gases available in the analytical sample. For example, to analyse the outlet gas stream of the reactor using the method defined for the direct decomposition studies took less time than the method used for SCR studies. The air supply for the GC switching valve was turned on. The air and hydrogen flow were also turned on in the case of using FID when SCR experiment. The mass flow controllers were set to use a combination of gases depending on the amounts required for the experiment. For direct decomposition of NO, two mass flow controllers were used to control the NO and the helium concentrations. In some cases, oxygen was also used to investigate the effect of the presence of O_2 on direct decomposition of NO. For selective catalytic reduction, besides NO, O_2 and helium, the flow rate of the hydrocarbon used had to be set also.

4.8.2 Operation

The experiment commenced by turning on the mass flow controllers and analysis of the inlet gas stream started once the GC was ready for injection. The GC sample list was activated and a proper file name was given to each injection. The mass flow controller readings were checked during the experiment to ensure that the gases passed to the system. After 20 to 30 minutes operation, the first series of GC analysis was taken. This was repeated until the recorded amount of N_2 reached a relatively constant value. Each time, after achieving a steady-state, the results were recorded in a Table of results. Ten injections were usually required to be taken by the GC to

achieve a relatively constant value. However, sometimes at the beginning of a run, more injections were required as some nitrogen gas may have penetrated into the system while each sample was replaced. Also, when a large increment in N_2 concentration was occurred, more injections were required. This was because the outlet gas concentrations, especially N_2 concentration, often fluctuated at that temperature and took longer time to reach to the stable condition.

At each temperature, the experiments were continued until a steady-state of NO conversion achieved. For this purpose, the results of the gas analysis of the outlet gas stream were checked until identical values obtained for N_2 concentration in the outlet gas stream. Sometimes, it was required to carry out the experiments for an extended time to reach a steady-state condition. For example, the GC took forty samples until the N_2 concentration in the outlet reached a relatively constant value when H-Cu-ZSM-5-32.2.101.7 catalyst was tested at 300 °C. As seen in Figure 4.10, there were

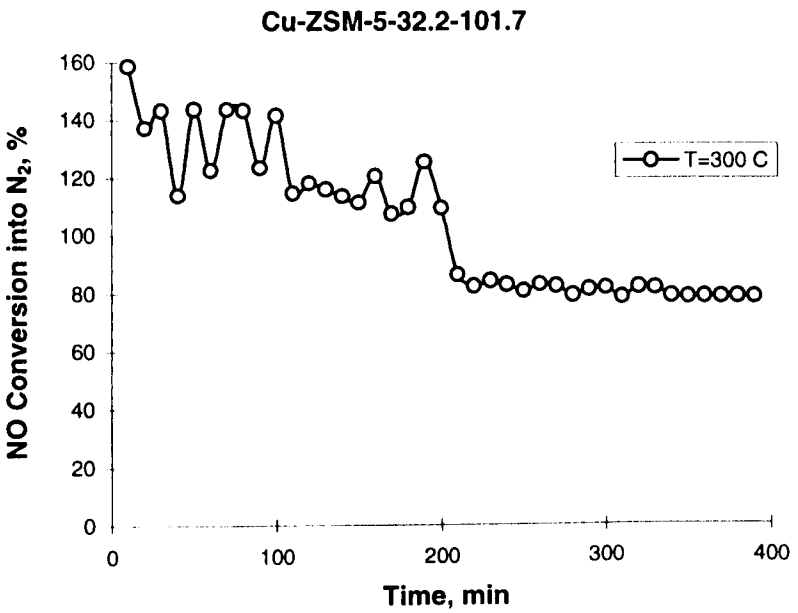

Figure 4.10. The dependence of NO conversion into N_2 on operation time at 300 °C over H-Cu-ZSM-5-32.2-101.7 catalyst. Reaction conditions: 2000 ppm NO, 2000 ppm C_3H_6, 2% O_2, balance He, 1 g catalyst weight, and 100 ml min^{-1} total flow rate.

some fluctuations in N_2 concentration values analysed by the GC when the experiment commenced at 300 °C. This took almost six hours until the steady-state condition was achieved. Then the experiment was continued for almost one more hour to ensure that there was no more fluctuations in the N_2 concentrations.

Fluctuation in the NO concentration was usually observed when a great deal of increment in N_2 concentration occurred. It may be postulated that the reaction intermediates attached to the active sites which were involved in N_2 production, started to desorb at this temperature. At 350 °C, as shown in Figure 4.11, it took two hours to achieve a steady-state value for N_2 concentration and the experiment was continued for almost four more hours but no more changes were observed. The average of the results obtained within the last hour of the experiment were considered as the NO conversion at this temperature.

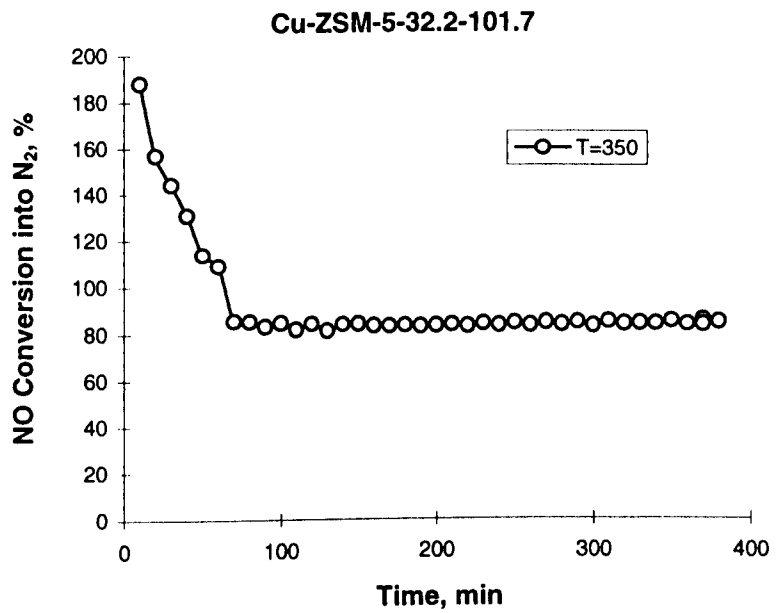

Figure 4.11. The dependence of NO conversion into N_2 on operation time at 350 °C over H-Cu-ZSM-5-32.2-101.7 catalyst. Reaction conditions: 2000 ppm NO, 2000 ppm C_3H_6, 2% O_2, balance He, 1 g catalyst weight, and 100 ml min^{-1} total flow rate.

After achieving a steady-state result at a certain temperature, the condition of the operation was changed to another interested condition, e.g. in the case of investigation of the effect of temperature, the electric furnace temperature was set at another temperature of interest and the experiments were repeated.

4.8.3 Shut-down

After each experiment run, the reverse order of the start up procedure was performed. The electric heater was turned off if the catalyst was not going to be used for further investigation. After the reactor was cooled down, it was opened and the catalyst was removed and stored for further use or analysis if required. If the catalyst was going to be used for a new run of experiment, the pre-treatment of the catalyst was performed. Therefore all mass flow controllers were shut down (according to the following procedure) except the one used for helium flow.

All gas cylinders but helium were closed. The mass flow controllers were left on until the readout of the mass flow controllers showed that no gas passed through the system. Then, the mass flow controllers were switched off and the valves of the gas cylinders were closed. The helium was left to flow through the system until the reactor had been purged of all other gases. For helium, again the same shut-down procedure had to be repeated.

To prevent ruining the GC columns, helium was sent through the columns until the columns were cooled down to below 70 ^{o}C. Then, the valve of the helium gas cylinder providing the GC carrier gas was closed.

4.9 Data Analysis

In order to compare the catalytic activity of the catalysts, it was necessary to analyse the catalysts. For this purpose, 0.5 g of each catalyst was sent to Amdel Laboratories, Ltd., South Australia, prior to being used. The catalysts were analysed using the

whole rock fusion and Inductively Coupled Plasma (ICP) methods to determined the quantity of the elements and oxides available in the catalyst and the results are presented in Appendix C. The most important compounds and elements which were required to evaluate the catalyst quantitatively were SiO_2, Al_2O_3, Na_2O and Cu and/or Co. Typical results of analysis received from Amdel Laboratories for three samples are shown in Tables 4.5 and 4.6.

Table 4.5. Typical analytical results of SA-C5, STM-C5 and Cu-H-NT catalysts.

Sample	Al_2O_3, %	CaO, %	Fe_2O_3, %	K_2O, %	MgO, %	MnO, %
SA-C5	12.6	0.08	0.10	0.02	0.08	<0.01
STM-C5	0.46	0.08	0.23	0.04	0.09	<0.01
Cu-H-NT	4.06	0.02	0.07	<0.01	<0.01	<0.01

Table 4.6. Typical analytical results of SA-C5, STM-C5 and Cu-H-NT catalysts.

Sample	Na_2O, %	P_2O_5, %	SiO_2, %	TiO_2, %	Cu, %	Co, ppm
SA-C5	0.017	0.02	78.0	0.060	1.39	<20
STM-C5	0.12	0.08	72.8	15.8	2.73	90
Cu-H-NT	0.11	0.02	82.1	0.010	2.59	260

From the results of these analysis, copper ion-exchange levels and SiO_2/Al_2O_3 ratios of the catalysts were calculated. Cu ion-exchange level was calculated as twice (oxidation number of copper) the number of copper atoms divided by number of Al atoms. According to this definition, for instance, copper ion-exchange level and SiO_2/Al_2O_3 ratio of a sample containing 1.06% Cu (w/w %), 1.56% (w/w %) Al_2O_3 and 88.6% SiO_2 (w/w %) are calculated as:

$$\text{Copper ion-exchange level (\%)} = 2\frac{1.06}{64} / \left(\frac{1.56}{102} \times 2\right) \times 100 = 108.3\ \%$$

$$SiO_2/Al_2O_3 = \frac{88.6 / 60.06}{1.56 / 102} = 96.454$$

The NO conversion into N_2 was calculated using the Equation (2-1).

Turnover Frequency (TOF) is often used to express the reaction rate in catalytic reactions. TOF which is defined as the number of NO molecules converted to N_2 per copper site per second, was calculated using the following formula:

$$TOF = \frac{F[NO]_{in}(X_{NO} / 100)}{m_{Cu} / 64} \qquad (4\text{-}2)$$

where:

F is the inlet gas flow rate, [l s^{-1}],

$[NO]_{in}$ is concentration of NO in the inlet stream, [mol l^{-1}],

X_{NO} is the NO conversion into N_2, [%], and

m_{Cu} is copper mass available in the catalyst, [g].

For example, TOF for NO decomposition at 450 °C when 100 ml min^{-1} gas including 2000 ppm (0.2%) NO in helium passed over 0.5 g of Cu-ZSM-5 was calculated as follows. The catalyst included 2.59% copper. The analysis of the outlet gas of the reactor showed that 0.0400 % of this gas was N_2 which was produced due to NO conversion at 450 °C.

$$X_{NO} = \frac{2 \times 0.0400}{0.2} = \frac{40}{100}$$

and:

$$TOF = \frac{100\,(\frac{ml}{min}) \times \frac{1min}{60s} \times \frac{0.2}{100} \times \frac{1}{22400}(\frac{mole}{ml}) \times \frac{40}{100}}{0.5g \times \frac{2.59}{100} \times \frac{1mole}{64g}} = 2.94 \times 10^{-4} \quad s^{-1}$$

4.10 Experimental Error Analysis

There are several sources of errors in the results relating to the operation of the experimental system. These were identified as follows in the early stages of this research and precautions were taken in order to minimise the errors involved in this study.

Converting NO to the other forms of oxides of nitrogen especially NO_2 and N_2O when doing an experiment in the presence of O_2 is one of the possible errors. NO_2 is formed in a homogeneous reaction of the O_2 and NO at ambient temperatures upstream to the reactor. This can occur if NO and O_2 have a possibility of mixing before entering the reactor. In the present study, the oxygen stream in the inlet was mixed with reactants including NO exactly before the inlet gas entered the reactor to prevent NO conversion to other oxides of nitrogen especially to NO_2.

Penetration of N_2 into the experimental system before and while the experiment is in progress can change the results. All the joints were checked with soapy water after each change of catalyst to ensure that there was not any leakage or air penetration into the system. In addition, the catalyst had undergone pre-treatment by flushing helium through the system. Therefore, if any N_2 might penetrated into the tubing system before starting an experiment, it would have been cleaned by the helium gas. Furthermore, the gas streams were continuously fed to the gas chromatograph, so that no N_2 contamination occurred.

Moving the catalyst from its place due to the flowing gas may occur during the experiment. Therefore, the catalyst may not be in that part of tube which is located in the furnace. A steel shape, resembling a cross, was welded behind the catalyst bed inside the tube to prevent the catalyst moving with the flowing the gas over the catalyst. This was done to ensure that the catalyst was located at its position in the furnace.

To ensure that the temperature control of the furnace worked correctly and the temperature reading was reliable, a thermocouple was utilised to check the temperature of the catalyst bed. The thermocouple rod was located inside the catalyst bed. It was also checked to see that it did not touch the body of the reactor or the welded cross.

In performing the necessary calculations for determining NO conversion and TOF, errors enter the end results from manual measurements made in performing the experiment. The uncertainty of the measured volumetric flow rates by mass flow controllers are ±1% of the full-scale of each mass flow controller. The full-scale of the mass flow controller for NO measurement was 10 ml min^{-1}. Therefore, 0.1 ml min^{-1} error could be involved in each NO measurement. The error of the gas analysis by GC is very small as it is shown in Table 4.8 and is negligible compared to the error of mass flow controllers. This is exhibited in Chapter 8 when validity of the data is discussed. Based on these facts, uncertainties involved in calculation of NO conversion calculated and was 11.7% and 11.9% for direct decomposition and SCR when an inlet gas including 2000 ppm NO with a total flow rate of 100 ml min^{-1} was used respectively. The details of the error analysis are given in Chapter 8 where the results of this study are evaluated.

Random errors for gas concentration measurements from the GC were analysed using standard statistic procedure (Taylor, 1982). For a given set of experimental conditions, the last five members of each set of data were taken after the system reached the steady-state. It was understood that the repeatability of the data was very high and the uncertainty was less than 1%. For example, from the data used in Figures 4.10 and 4.11, the last five N_2 concentrations, shown in Table 4.7 at both temperatures, 300 and 350 °C were considered.

The obtained uncertainties in the N_2 concentrations were 0.05% and 0.43%. These values were obtained by calculating the standard deviations, σ_x, and standard deviation of the mean, $\sigma_{\bar{x}}$ using Equations (4-3) and (4-4) for the last five NO

Table 4.7. The last five data reported by GC for N_2 concentrations over H-Cu-ZSM-5-32.2-101.7. Reaction condition: 2000 ppm NO, 2000 ppm C_3H_6, 2% O_2, balance helium, 1 g catalyst weight, and 100 ml min^{-1} total flow rate.

Temperature	N_2 concentrations in the outlet gas obtained using GC				
300 °C	0.0787	0.0874	0.0785	0.0784	0.0785
350 °C	0.0837	0.0839	0.0835	0.0855	0.0845

conversions presented in Figures 4.10 and 4.11. These values are detailed in Table 4.8.

$$\sigma_x = \sqrt{\frac{1}{N}\sum_{i=1}^{N}\left(x_i - \bar{x}\right)^2} \qquad (4\text{-}3)$$

$$\sigma_{\bar{x}} = \frac{\sigma_x}{\sqrt{N}} \qquad (4\text{-}4)$$

Table 4.8. Standard deviation, standard deviation of the mean, and uncertainty for the last five data used in Figures 4-10 and 4-11 at 300 °C and 350 °C respectively.

Temperature	σ_x	$\bar{x}$	$\sigma_{\bar{x}}$	uncertainty, %	final answer
300 °C	0.0001	0.0785	0.00004	0.05%	0.0785±0.00004
350 °C	0.0007	0.0844	0.00031	0.37%	0.0845±0.00031

From these calculations, it is concluded that despite the different errors involved in the experiment, repeatability of the data is very high. The maximum uncertainty of the results obtained in this study are calculated and reported in Chapter 8. These calculations are the base of the error bars used in the following Chapters.

CHAPTER FIVE

DIRECT DECOMPOSITION OF NITROGEN MONOXIDE

5.1 Introduction

In Chapter 4, catalyst preparation methods, experimental technique and procedure, and data analysis methods were discussed. In this Chapter, the results obtained for several aspects of the direct decomposition of NO are presented and discussed. This Chapter includes two sections: 1. the effect of catalyst preparation on copper ion-exchange level and the activity of the catalyst for the direct decomposition; and 2. kinetic studies for the direct decomposition.

In order to investigate the effect of catalyst preparation conditions on the direct decomposition of NO, nine samples were prepared under different ion-exchange conditions. In the first section, after description of the preparation procedure for these catalysts, the effect of ion-exchange temperature and number of repetition of the ion-exchange procedure on copper ion-exchange level are presented. The effect of catalyst preparation methods on the direct decomposition of NO with and without the presence of oxygen are also presented and discussed.

In the second part of this Chapter, the results obtained in the kinetic studies over Cu-ZSM-5-32.2-101.7 catalyst for the dependence of the NO decomposition rate on partial pressure or concentration of NO are presented and discussed.

5.2 The Effect of Preparation Method on Cu Ion-Exchange Level

5.2.1 Preparation of Catalysts from ZSM-5 Support

In order to convert ZSM-5 zeolite into a proper catalytic form, different preparation techniques can be employed (Acres et al., 1981). Ion-exchange is widely accepted (Li and Hall, 1990; Hirabayashi et al., 1992; Zhang and Flytzani-Stephanopoulos, 1996) as an effective technique for preparation of an active, selective and stable catalyst from ZSM-5 zeolite, as this zeolite exhibits special ion-exchange properties. This zeolite is usually synthesised in sodium or hydrogen form. The sodium or hydrogen ions available in the zeolite framework are ion-exchanged with a desirable cation. For example, in Cu-ZSM-5 catalysts, copper ions have been ion-exchanged with sodium or hydrogen ions in Na-ZSM-5 or H-ZSM-5 zeolite. The ion-exchange level for Cu-ZSM-5 catalyst is defined by $2Cu/Al \times 100$ where 2Cu is equal to the amount of exchanged copper with Na^+ or H^+ ions. For stoichiometric exchange of copper ions for sodium or hydrogen ions, the Cu/Al ratio should be 0.5 assuming that one Cu^{2+} charge compensates two aluminium sites or exchanges for two sodium ions (Iwamoto et al., 1989). Similar definition has been given for stoichiometric exchange of cobalt ions for sodium or hydrogen ions (Zhang et al., 1995a).

It was reported that Cu ion-exchange level above 100%, achieved by either repetition of ion-exchange procedures (Iwamoto et al., 1989) or by adjusting the pH of ion-exchange solution (Curtin et al., 1997), showed high catalytic activity for direct decomposition of NO. However, there is no systematic approach reported in the literature for preparing a catalyst with a certain copper ion-exchange level. In order to devise a systematic preparation method for ZSM-5 zeolite supported catalysts, it was essential to investigate the effects of different factors which affect the copper ion-exchange level of the zeolite. The following parameters could affect the type of cation sites or the ion-exchange level of a cation with sodium or hydrogen in Na-ZSM-5 or H-ZSM-5 parent zeolites respectively:

- Ion-exchange temperature (Ward, 1984)
- Ion-exchange time (Dyer, 1988)
- Type of copper salt solution (Wichterlova et al., 1995)
- The concentration of the cation exchange solution (Ward, 1984)
- Number of repetitions of ion-exchange procedure (Iwamoto et al., 1989)
- pH level of the ion-exchange solution (Zhang et al., 1995b)
- Thermal pre-treatment time of the ZSM-5 (Wendlandt et al., 1987)

From these parameters, the effect of ion-exchange temperature and repetition of ion-exchange procedure on the copper ion-exchange level is investigated. In order to further elucidate the effect of catalyst preparation on the activity of the catalyst, the prepared samples are tested for NO decomposition with and without the presence of oxygen. Without the use of any reducing agent such as a hydrocarbon, this type of NO decomposition is called direct decomposition.

5.2.2 Catalyst Preparation and Specification

H-ZSM-5 zeolite with SiO_2/Al_2O_3 ratio of 50 provided by Zeolyst International Incorporation was used as the parent zeolite. The copper ion-exchange temperature and time were varied in order to investigate the effect of the temperature and repetition of ion-exchange procedure on the copper ion-exchange level. Nine samples of copper ion-exchanged ZSM-5 zeolite were ion-exchanged at three different temperatures, and by repetition of the ion-exchange procedures. The samples can be classified in three groups, depending on the temperature of ion-exchange (25, 45 and 80 °C). At each temperature, three samples were ion-exchanged with copper acetate for 24, 2×24 and 3×24 hours. The specifications of the preparation procedures are summarised in Table 5.1 .

To prepare the above samples, the following sequential steps were performed:

Table 5.1. Specifications of preparation of Cu-ZSM-5 catalysts prepared from H-ZSM-5.

Sample No.	Ion-exchange temperature, °C	Ion-exchange times hours	Catalyst Identification
1	25	1×24	H-Cu-ZSM-5-50-58.0
2	25	2×24	H-Cu-ZSM-5-50-77.3
3	25	3×24	H-Cu-ZSM-5-50-99.3
4	45	1×24	H-Cu-ZSM-5-50-62.3
5	45	2×24	H-Cu-ZSM-5-50-106.7
6	45	3×24	H-Cu-ZSM-5-50-139.3
7	80	1×24	H-Cu-ZSM-5-50-132.6
8	80	2×24	H-Cu-ZSM-5-50-111.1
9	80	3×24	-

1 Three separate 9 g portions of H-ZSM-5 zeolites (SiO_2/Al_2O_3 = 50), were stirred in 900 ml of copper acetate solution at three different temperatures, 25, 45, and 80 °C.

2 After 24 hours, each solution was filtered. The obtained cake was transferred to a flask and the sample was stirred in 900 ml of deionised water for two hours at room temperature. The solution was again filtered, washed with deionised water, and dried at 105-110 °C for 24 hours.

3 2 g of each sample was taken out, and named as Cu-ZSM-5(24h, 25 °C), Cu - ZSM-5(24h, 45 °C) and Cu-ZSM-5(24h, 80 °C), respectively. The rest of each sample was ion-exchanged again in 700 ml of a fresh copper acetate solution. All the three samples were ion-exchanged for a further 24 hours at the same temperatures as in Step 1.

4 After repeating Step 2, 2 g of each sample was taken out and named as Cu-ZSM-5(24×2h, 25 °C), Cu -ZSM-5(24h×2, 45 °C) and Cu-ZSM-5(24×2h, 80 °C), respectively. The rest of each sample was once again ion-exchanged using 500 ml of copper acetate solution.

5 After the samples had been ion-exchanged three times, they were washed with deionised water at room temperature and filtered. Then, the samples were dried for 24 hours. These samples were denoted as Cu-ZSM-5(24×3h, 25 °C), Cu - ZSM-5(24×3h, 45 °C) and Cu-ZSM-5(24×3h, 80 °C).

After preparation, a portion of each sample was analysed by Amdel Laboratories, SA, to determine the silica to alumina ratios and copper loading of the catalysts. The results of the analysis are given in Appendix C. To investigate the effect of preparation on the direct decomposition, NO decomposition experiments with and without the presence of oxygen, were performed over two group of samples. The first group included three samples ion-exchanged for 24 hours at different temperatures (25, 45 and 80 °C). The second group included three samples ion-exchanged at 45 °C once, twice, and three times, each time for 24 hours.

NO conversions to N_2 were determined using the concentrations of nitrogen in the inlet and outlet gas streams. The inlet gas stream contained 0.2% (2000 ppm) NO which was checked randomly to ensure that the mass flow controllers were working accurately. The NO conversion into N_2 was calculated using Equation (2-1).

$$X_{NO} = 2\left(\frac{[N_2]_{out}}{[NO]_{in}}\right)\times 100 \qquad (2\text{-}1)$$

5.2.3 The Direct Decomposition of NO

The effects of ion-exchange temperature and ion-exchange time on copper ion-exchange level were investigated using H-ZSM-5-50 zeolites. The results are shown in Figure 5.1. The influence of the ion-exchange temperature was examined by using the nine samples classified in three groups, and each group was ion-exchanged at one of the following three temperatures: 25, 45 and 80 °C. The results proved that the effect of ion-exchange temperature depends on ion-exchange time. For example, if the ion-exchange procedure is performed for 24 hours, increasing temperature leads

to a higher ion-exchange level. Increasing temperature from 25 to 45 °C still increases copper ion-exchange level if the ion-exchange procedure is repeated twice (48 hours) or three times (48 hours). However, from 45 to 80 °C, repetition of ion-exchange results in a lower ion-exchange level if ion-exchange is performed for 48 hours. This indicates that at higher temperatures, copper ions may hydrolyse and convert to copper hydroxide and then decompose to cupric oxide which is insoluble in water.

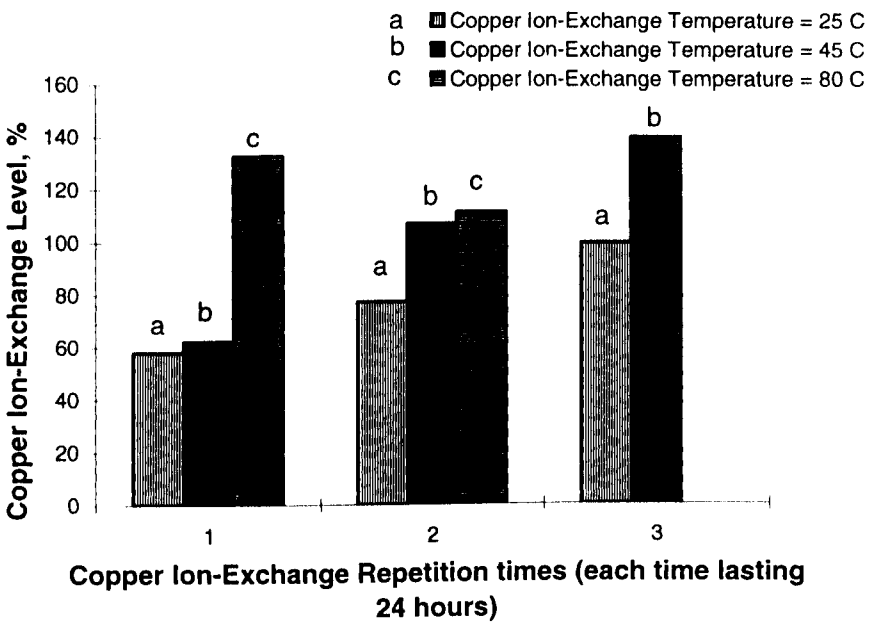

Figure 5.1. The dependence of copper ion-exchange level on ion-exchange temperature and the number of repetition of ion-exchange.

The effect of repetition of ion-exchange procedure depends on ion-exchange temperature. Repetition of ion-exchange procedure increased the copper ion-exchange level when the catalyst was ion-exchanged at 25 °C or 45 °C. However, this was not observed when the catalyst was ion-exchanged at 80 °C. At this temperature, after 24 hours of ion-exchange, 132.6% copper ion-exchange level was achieved however, by repetition of ion-exchange procedure for a further 24 hours, it was reduced to 111.1%, while after 72 hours copper ion-exchange at 80 °C, the slurry turned black. Based on the author's knowledge, this phenomenon has not been reported in the literature. It seems that at such a high temperature, some of copper

acetate may hydrolyse and convert to copper hydroxide, which then decomposes to cupric oxide, according to the following two reactions:

$$Cu\ (CH_3COO)_2 + 2H_2O \rightleftharpoons Cu(OH)_2 + 2CH_3COOH \quad \text{(R5-1)}$$

$$Cu(OH)_2 \rightleftharpoons 2H_2O + CuO \quad \text{(R5-2)}$$

A comparison among the ion-exchange levels of the samples prepared at the three different temperatures for 24 hours revealed that increasing the temperature from 25 to 45 °C only increased the ion-exchange level by 4%. This was low compared to when the temperature was increased from 45 to 80 °C, which resulted in enhancement of the ion-exchange level by 70%. In contrast, comparison among the samples ion-exchanged twice (each time for 24 hours) revealed that the effect of increasing the temperature from 25 to 45 °C is more pronounced (increasing copper ion-exchange level by 30%) than from 45 to 80 °C (the ion-exchange level was increased by only 4%).

The catalysts were tested for direct decomposition of NO using a gas of 2000 ppm (0.2%) NO in helium. The catalyst weight and the total flow rate of the gas were 1 g and 150 ml min^{-1} respectively. As Figure 5.2 shows, increasing the ion-exchange temperature from 25 to 45 °C improved the NO conversion over the whole temperature range. The improvement was due to enhancement in the ion-exchange level from 58% to 62.3%. By increasing the temperature from 45 to 80 °C, the ion-exchange level improved from 62.3 to 132.6% and as a result, the catalytic activity of the catalyst also improved. However, this only occurred over a narrow temperature range (380-550 °C). On either side of this range, the conversion level of NO over the catalyst was reduced.

In order to investigate the effect of ion-exchange time on the activity of Cu-ZSM-5 zeolites for direct decomposition of NO, the catalysts which were prepared by conducting an ion-exchange once, twice, and three times, each time being 24 hours at 25 °C, were tested. The copper ion-exchange level achieved after one, two and three

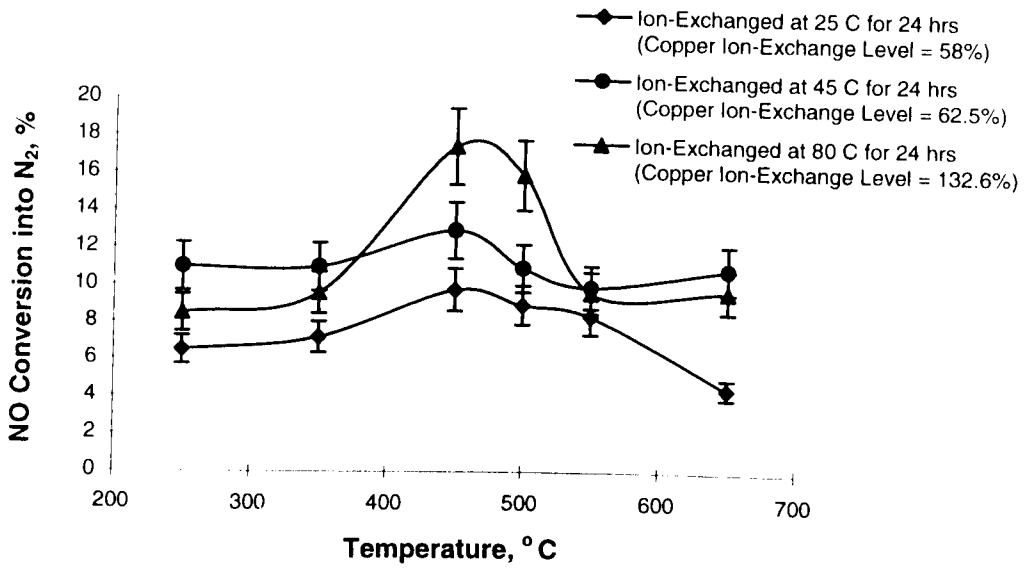

Figure 5.2. The dependence of NO conversion into N_2 on operation temperature and ion-exchange temperature for H-Cu-ZSM-5-50 zeolites. Reaction conditions: 2000 ppm NO, balance He, catalyst weight 1.0 g, and total flow rate 150 ml min^{-1}.

times were 58, 77.3 and 99.3%, respectively. This concurs with what was reported by Iwamoto et al. (1989) that the extent of copper ion-exchange level can be raised by repetition of ion-exchange procedure. After testing the samples, the results revealed that the NO conversion to N_2 did not follow the same trend, as shown in Figure 5.3. The catalyst which ion-exchanged at 45 °C twice (ion-exchange level of 106.7%) was less active than the catalyst ion-exchanged only for a period of 24 hours (ion-exchange level of 62.3%). The former was tested using XRD as less activity of this catalyst was unexpected. It was found that less than 1% of the catalyst was CuO indicating that some of the copper atoms available in the catalyst were converted to CuO. However, the quantitative amount of CuO could not be determined due to the low accuracy of the system.

The reason could be also different activities of copper ions due to different locations of the ions in the zeolite framework. As Dedecek et al. (1995) postulated in the first stage of the ion-exchange, Cu^{2+} ions can occupy the sites in large cavities adjacent to two Al framework atoms, while by increasing copper loading small cavities are then

occupied. However, the question why the same trend was not observed when the catalyst was ion-exchanged three times, remains unanswered.

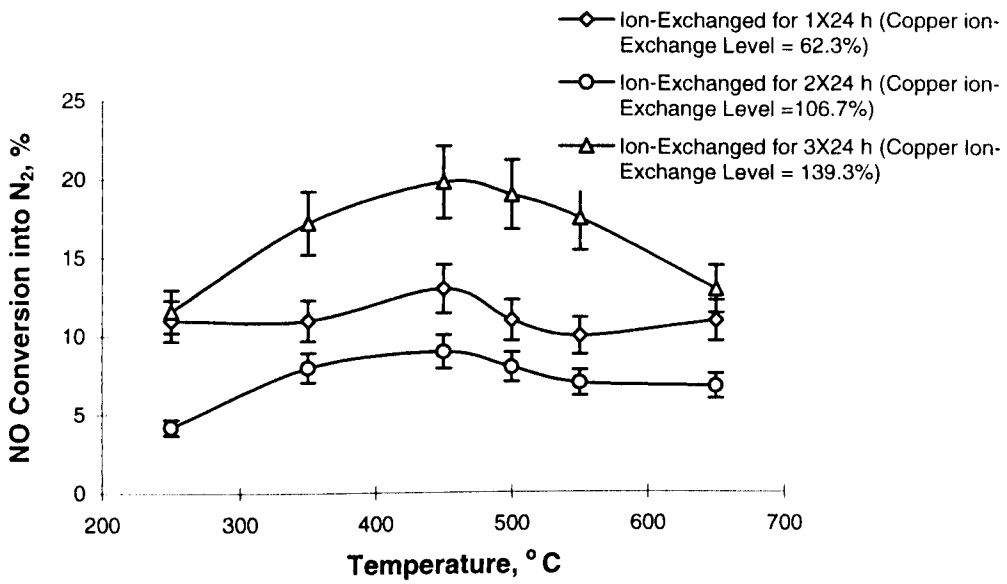

Figure 5.3. The dependence of NO conversion into N_2 on operation temperature and repetition of ion-exchange at 45 °C for H-Cu-ZSM-5-50 zeolites. Reaction conditions: 2000 ppm NO, balance He, 1.0 g catalyst weight, and 150 ml min^{-1} total flow rate.

NO conversion to N_2 as a function of copper-exchange level is shown in Figure 5.4. The overall trend shows that NO conversion was enhanced as the copper ion-exchange level increased. It was observed that when increasing the ion-exchange temperature, the NO conversion increased. Repeating the ion-exchange procedure increased copper ion-exchange level, but NO conversion reduced and then increased indicating that existing different locations for copper sites, or stabilising different types of copper on the zeolite framework, may results in different activities for copper sites. The reason for the latter could be due to changing of the pH value of the ion-exchange solution when a new copper acetate solution was used to repeat the ion-exchange procedure. Hydrolysis of acetate ions may have occurred and led to formation of hydroxide ions which may produce complexes of the type $Cu(OH)^+$ and

$Cu(OH)_2$. These species can be then ion-exchanged or precipitated on the zeolite support (Schoonheydt et al., 1976).

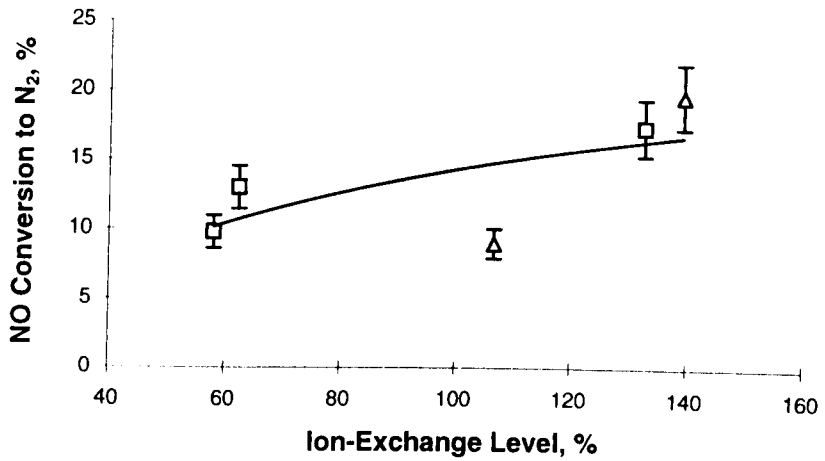

Figure 5.4. The dependence of maximum NO conversion into N_2 on ion-exchange level and catalyst preparation for H-Cu-ZSM-5-50 zeolites. (Δ) Ion-exchange level changed by repetition of ion-exchange procedure, (□) ion-exchange level changed by changing ion-exchange temperature. Reaction conditions: 2000 ppm NO, balance He, 1.0 g catalyst weight, and total flow rate 150 ml min^{-1}.

The effect of the presence of 2% O_2 in the feed gas on the conversion of NO into N_2, as well as a comparison between the effect of ion-exchange temperature and ion-exchange repetition, are shown in Figures 5.5 and 5.6. The presence of O_2 decreased NO conversion sharply. This effect even prevented any NO conversion over H-Cu-ZSM-5-50-106.7 as the lowest NO conversion achieved over this catalyst compared to the others when the oxygen was absent.

The graphs show the highest conversion at the relatively wide temperature range achieved over H-Cu-ZSM-5-50-139.3. However, the catalyst did not show any activity up to 350 °C and the maximum conversion achieved at 450 °C decreased from 20% to 5% when oxygen was added to the inlet gas. H-Cu-ZSM-5-50-58 with a

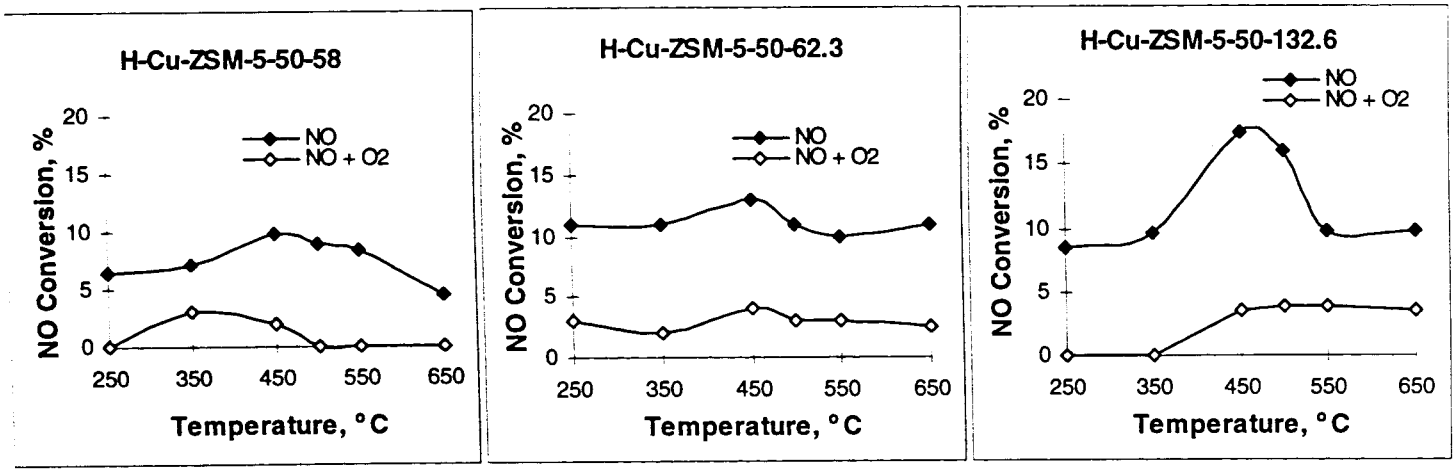

Figure 5.5. The dependence of NO conversion on temperature with and without the presence of O_2 over: (a) H-Cu-ZSM-5-50-58, ion-exchanged at 25 °C once for 24 h, (b) H-Cu-ZSM-5-50-62.3, ion-exchanged at 45 °C once for 24 h, (c) H-Cu-ZSM-5-50-132, ion-exchanged at 80 °C once for 24 h. Reaction conditions: 2000 ppm NO, 0.0% or 2% O_2, balance He, 1.0 g catalyst weight, and 150 ml min^{-1}.

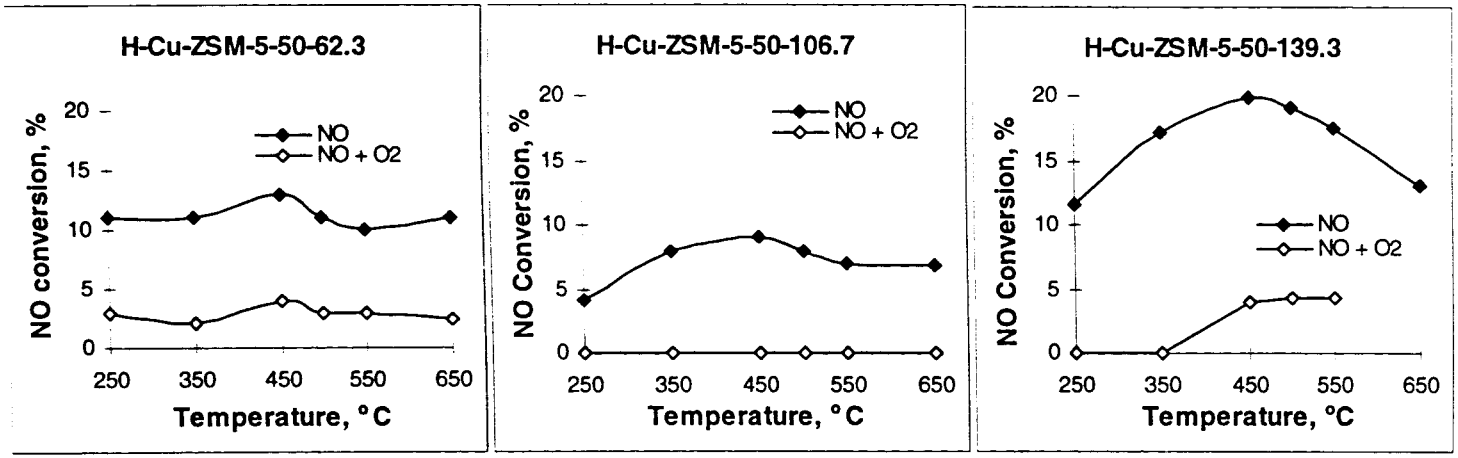

Figure 5.6. The dependence of NO conversion with and without the presence of O_2 over: (a) H-Cu-ZSM-5-50-62.3, ion-exchanged at 45 °C once for 24 h (b) H-Cu-ZSM-5-50-106.7, ion-exchanged at 45 °C twice for 24 h, (c) H-Cu-ZSM-5-50-139.3, ion-exchanged at 45 °C three times for 24 h. Reaction conditions: 2000 ppm NO, balance He, 1.0 g catalyst weight, and 150 ml min^{-1} total flow rate.

low copper exchange level was not active at temperatures greater than 500 °C and H-Cu-ZSM-5 132.6 and of H-Cu-ZSM-5-139.3 catalysts with close ion-exchange levels did not show any activity up to 350 °C. It can be concluded that the NO conversion profile over copper ion-exchanged ZSM-5 catalysts are shifted towards higher temperature when copper ion-exchange level increases.

The results obtained indicated that the direct decomposition over Cu-ZSM-5 is not suitable for practical use especially for engines working under an oxidising atmosphere. The catalyst showed low activity and this activity decreased sharply by adding oxygen to the inlet gas stream. The activity of Cu-ZSM-5 catalysts is not sufficient for practical implementation, but the study of the direct decomposition over these catalysts is important as it may indicate ways to devise more active catalysts (Shelef, 1995).

5.3 Kinetic Studies of the Direct Decomposition of NO

The dependence of NO decomposition rate on partial pressure or concentration of NO and O_2 was investigated over H-Cu-ZSM-5-32.2-101.7 zeolite. The dependence of NO conversion into N_2 on contact time was examined to ensure that the reaction was not diffusion-limited under the experimental conditions. The reaction order in NO concentration and the rate constants at 350, 450 and 550 °C were determined by varying NO concentrations in the feed while the oxygen was absent. Then, oxygen was added to the inlet gas and the dependence of the reaction rate on oxygen concentration was examined by varying O_2 concentration for NO concentration of 0.2%. The reaction order for O_2 was negative and strongly dependent on reaction temperature. The reaction order for O_2 and reaction constants at 450 and 550 °C were determined. The results were finally compared to suggested reaction rate addressed in the literature. On the basis of the experimental results obtained in this study, a new reaction rate equation at temperatures less than the most effective temperature as well as the mechanism involved were proposed.

5.3.1 Theory and Background

The following steps are mainly involved in a catalytic reaction using porous catalysts (Hughes, 1984):

1. Diffusion of reactants from the bulk fluid to the external surface of the catalyst,
2. Diffusion of reactants from the pore mouth through the catalyst pores,
3. Adsorption of reactants onto active sites on the catalyst surface,
4. Reaction on the surface of the catalyst,
5. Desorption of the products from the active sites,
6. Diffusion of the products from the catalyst pores to the pore mouth on the external surface,
7. Diffusion of the products from the external surface of the catalyst to the bulk fluid.

To determine the reaction rate of a catalytic reaction, the diffusion steps (steps 1,2,6, and 7) must be extremely rapid to avoid diffusion limitations. Under these circumstances, the dependence of NO conversion on contact time must be linear.

The following reaction rate was suggested by Li and Hall (1991) for the direct decomposition of NO over Cu-ZSM-5-26-166. The description of each term in the reaction rate has been detailed in Chapter 2.

$$r = \frac{k[NO]}{1 + K[O_2]^{1/2}} \qquad (2\text{-}8)$$

They determined the order of NO concentration, the rate constants, k and K based on experimental results. The later constant (K) was defined as the equilibrium constant for O_2 adsorption on the catalytic sites.

5.3.2 Catalyst Preparation

The catalyst was prepared from Na-ZSM-5 zeolite synthesised using the template-free method as described in Chapter 3. The synthesised zeolite was ion-exchanged with ammonium nitrate (0.1 M) at 60 °C three times, each time for 24 hours. The catalyst was dried at 110 °C for 24 hours and calcined at 500 °C for 4 hours to remove ammonia from the zeolite lattice prior to being ion-exchanged with copper ions. The catalyst was then ion-exchanged twice with copper acetate 0.01 M at 45 °C, each time for 24 hours. After filtration and washing with deionised water, the obtained cake was dried at 110 °C for 24 hours. The detailed analysis of the obtained catalyst, Cu-ZSM-5-32.2-101.7, is given in Table 5.2. This catalyst was used for kinetic studies of the direct decomposition of NO.

Table 5.2. The detailed analysis of the catalyst used for kinetic studies (weight %).

Al_2O_3, %	4.06	MgO, %	<0.01	SiO_2, %	82.1
CaO, %	0.02	MnO, %	<0.01	TiO_2, %	0.01
Fe_2O_3, %	0.07	Na_2O, %	0.11	Cu, %	2.59
K_2O, %	<0.01	P_2O_5, %	0.02	Co, %	0.02

5.3.3 Dependence of NO Conversion on Temperature

The catalyst was first tested for the direct decomposition of NO over a temperature range of 250-650 °C in order to determine the temperature at which the maximum conversion occurs. The results are shown in Figure 5.7. It is seen that a relatively high conversion was achieved over the catalyst and the maximum NO conversion into N_2 occurred at 400-450 °C. The kinetic studies were performed at 350, 450 and 550 °C to examine the reaction mechanisms close to the temperature with the maximum NO conversion, and at both sides of that temperature where the NO conversions into N_2 decrease.

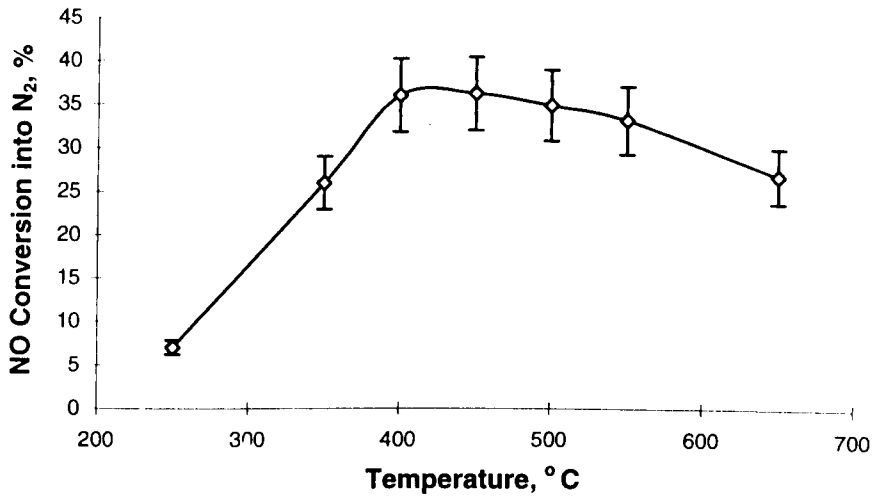

Figure 5.7. The dependence of NO conversion into N_2 on temperature over 1 g of H-Cu-ZSM-5-32.2-101.7. Reaction conditions: 2000 ppm NO, balance He, 1.0 g catalyst weight, and 100 ml min^{-1} total flow rate.

5.3.4 Dependence of NO Conversion on Contact Time

To ensure that the reaction rate is not diffusion-limited, the dependence of NO conversion into N_2 on contact time (W/F, catalyst weigh/ inlet gas flow rate) was investigated. The contact time was varied from 0.15 to 0.6 g s ml^{-1} by using 0.25, 0.5 and 1g of the catalyst. The results obtained at 450 °C and 500 °C are presented in Figures 5.8 and 5.9. The experiment was also conducted at 350 °C. However, the data could not be collected due to very low concentrations of N_2 in the outlet gas. The results show the NO conversion as a function of contact time were linear with 96.89% and 99.20% confidence intervals (R^2 values) at 450 °C and 500 °C, respectively. This indicated that the reaction was not diffusion limited. These confidence intervals will be closer to 100% if the experiment is conducted for a narrower range of contact time, for example from 0.0 to 0.30 g s ml^{-1}. Therefore, 0.5 g of the catalyst was used for kinetic study in order to keep the contact time as low as 0.30 g s ml^{-1}, to obtain the higher confidence intervals.

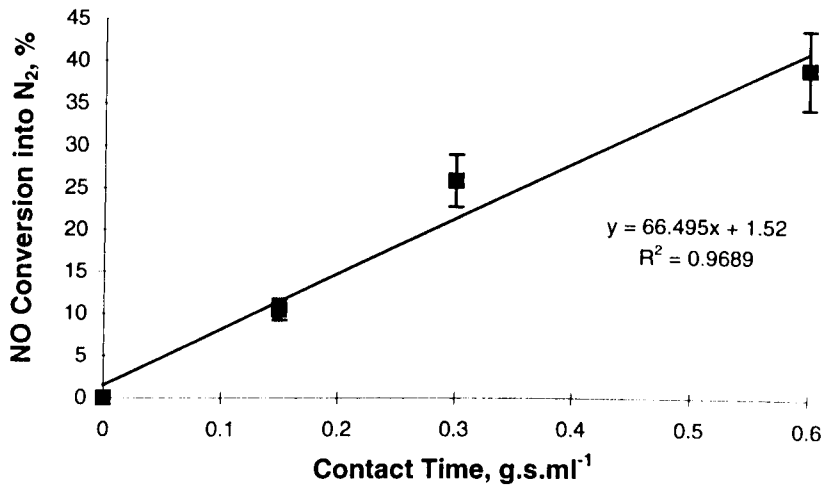

Figure 5.8. The dependence of NO conversion on contact time at 450 °C. Reaction conditions: 2000 ppm NO, balance He, 0.25 to 1.0 g catalyst weight, and 100 ml min^{-1} total flow rate.

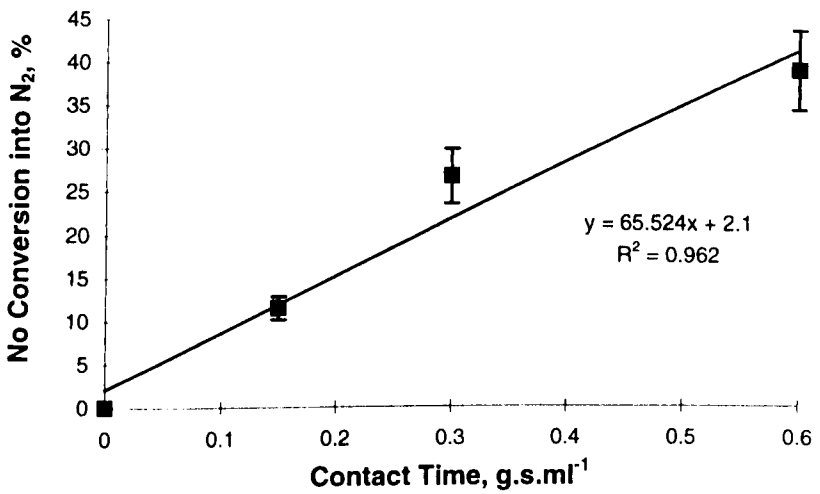

Figure 5.9. The dependence of NO conversion on contact time at 500 °C. Reaction conditions: 2000 ppm NO, balance He, 0.25 to 1.0 g catalyst, and 100 ml min^{-1} total flow rate.

5.3.5 Determination of the Reaction Rate

Based on the reaction rate suggested by Li and Hall (1991) and Valyon and Hall (1993), the following reaction rate is assumed for NO decomposition.

$$r = \frac{k[NO]^n}{1 + K[O_2]^m} \qquad (5\text{-}1)$$

In order to determine the order of NO concentration in reaction rate equation, the experiment was carried out over 0.5 g of the catalyst with varying NO concentration in the absence of oxygen. These experiments were performed at three different temperatures, 350, 450 and 550 °C. The results obtained at these temperatures are shown in Figures 5.10 and 5.11. It is seen that the orders of NO concentration in the reaction rate are 1.05, 1.13 and 1.63 at 350, 450 and 550 °C respectively. The plots indicate that the order of NO in the reaction rate is very close to 1 at 350 °C whereas at 450 and 550 °C derivation from the first order is observed.

The dependence of the turnover frequency and therefore the reaction rate on the concentration of NO over the catalyst at 550 °C (Figure 5.11) exhibited that the reaction rate is not first order in NO concentrations at temperatures higher than 450 °C at which the catalyst showed the most activity. The reaction order in NO concentration at 550 °C is 1.63 with a very high confidence factor (0.99) indicating that the reaction mechanism is different once the temperature passed over 450 °C. This is discussed further in this chapter.

The reaction order of NO and the rate constant, k, at 350, 450 and 550 °C are shown in Table 5-3. These values were calculated from the slops and y intercepts on Figures 5-10 and 5-11. These results are further compared with the literature data (Li and Hall, 1991) later in this Chapter.

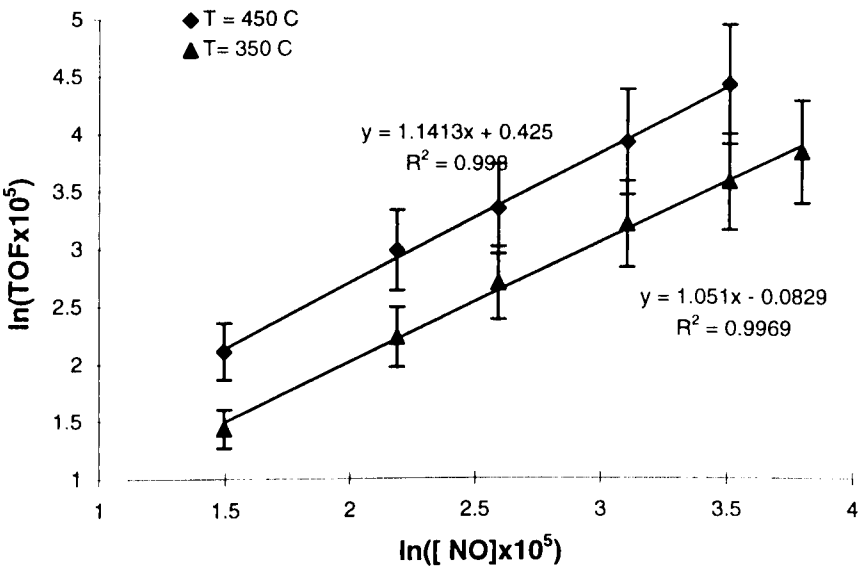

Figure 5.10. The dependence of turnover frequency (TOF) on NO concentration for H-Cu-ZSM-5-32.2-101.7 catalyst at 350 and 450 °C. Reaction conditions: 1000 to 10000 ppm NO, 0.5 g catalyst weight, and 100 ml min^{-1} total flow rate.

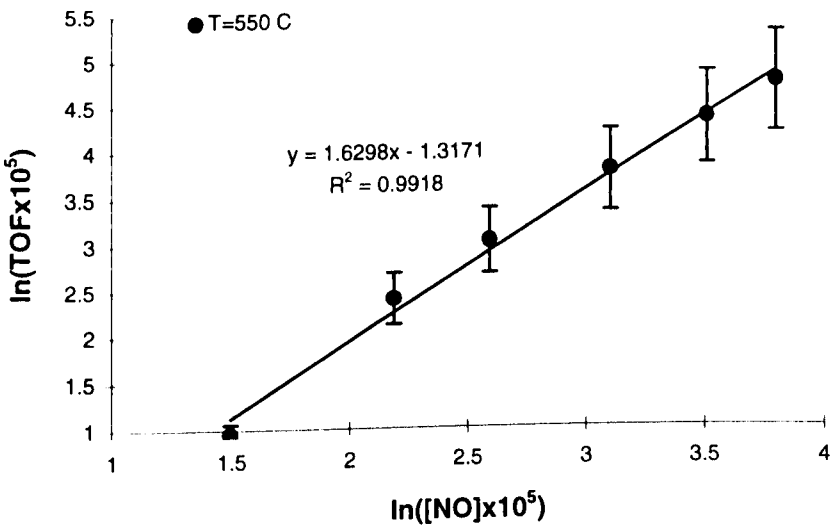

Figure 5.11. The dependence of turnover frequency (TOF) on NO concentration for H-Cu-ZSM-5-32.2-101.7 catalyst at 550 °C. Reaction conditions: 1000 to 10000 ppm NO, 0.5 g catalyst weight, and 100 ml min^{-1} total flow rate.

Table 5.3. The orders of NO in reaction rate and rate constants.

Temperature, °C	Order of NO, n	Rate Constant, k s^{-1} $site^{-1}$ $(mol\ l^{-1})^{-1}$
350	1.05	1.67
450	1.14	7.78
550	1.63	377

The dependence of the turnover frequency (TOF), as defined in Equation (4-2), and therefore decomposition rate on the concentration of O_2 over the catalyst was investigated by keeping NO concentration constant (0.2% NO) while the concentration of the O_2 in the feed was varied from 0.2 to 2 %. The results obtained at 450 and 550 °C are shown in Figure 5.12. It is observed that the reaction order for O_2 was negative and changed with changing the reaction temperature. Although, ln(TOF) was a linear function of the $\ln[O_2]$ and the reaction order in O_2 was -0.66 at 450 °C and -0.30 at 550 °C, the reaction rate can not be written as:

$$r = k\,[NO]^n\,[O_2]^{-m} \qquad (5\text{-}2)$$

The reason is that if the Equation (5-2) was a true indication of the reaction rate, the reaction rate would become infinity in the absence of O_2, which can not be correct.

In order to calculate the reaction order in O_2, m, and the reaction rate constant, K, in Equation 5-1, the equation is rewritten in the following form:

$$\frac{k[NO]^n}{r} - 1 = K[O_2]^m \qquad (5\text{-}3)$$

$$\ln\left[\frac{k[NO]^n}{r} - 1\right] = m\ln[O_2] + \ln K \qquad (5\text{-}4)$$

Thus, to determine the reaction order for O_2, values of $\ln\left[\frac{k[NO]^n}{r} - 1\right]$ were plotted

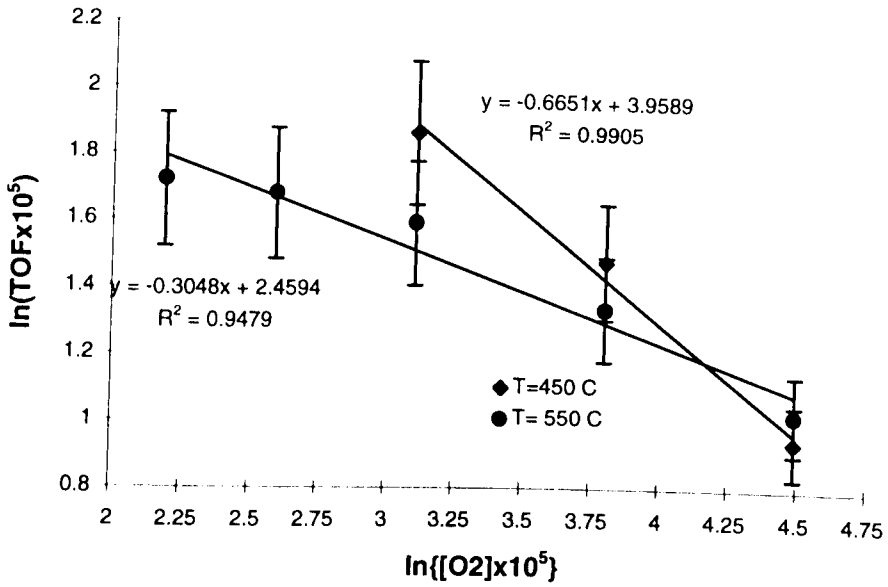

Figure 5.12. The dependence of turnover frequency (TOF) on O_2 concentration for H-Cu-ZSM-5-32.2-101.7 catalyst. Reaction conditions: 2000 ppm NO, 2000 to 20000 ppm O_2, 0.5 g catalyst weight, and 100 ml min^{-1} total flow rate.

against ln $[O_2]$. The plots are shown in Figures 5.13 and 5.14. The reaction order in O_2, m, and K constant were obtained using slops and y intercepts of the two plots at 450 and 550 °C (Figures 5.13 and 5.14). The obtained values for m and K are listed in Table 5.4. The experiments were also carried out at 350 °C, however the conversion of NO in the presence of O_2 was very low at 350 °C and therefore no data was obtained.

Table 5.4. The reaction orders in O_2 concentration in the reaction rate and the K values in Equation (5-3).

Temperature, °C	Reaction order in O_2, m	K
450	0.87	2668
550	0.55	104.8

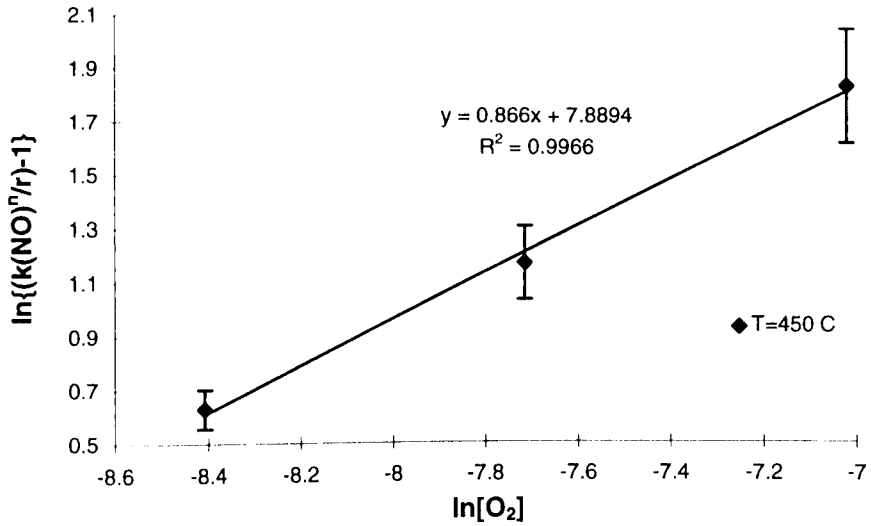

Figure 5.13. The dependence of $\ln\left[\frac{k[NO]^n}{r}-1\right]$ on $\ln[O_2]$ at 450 °C. Reaction conditions: 2000 ppm NO, 5000 to 20000 ppm O_2, 0.5 g catalyst weight, and 100 ml min^{-1} total flow rate.

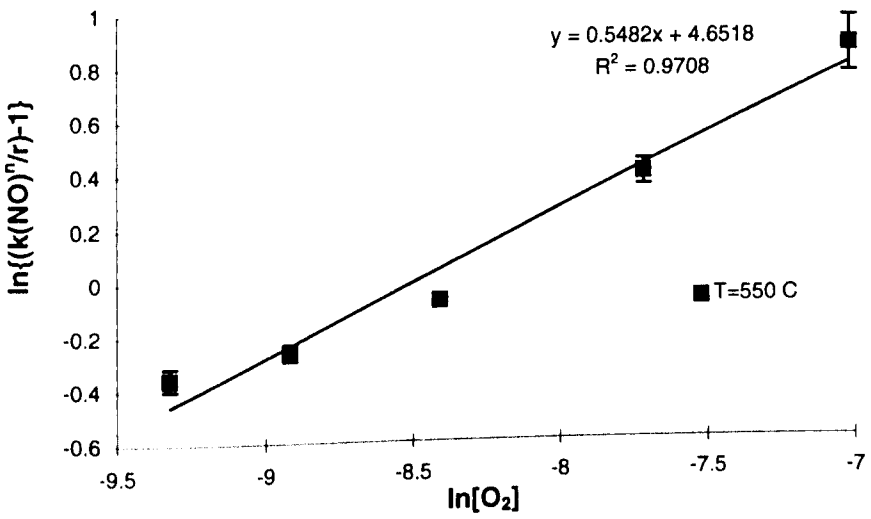

Figure 5.14. The dependence of $\ln\left[\frac{k[NO]^n}{r}-1\right]$ on $\ln[O_2]$ at 550 °C. Reaction conditions: 2000 ppm NO, 1000 to 10000 ppm O_2, 0.5 g catalyst weight, and 100 ml min^{-1} total flow rate.

Table 5.5. The reaction orders in NO (n) and in O_2 (m) concentrations in the reaction rate.

Temperature, °C	n This study	n Li and Hall	m This study	m Li and Hall study
350	1.05	0.9	-	-
450	1.14	1.0	0.87	0.5
550	1.63	1.1	0.55	0.5

A comparison between the reaction order in NO and reaction order in O_2 in the reaction rate at different temperatures obtained in this study and reported by Li and Hall is shown in Table 5.5. In both studies, the reaction order in NO increases with increasing reaction temperature. However, the reaction order in NO in Li and Hall's study only slightly increased with an increase in temperature whereas this increment is more pronounced in the data obtained in this study. It is seen that the reaction order in O_2 decreases with an increasing temperature. Li and Hall assumed a constant reaction order in O_2 was equal to 0.5 and calculated K. They postulated that the reaction rate is limited by desorption of O_2 from the active sites which results in self reduction of the sites. The half order in the O_2 concentration term in their model was justified by the formation of O_2 from combination of two adsorbed oxygen atoms. However, this can be the case if we accept that dinitosyl species are reaction intermediates.

The values of k and K, reaction rate constants, obtained in this study and reported by Li and Hall (1991) are compared in Table 5.6. These values obtained considering Equation (2-8) as the reaction rate. The rate constant increases with increasing temperature. Once again, it was found in this study that k is more dependent on temperature.

In reference to the values reported for the reaction orders in NO (n) and O_2 (m) concentrations in Table 5.4, the results obtained in this study supports n at temperatures lesser and m at temperatures greater than the most effective

temperature, as reported by Li and Hall. The order in the NO concentration at 550 °C is 1.6 which is higher than 1 and the order in the O_2 concentration is nearer to 1 rather that 0.5 at 450 °C. If the uncertainties for the NO conversion obtained are considered, then m could be 1. A new reaction rate for temperatures lower than the most effective temperature can be considered. It is imperative that the reaction rate be derived by a reaction mechanism which is discussed in the following section.

Table 5.6. The reaction rate constants.

Temperature, °C	k This study	k Li and Hall	K This study	K Li and Hall study
350	1.67	0.95	-	-
450	7.78	5.03	2668	157.5
550	377.4	7.43	104.8	53.0

5.3.6 Reaction Mechanism at Temperatures Lower Than the Most Effective Temperature

In order to obtain a reaction rate equation for the direct decomposition of NO at temperatures lower than the most effective temperature, the following reaction mechanism is suggested;

$$NO + (S) \longrightarrow NO\text{-}(S) \qquad \text{(R5-3)}$$

where (S) and NO-(S) represent active sites, and NO adsorbed on active sites. Then another NO molecule reacts with a NO-S as follows:

$$2NO\text{-}(S) + 2NO \longrightarrow N_2 + 2(S)\text{-}NO_2 \qquad \text{(R5-4)}$$

(S)-NO_2 represents NO_2 molecule attached to the active site left behind after desorption of nitrogen. In the first step, Reaction (R5-3), NO molecules adsorb on the

active sites to produce NO-(S) species. NO molecules also adsorb on NO-(S) species either after or parallel to the first step which leads to desorption of N_2 and production of (S)-NO_2 species as shown in Reaction (R5-4). These two steps continue until all the active sites are covered by NO and converted to (S)-NO_2 species. It is assumed that Reactions (R5-3) and (R5-4) are fast. In the next step, the following reaction, Reaction (R5-5) occurs.

$$NO + (S)\text{-}NO_2 \underset{k_2}{\overset{k_1}{\rightleftharpoons}} O_2 + (S)\text{-}N_2O \qquad \text{(R5-5)}$$

where N_2O-(S) represent N_2O molecules attached to the active sites left behind after desorption of oxygen. Reaction (R5-5), a reversible reaction, occurs between NO molecules and (S)-NO_2 species results in desorption of O_2 leaving (S)-N_2O species behind. These species then react with NO molecules to produce N_2 molecules and (S)-NO_2 species which are again reactants for Reaction (R5-5).

$$N_2O\text{-}(S) + NO \xrightarrow{k_3} N_2 + NO_2\text{-}(S) \qquad \text{(R5-6)}$$

Reactions (R5-5) and (R5-6), are asumed to be reaction limited steps. Accordingly, the reaction rate is determined by Reactions (R5-5) and (R5-6). Therefore, in steady state, the reaction rate can be written only using these two reactions as below:

$$r = k_1 [NO][(S)\text{-}NO_2] - k_2 [O_2][(S)\text{-}N_2O] + k_3 [(S)\text{-}N_2O][NO] \qquad (5\text{-}5)$$

The conservation of surface sites gives

$$[(S)\text{-}NO_2] + [(S)\text{-}N_2O] + [(S)\text{-}NO] + [S] = C \qquad (5\text{-}6)$$

where C is total number of active sites which is constant. [(S)-NO] and [S] are negligible in steady state since it is assumed that in the first two steps they are quickly converted to (S)-NO_2. Therefore, it can be written as:

$$[(S)\text{-}NO_2] = C - [(S)\text{-}N_2O] \quad (5\text{-}7)$$

The overall production rate of (S)-NO_2 and (S)-N_2O in the reactions is zero thus,

$$\frac{d[(S)-NO_2]}{dt} = \frac{d[(S)-N_2O]}{dt} =$$

$$-k_1[NO][(S)-NO_2] + k_2[O_2][(S)-N_2O] + k_3[S-N_2O][NO] = 0 \quad (5\text{-}8)$$

Therefore:

$$k_1[NO][(S)-NO_2] - k_2[O_2][(S)-N_2O] = k_3[S-N_2O][NO] \quad (5\text{-}9)$$

Combining Equations (5-5) and (5-9) results in:

$$r = 2k_3[NO][(S)\text{-}N_2O] \quad (5\text{-}10)$$

and

$$[(S)\text{-}N_2O] = \frac{Ck_1[NO]}{(k_1+k_2)[NO]+k_2[O_2]} \quad (5\text{-}11)$$

Substitution of Equation (5-11) into Equation (5-10) yields

$$r = \frac{2Ck_1k_3[NO]^2}{(k_1+k_2)[NO]+k_2[O_2]} = \frac{k[NO]^2}{[NO]+K[O_2]} \quad (5\text{-}12)$$

where $K = \frac{k_2}{k_1+k_2}$ and $k = \frac{2Ck_1k_3}{k_1+k_2}$.

The above reaction mechanism suggests that (S)-N_2O and (S-NO_2) species participate in the formation of the reaction intermediates. The adsorption of these two species

were observed by infra red (IR) spectroscopy technique by Valyon and Hall (1993) and Hoost et al. (1995) at low temperatures. The band of N_2O adsorbed on Cu-ZSM-5 detected by IR adsorption at 2224 cm^{-1} at room temperature (Valyon and Hall, 1993) and at 25, 150, 225 and 300 °C (Hoost et al., 1995). The peak intensity attenuation resulting from the adsorption of N_2O decreased when the temperature was increased. It can be postulated that (S)-N_2O species can be intermediates at temperatures lower than the most effective temperature. Spectra of adsorbed NO_2 began to appear after an hour in the 1630-1530 cm^{-1} region and started to grow which was evident that NO_2 had been produced at 100 °C.

Equation (5-12) is considered in a general form

$$r = \frac{k[NO]^{n'}}{[NO] + K[O_2]^m} \qquad (5\text{-}13)$$

In the absence of O_2, Equation (5-13) is converted to $r = k[NO]^{n'-1}$ and therefore $n' - 1 = n$ which was defined in previous section in this chapter.

Equation (5-13) is rearranged into the following form.

$$\ln\left[\frac{k[NO]^n}{r} - 1\right] + \ln[NO] = m.\ln[O_2] + \ln K \qquad (5\text{-}14)$$

The data obtained at 450 °C in this study was fitted with Equation (5-12) and the same values for k, reaction orders in NO and O_2 concentrations but different value for K were obtained. To obtain K in Equation 5-14, values of $\ln\left[\frac{k[NO]^n}{r} - 1\right] + \ln[NO]$ at 450 °C were plotted against ln $[O_2]$. This plot is shown in Figures 5.15. The values for m and K are found to be 0.866 and 0.21, respectively.

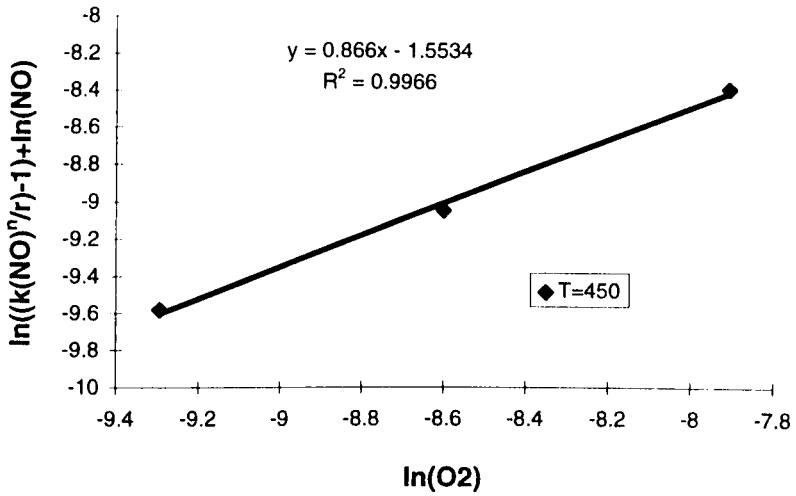

Figure 5.15. The dependence of $\ln\left[\frac{k[NO]^n}{r}-1\right]+\ln[NO]$ on $\ln[O_2]$ at 450 °C. Reaction conditions: 2000 ppm NO, 5000 to 20000 ppm O_2, 0.5 g catalyst weight, and 100 ml min^{-1} total flow rate.

It is concluded that the reaction mechanism on both sides of the most effective temperature are different. The general form of the reaction rate reported by Li and Hall (1991) and Valyon and Hall (1993) is confirmed for temperatures greater than the most effective temperature and Equation 5-12 is now suggested for the reaction rate at temperatures below the most effective temperature.

It is acknowledged that the data used to obtain K value were taken at 450 °C as no data could be collected at lower temperatures. The deduced reaction rate is also considered to be valid at temperatures below the most effective temperature. The reason is that the reaction order in O_2, m, increases as reaction temperature decreases and postulate to be approached to 1 at lower temperatures, as shown in Table 5.5. In addition, N_2O adsorbed on Cu-ZSM-5 zeolites were detected at low temperatures (Valyon and Hall, 1993; Hoost et al., 1995) as described in Section 5.3.6.

5.4 Summary

Based on the results presented in this Chapter, it can be concluded that the ion-exchange conditions have a significant effect on copper ion-exchange level and properties of the Cu-ZSM-5 zeolite catalyst. Increasing the temperature of the ion-exchange solution from 25 to 45 °C leads to an increase in ion-exchange level for the same ion-exchange time. In contrast, increasing the temperature from 45 to 80 °C increases the ion-exchange level if the catalyst is ion-exchanged for 24 hours but this level decreases severely by further repetition of ion-exchange procedure. Therefore, the ion-exchange level of a catalyst can be controlled by either changing the temperature or repeating the ion-exchange procedure. For example, to prepare a catalyst having a very high copper ion-exchange level, the catalyst can be ion-exchanged at 45 °C several times. The number of times that the process is required to be repeated, depends on the desired ion-exchange level.

It is also shown that the ion-exchange temperature has a considerable effect on the activity of the catalyst. Repetition of ion-exchange procedure leads to increasing ion-exchange level, however the activity of the catalyst is not always directly proportional to the catalyst ion-exchange level. In this study, it was shown that the activity of the catalyst is directly proportional to the ion-exchange level if the catalyst is ion-exchanged at 25 °C, but not at 45 °C. This could be due to hydrolysis of the ions which is more probable at higher temperatures. The hydrolysis of the copper ions definitely occurs at 80 °C as the catalyst turns black at this temperature, whereas this phenomenon slightly occurs at 45 °C. Therefore, two ion-exchanged catalysts with the same copper ion-exchange level may show different activities for the direct decomposition of NO depending on the preparation method used. This has not been reported in the literature. It can be concluded that considering only the copper ion-exchange level, which has been a criterion for the activity of Cu-ZSM-5 catalysts for the direct decomposition of NO (Iwamoto et al., 1989) is not enough to recognise the activity of the catalyst however, catalyst preparation method must be considered.

Adding oxygen to the inlet gas stream always reduces NO conversion severely and the NO conversion profile shifts towards higher temperatures when copper ion-exchange level increases. Although the direct decomposition of NO is thermodynamically favoured, Cu-ZSM-5 catalysts are not suitable for practical use due to insufficient catalytic activity and inhibition of the reaction by presence of oxygen.

In kinetic studies for the direct decomposition, it is postulated that the reaction mechanisms for the direct decomposition of NO at temperatures below and above the most effective temperatures, i.e. 400-450 °C, are different. For temperatures greater than 450 °C, the reaction rate reported by Li and Hall (1991) and Valyon and Hall (1993) and the reaction mechanism involved reported by Valyon and Hall (1993) are supported. In the present study, at temperatures lower than the most effective temperature, a new reaction rate is proposed which shows that the dependence of NO decomposition is first order in NO concentration in the absence of oxygen and the reciprocal of the rate increases linearly with the oxygen concentration when oxygen is present.

CHAPTER SIX

SELECTIVE CATALYTIC REDUCTION OF NITROGEN MONOXIDE

6.1 Introduction

In Chapter 5 studies of the direct decomposition of NO were reported. This chapter presents the results obtained for selective catalytic reduction (SCR) of NO over synthesised ZSM-5 zeolites ion-exchanged with copper or cobalt ions. The zeolites were synthesised according to Method 1 and Method 3 described in Chapter 3. Then, they were ion-exchanged with copper or cobalt ions and tested in the system described in Chapter 4.

In the first stage, SCR of NO using methane or propene as the reducing agent was investigated over two samples ion-exchanged with copper and cobalt ions, respectively. The results obtained showed that the highest NO conversion into N_2 was achieved over Cu-ZSM-5 catalyst, when propene was used as a reducing agent. In contrast, when propene was replaced with methane, Co-ZSM-5 was more active than Cu-ZSM-5 catalyst. These observations led us to carry out further investigations in the next two stages for SCR of NO over Cu-ZSM-5 using propene and over Co-ZSM-5 using methane. The outline of these investigations are as follows:

- The effect of SiO_2/Al_2O_3 ratio, copper loading and copper ion-exchange level on the SCR of NO using propene as the reducing agent over Cu-ZSM-5 zeolites,
- The effect of catalyst preparation, SiO_2/Al_2O_3 ratio and cobalt loading on SCR of NO using methane as the reducing agent over Co-ZSM-5 zeolites.

6.2 SCR of NO over Cu-ZSM-5 and Co-ZSM-5 Catalysts

Methane and propene are well-known as effective reducing agents for SCR of NO over Co-ZSM-5 (Li and Armor, 1992) and Cu-ZSM-5 (Iwamoto and Mizuno, 1993) respectively. Methane is known as a non-selective reducing agent for the reduction of NO over Cu-ZSM-5 zeolite. However there is a little knowledge about the activity of Co-ZSM-5 for SCR of NO by propene.

In order to compare the activity of Co- and Cu-ZSM-5 catalysts for the SCR of NO, Na-form of ZSM-5 zeolite with a SiO_2/Al_2O_3 ratio of 40 was synthesised via the template-free method detailed in Chapter 3. The zeolite was ion-exchanged with ammonium nitrate and calcined to obtain the H-form of the zeolite. One part of the sample was ion-exchanged with copper acetate and another part with cobalt acetate. Co-ZSM-5 catalyst was prepared using the semi-continuous method. The preparation methods have been explained in detail in Chapter 4. The resulting catalysts were H-Cu-ZSM-5-40-101.7 and H-Co-ZSM-5-40-45 which are simply called Cu-ZSM-5 and Co-ZSM-5 in this section. The catalysts were analysed and the details of the analysis are given in Appendix C.

The SCR of NO into N_2 by methane and propene over 1.0 g of each catalyst using a mixture of 2000 ppm NO, 2000 ppm CH_4 or C_3H_6, 2% O_2, balance He, and 100 ml min^{-1} total flow rate was investigated. The activity of the catalysts were found to be dependent on temperature. NO conversion and CH_4 or C_3H_6 oxidation as a function of temperature are shown in Figure 6.1(a) and (b) respectively. The highest NO conversion into N_2 was achieved over Cu-ZSM-5 when propene was the reducing agent. This catalyst showed very low activity for SCR of NO by methane as shown in Figure 6.1(a). Similar NO conversions were achieved over Co-ZSM-5 using either methane or propene at temperatures between 250 and 450 °C, while this catalyst showed slightly more activity at temperatures between 450 and 625 °C when propene was the reducing agent.

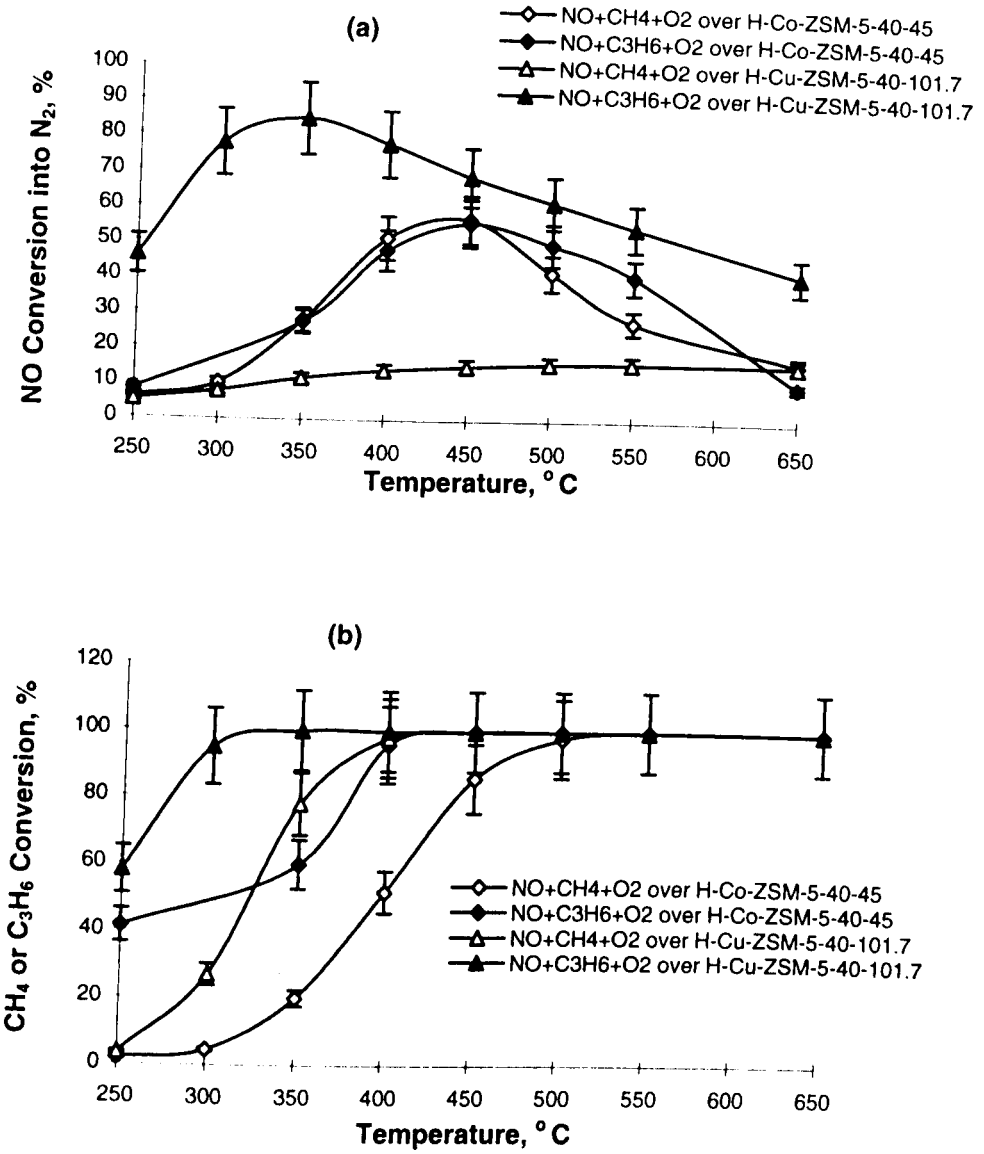

Figure 6.1. The dependence of NO conversion (a) and CH_4 or C_3H_6 conversion (b) on temperature over H-Cu-ZSM-5-40-101.7 and H-Co-ZSM-5-40-45. Reaction conditions: 2000 ppm NO, 2000 ppm CH_4 or C_3H_6, and 2% O_2, balance He, 1.0 g catalyst, and 100 ml min^{-1} total flow rate.

NO conversion increased by increasing temperature, reached a maximum, and then decreased. The *most effective temperature*, the temperature of the maximum NO conversion, was around 450 °C over Co-ZSM-5 using either propene or methane as the reducing agent, and 350 °C over Cu-ZSM-5 using propene. The decreases in the catalytic activity of the catalysts at temperatures greater than the most effective

temperature could not be related to the deactivation of the catalyst or collapse of the zeolite structure. This is because the experiments were also repeated in reverse order of temperature, and the results were repeatable and consistent. The decrease in catalytic activity at high temperatures could be due to a change in reaction mechanism or an increase of the oxidation of propene at higher temperatures.

Figure 6.1(b) reveals that the maximum propene conversion is associated with the maximum nitrogen monoxide reduction when either Cu-ZSM-5 or Co-ZSM-5 catalyst is used. 85% and 56% NO conversions were achieved over Cu-ZSM-5 and Co-ZSM-5 respectively, although the catalysts were more active for propene oxidation than NO reduction over the entire range of temperature. These two catalysts were very active for propene oxidation even at temperatures as low as 250 °C, achieving 55% and 40% propene conversion respectively. The propene oxidation then increased by increasing the temperature. High oxidation of propene at 250 °C is contrary to methane oxidation over both catalysts which were less than 10% at this temperature. In addition, Cu-ZSM-5 which was less active for NO reduction by methane, was a more effective catalyst for methane oxidation than Co-ZSM-5 at temperatures between 250 and 500 °C. This indicates that the methane oxidation is not a precursor for reduction of NO over Cu-ZSM-5 and/or the copper active sites may compete for oxidation of methane rather than for reduction of NO.

In the current study, it was found that the catalytic activities shown by Co-ZSM-5 zeolite for reduction of NO using either methane or propene were the same. Almost 54% NO conversion was achieved at the most effective temperature. Witzel et al. (1994) investigated the activity of Co-ZSM-5 by either methane or isobutane and reported that the maximum NO conversion achieved using methane and isobutane was 62% and 88%, respectively. Figure 6.2 compares NO conversion as a function of temperature obtained over Co-ZSM-5 catalyst in this study using either methane or propene with the data reported by Witzel et al. (1994). Although the reaction conditions are different and they achieved relatively higher NO conversions considering the contact times, it is seen that higher conversions were achieved when isobutane was used, compared to methane or propene.

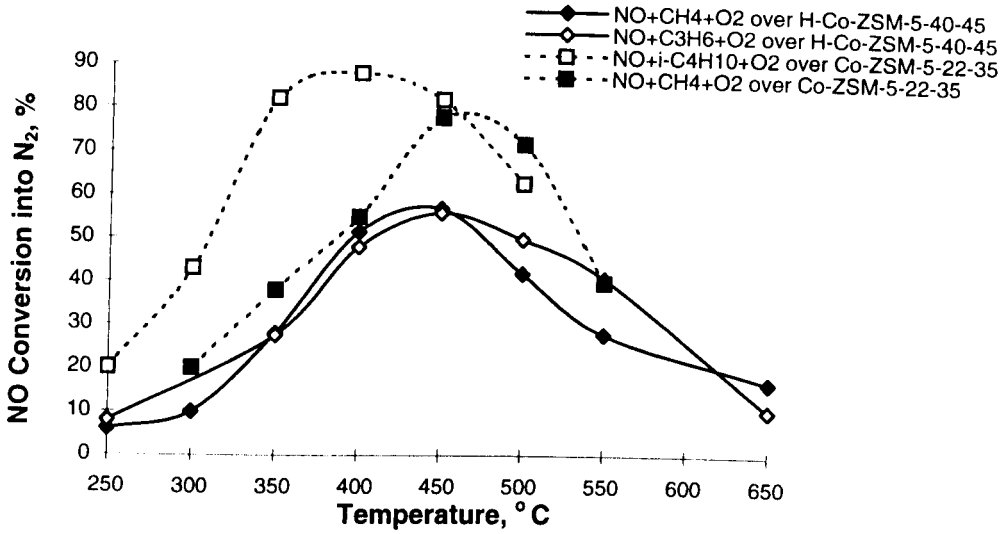

Figure 6.2. The dependence of NO conversion on temperature for SCR of NO over Co-ZSM-5 using CH_4 or C_3H_6 in this study (solid-lines) and using CH_4 or i-C_4H_{10} reported by Witzel et al. in 1994 (dashed-lines). Reaction conditions of this study: 2000 ppm NO, 2000 ppm CH_4 or C_3H_6, and 2% O_2, balance He, 1.0 g catalyst, 100 ml min^{-1} total flow rate. Reaction conditions of Witzel et al. study: 2000 ppm NO, 8000 ppm CH_4 or 2000 i-C_4H_{10} and 10% O_2, balance He, 0.25 g catalyst, and 75 ml min^{-1} total flow rate.

In other studies, Cu-ZSM-5 was reported to be very different in its response to different hydrocarbons, achieving maximum 40% NO conversion if ethene was present (Sato et al., 1991), 70 % when propene was used (Iwamoto and Mizuno, 1993) and was a non-selective catalyst when methane was used in the reaction system (Iwamoto and Hamada, 1991). d'Itri and Sachtler (1992) also reported that methane has an unselective nature for NO reduction over H-Cu-ZSM-5 catalyst prepared via the impregnation method. It is postulated that almost 18% NO conversion obtained over H-Cu-ZSM-5 zeolite in the presence of methane was not due to the presence of the catalyst but this conversion could occur in a reaction system even with no catalyst. This phenomenon is shown in Section 7.4.3 of Chapter 7.

It was reported that methane was a selective reducing agent for reduction of NO over copper ion-exchanged natural zeolite (Headon and Zhang, 1997) and over Co-ZSM-5 catalyst (Amiridis et al., 1996). However, for the natural zeolite, 30% NO conversion was achieved using a mixture of 2% NO, 2% O_2, 1% CH_4, and balance helium with a total flow rate of 100 ml min^{-1} over 1.5 g catalyst. However, the gas composition is very far from realistic conditions for practical use.

Adelman et al. (1996) reported that different types of adsorbed nitrogen oxide complexes were produced over Co-ZSM-5 and Cu-ZSM-5 catalysts when these catalysts were exposed to a mixture of NO and O_2. These complexes were collectively called NO_y. They believed that due to the different chemistry of these two catalysts, the types of the complexes formed were different. They employed Fourier Transform Infra Red (FTIR) spectroscopy technique to identify the type of NO_y complexes in these catalysts. It was shown that both nitro or nitrito complexes can form over both catalysts, but prominent complexes formed over Co-ZSM-5 were O bound nitrito complexes (Co^{2+}.ONO) whereas predominant complexes formed on Cu-ZSM-5 were N bound nitro complexes (Cu^{2+}.NO_2). This produced a variety of Cu species in ZSM-5 including Cu^{2+} ions, oxo-complexes and oxide clusters. CH_4 can react with nitrito groups (Co^{2+}.ONO) but not with the complexes formed over Cu-ZSM-5. This could be the reason why CH_4 is an effective reducing agent for SCR of NO over Co-ZSM-5 but not over Cu-ZSM-5. On the other hand, higher alkanes can react with different NO_y complexes. Therefore, these reducing agents are suitable for SCR of NO over Cu-ZSM-5 catalysts.

6.3 SCR of NO by Propene over Cu-ZSM-5 Zeolites

It is well-known that for ZSM-5 zeolite the SiO_2/Al_2O_3 ratio determines the number of Bronsted acid sites and the capacity of the zeolite for ion-exchange. Therefore, the catalytic activity of a metal ion-exchanged ZSM-5 zeolite can be a function of the SiO_2/Al_2O_3 ratio and metal loading of the zeolite. For example, the catalytic activity

of Cu-ZSM-5 depends on the copper loading, SiO_2/Al_2O_3 ratio of the zeolite and therefore copper ion-exchange level of the catalyst.

The effect of SiO_2/Al_2O_3 ratio on the activity of Cu-ZSM-5 prepared from H-form of the zeolite on the SCR of NO by propene was investigated by Torre-Abreu et al. (1997a). In this study, the effect of SiO_2/Al_2O_3 ratio on the activity of Cu-ZSM-5 catalysts using the catalysts prepared from Na-form is presented and discussed.

The effect of copper ion-exchange level on the activity of Cu-ZSM-5 for SCR of NO in the presence of ethene and propene was reported by Sato et al. (1991) and Kharas (1993). It was shown that the activity of Cu-ZSM-5 catalysts increased with increasing copper ion-exchange level up to 80-100% when ethene was used as the reducing agent. The activity leveled off when the ion-exchange level increased beyond 100%. Kharas reported that the most effective catalysts for reduction of NO using propene have copper ion-exchange levels of 150 to 200. In this study, the performance of the catalysts prepared from the H-form and the Na-form of Cu-ZSM-5 for SCR of NO using propene are investigated. Also, two catalysts with the same SiO_2/Al_2O_3 ratios and almost 80 and 100 copper ion-exchange levels are examined for SCR of NO by propene. In order to compare the reducibility of ethene and propene, the results obtained in this study are compared with those reported by Sato et al. (1991) when ethene was used.

Cu-ZSM-5 catalysts used in this section of the study are classified in three groups:

1. catalysts with different SiO_2/Al_2O_3 ratios but the same copper loading;
2. catalysts with different copper loading but the same SiO_2/Al_2O_3 ratios and;
3. catalysts with the same copper ion-exchange level but different copper loading and different SiO_2/Al_2O_3 ratios.

The results of the analytical tests of the catalysts are given in Appendix C. All experiments were carried out using a mixture of NO 2000 ppm, 2000 ppm C_3H_6, 2%

O_2, balance helium, at a flow rate of 150 ml min^{-1} over 1 g of catalyst. The contact time was therefore 0.4 g s ml^{-1}.

6.3.1 The Effect of SiO_2/Al_2O_3 Ratio

To investigate the effect of SiO_2/Al_2O_3 ratio on the activity of Cu-ZSM-5 prepared from the Na-form of the zeolite for SCR of NO by propene, three over-exchanged samples of Cu-ZSM-5 zeolite catalysts with different SiO_2/Al_2O_3 ratios of 176, 140 and 100 but the same copper loading (i.e. about 1.3 wt.-%) were prepared. The main characteristics of the catalysts are classified in Table 6.1. The activity of the catalysts were tested at temperatures between 250 and 650 °C.

Table 6.1. Specifications of the three copper ion-exchanged ZSM-5 catalysts with the same copper loading but different SiO_2/Al_2O_3 ratios.

Catalyst	Initial SiO_2/Al_2O_3 ratio	Resulting SiO_2/Al_2O_3 ratio	Cu loading, (wt. %)	Cu/Al	Cu ion-exchange level, %
Cu-ZSM-5-176-199.2	176	145	1.3	0.99	199.2
Cu-ZSM-5-140-160.7	140	144	1.24	0.80	160.7
Cu-ZSM-5-100-127.5	100	97	1.24	0.64	127.5

The dependence of catalytic activity on SiO_2/Al_2O_3 ratio for over-exchanged Cu-ZSM-5 catalysts is shown in Figure 6.3. Results revealed that increasing the SiO_2/Al_2O_3 ratio led to a slight increase in catalytic activity. This was in contrast to the results obtained over H-form by Torre-Abreu et al. (1997a) who reported that a catalyst with SiO_2/Al_2O_3 ratio of 54 was the most active catalyst among catalysts with the same copper loading and SiO_2/Al_2O_3 ratios of 22, 54, 90 and 200. However, they examined only one catalyst with SiO_2/Al_2O_3 ratio greater than 100.

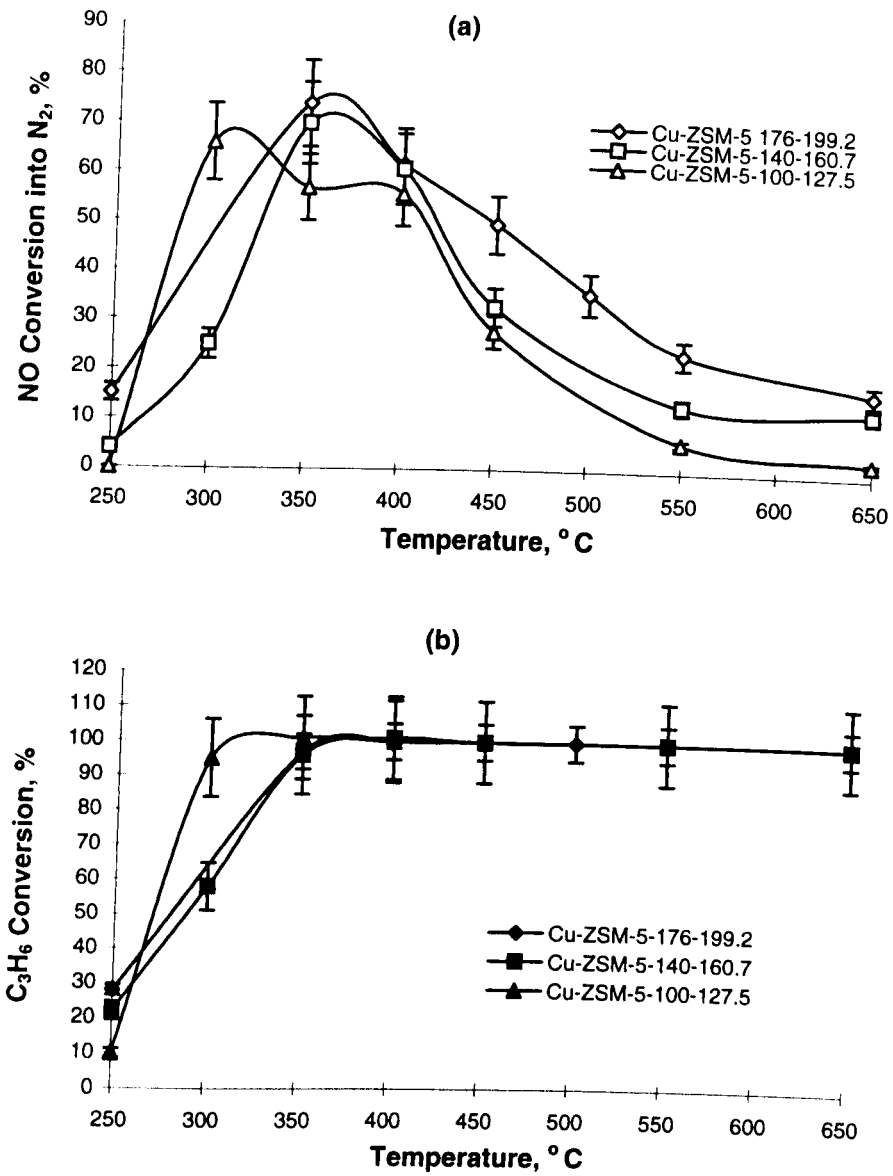

Figure 6.3. The dependence of NO conversion (a) and C_3H_6 conversion (b) on temperature and SiO_2/Al_2O_3 ratio. All catalysts have a 1.3% copper loading. Reaction conditions: 2000 ppm NO, 2000 ppm C_3H_6, 2% O_2, balance He, 1.0 g catalyst weight, and 150 ml min^{-1} total flow rate.

It can be postulated that the copper sites incorporated in the zeolites prepared from H-form or Na-form are different. In addition, the zeolite with different SiO_2/Al_2O_3 ratios did not have equal activity for SCR of NO, indicating that different active sites may be involved. It is believed that Cu ions in zeolite framework are involved in a

redox reaction in SCR of NO with hydrocarbons (Dedecek et al., 1995). The Cu^{2+} ions in zeolite with a higher SiO_2/Al_2O_3 ratio, and therefore a smaller number of Al acid sites in the zeolite framework, can be reduced to Cu^+ more easily than in zeolites with a lower SiO_2/Al_2O_3 ratio (Wichterlova et al., 1995). The higher activity in the zeolite higher SiO_2/Al_2O_3 ratios could be due to this redox property of the catalyst.

The most effective temperature was slightly decreased with decreasing SiO_2/Al_2O_3 ratio. This temperature was 350 °C for the two catalysts with higher SiO_2/Al_2O_3 ratios, i.e. 176 and 140, and was 300 °C for the catalyst with a SiO_2/Al_2O_3 ratio of 100. The maximum NO conversion and the complete propene oxidation occurred at the same temperature. Torre-Abreu et al. (1997a) reported that the most effective temperature decreased when the SiO_2/Al_2O_3 ratio increased. Their data shows that for under-exchanged catalysts, this temperature decreased from 500 to 350 °C and was 350 °C for Cu-ZSM-5-90-140 and Cu-ZSM-5-200-280 catalysts. However, in both studies, the temperature interval for the data measurements was 50 °C which means that the actual value for the most effective temperature involves ±25 °C uncertainty. Therefore, it can be concluded that the most effective temperature for over-exchanged catalysts could be 300 to 350 °C whether or not the catalyst was prepared from H-form or Na-form of ZSM-5 zeolite.

According to Figure 6.3(a), NO conversion over Cu-ZSM-5-100-127.5 catalyst increased with increases in temperature up to 300 °C, then decreased and remained constant from 350 °C to 400 °C, and then decreased again. The experiment was repeated in reverse order of temperature and the same results obtained. Although the error bars indicate that almost 12% errors were involved in the NO conversions, this phenomenon can not be related to the errors involved as the same results were obtained when the experiment was repeated.

Propene conversion showed the same trend as that of NO conversion into N_2 at temperatures lower than the most effective temperature, as shown in Figure 6.3(b). For example, the total propene oxidation was low at low temperatures where NO conversion was low, and increased sharply to 100% where the maximum conversion

of NO, 70 to 78%, occurred. The conversion of NO decreased with further increasing temperature, while the conversion of propene remained 100%. The reason could be different reaction mechanisms at temperatures below and greater than the most effective temperature, or competition of propene oxidation reaction with NO reduction.

6.3.2 The Effect of Copper Loading

The dependence of the activity of copper ion-exchanged ZSM-5 zeolites on copper loading using four over-exchanged samples with SiO_2/Al_2O_3 ratio of 100 but different copper loading was investigated. The main characteristics of the samples are shown in Table 6.2 and the details of the analysis of the catalysts are given in Appendix C. Figure 6.4 shows the conversions of NO at 350, 450 and 550 °C over Cu-ZSM-5 catalysts with a SiO_2/Al_2O_3 ratio of 100 but with different copper ion-exchange levels. It is shown that the NO conversion for over-exchanged Cu-ZSM-5 catalysts decreased with increase in copper ion-exchange level, and leveled off at a certain copper ion-exchange level depending on the operating temperature. The effect of the copper ion-exchange level is more pronounced at lower temperatures which could be due to less competition for propene combustion than to NO reduction at lower temperatures.

Table 6.2. Specifications of two groups of copper ion-exchanged ZSM-5 catalysts with the same SiO_2/Al_2O_3 ratios but different copper loadings.

Catalyst	Initial SiO_2/Al_2O_3 ratio	SiO_2/Al_2O_3 ratio after ion-exchange	Cu loading, (wt. %)	Cu/Al	Cu ion-exchange level, %
Cu-ZSM-5-100-168.6	100	91.1	1.58	0.84	168.6
Cu-ZSM-5-100-127.5	100	97	1.24	0.64	127.5
Cu-ZSM-5-100-108.3	100	96.5	1.06	0.54	108.3
Cu-ZSM-5-100-99.3	100	96	1.29	0.50	99.3

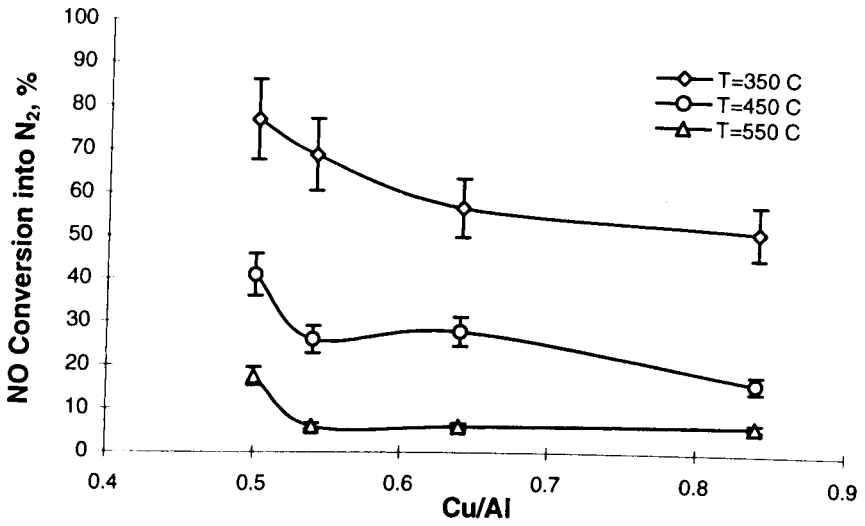

Figure 6.4. The dependence of NO conversion on Cu/Al and temperature over Cu-ZSM-5-100 catalysts. Reaction conditions: 2000 ppm NO, 2000 ppm C_3H_6, 2% O_2, balance He, 1.0 g catalyst weight, and 150 ml min^{-1} total flow rate.

NO conversion as a function of temperature is shown in Figure 6.5. It is seen that for over-exchanged samples, increasing copper loading results in a decrease in the activity of the catalysts. This could be due to aggregation of the copper or copper oxides in the zeolite pores. Therefore blockage of the pores may occur and prevent the passage of the gas through the zeolite channels. Another reason could be due to different coordination environments of copper sites associated in Cu-ZSM-5 zeolites as Larsen et al. (1994) showed that the fraction square-pyramidal component increased by increasing copper ion-exchange level. From the results obtained in this section, it is concluded that among Cu-ZSM-5 catalysts prepared from Na-form of ZSM-5 zeolites with the same SiO_2/Al_2O_3 ratio, the highest activity is shown by a catalyst with 100% copper ion-exchange level.

Dedecek et al. (1995) believed that the activity of the copper ions relates to the Al atoms which form localised Bronsted acid sites in the zeolite. They reported that Cu

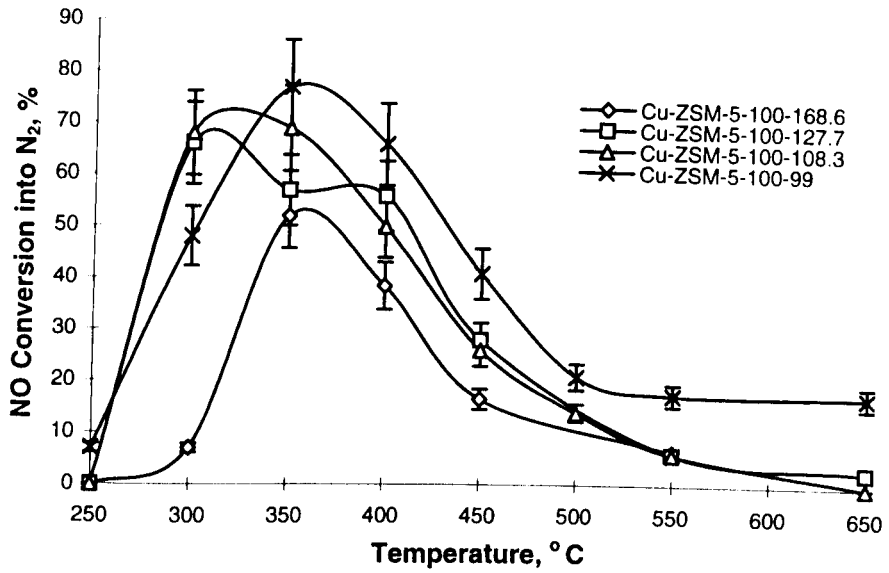

Figure 6.5. The dependence of NO conversion on temperature and copper loading for SCR of NO. All the catalysts have SiO_2/Al_2O_3 ratio of 100. Reaction conditions: 2000 ppm NO, 2000 ppm C_3H_6, 2% O_2, balance helium, 1.0 g catalyst weight, and 150 ml min^{-1} total flow rate.

sites in ZSM-5 zeolites were associated with two environments, depending on the number of aluminium atoms in the vicinity of the copper site. When a copper ion was adjacent to one Al atom a square planer coordination was assumed to form from a $(Cu^{2+}\text{-}OH)^+$ precursor. The other form of coordination was a square pyramidal coordination which was exhibited by a copper site balanced by two framework Al atoms. The Cu site distribution changed in different samples depending on Cu loading and SiO_2/Al_2O_3 ratio. Dedecek et al. (1995) assigned those sites adjacent to single framework Al atoms to Cu sites responsible for the Cu over-exchange. These sites are also well occupied below 100% copper exchange level. They concluded that these sites are responsible for the high activity of Cu-ZSM-5 in the direct decomposition of NO, as NO decomposition increases by increasing catalyst copper loading. It is postulated that these sites may not be attributed to the activity of the catalyst for SCR, as it was shown that the activity of Cu-ZSM-5 catalysts decreases by increasing copper loading.

Torre-Abreu et al. (1997a) employed Electron Spin Resonance (ESR) technique to determine the oxidation state of copper ions in zeolite. They reported that copper mainly existed as isolated Cu^{2+} in the catalysts with ion-exchange levels less than 100%, while in over-exchanged catalysts, Cu^{+1} ions and CuO were also detected.

In order to investigate the effect of copper loading on the activity of the catalysts prepared from the H-form of ZSM-5 zeolite for SCR of NO using propene, two catalysts with copper ion-exchange levels of 77 an 99.3 were prepared from H-ZSM-5 zeolite with a SiO_2/Al_2O_3 ratio of 50. The specifications of the catalysts and the details of the analysis of the catalysts are given in Table 6.3 and Appendix C, respectively. The catalysts were tested and the results are shown in Figure 6.6. The maximum NO conversion achieved over both catalysts was 68%, indicating that increasing ion-exchange level from 77 to 99.3% did not improve the maximum NO conversion. However, the catalyst with a higher copper ion-exchange level was more active at temperatures between 250 and 350 °C, and slightly less active at temperatures between 400 and 550 °C. The most effective temperature over both catalysts was 350 °C which is the same as the most effective temperature obtained for the catalyst prepared from the Na-form. Achieving the same maximum conversion over the catalysts with copper ion-exchange level of almost 80 to 100% reveals that SCR of NO over copper ion-exchanged zeolites prepared from H-form by propene is similar to SCR of NO using ethene as was reported by Sato et al. (1991).

Table 6.3. Specifications of two copper ion-exchanged ZSM-5 catalysts prepared from H-ZSM-5 zeolite with the same SiO_2/Al_2O_3 ratio.

Catalyst	Initial SiO_2/Al_2O_3 ratio	SiO_2/Al_2O_3 ratio after ion-exchange	Cu loading, (wt. %)	Cu/Al	Cu ion-exchange level, %
H-Cu-ZSM-5-50-99.3	50	50.7	1.85	0.5	99.3
H-Cu-ZSM-5-50-77.3	50	50.8	1.44	0.38	77.3

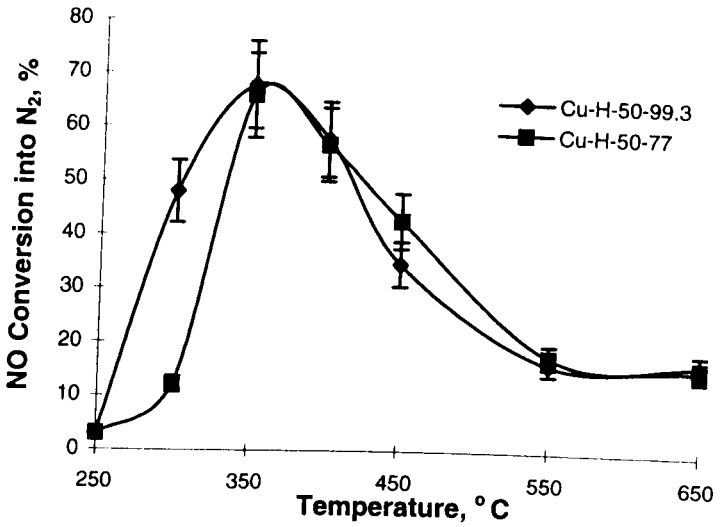

Figure 6.6. The dependence of NO conversion on temperature and copper loading of the catalysts prepared from H-ZSM-5 zeolites with SiO_2/Al_2O_3 ratios of 50 for SCR of NO. Reaction conditions: 2000 ppm NO, 2000 ppm C_3H_6, 2% O_2, balance helium, 1.0 g catalyst weight, and 150 ml min^{-1} total flow rate.

6.3.3 The Effect of Copper Ion-Exchange Level

Cu-ZSM-5-140-160.8 and Cu-ZSM-5-100-168.6 catalysts with almost the same copper ion-exchange level but different SiO_2/Al_2O_3 ratios were also tested. The temperature dependence of catalytic activity of the catalysts is shown in Figure 6.7. These catalysts also had different copper loadings, i.e. 1.58 and 1.24 wt.-% respectively. The specifications and the detailed analysis of the catalysts are given in Table 6.4 and Appendix C, respectively. It is worth noting that copper ion-exchange level can be increased by either increasing copper loading or increasing the SiO_2/Al_2O_3 ratio (i.e. decreasing aluminium Bronsted acid sites) of the catalyst. The results revealed that the catalyst with the higher SiO_2/Al_2O_3 ratio and lower copper loading showed higher activity as indicated in Figure 6.7. This is in agreement with the results obtained in previous sections that a higher SiO_2/Al_2O_3 ratio and lower copper loading cause higher activity for a catalyst.

Table 6.4. Specifications of two copper ion-exchanged ZSM-5 catalysts with almost the same copper ion-exchange level but different SiO_2/Al_2O_3 ratios.

Catalyst	Initial SiO_2/Al_2O_3 ratio	SiO_2/Al_2O_3 ratio after ion-exchange	Cu loading, (wt. %)	Cu/Al	Cu ion-exchange level, %
Cu-ZSM-5-100-168.6	100	91.1	1.58	0.84	168.6
Cu-ZSM-5-140-160.7	140	144	1.24	0.80	160.7

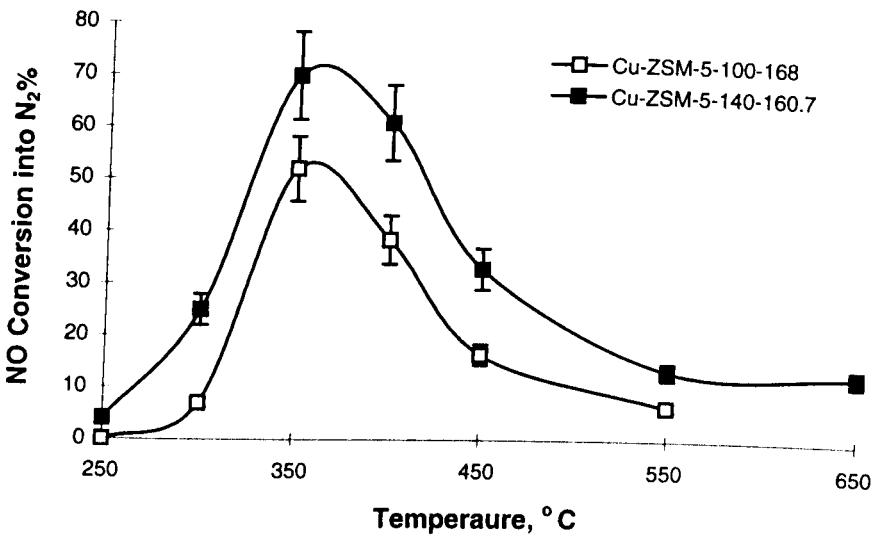

Figure 6.7. The dependence of NO conversion on temperature for two samples of Cu-ZSM-5 with almost the same copper ion-exchange level but different SiO_2/Al_2O_3 ratios. Reaction conditions: 2000 ppm NO, 2000 ppm C_3H_6, 2% O_2, balance helium, 1.0 g catalyst weight, and 150 ml min^{-1} total flow rate.

It can be concluded that for over-exchanged catalysts, the effect of copper ion-exchange level depends on the SiO_2/Al_2O_3 ratio of the catalyst. For catalysts with the same copper loading (Figure 6.3), the activity of the catalysts increased with increasing copper ion-exchange level, but for catalysts with the same SiO_2/Al_2O_3 ratios (Figure 6.4), increasing copper ion-exchange level resulted in a decrease in the

activity of the catalysts. It is suggested that both SiO_2/Al_2O_3 ratio and copper loading should be considered together when evaluating a copper ion-exchanged ZSM-5 zeolite catalyst. For example, when two over-exchanged catalysts with the same copper ion-exchange level are compared, the catalyst with the higher SiO_2/Al_2O_3 ratio is more effective for SCR of NO using propene as shown in Figure 6.7.

Torre-Abreu et al. (1997a) concluded that the catalysts with the same copper ion-exchange level but different copper loadings and different SiO_2/Al_2O_3 ratios show the same activity for SCR of NO using propene. They came to this conclusion by testing two groups of samples, each group including two samples with ion-exchange levels of 40% and 80%. From the results presented in this section, it is seen that the behaviour of the over-exchanged catalysts prepared from Na-form was different to the catalysts prepared from H-form. For the former with the same copper ion-exchange level, the higher the SiO_2/Al_2O_3 ration the higher the activity.

For each run of experiments material balance was conducted. However, 100% carbon balance was not achieved for SCR of NO using C_3H_6 at each reaction temperature. There was less carbon in the output stream than in the inlet gas at lower temperatures where propene was oxidised partially. For example, in an experiment over H-Cu-ZSM-5-140-109.5 (Figure 4.7), 8 to 10% less carbon was detected in the outlet gas at 250 and 300 °C (considering all carbon available in forms of CO_2, C_3H_6 and very small amounts in forms of CO and CH_4). However, at 350 °C and at temperatures greater than 350 °C, 6 to 7% more carbon atoms were detected in the output gas than in the input gas. It seems that carbon atoms available on catalysts in any form converted to CO_2 where 100% oxidation of C_3H_6 occurred. It is worth noting that at temperatures ≥ 350 °C, all carbon atoms were converted to CO_2, and neither CO nor other molecules containing carbon were detected. This indicates that carbonaceous species were deposited to the catalyst surface at lower temperatures, and then they were completely oxidised to CO_2 at higher temperatures. This was also confirmed by d'Itri and Sachtler (1992) who conducted temperature-programmed studies and reported the deposition of carbonaceous species to Cu sites by the interaction of propene with copper ion-exchanged ZSM-5 at temperatures below 600 K. They also

confirmed the oxidation of carbonaceous species to CO_2 by oxygen at temperatures above 600 K.

6.4 SCR of NO by Methane over Co-ZSM-5 Zeolites

It is well documented that methane is a non-selective reducing agent for the SCR of NO_x over Cu-ZSM-5. Li and Armor (1992) found that NO_x could be selectively reduced with methane in the presence of oxygen over a class of metal exchanged zeolites including cobalt. According to Li and Armor (1994), two parallel catalytic reactions occur over the catalyst, 1. NO reduction (R6-1) and 2. methane combustion (R6-2). The reaction equation for NO reduction was demonstrated by Equation (R6-1) as the presence of O_2 was essential for NO reduction and was also based on the product analysis.

$$2NO + CH_4 + O_2 \rightarrow N_2 + CO_2 + 2H_2O \qquad \text{(R6-1)}$$

$$CH_4 + 2O_2 \rightarrow CO_2 + 2H_2O \qquad \text{(R6-2)}$$

Li and Armor (1994) also pointed out that Co^{2+} ions are responsible for reduction of NO, and catalytic activity of the catalyst is proportional to the Co^{2+} exchange level. They believed that the importance of the Co-ZSM-5 catalyst lies in its ability to reduce NO in the presence of excess O_2, and simultaneously minimising the methane combustion rate.

In this project, systematic studies were undertaken with the aim of understanding the activity dependency of Co-ZSM-5 on many parameters. This section presents the effect of catalyst preparation method, SiO_2/Al_2O_3 ratio, cobalt loading and cobalt ion-exchange level on the activity of cobalt ion-exchanged ZSM-5 zeolites. The experiments were carried out over four groups of Co-ZSM-5 catalysts by passing a gas stream of 2000 ppm NO, 2000 ppm CH_4 2% O_2, and balance He at a rate 150 ml min^{-1}. In each run of experiment, 1 g catalyst was used and therefore, contact time was 0.4 g s ml^{-1}.

6.4.1 The Effect of Catalyst Preparation Method

Two samples of cobalt ion-exchanged ZSM-5 zeolites were prepared using two different preparation methods. The first sample was prepared using a semi-continuous system and the second using a batch system. These preparation methods are described in detail in Chapter 4. The specifications and the detailed analysis of the samples are given in Table 6.5 and Appendix C, respectively.

Table 6.5. Specifications of the two cobalt ion-exchanged ZSM-5 catalysts prepared using different preparation methods.

Catalyst	Preparation Method	Co Loading, (wt. %)	Co/Al	Co ion-exchange level, %
H-Co-ZSM-5-80-71	Semi-continuous	0.76	0.35	71
H-Co-ZSM-5-80-77.9	Batch	0.87	0.39	77.9

Although these samples were not very different in cobalt loading, they showed very different catalytic activities for reduction of NO using methane as shown in Figure 6.8. The activity of the sample prepared using the semi-continuous system was considerably higher than that of the sample prepared using the batch system over the entire range of temperatures. The maximum activity of the former was about two times that of the latter sample. The low activity of the catalyst prepared via the batch system could be due to precipitation of cobalt acetate or cobalt hydroxide in zeolite pores or on the external surface of the zeolite. Evaporation of acetic acid and water at the ion-exchange temperature, i.e. 80 °C, may have led to saturation of the cobalt acetate solution. Precipitation of cobalt hydroxide which can precipitate from all Co^{2+} salts may also occur. Therefore, even the sample with 10% more in cobalt loading but the same SiO_2/Al_2O_3 ratios showed less catalytic activity.

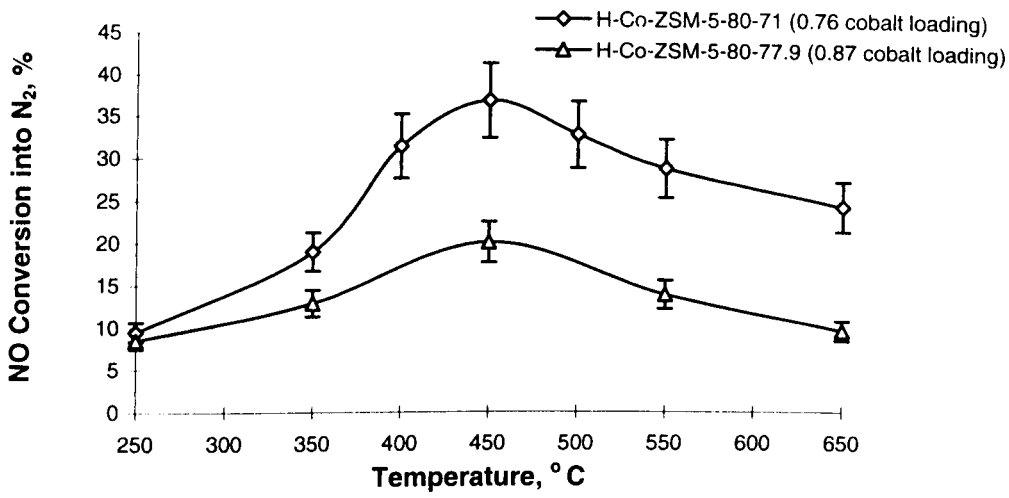

Figure 6.8. The effect of catalyst preparation on SCR of NO over Co-ZSM-5. The catalysts had the same SiO_2/Al_2O_3 ratio. Co-ZSM-5 catalyst prepared using batch (Δ) or semi-continuous system (◊).Reaction conditions: 2000 ppm NO, 2000 ppm CH_4, 2% O_2, balance He, 1.0 g catalyst weight, 150 ml min^{-1} total flow rate.

6.4.2 The Effect of SiO_2/Al_2O_3 Ratio

Two samples with SiO_2/Al_2O_3 ratios of 80 and 40, and with 1% cobalt loading were prepared using the semi-continuous system. The specifications of the samples are shown in Table 6.6. Figure 6.9 compares the catalytic activity of the two H-Co-ZSM-5 catalysts over a wide range of temperatures. The maximum NO conversion occurred at 450 °C for both catalysts, indicating that the most effective temperature is independent of the SiO_2/Al_2O_3 ratio of the catalysts. The results revealed that the NO conversion over the catalyst increases with decreasing SiO_2/Al_2O_3 ratio.

Increasing the activity of Co-ZSM-5 zeolite by decreasing the SiO_2/Al_2O_3 ratio was also reported by Li and Armor (1993). They came to this conclusion by conducting the experiment over three over-exchanged Co-ZSM-5 catalysts and considering that excess amounts of cobalt ions did not contribute to the NO reduction. In the other

words, they assumed that the NO conversion obtained over the over-exchanged catalysts served the activity of the fully exchanged catalysts. The suggested trend was correct, however they did not consider that increasing cobalt loading may result in decreasing the activity of the catalysts.

Methane conversion was very low at temperatures as low as 250 °C, increased slightly up to 350 °C, and then increased sharply. A complete conversion of CH_4 was observed at 500 °C. The highest NO conversions over the catalysts were achieved where the methane combustion was not completed, indicating that the selectivity of the catalyst for NO conversion into N_2 is higher than that of methane oxidation reaction.

Table 6.6. Specifications of the two cobalt ion-exchanged ZSM-5 catalysts with different SiO_2/Al_2O_3 ratios.

Catalyst	SiO_2/Al_2O_3 Ratio	Co Loading, (wt. %)	Co/Al	Co ion-exchange level, %
H-Co-ZSM-5-80-96.6	80	1.04	0.48	96.6
H-Co-ZSM-5-40-45	45	1.05	0.23	45

6.4.3 The Effect of Cobalt Loading

Three catalysts with different cobalt loadings were prepared from an H-form of ZSM-5 with a SiO_2/Al_2O_3 ratio of 80. The cobalt ion-exchange level of the catalysts varied from 71% to 428%. The specifications and detailed analysis of the samples are given in Table 6.6 and Appendix C respectively. Figure 6.10 compares the NO conversions for SCR of NO over the three catalysts in a temperature range of 250-650 °C. Similar conversion profiles were obtained using the three catalysts. Although the cobalt loadings were vastly different, the most effective temperature was the same for the three cases, i.e. 450 °C.

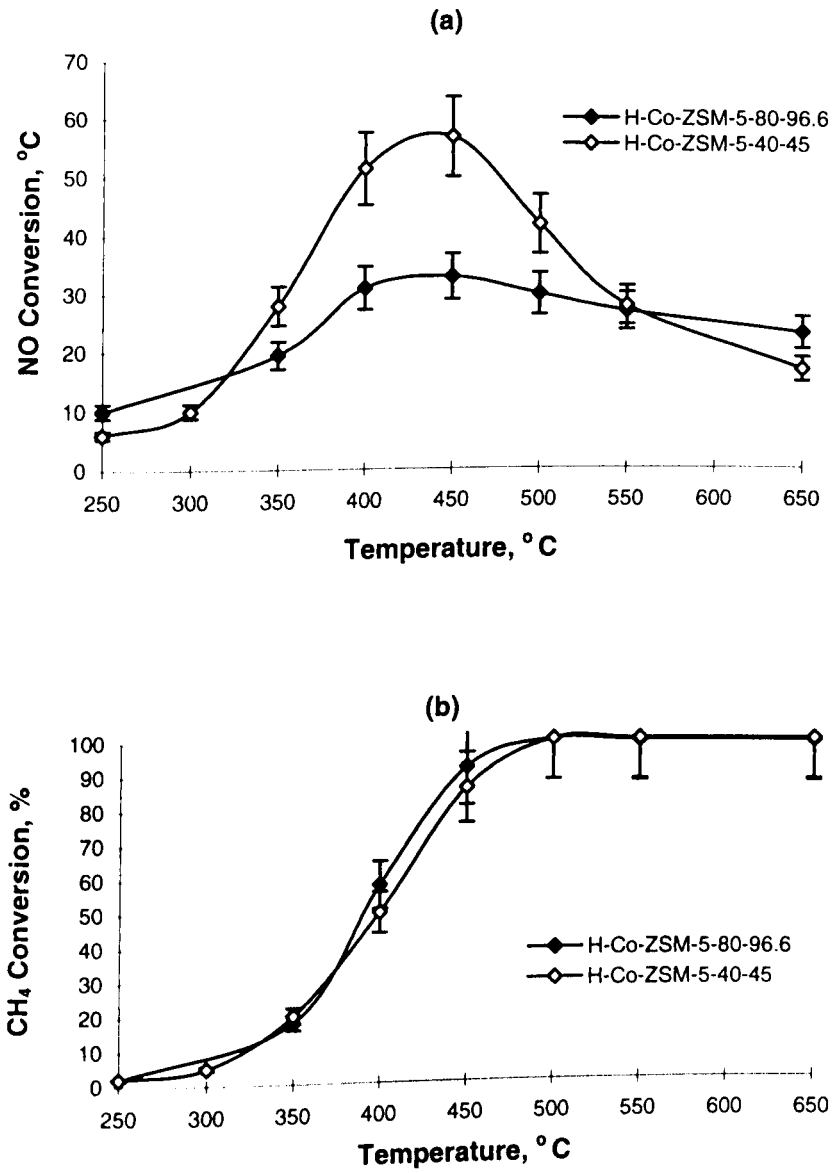

Figure 6.9. The dependence of NO conversion (a) and CH_4 conversion (b) on temperature and SiO_2/Al_2O_3 ratio for SCR of NO and oxidation of methane over Co-ZSM-5. Both catalysts included 1% copper loading. Reaction conditions: 2000 ppm NO , 2000 ppm CH_4 , 2% O_2, balance He, 1.0 g catalyst weight, and 150 ml min^{-1} total flow rate.

The activities of the catalysts for the two under-exchanged catalysts were similar at temperatures below 400 °C but slightly different at higher temperatures. The catalyst with very high cobalt loading showed less activity over the whole range of temperatures.

Table 6.7. Specifications of the three cobalt ion-exchanged ZSM-5 catalysts with same SiO_2/Al_2O_3 ratio but different cobalt loadings.

Catalyst	SiO_2/Al_2O_3 Ratio	Co Loading, (wt. %)	Co/Al	Co ion-exchange level, %
H-Co-ZSM-5-80-428	80	4.45	2.14	428
H-Co-ZSM-5-80-96.6	80	1.04	0.48	96.6
H-Co-ZSM-5-80-71	80	0.76	0.35	71

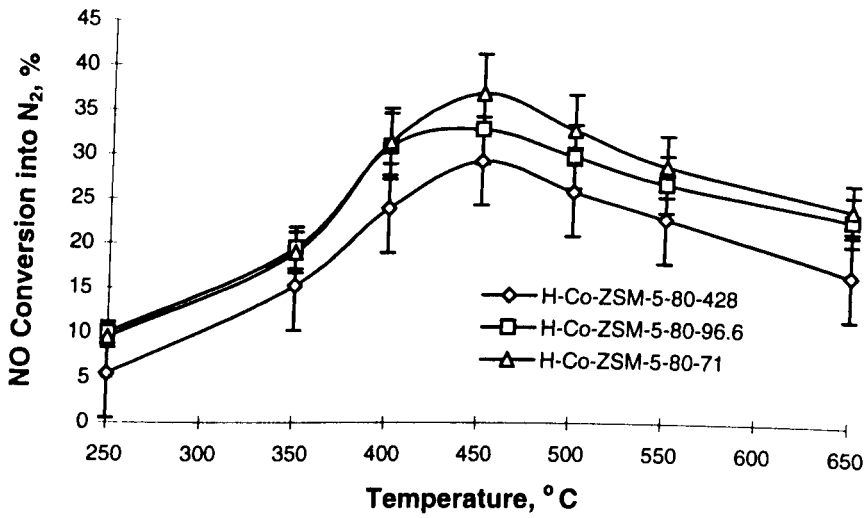

Figure 6.10. The dependence of NO conversion on temperature and cobalt loading for SCR of NO over Co-ZSM-5 with SiO_2/Al_2O_3 Ratio of 80. Reaction conditions: 2000 ppm NO, 2000 ppm CH_4 , 2% O_2, balance helium, 1.0 g catalyst weight, and 150 ml min^{-1} total flow rate.

The effect of metal loading on the activity of Co-ZSM-5 catalysts for NO reduction by methane was different from that of Cu-ZSM-5 when propene was used as shown in Figure 6.3 and Figure 6.10, respectively. In Co-ZSM-5, the activity decreased due to increasing copper loading for over-exchanged samples while the results obtained over Cu-ZSM-5 showed an opposite trend. This could be due to different reaction mechanisms. Li and Armor (1993) reported that a redox process could not involve

the reduction of NO over Co-ZSM-5. They also believed that an active site was a single Co^{2+} cation. This is different from the reaction mechanism over Cu-ZSM-5 because it is believed that a redox mechanism is involved for the reduction over Cu-ZSM-5 catalysts.

The most effective temperatures for SCR of NO by methane over H-Co-ZSM-5 catalysts are much higher than the most effective temperatures of Cu-ZSM-5 using propene as the reducing agent. This could be due to the high stability of methane which is related to the strong C-H bond (422 KJ $mole^{-1}$). Therefore, high temperatures are required to activate methane.

6.5 Summary

Selective catalytic reduction of NO over copper and cobalt ion-exchanged with H-form ZSM-5 zeolites using methane and propene was investigated and compared under the same conditions. The experimental results proved that the highest NO conversion was achieved over the H-Cu-ZSM-5 when propene was the reducing agent. Similar NO conversion profiles were obtained over the H-Co-ZSM-5 catalyst using either methane or propene. The lowest NO conversion was observed over H-Cu-ZSM-5 when methane was the reducing agent.

The effect of SiO_2/Al_2O_3 ratio, copper loading and copper ion-exchange level on reduction of NO by propene over Cu-ZSM-5 zeolites with more than 100% copper ion-exchange level was investigated. Catalysts with the same copper loading but different SiO_2/Al_2O_3 ratios showed slightly different activities. It was observed that at temperatures $\geq$ 350 °C, the higher the SiO_2/Al_2O_3 ratio, the higher the NO conversion. The effect of copper loading for the catalysts with the same SiO_2/Al_2O_3 ratio was more pronounced. Maximum NO conversion decreased by increasing copper loading. In addition, the results indicated that two catalysts with the same copper ion-exchange levels may not show the same activities, as they may have different SiO_2/Al_2O_3 ratios and different copper loadings. Therefore, the SiO_2/Al_2O_3

ratio as well as copper loading should be considered together to compare the activities of the two Cu-ZSM-5 catalysts.

The effect of catalyst preparation, SiO_2/Al_2O_3 ratio, and cobalt loading on reduction of NO by methane over Co-ZSM-5 zeolites was investigated. A comparison between two catalysts with the same cobalt ion-exchange levels revealed that a higher NO conversion was achieved over a catalyst ion-exchanged in a semi-continuous system than the catalyst ion-exchanged in a batch system. It was also required to use a refluxing system as the cobalt ion-exchange process is carried out at high temperatures, i.e. 80 °C. In addition, from a comparison between NO conversions achieved over the two catalysts with the same cobalt loadings but different SiO_2/Al_2O_3 ratios, it was found that the lower the SiO_2/Al_2O_3 ratio, the higher the activity. Furthermore, for catalysts with the same SiO_2/Al_2O_3 ratios, the activity of Co-ZSM-5 catalysts slightly decreased by increasing cobalt loading, whereas the decrease was more pronounced for over-exchanged catalysts. This was concluded based on the activity profiles obtained over several Co-ZSM-5 catalysts with cobalt ion-exchange levels greater than 71%. Therefore, the highest NO reduction may be obtained over catalysts with cobalt ion-exchange levels less than 70%.

CHAPTER SEVEN

NO CONVERSION STUDIES USING OTHER CATALYSTS

7.1 Introduction

The previous Chapters have investigated the ability of the various catalysts supported on ZSM-5 zeolites for decomposition of NO either directly or via SCR. ZSM-5 zeolites used to prepare the catalysts were synthesised in our laboratory or obtained from Zeolyst International. This Chapter extends the previous work to cover a wider range of different catalysts, particularly, those supported on MCM-41 molecular sieves and pillared clays. This part of the work was done in collaboration with Dr. Max Lu of Department of Chemical Engineering at the University of Queensland. Two groups of catalysts were received from the University of Queensland to evaluate their catalytic activities for the direct decomposition or selective catalytic reduction (SCR) of NO. These two groups are outlined as follows:

- Ten samples including synthesised ZSM-5 zeolite and MCM-41 molecular sieve as well as SiO_2+Al_2O_3, ZSM-5+TiO_2 and MCM-41+MoO_3+TiO_2.

  The catalysts supports, i.e. ZSM-5 zeolite and MCM-41 molecular sieve, were synthesised and the catalysts were prepared using different preparation methods including ion-exchange, impregnation, and incorporation of cations during zeolite synthesis with copper.

- Twenty one samples of pillared clays (PILC).

These catalysts were prepared using montmorillonite (clay) and left in contact with pillaring solution to obtain a more porous structure. They were then calcined and ion-exchanged with different cations.

The catalytic activities of the first group of samples were evaluated by testing the samples for direct decomposition of NO with and without the presence of oxygen and also in the presence of methane. Some of the samples showed reasonable (e.g. up to 28% NO_x conversion) catalytic activity, comparable with the activity of zeolites reported in the literature (Iwamoto et al., 1986a). However, the catalytic activities of some other samples were very low which indicated that the nature of the samples or the preparation methods were responsible for the low NO conversion. The effect of the presence of oxygen on the catalytic activities of the samples was also examined. NO_x conversion was significantly enhanced by the presence of oxygen at temperatures below 400 °C and slightly decreased at temperatures greater than 450 °C. The effect of the addition of methane on NO decomposition for several samples was also examined. The presence of methane in the reacting stream sharply increased the catalytic activity in the absence of oxygen at temperatures greater than 500 °C. SCR of NO using methane or propene over the most active sample selected was also examined and 95% conversion was achieved using propene as the reducing agent.

The catalytic activities of the second group were evaluated in the presence of methane and oxygen. However, these samples did not show any catalytic activity for the selective catalytic reduction of NO.

7.2 Catalyst Synthesis and Preparation Methods

As mentioned in the previous section, ZSM-5 zeolites and MCM-41 molecular sieve used in this part of the experiments were synthesised and prepared at the University of Queensland. The procedures for the synthesis and preparation methods used are described in detail below.

7.2.1 ZSM-5 Zeolites and MCM-41 Molecular Sieve

The zeolites were synthesised in a hydrothermal system containing a silica source (sodium silicate), an aluminium source (aluminium sulphate) and a template (H_2N-$(CH_2)_6$-NH_2).

The preparation procedures for the samples are classified in Table 7.1. The preparation methods used for the samples were: 1. ion-exchange of the samples to a Cu-form or H-form; 2. incorporation of Cu into the ZSM-5 framework during synthesis; 3. impregnation; and 4. mixing mechanically with $CuCl_2$.

The H-form of the zeolite was obtained by ion-exchange of the zeolite in NH_4NO_3 or NH_4Cl solutions. The ion-exchange procedure was carried out at room temperature, and this process was repeated until the required level of ion-exchange was achieved.

The structure of the zeolite samples were identified using XRD. Two samples with different SiO_2/Al_2O_3 ratios were received from Hamada at the National Chemical Laboratories for Industry in Japan were used as references.

7.2.2 Pillared Clays (PILCs)

To prepare a pillared clay catalyst, montmorillonite (bentonite) was left in contact with a pillaring solution in order to obtain a more porous structure. Accordingly, aluminium pillaring solution containing polycations $[Al_{13}O_4(OH)_{24}(H_2O)_{12}]^{7+}$, referred to as the Keggin ion, was prepared by controlled hydrolysis of an aluminium salt solution, i.e., aluminium nitrate ($Al(NO_3)_3.9H_2O$) or aluminium chloride ($AlCl_3.6H_2O$) with sodium hydroxide (NaOH). For instance, a 1200 ml of 1.0 M NaOH was added drop-wise, with constant stirring, into 600 ml of 1.0 M aluminium chloride solution for approximately 2 hours.

Table 7.1. Preparation conditions of the first group of samples and their specifications.

Sample No. and code	Sample identification	Copper loading (%)	Preparation method
Sample 1 (53C)	Cu-ZSM-5-25.4-81.2 SiO_2/Al_2O_3=25.4	1.55	Na-ZSM-5 was ion-exchanged with 0.015M $Cu(CH_3COO)_2$ (Solid/liquid =1 g : 50 ml) at 65 °C overnight 4 times, then calcined at 500 °C for 12 hours.
Sample 2 (53MC)	Cu-ZSM-5-25.4-140.9 SiO_2/Al_2O_3=25.4	2.69	H-ZSM-5 was physically mixed with $CuCl_2$ (2.5% Cu in total), then calcined at 500 °C for 12 hours.
Sample 3 (541-C5)	Cu-ZSM-5-25 + MCM-41 SiO_2/Al_2O_3 (ZSM-5)=25	1.81	The support included a mixture of ZSM-5 and MCM-41 (1:1, weight ratio), ion-exchanged as for Sample 1 but calcination was carried out at 400 °C for 12 hours.
Sample 4 (54C)	Cu-ZSM-5-26 SiO_2/Al_2O_3=26	2.65	Cu was incorporated into ZSM-5 framework during synthesis, then ion-exchanged twice with $Cu(CH_3COO)_2$, and calcined at 500 °C.
Sample 5 (55H)	Cu-ZSM-5	2.21	Cu was incorporated into ZSM-5 framework during synthesis, then ion-exchanged to H form, and calcined at 500 °C.
Sample 6 (STM-C5)	Silicalite-1 + TiO_2	2.73	Silicalite-1 + TiO_2, impregnated with 5% Cu and calcined at 400 °C for 8 hours.
Sample 7 (57C5)	Cu-ZSM-5-15-119 SiO_2/Al_2O_3=15	2.88	Na-ZSM-5 was ion-exchanged with NH_4^+ first, then with Cu^{2+}. The sample was calcined at 550 °C for 10 hours.
Sample 8 (SA-C5)	SiO_2 + Al_2O_3	1.39	Cu was impregnated over the mixture of amorphous silica and alumina. SiO_2 and Al_2O_3 were added to $Cu(CH_3COO)_2$ solution. Sodium hydroxide was then added to adjust pH to about 12.
Sample 9 (H417)	Cu-MCM-41	-	Cu was incorporated during synthesis (Si/Cu = 30).
Sample 10 (41TM-V2)	MCM-41+ MoO_3+TiO_2	-	V was impregnated over MCM-41+ MoO_3 + TiO_2 (similar to Sample 8).

To prepare aluminium pillared clay (Al-PILC), the pillaring solution was diluted to 0.07 M and 10.0 g of bentonite was added to the solution, then stirred for 3 hours, while the Na^+ ions of the clay were exchanged with the Keggin-ions. It was then filtered and washed until the product became free of Cl^- and NO_3^- ions. The obtained cake was dried at 110 °C for 24 hours in air. Finally, the product was calcined at 500 °C for 24 hours. After calcination, the PILCs Cation Exchange Capacity (CEC) was restored at different pH as shown in Table 7.2 with Na^+-cations. Then Co^{2+}, Cu^{2+} and Ni^{2+} cations were doped into PILC.

LaAl-PILCs were prepared using $LaCl_3$. A La-Al pillaring solution was prepared by hydrothermal treatment of Al_{13} solution and $LaCl_3$. The hydrothermal treatments were carried out for 96 hours by refluxing of the solution or by treating the solutions in a stainless steel autoclaves at 120 °C. After filtration and washing until the filtrate was free of Cl^-, the obtained product was air dried at 100 °C for 24 hours. Afterwards the product was calcined at 500 °C for 3 hours. Then, cation exchange was performed using the same procedure described for aluminium pillared clay catalysts.

CeAl-PILCs were prepared using $Ce(NO_3)_3.6H2O$. The preparation procedure was the same as preparation of LaAl-PILC, except $Ce(NO_3)_3.6H_2O$ was used instead of $LaCl_3$.

PILCs were cation exchanged in two steps. First, the calcined PILCs were treated with an aqueous solution containing Na^+ cations at various pH values to restore the CEC, then obtained powder containing Na^+ cations (Na^+ doped PILC) was exchanged with an aqueous solution of desired transition cations like Cu^{2+}, Co^{2+} and Ni^{2+} at a pH value of about 3 to 5 to restore the Na^+ ions. The type and the pH value of the solution containing Na^+ which was used to restore cation exchange capacity of the clays are detailed in Table 7.2.

Table 7.2. The type and the pH value of the solutions used to restore the cation exchange capacity of the pillared clays.

Sample	Type	pH
1	Cu^{2+}-Al-PILC	8
2	Co^{2+}-Al-PILC	8
3	Ni^{2+}-Al-PILC	8
4	Cu^{2+}-LaAl-PILC	7
5	Co^{2+}-LaAl-PILC	7
6	Ni^{2+}-LaAl-PILC	7
7	Cu^{2+}-LaAl-PILC	9
8	Co^{2+}-LaAl-PILC	9
9	Ni^{2+}-LaAl-PILC	9
10	Cu^{2+}-LaAl-PILC	11
11	Co^{2+}-LaAl-PILC	11
12	Ni^{2+}-LaAl-PILC	11
13	Cu^{2+}-CeAl-PILC	7
14	Co^{2+}-CeAl-PILC	7
15	Ni^{2+}-CeAl-PILC	7
16	Cu^{2+}-CeAl-PILC	9
17	Co^{2+}-CeAl-PILC	9
18	Ni^{2+}-CeAl-PILC	9
19	Cu^{2+}-CeAl-PILC	11
20	Co^{2+}-CeAl-PILC	11
21	Ni^{2+}-CeAl-PILC	11

7.3 Experimental Technique

The equipment for evaluation of the catalytic activities of samples was described in Chapter 4. The first group of samples were tested using either a quartz or a stainless

steel tube reactor (I.D. 1.0 cm). The catalytic activity of this group of catalysts were evaluated by measuring NO_x conversion using the NO_x analyser or NO conversion into N_2 using a gas chromatograph. The gas cylinders contained on a mole basis, 4000 ppm of NO and 70 ppm NO_2 in nitrogen (when using NO_x analyser) or 12% NO in helium (for GC studies). To reduce the amount of error which may be caused by using a pure NO gas, low concentrations of NO were selected. In this case, the mass flow rates could be set at higher amounts to reduce errors due to the mass flow controller.

The NO_x analyser was calibrated before each run of experiment as described in Chapter 4. The GC calibration was checked using a verification run periodically and re-calibrated when it was required. The gas flow could be switched to pass or by-pass the reactor by a valve and then pass through either the NO_x analyser or GC. Therefore, the NO and NO_x concentrations in the gas streams before and after the reactor could be measured by the NO_x analyser or GC.

The synthesised materials were characterised by XRD. As a typical result, XRD pattern of silicalite-1 and MCM-41 molecular sieves are presented in Figure 7.1. The results confirmed the structure of the expected materials except for Sample 53C which, besides of ZSM-5 zeolites, contained some amorphous silica. The elemental analysis for the catalysts were carried out at Amdel Laboratories Ltd., SA. The catalysts were analysed using the whole rock fusion and Inductively Coupled Plasma (ICP) methods to determine silica to alumina ratio of the support as well as copper loading of the samples. The percentage of copper loadings and the SiO_2/Al_2O_3 ratios of the zeolites are also presented in Table 7.1.

To examine the first group of catalysts, a flow of synthetic gas containing 2000 ppm NO in N_2 or helium (depending whether the NO_x analyser or GC was used) at a flow rate of 100 ml min^{-1} passed over each catalyst. The O_2 concentration was 1.6 or 2%, the CH_4 concentration was 0.2 or 0.52% and the C_3H_6 concentration was 0.2%. The packed bed tubular reactor housed 1.5 g of a catalyst for each experimental run, so the contact time was 0.9 g s ml^{-1}. The experiments were carried out within a temperature range of 250-650 °C. NO_x conversion was calculated based on the inlet

and outlet concentrations of NO_x (Eq. (2-2)). NO conversion into N_2 was calculated based on the N_2 produced and NO concentration in the inlet gas stream (Eq. (2-7)).

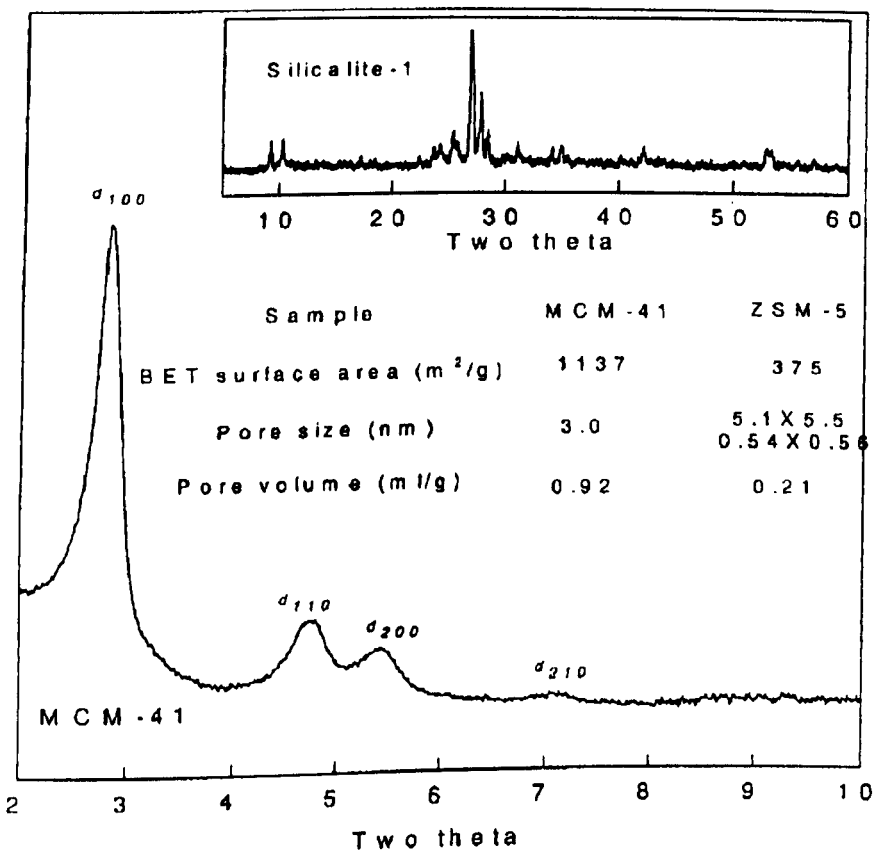

Figure 7.1. XRD patterns of silicalite-1 and MCM-41 molecular sieves as a typical example. Surface area, pore size, and pore volume of these two materials are also shown in this Figure.

For the second group of samples, a gas stream with a flow rate of 150 ml min^{-1} containing 1000 ppm NO, 500 ppm CH_4, 2% O_2, and balanced with helium was used to investigate selective catalytic reduction of NO. In each run of the experiments, 0.5 g of catalyst was located in a stainless steel tube reactor with a diameter of 0.5 cm, which gave a contact time of 0.2 g s ml^{-1}. The inlet and outlet gas streams of the reactor were analysed by the GC.

7.4 Results and Discussion for the First Group of Catalysts

The first group of samples were tested for direct decomposition of NO_x in the absence or presence of oxygen. The effect of the presence of methane was also examined over the most active catalysts. Sample 3 was selected for further investigation as this catalyst showed relatively high activity for NO_x conversion over a wide range of temperatures. The thermal stability and the effect of pre-treatment of the catalyst in a helium gas stream at 500 °C on the NO conversion into N_2 was examined. The catalyst was also tested for SCR of NO with methane or propene. The experiments were also carried out in order to examine whether the presence of MCM-41 had a significant effect on the kinetic behaviour of Cu-ZSM-5 catalyst.

7.4.1 NO_x Conversion Without the Presence of Oxygen

NO_x conversion was investigated over all the catalysts described in Table 7.1. The NO_x conversion measurements were carried out at temperatures between 300 °C and 700 °C. Among the catalysts tested, synthesised ZSM-5 zeolites as well as a mixture of ZSM-5 with a MCM-41 molecular sieve ion-exchanged with copper were found to be the most active for the NO_x conversion. The results indicated that the maximum NO_x conversion achieved over the catalysts, which did not contain any Cu-ZSM-5 zeolite, including MCM-41 molecular sieve alone, was only 6%.

NO_x conversions over the five samples exhibiting some activity are presented in Figure 7.2. Among them, Samples 3 and 7 were most active, both achieving a maximum conversion of nearly 30%. This conversion is however lower than the maximum NO conversion of 95% reported by Iwamoto et al. (1989) over Cu-ZSM-5-23.3-143 with a contact time of 4.0 g s ml^{-3}. The major difference is the decrease in contact time used in the present study (0.9 g s ml^{-3}). The effect of contact time on NO decomposition was tested on Sample 3 for contact times up to 2 g s ml^{-1}. It was observed that the NO conversion into N_2 was directly proportional to contact time

and 57% NO conversion was obtained at a contact time of 2 g s ml^{-1}. This is further shown in Figure 7.10 in this chapter. A similar observation was made by Li and Hall (1991) for conversions up to 8% in their kinetic studies. If the same linear trend is assumed for contact times higher than 2 g s ml^{-1}, the NO conversion achieved over Sample 3 would be comparable with what Iwamoto et al. reported for Cu-ZSM-5-23.3-143.

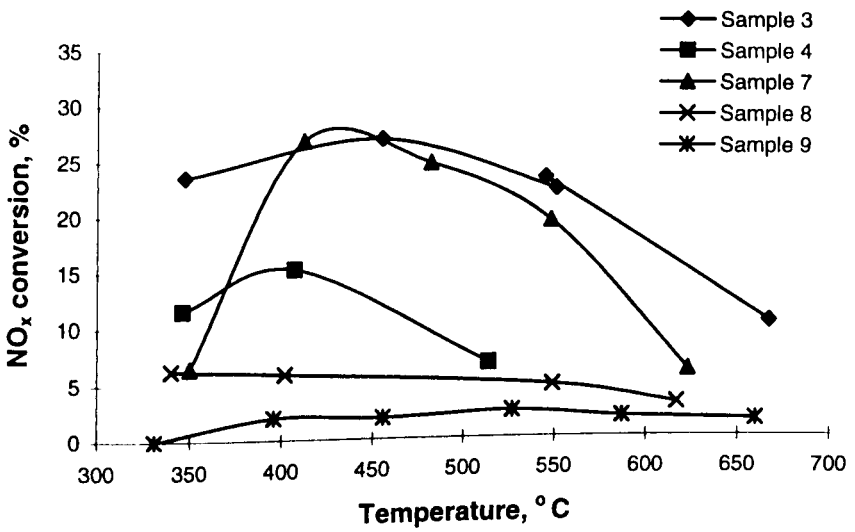

Figure 7.2. The dependence of NO_x conversion on temperature for 5 synthesised samples. Reaction conditions: 2000 ppm NO, balance He, 1.5g catalyst weight, and 100 ml min^{-1} total flow rate.

Sample 3, which contained a mixture of copper ion-exchanged ZSM-5 and MCM-41, also exhibited a greater stability for NO_x decomposition than other catalysts over the entire temperature range investigated. This indicates that the presence of MCM-41 did not reduce the activity of Cu-ZSM-5 but served to stabilise it over a wider temperature range than that observed for Cu-ZSM-5.

The catalytic activity exhibited by Sample 4 was considerably less than that of Samples 3 and 7, indicating the importance of the preparation method as Campa et al. (1994) stated. They reported that a Cu-ZSM-5 catalyst prepared using impregnation method showed only one-tenth of the activity of the catalyst prepared via an ion-

exchanged method. They postulated that different copper sites were produced by the different preparation methods. However, the type of the copper sites was not identified. Campa et al. (1994) also found that the impregnated catalyst could have the same activity as ZSM-5 catalysts prepared via ion-exchanged method if the excess copper was removed by washing with water after impregnation. Further investigations are required to see if this is correct for the catalysts incorporated with copper during zeolite synthesis. If it is, it could then come to the conclusion that the copper ion-exchange conducted via incorporation of copper during synthesis may result in copper aggregates formation in the zeolite, thus blocking the passage of NO to the active sites which leads to inhibiting the direct decomposition of NO.

The catalytic activities of Samples 1 and 7 were very different despite the fact that both used ZSM-5 zeolites as the catalyst support. Sample 1 exhibited no activity while nearly 30% NO_x conversion was achieved over Sample 7. The main difference between the two samples was that Sample 7 was ion-exchanged to the H-form prior to ion-exchange with copper. Calcination times and temperatures as well as copper ion-exchange conditions were similar. Hydrogen ion-exchange of ZSM-5 introduces bronsted acid sites of high and uniform strength into the zeolite (Shelef, 1995). Centi and et al. (1994) reported that the interaction of isolated Cu^{2+} species with the bronsted acid sites allowed the formation of mononitrosyl and dinitrosyl species to occur and for direct decomposition these species were believed to be the intermediates for nitrogen formation. This may be the reason Sample 7 was active and Sample 1 was not, however this observation has not been reported by other researchers. The specific catalytic activity of Cu-ZSM-5 was found to increase with increasing copper loading by Iwamoto et al. (1989) and hence this may also contribute to the high activity of Sample 7 which has a copper exchange level of 119% compared to 81% for Sample 1. Moretti (1994) also reported that the lower the silica to alumina ratio, the higher the catalytic activity for the same copper loading which was in agreement with the results obtained over Samples 1 and 7. However, this was in contrast to the results reported by Iwamoto et al. (1986b), who reported that the catalytic activity per Cu^{2+} site was increased by increasing SiO_2/Al_2O_3 ratio of Cu-ZSM-5 catalyst.

7.4.2 NO_x Conversion in the Presence of Oxygen

NO_x conversions when 1.6% O_2 was present in the stream of 2000 ppm NO in N_2 over eight samples are compared in Figures 7.3. A trend of increasing NO conversion with increasing temperature up to a maximum at 300 - 400 °C was observed for all samples. The maximum NO_x conversion was at least 20% for all samples except Sample 10 which also did not show any catalytic activity without the presence of oxygen. Referring to Figure 7.3, Sample 4 showed the maximum catalytic activity for NO_x conversion in the presence of oxygen, even though this sample did not achieve the highest NO_x conversion for the direct decomposition without the presence of oxygen. This is contrary to what Iwamoto et al. (1991a) concluded, that the presence of O_2 decreases NO conversion. The higher NO_x conversion achieved at lower temperatures when oxygen was added to the system could be due to conversion of a fraction of NO into N_2O which results in higher NO_x conversion.

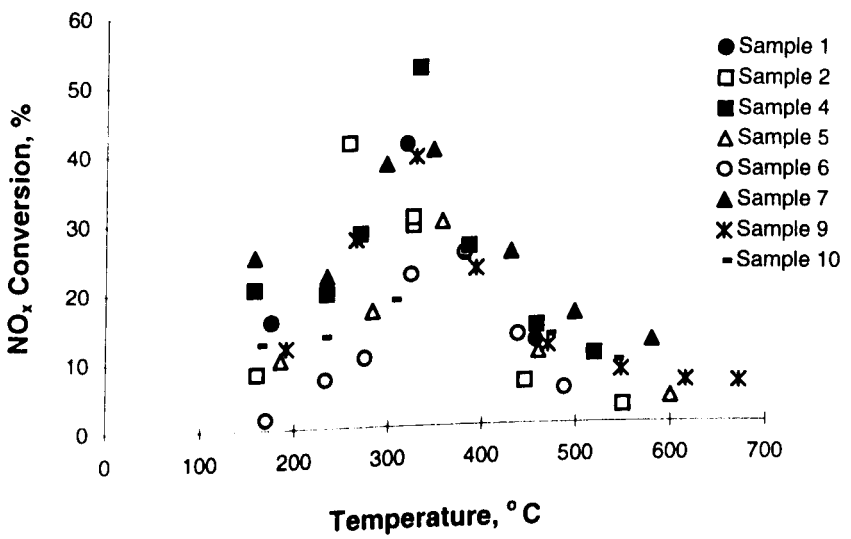

Figure 7.3. The dependence of NO_x conversion on temperature in the presence of O_2. Reaction conditions: 2000 ppm NO, 1.6% O_2, balance He, 1.5g catalyst weight, and 100 ml min^{-1} total flow rate.

NO_x conversions in the presence of oxygen achieved over Samples 4, 7, and 9 as a function of temperature are presented in Figure 7.4. These Samples were selected as they showed a wide range of performance (medium, high and low, respectively) for the direct decomposition without the presence of oxygen. It is shown that the activity of the three catalysts increased at lower temperatures by oxygen. Centi et al. (1994) also reported that adding oxygen promoted NO conversion at low temperatures (around 250 °C). On the other hand, Iwamoto et al (1991a) reported that the presence of O_2 decreased the catalytic activity of ZSM-5 zeolite. Li and Hall (1990) supported this observation in their investigation of the activity of Cu-ZSM-5 zeolite at the 500 °C which is not in contradiction with this study, as they tested their catalyst at 500 °C only. It can be concluded that the catalytic activity in the presence of O_2 which is a function of temperature differs at low and high temperatures. O_2 promotes the NO_x conversion at temperatures lower than 300 °C but decreases it at temperatures above 350 °C.

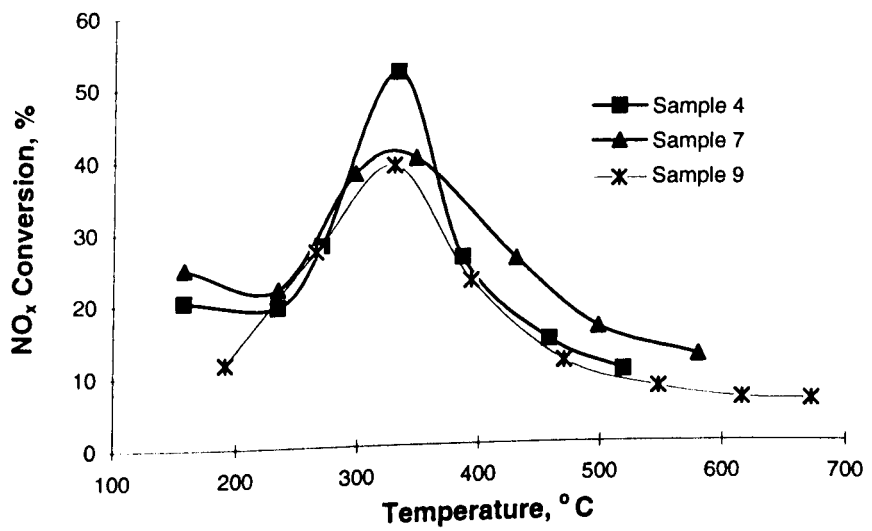

Figure 7.4. The dependence of NO_x conversion on temperature in the presence of O_2. Reaction conditions: 2000 ppm NO, 1.6% O_2, balance He, 1.5g catalyst weight, and 100 ml min^{-1} total flow rate.

7.4.3 NO_x Conversion in the Presence of Methane

NO_x conversions in the presence of 0.52% CH_4 over Samples 4, 6 and, 7 are compared in Figure 7.5. At low temperatures, NO_x conversion over Samples 6 and 7 are low, but increase with increasing temperature. It is noticeable that Sample 4 showed roughly 50% conversion at around 300 °C in the presence of methane which was much higher than the conversions exhibited by the other two samples. At temperatures greater than 600 °C, the catalytic activities of the three samples are similar, with NO_x conversions greater than 90%. Therefore, it can be concluded that Sample 4 could be more suitable for SCR of NO in the presence of methane than Samples 6 and 7.

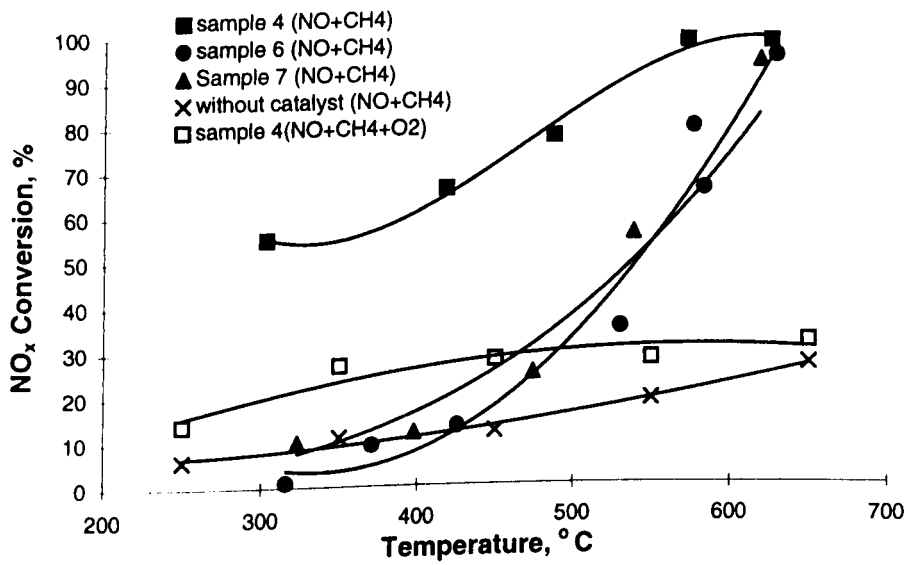

Figure 7.5. The dependence of NO_x Decomposition in the presence of CH_4 on temperature. Reaction conditions: 2000 ppm NO, 0.52% CH_4, balance He, 1.5g catalyst weight, and 100 ml min^{-1} total flow rate.

The support used to prepare Sample 6 was different with those of Samples 4 and 7. Therefore the effect of preparation method on the activity of Cu-ZSM-5 catalysts can be only compared by NO_x conversion achieved over Samples 4 and 7. The higher activity of Sample 4 over Sample 7 at low temperatures could be due to different active sites produced by the different preparation methods utilised. However, the type of copper sites provided by the incorporation method has not been reported in the

literature as discussed in Section 7.4.1. Trout et al. (1996) reported that autoreduction of Cu^{2+} to Cu^{+} species occur upon heating copper ion-exchanged ZSM-5 catalysts. Larsen et al. (1994) also showed that Cu^{2+} species decreased by ~50% due to heating Cu-ZSM-5 catalyst to temperatures up to 500 °C. This may be the reason why Sample 4 which was calcined at 500 °C, was more active than Sample 7 which was calcined at 550 °C.

As previously described, in addition to ion-exchange, copper was also incorporated into ZSM-5 zeolite framework during synthesis of the zeolite for preparation of Sample 4. This could be considered as an effective technique of preparing active Cu-ZSM-5 catalysts for SCR of NO by methane. It is worth noting that the catalyst prepared via this technique was less active for the direct decomposition compared to the catalysts prepared using ion-exchange method. Impregnation method was also reported (d'Itri and Sachtler 1992) to be an effective technique for SCR of NO when propane used as a reducing agent. According to Campa et al. (1994), it is not surprising that a catalyst exhibits higher activity for SCR than direct decomposition as different reaction mechanisms are involved in the two cases.

A comparison between the results presented in Figures 7.1 and 7.5 for Samples 4 and 7 revealed that the catalyst behaviour for NO_x conversion was influenced by methane. However, the catalyst behaviour has not been examined by both methane and oxygen. Therefore, it can not be concluded whether these two catalysts were suitable for SCR of NO_x. It should also be noted that reaction between CH_4 and NO can take place without using any catalyst as shown in Figure 7.5. it is seen that NO conversion increased by increasing temperature and up to 30% NO conversion was achieved at 650 °C without using any catalyst.

Figure 7.5 indicates that at high temperatures, different catalysts show similar behaviour in the presence of methane. However, NO_x conversions are not a true indication of selective catalytic reduction of NO over the catalysts. This is because NO may react with methane in the absence of oxygen in a homogeneous gas system or methane reacts with oxygen instead of NO when oxygen is present. In addition, as

mentioned previously, up to 30% conversion of NO which was observed at 650 °C without the presence of catalyst, is not related to the activity of the catalysts.

Sample 4 which was active at low temperatures was selected to test for the conversion of NO into N_2 in the presence of oxygen and methane. This investigation revealed that the activity of this catalyst was reduced when oxygen was added to the system. It is worth noting that the NO conversion achieved using methane in the presence of 2% oxygen was still twice that of the NO_x conversion for direct decomposition over the same catalyst (Sample 4). The incorporation of copper into the zeolite framework may result in different copper sites which make the ZSM-5 catalysts more active for SCR using methane in the presence of oxygen. Further studies are required to specify the type of the copper sites involved and their effects on the reaction intermediates when copper is incorporated in the zeolite framework during a ZSM-5 zeolite synthesis.

Figure 7.6 shows the temperature dependence of the NO_x decomposition with and without the presence of oxygen as well as the effect of methane on direct decomposition of NO over Sample 7. It is shown that oxygen promoted NO_x decomposition at lower temperatures (<450 °C), whereas at higher temperatures (>450 °C) oxygen inhibited the decomposition reaction. These observations clearly support the idea that the effect of oxygen presence on NO_x conversion differs at low and high temperatures as discussed in Section 7.4.2. It has been observed by Iwamoto et al. (1991a) that adding oxygen in the system inhibits the direct decomposition of NO into N_2. According to Figure 7.3, oxygen exhibited different effect on NO_x decomposition, depending on the reaction temperature. Adding oxygen promoted NO_x decomposition at temperatures lower than 450 °C whereas oxygen reduced the NO_x conversion at temperatures greater than 450 °C. This could be related to the conversion of NO to other nitrogen oxides such as NO_2 and N_2O at lower temperatures, therefore increasing NO_x conversion at temperatures less than 450 °C but not NO conversion into N_2. Centi et al. (1994) reported that oxygen promoted NO decomposition at temperatures below 350 °C. Our observations may also indicate that the reaction path or the nature of active sites in the Cu-ZSM-5 are different at

low and high temperatures. The effect of methane was found to be opposite to that of oxygen as methane decreased the NO_x conversions at temperatures < 450 °C and promoted the conversion of NO significantly at temperatures higher than 500 °C. These observations are not surprising as different reaction mechanisms are involved in the two reaction systems.

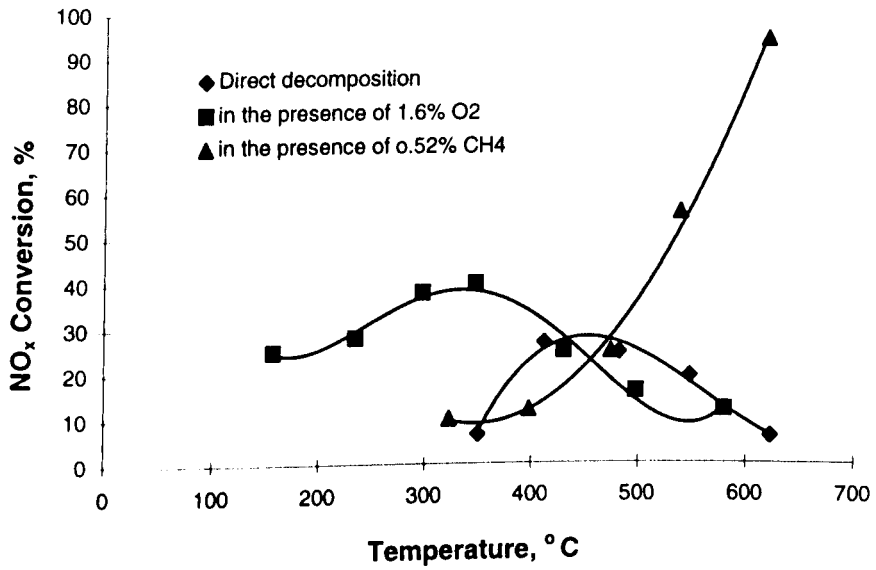

Figure 7.6. The dependence of NO_x Decomposition on temperature for sample 7. Reaction conditions: 2000 ppm NO, 0% or 0.52% CH_4, 0% or 1.6% O_2, balance He, 1.5g catalyst weight, 100 ml min^{-1} total flow rate.

7.4.4 A Mixture of ZSM-5 and MCM-41 Molecular Sieve

The effect of pre-treatment on the catalytic activity of Sample 3 (this sample showed activity over the entire range of temperature) was examined. The result is shown in Figure 7.7. The pre-treatment process was in-situ calcination of the catalyst at 500 °C for one hour in a stream of helium with a flow rate of 100 ml min^{-1} and then maintaining the helium flow until the catalyst bed reached the desired reaction temperature. The gas was then switched to a mixture of NO in helium and the activity of the catalyst was examined at different temperatures. The outlet gas was analysed using the GC to measure NO conversion into N_2. The experiments were conducted

under the same conditions that direct decomposition without the presence of oxygen performed for NO_x conversion measurements. The only difference being the catalyst was pretreated. Figure 7.7 compares this results with NO_x conversions obtained over Sample 3 presented in Figure 7.2. This comparison illustrates that NO conversion was enhanced by more than 15% when the catalyst was pre-treated. We can therefore conclude that the higher activity achieved after pre-treatment was in fact due to the pre-treatment process. These experiments were also repeated by decreasing the temperature to examine the thermal stability of the catalyst. It was observed that the catalytic activity of the catalyst did not decrease (Figure 7.7) when the experiment was repeated commencing from high temperatures to low temperatures. This indicates that the catalyst is stable when it has been subjected to the reaction conditions of 0.2 % NO in helium at 650 °C for two hours. This means that the catalyst is thermally stable for at least this period of time. This stability may be due to the inclusion of MCM-41 with ZSM-5 as MCM-41 is reported to have a high thermal stability (Zhao et al., 1996).

NO_x conversion and NO conversion into N_2 were determined using the NO_x analyser and the GC, respectively. To avoid the secondary oxidation of undecomposed NO to NO_2 as described in Section 2.5.4, the NO_x analyser was located near the reactor. In addition, a tube with the minimum required length was selected to carry the reactor outlet gas to the NO_x analyser. According to Equations (2-1) and (2-7), NO conversion into N_2 calculated from GC results must be less than NO_x conversion calculated using the data reported by NO_x analyser. However, the results showed an opposite trend as exhibited in Figure 7.7, indicating that the pre-treatment increased the activity of the catalyst. This is not unexpected, as the effect of different pre-treatment was reported to influence the NO conversion up to 15% (Li and Hall, 1991).

Sample 3 was also investigated for the selective catalytic reduction of NO using methane or propene, and the results are shown in Figure 7.8. The catalyst was pre-treated by exposing the catalyst to a helium stream with a flow rate of 100 ml min^{-1} for one hour at 500 °C. It was observed that propene increased NO conversion into

N_2 by approximately 60% whereas methane did not have any effect on catalytic activity of the catalyst in an oxidising atmosphere. This is in agreement with the literature that Cu-ZSM-5 zeolites are active for SCR of NO using propene but not methane (d'Itri and Sachtler, 1992). This indicates that the presence of MCM-41 did not change the effect of the type of the hydrocarbon (i.e. methane and propane) as compared to Cu-ZSM-5 for the SCR of NO.

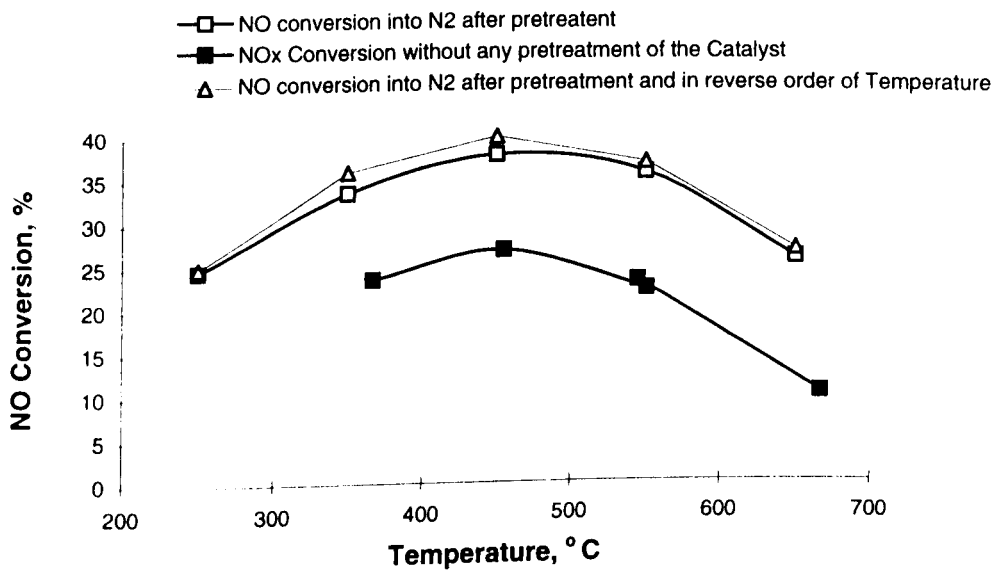

Figure 7.7. The dependence of NO/NO_x decomposition on temperature for Sample 3 with and without pre-treatment of the catalyst. Reaction conditions: 2000 ppm NO, balance He, 1.5g catalyst weight, and 100 ml min^{-1} total flow rate. The catalyst was exposed to a He stream with a flow rate of 100 ml min^{-1} for one hour at 500 °C before use.

To determine the role of the catalyst itself, the conversion of NO in the gas-phase reaction with methane and oxygen was examined. A mixture of NO, O_2 and CH_4 balanced with helium was used in a none catalytic system. The experiment was conducted using the same concentrations of NO and O_2 but 0.52% CH_4 and the same conditions as those employed over the catalyst previously. The results are shown in Figure 7.8. It was observed that NO conversion occurred even without the presence of a catalyst. This conversion was almost linearly increased by increasing the temperature from 5% at 250 °C to 20% at 650 °C. Therefore, a part of the NO conversions was not related to the activity of the catalyst. For example, from 24%

NO conversion into N_2 which was obtained at 450 °C, only 12% can be considered due to the presence of the catalyst itself. This must be considered in kinetic studies to show the real NO conversions achieved per active site.

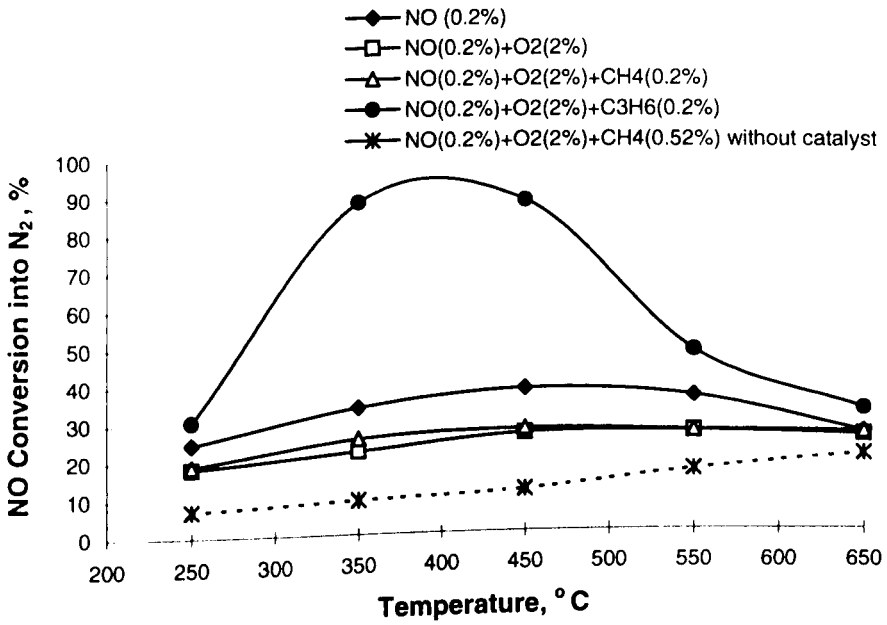

Figure 7.8. The dependence of NO conversion on temperature with and without the presence of oxygen and SCR of NO using methane or propene for Sample 3. Reaction conditions: 1.5g catalyst weight, and 100 ml min^{-1} total flow rate. The catalyst was exposed to a He stream with a flow rate of 100 ml min^{-1} for one hour at 500 °C before use.

The direct decomposition without and with the presence of oxygen and selective reduction of NO with propene over Cu-ZSM-5-23.3-152 was examined by Iwamoto and Mizuno (1993). A comparison among the results achieved over their catalyst and over the mixture of MCM-41 and ZSM-5 used in this study is shown in Figure 7.9. This comparison reveals that the conversion of NO occurs over a wider temperature range for both SCR as well as direct decomposition by adding MCM-41 to the ZSM-5 support. However, these results can not be quantitatively compared as the experiments were carried out under different conditions. It can only be concluded that the higher activity obtained in this study was due to the higher contact time.

The effect of contact time on NO conversion into N_2 with and without the presence of oxygen was also tested. The results are presented in Figure 7.10. The NO decomposition was directly proportional to the contact time whether in the presence or absence of oxygen. It is noticeable that the presence of oxygen decreased NO conversion by roughly 10% at any given contact time.

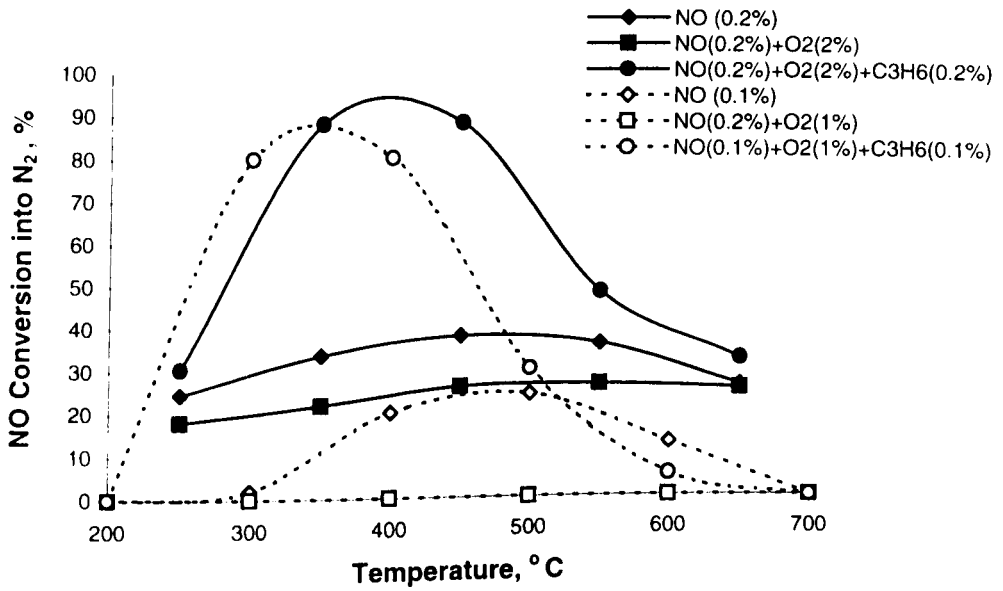

Figure 7.9. A comparison among the results obtained from this study for the dependence of NO conversion into N_2 on temperature for a mixture of MCM-41 and ZSM-5, Sample 3, (the solid lines) and the results reported by Iwamoto and Mizuno (1993) for Cu-ZSM-5-23.3-152 (the dashed-lines). The contact time was 0.9 g s ml^{-1} for the solid lines whereas it was 0.3 g s ml^{-1} for the dashed-lines.

Finally, NO conversion into N_2 over Sample 3 was investigated by changing NO or O_2 concentration as shown in Figures 11 and 12. The results reveal that NO conversion increases with increasing NO concentration but decreases with increasing oxygen concentration. This is in agreement with the behaviour of the ZSM-5 alone(Li and Hall, 1991), indicating that the kinetic behaviour of Cu-ZSM-5 zeolite may not be influenced by adding MCM-41 molecular sieve.

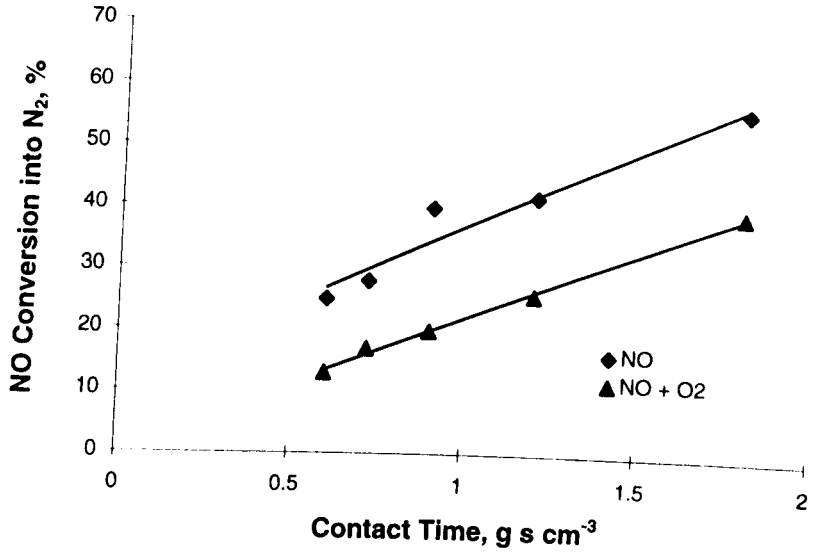

Figure 7.10. The dependence of NO Conversion on contact time for Sample 3 at 450 °C. Reaction conditions: 2000 ppm NO, 0.0% or 2% O_2, balance He, 1.5g catalyst weight, and 50 to 150 ml min^{-1} total flow rate. The catalyst was exposed to a He stream with a flow rate of 100 ml min^{-1} for one hour at 500 °C prior to use.

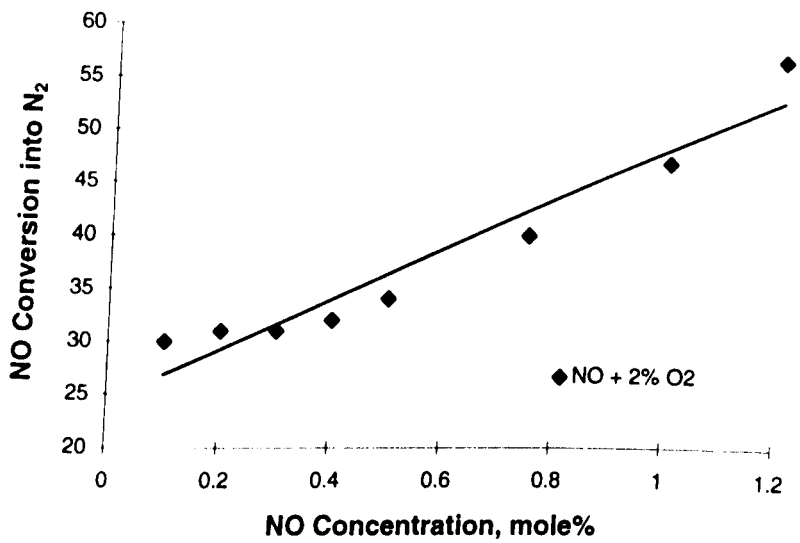

Figure 7.11. The dependence of NO conversion on NO concentration for Sample 3 at 450 °C. Reaction conditions: 0.1 to 1.2 ppm NO, 2%O_2, balance He, 1.5g catalyst weight, and 100 ml min^{-1} total flow rate. The catalyst was exposed to a He stream with a flow rate of 100 ml min^{-1} for one hour at 500 °C prior to use.

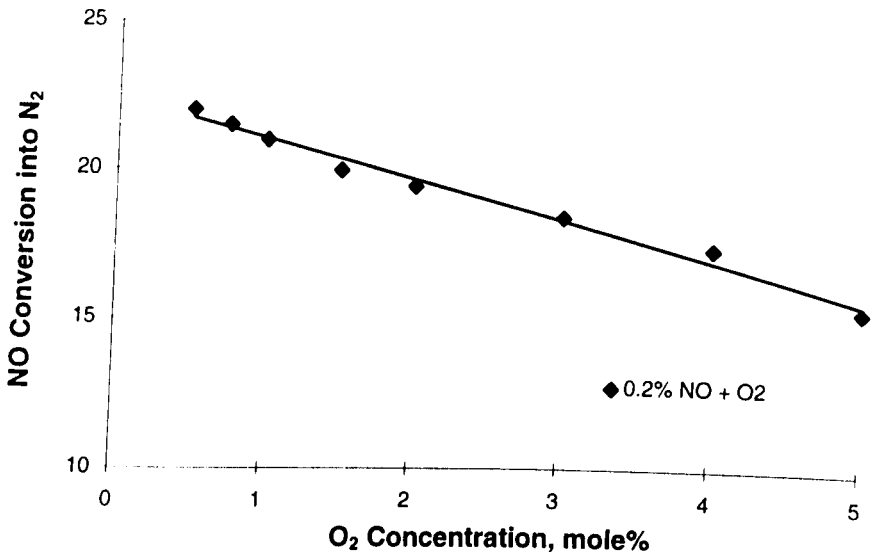

Figure 7.12. The dependence of NO conversion on O_2 concentration for Sample 3 at 450 °C. Reaction conditions: 2000 ppm NO, 0.5 to 5% O_2, He balance, 1.5g catalyst weight, and 100 ml min^{-1} total flow rate. The catalyst was exposed to a He stream with a flow rate of 100 ml min^{-1} for one hour at 500 °C prior to use.

7.5 Results and Discussion for the Second Group of Catalysts

The SCR of NO over the second group of catalysts was investigated over a temperature range of 200-500 °C. Methane was used as the reductant. It was found that none of the catalysts were active for SCR of NO by methane.

It was reported in the literature that ion-exchanged Pillared Clays, introduced as a new class of catalysts, were very active for selective catalytic reduction of NO by hydrocarbons and by ammonia (Yang and Li, 1995). The catalyst used was Cu^{2+} ion-exchanged TiO_2-pillared clay and the experiments were carried out using a combination of NO, O_2 and C_2H_4. It was reported that maximum NO conversion achieved was 40% more than that over Cu-ZSM-5 reported by Iwamoto and Mizuno

(1993). The presence of SO_2 and H_2O reduced the catalytic activity of the catalyst by 10-12% but NO conversion achieved was still much higher than over the Cu-ZSM-5. The reported results were interesting and encouraged us to investigate the catalytic activity of different type of cation exchanged clays. The coexistence of Ce on Cu^{2+} exchanged TiO_2 pillared clay promoted the NO conversion by 10% whereas it was observed that Cu^{2+}-CeAl-PILC did not show any catalytic activity for SCR of NO in the presence of methane. This is simply because the initial material, Al-PILC was different from TiO_2 pillared clay. The next reason could be due to using different reactants as in this study methane used instead of ethene. Ethene was reported to be a suitable reducing agent for SCR of NO over Cu-ZSM-5 zeolite whereas methane was not. Investigation over the same catalyst are required to determine the role of the reductant.

7.6 Summary

In this Chapter, the catalytic activity of two groups of catalysts received from the University of Queensland was investigated. The first group of catalysts including a mixture of silicalite-1 and TiO_2, a mixture of SiO_2 and Al_2O_3, Cu-MCM-41, Cu-ZSM-5, and a mixture of MCM-41, MoO_3 and TiO_2, were examined for NO_x conversion with and without the presence of oxygen. Among these catalysts, the only active catalysts were Cu-ZSM-5. A catalyst made from the mixture of copper ion-exchanged ZSM-5 zeolite and MCM-41 molecular sieve (Sample 3) was also active for NO_x conversion. This catalyst exhibited a higher activity than Cu-ZSM-5 alone for NO decomposition over the entire temperature range investigated. This finding is very important as maintaining a high activity over a wide temperature range is desirable for any practical application.

The effect of the presence of oxygen on NO_x conversion over the afore-mentioned catalysts was also investigated. Based on the results obtained, it can be concluded that the effect of O_2 in the inlet gas stream depends on the operating temperature. NO_x conversions increased at temperatures lower than 400 °C where the maximum

NO_x conversion achieved, and then decreased as the temperature was further increased.

These results also revealed that incorporation of copper into the zeolite structure during synthesis decreased the activity of the catalyst for NO_x conversion when no oxygen or methane was added to the system. On contrary, the activity of the catalyst at low temperatures increased when methane was added to the inlet gas stream. In addition, methane sharply increased the NO_x conversion over copper ion-exchanged zeolites in the absence of oxygen at high temperatures. However, the high activity for NO_x conversion in the presence of methane only does not indicate that the catalyst could be active if oxygen was also present. Further investigations are therefore required to confirm the conclusion if the catalyst is active for SCR.

Sample 3, a mixture of copper ion-exchanged ZSM-5 zeolite and MCM-41 molecular sieve, was selected for detailed investigations. The effect of pre-treatment of the catalyst on the direct decomposition was investigated and it was found that the pre-treatment including calcination of the catalyst at 500 ^{o}C in a flow of helium (flow rate of 100 ml min^{-1}) increased NO conversions into N_2 by more than 15%. SCR of NO using methane or propene over this catalyst was also investigated. It was observed that this catalyst was very active for SCR of NO by propene but not by methane as almost 90% and 25 % NO conversions into N_2 were achieved when propene and methane were used as the reducing agents, respectively. Therefore, using a mixture of MCM-41 molecular sieve and ZSM-5 zeolite as a catalyst support for SCR by propene seems to be a way to achieve high NO conversions over a wider range of temperatures.

The second group of catalysts including aluminium, lanthanum aluminium, and cerium aluminium pillared clays ion-exchanged with copper, cobalt, or nickel cations were tested for SCR of NO using methane as a reducing agent. It was found that none of these catalysts was active for SCR of NO using methane.

CHAPTER EIGHT

AN EVALUATION OF THE PRESENT STUDIES

8.1 Introduction

In Chapters 5 and 6, the results obtained for the direct decomposition over copper ion-exchanged, and selective catalytic reduction of NO over copper and cobalt ion-exchanged ZSM-5 zeolites were presented and discussed. Chapter 7 compared the performance of different catalysts as well as copper ion-exchanged ZSM-5 zeolites for the direct decomposition. The most active catalyst for the direct decomposition, a mixture of Cu-ZSM-5 and MCM-41 ion-exchanged with copper, was also examined for SCR of NO. The results presented in those three chapters will be evaluated in this chapter by comparing the performance of these catalysts with data available in the literature. Validity of the data obtained is examined by an error analysis. Practical relevance and significance of the results are also discussed.

8.2 Comparison of Present Results with Literature Data

Copper and cobalt ion-exchanged ZSM-5 zeolites as well as other catalysts as candidates for reduction of NO have been examined in this study. The maximum NO conversion achieved over the catalysts for the direct decomposition in this study and in the literature are summarised in Table 8.1. It is shown that the performance of the catalysts used in this study either synthesised or obtained from commercial sources

are comparable with the performance of the catalysts used by others, found in the literature. It is also shown that the most effective temperature for direct decomposition of NO is 450 °C regardless of the SiO_2/Al_2O_3 ratio or the copper ion-exchange level. In addition, a mixture of ZSM-5 zeolite and MCM-41 molecular sieve ion-exchanged with copper shows similar performance over the entire range of temperature (250 to 700 °C). This is a valuable finding as it is important to find an active catalyst over a wider temperature window.

Table 8.1. A Comparison between the maximum NO conversions obtained using different Cu-ZSM-5 catalysts in this study and the literature for the direct decomposition.

Catalyst	Reaction conditions	Maximum NO Conversion into N_2, %	The Most Effective Temperature, °C
H-Cu-ZSM-5-50-58.0 (This work)	2000 ppm NO, and 0.4 g s ml^{-1} contact time	9.8	450
H-Cu-ZSM-5-50-62.3 (This work)	"	13	450
H-Cu-ZSM-5-50-106.7 (This work)	"	9	450
H-Cu-ZSM-5-50-139.3 (This work)	"	19.8	450
H-Cu-ZSM-5-50-132.6 (This work)	"	17.5	450
H-Cu-ZSM-5-40-101.7 (This work)	"	36.4	450
A mixture of ZSM-5 and MCM-41 ion-exchanged with copper	2000 ppm NO, and 0.9 g s ml^{-1} contact time	40	450
H-Cu-ZSM-5-53-170 (Ganemi et al. 1998)	2000 ppm NO	36	450
H-Cu-ZSM-5-33-108 (Ganemi et al. 1998)	2000 ppm NO	12	450

It is worth noting that the effect of SiO_2/Al_2O_3 ratio on the performance of the catalysts used in this study and the data presented by Ganemi et al. (1998) are not in agreement. There are conflicting reports on the effect of SiO_2/Al_2O_3 ratio on the activity of copper ion-exchanged catalysts in the literature. Moretti (1994) summarised literature data and concluded that the turnover frequency decreases with increasing the SiO_2/Al_2O_3 ratio of Cu-ZSM-5 catalysts. However, Ganemi et al. (1998) and Iwamoto et al. (1986b) reported that the activity of Cu-ZSM-5 catalysts increases with increasing SiO_2/Al_2O_3 ratio of the catalyst for direct decomposition. This study supports the trend reported by Moretti (1994).

Tables 8.2 and 8.3 compare the NO conversions for SCR of NO obtained over Cu-ZSM-5 and Co-ZSM-5 used in this study, and over several catalysts used by others. Although it is difficult to compare the results due to different conditions used in different studies, it is shown that the activity of all catalysts used either in this study or in the literature are relatively comparable. The NO conversions reported by Iwamoto and Mizuno (1993) seem to be higher than the NO conversions achieved in this study, considering the contact times. However, there is no information in the literature as to whether the catalyst used by Iwamoto and Mizuno was prepared from H-form or Na-form of the zeolite.

The most effective temperature seems to be dependent on the reductant used as well as on the type of the cations ion-exchanged. The uncertainty as to the most effective temperatures can be considered within ± 25 °C as explained in Chapter 6. It seems that the most effective temperature for reduction of NO using propene over Cu-ZSM-5 catalysts lies between 300 and 350 °C. This temperature almost decreases by 100 °C when ethene or propane is used as the reducing agent. It is interesting that the mixture of ZSM-5 and MCM-41 ion-exchanged with copper shows a high activity over a wider range of temperature for SCR as well. It is seen that the most effective temperature is from 350 to 450 °C, which has not been observed for the other catalysts. It is also shown that the activity of the metal ion-exchanged ZSM-5 catalysts can be improved by controlling their properties. For example, the activity of

Table 8.2. A Comparison between the maximum NO conversions achieved for SCR of NO over several Cu-ZSM-5 catalysts in this study and literature data.

Catalyst	Reaction Conditions	NO Conversion into N_2, %	The Most Effective Temperature °C
Cu-ZSM-5-176-199.2 (This work)	2000 ppm NO, 2000 ppm C_3H_6, 2% O_2, and 0.4 g s ml^{-1} contact time	74	350
Cu-ZSM-5-140-160.7 "	"	70	350
Cu-ZSM-5-100-127.5 "	"	66	300
Cu-ZSM-5-100-168.6 "	"	52	350
Cu-ZSM-5-100-108.3 "	"	69	300-350
Cu-ZSM-5-100-99 "	"	77	350
H-Cu-ZSM-5-50-99.3 "	"	68	350
H-Cu-ZSM-5-50-77.3 "	"	66	350
A mixture of ZSM-5 and MCM-41 ion-exchanged with copper	2000 ppm NO, , 2000 ppm C_3H_6, 2% O_2, and 0.9 g s ml^{-1} contact time	90	350-450
Cu-ZSM-5-23.3-152 (Iwamoto and Mizuno, 1993)	1000 ppm NO, 1000 ppm C_3H_6, 1% O_2, and 0.3 g s ml^{-1} contact time	75	325
Cu-ZSM-5-23.3-102 (Iwamoto and Mizuno, 1993)	1000 ppm NO, 250 ppm C_2H_4, 2% O_2, and 0.2 g s ml^{-1} contact time	41	250
Cu-ZSM-5-34, 3.2% Cu (Sasaki et al., 1992)	1079 ppm NO, 323 ppm C_3H_8, 10% O_2, and ~1 g s ml^{-1} contact time	15	250

over-exchanged Cu-ZSM-5 catalysts increases by increasing SiO_2/Al_2O_3, and decreases with further increasing the copper loading. As recorded in Table 8.3, the

most effective temperature for SCR of NO using methane over Co-ZSM-5 catalysts obtained in this study and reported in the literature lies between 400 and 450 °C.

Table 8.3. A Comparison between the maximum NO conversions achieved for SCR of NO over Co-ZSM-5 catalysts in this study and literature data.

Catalyst	Reaction conditions	NO Conversion into N_2, %	The Most effective Temperature °C
H-Co-ZSM-5-80-71 (This work)	2000 ppm NO, 2000 ppm CH_4, 2% O_2, and 0.4 g s ml^{-1} contact time	37	450
H-Co-ZSM-5-80-77.9 (This work)	"	20.2	450
H-Co-ZSM-5-80-96.6 (This work)	"	33	450
H-Co-ZSM-5-40-45 (This work)	"	86	450
H-Co-ZSM-5-80-428 (This work)	"	29.5	450
H-Co-ZSM-5-13.6-70 (Li and Armor 1992)	820 ppm NO, 2000 ppm CH_4, 2.5% O_2, 0.4 g catalyst	95	450
H-Co-ZSM-5-13.6-70 (Li and Armor 1992)	1840 ppm NO, 820 ppm CH_4, 2.5% O_2, 0.4 g catalyst	40	450
H-Co-ZSM-5-13.6-70 (Li and Armor 1992)	820 ppm NO, 820 ppm CH_4, >0.5% O_2, 0.4 g catalyst	60	400

Tables 8.1, 8.2, and 8.3 show that the NO conversions obtained for direct decomposition are much lower than those of SCR. Direct decomposition is also not favourable when oxygen is present in the reaction system, while the presence of oxygen is essential for SCR. Direct decomposition is therefore not suggested for practical use due to the presence of oxygen in exhaust gases of engines which mostly work under oxidising atmosphere. Therefore, SCR is considered to be a possible way to reduce NO emissions from the exhaust gas of motor vehicles.

8.3 Validity of the Data Presented in This project

In this project, NO conversion into N_2 was calculated using Equation (2-1). To calculate NO concentration in the inlet gas stream of the reactor, $[NO]_{in}$, Equation (4-1) which was described in Section 4.7.2 was used. Substituting N_2 concentration in the outlet gas measured by GC and $[NO]_{in}$ in Equation (2-1), Equation (8-1) is obtained. Accordingly, the following equation is considered for calculation of NO conversion into N_2.

$$X_{NO} = \frac{2[N_2]}{\frac{F_{NO}[NO]_{cyl.}}{(F_{NO} + F_{He} + F_{C_nH_m} + F_{O_2})}} \qquad (8\text{-}1)$$

As shown in Equation (8-1), the X_{NO} value is proportional to N_2 concentration measured using GC (in GC studies), the gas total flow rate and inversely proportional to the NO flow rate and the NO concentration in the NO gas cylinder. Each of these parameters which have been used to calculate NO conversion has been measured with some uncertainty. The uncertainties for $[N_2]$, $[NO]_{cyl.}$, F_{NO}, F_{He}, $F_{C_nH_m}$ and F_{O_2} are named $\delta[N_2]$, $\delta[NO]_{cyl}$, δF_{NO}, δF_{He}, $\delta F_{C_nH_m}$ and δF_{O_2}, respectively. The extreme probable value for each measurement such as F_{NO} is $F_{NO} \pm \delta F_{NO}$. The uncertainties contributing to the GC measurements were found to be different and dependent on calibration curves used for each gas analysis. The repeatability of the data was relatively high, as shown in Figures 4.10 and 4.11 in Chapter 4. Typical values for the uncertainties for the two series of N_2 concentration measurements were 0.05 and 0.37 % as detailed in Chapter 4. The maximum uncertainty was considered to be 2%, taking into account any possible calibration drift. The concentration of the NO gas cylinder was 12% with ±1.2% uncertainty. The uncertainty of measurements given by each mass flow controller was ±1% of its full scale. The full-scale of the mass flow controllers and the errors involved are given in Table 8.4.

The uncertainty of $NO_{conv.}$ can be calculated using the following equation (Taylor, 1982):

$$\delta(NO_{conv.}) = \frac{\partial(NO_{conv.})}{\partial[F_{N_2}]}\delta[F_{N_2}] + \frac{\partial(NO_{conv.})}{\partial[NO_{cyl.}]}\delta(NO_{cyl.}) + \frac{\partial(NO_{conv.})}{\partial(F_{NO})}\delta F_{NO} +$$

$$\frac{\partial(NO_{conv.})}{\partial(F_{He})}\delta F_{He} + \frac{\partial(NO_{conv.})}{\partial(F_{C_nH_m})}\delta F_{C_nH_m} + \frac{\partial(NO_{conv.})}{\partial(F_{O_2})}\delta F_{O_2} \qquad (8\text{-}2)$$

Considering Equation (8-1) in Equation (8-2), and recalling that the partial derivatives may be positive or negative, the uncertainty in $NO_{conv.}$ is calculated as:

$$\delta(NO_{conv.}) = \left|2\frac{[N_2]}{[NO]_{cyl}}\left(\frac{F_{He} + F_{C_nH_m} + F_{O_2}}{F_{NO}^2}\right)\right|\delta F_{NO} +$$

$$\left|2\frac{[N_2]}{[NO]_{cyl}}\left(\frac{1}{F_{NO}}\right)^2\right|(\delta F_{He} + \delta F_{C_nH_m} + \delta F_{O_2}) +$$

$$\left|2\frac{1 + (F_{He} + F_{C_nH_m} + F_{O_2})/F_{NO}}{[NO_{cyl.}]}\right|\delta[N_2] +$$

$$\left|2\left(1 + \frac{F_{He} + F_{C_nH_m} + F_{O_2}}{F_{NO}}\right)\frac{[N_2]}{[NO]^2_{cyl.}}\right|\delta[NO_{cyl.}] \qquad (8\text{-}3)$$

Table 8.4. Full-scale flow rates and uncertainties of the mass flow controllers used in this study.

	Mass flow controllers				
Gas	NO	He	CH_4	O_2	C_3H_6
full-scale, ml min^{-1}	10	200	10	200	10
uncertainty, ml min^{-1}	0.1	2	0.1	2	0.1

It is possible to overestimate δ ($NO_{conv.}$) when Equation (8-3) is used (Taylor, 1982). This happens because full amounts of $\delta[N_2]$, $\delta[NO]_{cyl}$, δF_{NO}, δF_{He}, $\delta F_{C_nH_m}$ and δF_{O_2} are considered. Obviously, there is a low probability that maximum uncertainties for all measurements occur at the same time. When the uncertainties are independent of each other and the errors are random in nature, there is a 50% chance that an underestimate of a variable will be accompanied by an overestimate of another variable. Clearly, the probability of the underestimation or overestimation of all variables by the full amounts of $\delta[N_2]$, $\delta[NO]_{cyl}$, δF_{NO}, δF_{He}, $\delta F_{C_nH_m}$ and δF_{O_2} is fairly low. Therefore, the sum in Equation (8-3) can be replaced by addition by quadrature (Taylor, 1982) which results in Equation (8-4).

$$\delta(NO_{conv.}) = \left\{ \left(2\frac{[N_2]}{[NO]_{cyl}} \left(\frac{F_{He} + F_{C_nH_m} + F_{O_2}}{F_{NO}^2} \right) \delta(F_{NO}) \right)^2 + \left(2\frac{[N_2]}{[NO]_{cyl}} \frac{1}{F_{NO}} \right)^2 \left((\delta F_{He})^2 + (\delta F_{C_nH_m})^2 + (\delta F_{O_2})^2 \right) \left(2\frac{1 + F_{He} + F_{C_nH_m} + F_{O_2}/F_{NO}}{[NO_{cyl}]} \delta[N_2] \right)^2 + \left(2\left(1 + \frac{F_{He} + F_{C_nH_m} + F_{O_2}}{F_{NO}} \right) \frac{[N_2]}{[NO]^2_{cyl.}} \delta[NO_{cyl.}] \right)^2 \right\}^{1/2} \quad (8\text{-}4)$$

For justification of the data presented in the current project, three groups of uncertainties in NO conversions calculated using Equation (8-4) are presented in Tables 8.5 to 8.7. Table 8.5 demonstrates calculated uncertainties for NO conversions using the direct decomposition technique over H-Cu-ZSM-5-32.2-101.7. NO conversions were taken from Figure 5.7 in Chapter 5. Tables 8.6 and 8.7 present uncertainties for NO conversions for SCR of NO over H-Cu-ZSM-5-40-101.7 and H-Co-ZSM-5-40-45 using propene and methane, respectively. The data were taken from Figure 6.1 in Chapter 6.

Table 8.5. NO conversions and the uncertainties involved for the direct decomposition of NO over H-Cu-ZSM-5-32.2-101.7 catalyst.

Temperature, °C	250	350	400	450	500	550	650
$NO_{conv.}$, %	7	26	36.1	36.4	35.1	33.4	27
δ ($NO_{conv.}$), %	0. 82	3.06	4.24	4.28	4.13	3.93	3.17
uncertainty, %	11.8	11.8	11.8	11.8	11.8	11.8	11.8

Table 8.6. NO conversions and the errors involved for SCR of NO using propene over H-Cu-ZSM-5-40-101.7 catalyst.

Temperature, °C	250	350	400	450	500	550	650
$NO_{conv.}$, %	46	85	78	69	62	55	42
δ ($NO_{conv.}$), %	5.48	10.13	9.29	8.22	7.39	6.56	5.01
uncertainty, %	11.9	11.9	11.9	11.9	11.9	11.9	11.9

Table 8.7. NO conversions and the errors involved for SCR of NO using methane over H-Co-ZSM-5-40-45 catalyst.

Temperature, °C	250	350	400	450	500	550	650
$NO_{conv.}$	6	28	51.5	57	42	28	17
δ ($NO_{conv.}$), %	0.72	3.34	6.14	6.79	5.00	3.34	2.03
uncertainty, %	12.0	11.9	11.9	11.9	11.9	11.9	11.9

It can be seen that the uncertainties calculated for NO conversions are reasonable. It is also evident that the uncertainties obtained for the NO conversions calculated for the direct decomposition and for the SCR are very close. This is due to the relatively high uncertainty, 10% in concentration of NO in the gas cylinder and also 1% uncertainty for inlet NO gas flow rate which were exactly the same in the three sets of experiments. These two uncertainties had the original role in the uncertainty calculations. In addition, exactly the same uncertainties were obtained for both cases

of SCR because C_3H_6 and CH_4 gas cylinders contained C_3H_6 and CH_4 with very close concentrations, and therefore the uncertainties involved were the same.

To calculate the error bars in the kinetic study presented in Chapter 5, the relative uncertainty for the turnover frequency (TOF) which according to Equation (4-2) is defined as a number of NO molecules converted to N_2 per second per copper site,

$$TOF = \frac{F[NO]_{in}(X_{NO}/100)}{m_{Cu}/64} \qquad (4\text{-}2)$$

the following equation is used.

$$\frac{\delta TOF}{TOF} = \left(\left(\frac{\delta F}{F}\right)^2 + \left(\frac{\delta[NO]_{in}}{[NO]_{in}}\right)^2 + \left(\frac{\delta X_{NO}}{X_{NO}}\right)^2 + \left(\frac{\delta m_{Cu}}{m_{Cu}}\right)^2\right)^{1/2} \qquad (8\text{-}5)$$

As a typical example, a relative uncertainty for TOF was calculated for the dependence of TOF on NO concentration for H-Cu-ZSM-5-32.2-101.7 under reaction conditions of 1000 to 10000 ppm NO, 0.5 g of catalyst, and 100 ml min^{-1} of the total flow rate, and found to be 12%. Again this is because the errors involved in the concentration of the NO gas cylinder had the main role in Equation (8-6). Considering 12% uncertainty for TOF on one hand and on the other hand linearity of the plots obtained for the kinetic study (for example, Figures 5.10 and 5.11) reveals that the uncertainties are overestimated, and the relative uncertainty for NO conversion as well as TOF should be much less than 12%. This leads to high confidence in the results presented in this study.

8.4 Practical Implication of the Present Studies

The current study of the direct decomposition and selective catalytic reduction of nitrogen oxides was initially motivated by the concern for public health and the

environment which are both being threatened by NO_x emissions. Although many researchers have focused on using ZSM-5 zeolite-supported catalysts as an alternative for the three-way catalysts which are not able to work in the presence of oxygen, this has not yet been put in practice. In general, the present study is aimed at obtaining improved knowledge of NO decomposition that may lead to the development of NO_x emission control technology applicable to the engines working under oxidising atmosphere. In particular, this study is aimed at providing a systematic approach to catalyst preparation and deduction of a reaction rate as well as reaction mechanisms for the direct decomposition. The effect of zeolite properties on the activity of copper and cobalt ion-exchanged ZSM-5 catalysts for SCR of NO is also investigated. These investigations have certainly improved the understanding of this area of research, especially the reaction mechanism of the direct decomposition, and reveals the importance of details in the synthesis of ZSM-5 zeolite on reduction of NO.

Although ZSM-5 zeolites are synthesised commercially and there are many papers concerning the methods of their synthesis, not enough details are given in the literature. In addition, the methods of synthesis reported in the literature are usually very different. In this study, four synthesis methods are introduced in Chapter 3. ZSM-5 zeolites with 100% crystallinity are synthesised using two of them, Method 1 and Method 3. Method 3, the method in which no template was used, was found to be the easiest, safest, and quickest method for ZSM-5 zeolite synthesis. The results obtained in this study showed that the zeolite synthesised using this method had a high performance as a catalyst support. Furthermore, it revealed that the zeolites synthesised, either with or without template, were similar in performance to the zeolites provided by the commercial sources.

A systematic approach to the catalyst preparation, and investigation into the effect of the preparation method on the direct decomposition of NO, were addressed in the present project. This helps to select a method for preparation of a Cu-ZSM-5 catalyst with a specific copper ion-exchange level. This also reveals the relationship between the preparation method and the activity of the catalyst. It was shown that the reaction

rate and reaction mechanisms for the direct decomposition at temperatures below and above the most effective temperatures were different. The reaction rate equation as well as the reaction mechanisms involved as reported in literature were only supported for temperatures greater than the most effective temperature. A new reaction rate as well as the reaction mechanisms were deduced for the direct decomposition at lower temperatures.

The effect of the SiO_2/Al_2O_3 ratio of over-exchanged Cu-ZSM-5 zeolites on reduction of NO by propene prepared from H-form of ZSM-5 zeolites has been investigated (Torre-Abreu et al., 1997a; Kharas, 1993) and conflicting results reported. This effect, which has not been addressed in the literature for the catalysts prepared from Na-form of ZSM-5 zeolites, has been reported for the first time in this study. The results indicated that for two catalysts with the same copper loading, the catalyst with the higher SiO_2/Al_2O_3 ratio was more active. This trend was different from the results reported by Torre-Abreu et al. (1997a) for the catalysts prepared from H-form of the zeolites. The effect of the SiO_2/Al_2O_3 ratio of over-exchanged Co-ZSM-5 zeolites prepared from acid form of ZSM-5 zeolites on SCR of NO by methane is also reported in this study. The results indicated that the lower the SiO_2/Al_2O_3 ratio, the higher the activity. This clear trend assists to optimise the condition under which the highest performance of the catalyst can be achieved. This also helps to identify the reaction mechanisms as different copper species have been identified for under-exchange and over-exchange catalysts.

It is acknowledged that the reaction rate for the direct decomposition is lower than required for practical use. However, the experimental results still help to provide an improved understanding of the various factors that affect the decomposition of NO. In addition, studies on direct decomposition may help in devising catalysts with higher activities (Shelef, 1995).

It is also acknowledged that due to water vapour suppression and sulfur dioxide poisoning, the direct decomposition of NO over Cu-ZSM-5 cannot be used in practice. The levels of sulfur compounds in most fuel sources that we use today result

in producing SO_2 by-product which has a poisoning effect on the direct decomposition, and an inhibiting effect on SCR of NO. This difficulty can possibly be overcome by reducing the SO_x concentration in exhaust gas, through reducing the concentration of sulfur in the fuels. As an example, the standard concentration of sulfur in diesel fuel has been reduced from 2000 ppm to 500 ppm in Japan as of September 1997 (Nakatsuji et al., 1998). This example paves the way to reduce the SO_x concentrations in exhaust gases which provides a condition for using metal ion-exchanged ZSM-5 catalysts for decomposition or reduction of NO.

Nakatsuji et al. (1998) estimated that with 500 ppm sulfur in the fuel, the exhaust gas of diesel engines will contain 20 ppm of SO_x. They examined the activities of a wide range of catalysts including Cu-ZSM-5 and achieved 20% NO_x conversion over Cu-ZSM-5 using a synthetic gas with a combination close to that of diesel engine exhausts, i.e. 500 ppm NO, 11% O_2, 20 ppm SO_2, 6% H_2O, and 2000 ppm of the fuel (four times of NO concentration). Although silver aluminate supported on alumina was the most active catalyst, achieving 50% NO conversion, 20% NO conversion achieved over Cu-ZSM-5 still encourages the development and supports the possibility of using ZSM-5 for SCR of NO.

Although Cu-ZSM-5 and Co-ZSM-5 catalysts are well known for the reduction of NO using propene and methane respectively, it is revealed in this study that Co-ZSM-5 shows the same performances for SCR of NO using either methane or propene. The presence of SO_2 and H_2O both reduce catalytic activity of Co-ZSM-5 catalyst when methane is used as the reducing agent (Li and Armor, 1995). According to the knowledge of the author, the effect of the presence of these two gases has not been thoroughly investigated when propene is used as a reducing agent. Future studies will reveal whether Co-ZSM-5 would be a suitable catalyst for SCR of NO by propene.

Although it is acknowledged that ZSM-5 zeolite catalysts alone are yet not suitable for practical applications at this stage, a combination of them with other catalysts can be used in practice. As an example, a combination of silver/proton exchanged zeolite

such as ferrite loaded with silver ions (Ag/H-FER) and Pt-ZSM-5 can be a potential catalytic converter for reducing NO_x emissions from lean-burn petrol and diesel engines (Freestone, 1998). The former catalyst is known to be good for the reduction of NO_2, and therefore the latter is required as an oxidative catalyst to convert NO to NO_2.

CHAPTER NINE

CONCLUSIONS AND RECOMMENDATIONS

9.1 Conclusions

1. ZSM-5 zeolites with 100% crystallinity are synthesised using two different methods, with and without a template. In the former, the zeolites with a wide range of SiO_2/Al_2O_3 ratios from 70 to infinity are synthesised using tetrapropylammonium bromide as a template whereas in the latter, the zeolite with a SiO_2/Al_2O_3 ratio of 40 is synthesised. The zeolites synthesised using different methods are different in shape, but they have the same structure. The size of the crystals changes with the composition of the initial materials and the conditions of the process.

2. The zeolite is used as a catalyst support, ion-exchanged with copper or cobalt ions to prepare a catalyst. The ion-exchange level of copper ion-exchanged ZSM-5 catalysts can be controlled by ion-exchange temperature and repetition of ion-exchange. The copper ion-exchange level increases linearly by repetition of ion-exchange at 25 °C and 45 °C. However, the copper ion-exchange level will decrease by repetition of ion-exchange at 80 °C and the solution will turn black indicating conversion of copper ions to copper oxide if the ion-exchange is performed for the third time.

3. Increasing temperature from 25 to 45 °C is not very effective if the ion-exchange is performed for a period of 24 hours whereas it is very effective if the ion-exchange is repeated and performed for 48 hours. In contrast, increasing temperature from 45 to

80 °C sharply enhances the copper ion-exchange level if the ion-exchange is performed for 24 hours and only slightly increased if the ion-exchange is repeated.

4. Different reaction rates and therefore reaction mechanisms are involved in direct decomposition of NO at temperatures lower and greater than the most effective temperature. The following reaction rate equation reported in the literature (Li and Hall, 1991) is supported only for temperatures greater than the temperature at which the maximum NO conversion is achieved.

$$r = \frac{k[NO]}{1 + K[O_2]^{1/2}} \qquad (2\text{-}8)$$

At temperatures lower than the most effective temperature, the following reaction rate equation is derived. This equation is obtained based on a suggested reaction mechanism. This reaction rate is supported by the experimental data.

$$r = \frac{k[NO]^2}{[NO] + K[O_2]} \qquad (5\text{-}12)$$

5. A comparison between the activity of Cu-ZSM-5 and Co-ZSM-5 catalysts for SCR of NO using methane or propene reveals that the highest NO conversion is achieved over Cu-ZSM-5 zeolite when propene is the reducing agent. Co-ZSM-5 shows similar activities for NO conversion when either methane or propene is the reducing agent. The lowest NO conversion is obtained over Cu-ZSM-5 when methane is the reductant.

6. Slightly different NO conversions are achieved using over-exchanged Cu-ZSM-5 zeolites prepared from the Na-form with the same copper loading but different SiO_2/Al_2O_3 ratios. The higher the SiO_2/Al_2O_3 ratio, the higher the NO conversion. Among catalysts with the same SiO_2/Al_2O_3 ratios, an over-exchanged catalyst with higher copper loading is less active.

7. Copper ion-exchange level alone is not a good criterion for the activity of a catalyst. This is because two catalysts with the same copper ion-exchange level do not show similar activities if they have different SiO_2/Al_2O_3 ratios. As a result, it is necessary to consider both SiO_2/Al_2O_3 ratio and copper loading.

9. Catalyst preparation method has an important role on the activity of Co-ZSM-5 zeolites. Two catalysts prepared via different preparation methods with the same cobalt ion-exchange levels and SiO_2/Al_2O_3 ratios do not necessarily show similar activities for NO conversion in the presence of methane. Catalysts prepared via the semi-continuous system are more active than the catalysts prepared via the batch system.

10. Co-ZSM-5 catalysts with the same cobalt loading but different SiO_2/Al_2O_3 ratios show different activities for NO reduction using methane. The lower the SiO_2/Al_2O_3 ratio, the higher the activity. Lower NO conversions are obtained using an over-exchanged catalyst rather than under-exchanged for the catalyst with the same SiO_2/Al_2O_3 ratios.

11. ZSM-5 zeolite as a support is more active than a mixture of silicalite-1 and TiO_2, a mixture of SiO_2 and Al_2O_3, Cu-MCM-41, Cu-ZSM-5, or a mixture of MCM-41, MoO_3 and TiO_2 for NO_x conversion, with and without the presence of oxygen. A mixture of ZSM-5 and MCM-41 molecular sieve is as active as ZSM-5 at the most effective temperature and more active at temperatures between 250 and 650 °C. Therefore, adding MCM-41 molecular sieve to ZSM-5 zeolite results in a wider NO_x conversion profile.

12. The effect of the presence of oxygen on NO_x conversion depends on the operating temperature. The maximum NO_x conversion is achieved at about 400 °C. The presence of oxygen increases NO_x conversion at temperatures lower than 400 °C, but decreases as the temperature is further increased.

13. Incorporation of copper into the zeolite framework during synthesis decreases the activity of ZSM-5 for NO_x conversions in the absence of oxygen and methane. This activity increases at low temperatures by adding methane to the inlet gas. In addition, NO_x conversion over copper ion-exchanged ZSM-5 catalysts sharply increases by adding methane into the reactant stream at high temperatures.

14. NO conversion into N_2 increases by 15% when a mixture of ZSM-5 and MCM-41 undergoes a pre-treatment including calcination at 500 °C in a helium flow with a flow rate of 100 ml min^{-1}. This catalyst is very active for SCR of NO using propene but not using methane.

15. Aluminium, lanthanum aluminium and cerium aluminium pillared clays, when ion-exchanged with copper, cobalt or nickel, are not active catalysts for SCR of NO when methane is used as the reducing agent.

9.2 Recommendations for Future Work

1. In this study the zeolites with different SiO_2/Al_2O_3 ratios were synthesised and examined for reduction of NO. ZSM-5 zeolites can also be synthesised with different OH^-/SiO_2 ratios. It is important to investigate the effect of alkalinity on decomposition and SCR of NO. For this purpose, several series of the zeolite with the same SiO_2/Al_2O_3 but different OH^-/SiO_2 ratios can be synthesised and examined.

2. ZSM-5 zeolites with the same OH^-/SiO_2 and SiO_2/Al_2O_3 ratios synthesised using different synthesis methods can be used to investigate the effect of zeolite synthesis method and the condition of synthesis on the activity of the catalysts.

3. It is suggested that mass flow controllers with full scales very close to the flow rate of each gas should be used in future work as this will result in less uncertainties.

4. The effect of the order of ion-exchange with cobalt and copper has yet not been determined. A comparison between the activity of the catalysts ion-exchanged with copper, cobalt, cobalt first and then copper, and copper first and then cobalt, will identify the most active catalysts among these catalysts.

5. Determination of the type of the copper sites in impregnated ZSM-5 catalysts with copper and the catalysts incorporated with copper during synthesis will provide a better understanding of the effect of preparation method. It will also reveal why catalysts prepared in this way show one-tenth of the activity of the catalysts prepared via the ion-exchange method for direct decomposition.

6. Methane can be available in the exhaust gas of combustion systems which use natural gas. Investigation of SCR of NO over Co-ZSM-5 catalyst with methane under practical conditions will reveal the capability of the catalyst for practical use. This can be performed using a synthetic gas mixture having similar composition to the real exhaust gas.

7. Using several mixtures of ZSM-5 and MCM-41 molecular sieves with different fractions may lead to finding a better catalyst for decomposition of SCR of NO.

ABBREVIATIONS AND NOMENCLATURE

Abbreviations

FID	Flame Ionisation Detector
FTIR	Fourier Transform Infra Red
HC	Hydrocarbon
He	Helium
IR	Infra Red
SCR	Selective Catalytic Reduction
SNCR	Selective Non-Catalytic Reduction
TCD	Thermal Conductivity Detector
TPABr	Tetrapropylammonium Bromide
TPAOH	Tetrapropylammonium Hydroxide
TWC	Three-Way Catalysts
XRD	X-Ray Diffraction

Nomenclature

E	apparent activation energy	cal mol^{-1}
[i]	concentration of i species	mol l^{-1}
F	total gas flow rate	
F_i	flow rate of gas stream containing i species	
He	helium	
k	rate constant	l mol^{-1} s^{-1} $site^{-1}$
K	equilibrium constant for O_2 adsorption	$l^{1/2}$ $mol^{-1/2}$
m	reaction order in NO	-
m′	reaction order in NO in Equation (5-14)	-
n	reaction order in O_2	-
n′	reaction order in O_2 in Equation (5-14)	-
O_2	oxygen	
r	reaction rate	s^{-1} $site^{-1}$

t	time	s
T	temperature	K
TOF	turnover frequency	s^{-1} $site^{-1}$
$\bar{x}_i$	mean value of i	
X_{NO}	NO conversion into N_2	%
X_{NOx}	NO_x conversion	%
X'_{NO}	NO conversion	%
m	mass	g

Greek Symbols

σ_x	standard deviation	
$\sigma_{\bar{x}}$	standard deviation of mean	
ρ_b	apparent density of catalyst	g ml^{-1}

Subscripts

in	inlet gas stream
NO	nitrogen monoxide
NO_x	nitrogen oxides
ox	oxidation
C_nH_m	methane or propene
out	outlet gas stream
Cu	copper
cyl.	NO gas cylinder

REFERENCES

Acres, G. J. K., Bird, A. J., Jenkins, J. W., and King, F. (1981). "*The Design and Preparation of Supported Catalysts.*" Catalysis, A Specialist Periodical Report, The Royal Society of Chemistry, Vol. 4, Chapter 1.

Adelman, B. J., Beutel, T., Lei, G.-D., and Sachtler. (1996). "Mechanistic Cause of Hydrocarbon Specificity over Cu/ZSM-5 and Co/ZSM-5 Catalysts in the Selective Catalytic Reduction of NO_x." *J. Catal.*, **158**, 327-335.

Amiridis, M. D., Zhang, T., and Farrauto, R. J. (1996). "Selective Catalytic Reduction of Nitric Oxide by Hydrocarbons." *Appl. Catal. B*, **10**, 203-227.

Ansell, G. P., Diwell, S. E., Golunski, J. W., Hayes, J. W., Rajaram, R. R., Truex, T. J., and Walker, A. P. (1993). "Mechanism of the Lean NO_x Reaction over Cu/ZSM-5." *Appl. Catal. B*, **2**, 81-100.

Argauer, R. J., and Landolt, G. R. (1972). US Pat. **3 702 886**.

Armor, J. N. (1994). "*NO_x Removal: An Overview.*" ACS Symposium series 552: Environmental Catalysis, Ed. J. N. Armor, American Chemical Society, Washington, DC, Chapter 1.

Baggley, G. W. (1993). "NO_x and Carbon Dioxide Control Using Burner Design." *First International Conference on Processing Materials for Properties.*, Ed. H. Henein and T. Oki, The Minerals, Metals & Material Society, 125-128.

Barrer, R. M. (1982). *Hydrothermal Chemistry of Zeolites*, Academic Press, London.

Bell, A. T., Manzer, L. E., Chen, N. Y., Weekman, V. W., Hegedus, L. L., and Pereira, C. J. (1995). "Catalysts for Environmental Protection: Protecting the Environment Through Catalysis." *Chem. Eng. Progr*, February 1995, 26-34.

Beutel, T., Adelman, B. J., and Sachtler, W. M. H. (1996). "FTIR Study of the Nitrogen Isotopic Exchange Between Adsorbed $^{15}NO_2$ Complexes and ^{14}NO over Cu/ZSM-5 and Co/ZSM-5." *Appl. Catal. B*, **9**, L1-L10.

Bosch, H., and Janssen, F. J. J. G. (1988). "Catalytic Reduction of Nitrogen Oxides. A Review on the Fundamentals and Technology." *Catal. Today*, **2**(4), 369-521.

Breck, D. W. (1974). "*Introduction.*" Zeolite Molecular Sieves, John Wiley & Sons, New York, Chapter 1.

Brunauer, S., Emmett, P. H., and Teller, E. (1938). "Adsorption of Gases in multimolecular Layers." *J. Am. Chem. Soc.*, **60**, 309-319.

Burch, R., and Millington, P. J. (1993). "Role of Propene in the Selective Reduction of Nitrogen Monoxide in Copper Exchanged Zeolites." *Appl. Catal. B*, **2**, 101-116.

Buzanowski, M. A., and Yang, R. T. (1990). "Simple Design of Monolith Reactor for Selective Catalytic Reduction of NO for Power Plant Emission Control." *Ind. Eng. Chem. Res.*, **29**, 2074-2078.

Campa, M. C., Indovina, V., Minelli, G., Moretti, G., Pettiti, I., Porta, P., and Ricio, A. (1994). "The Catalytic Activity of Cu-ZSM-5 and Cu-Y Zeolites in NO Decomposition: Dependence on Copper Concentration." *Catal. Lett.*, **23**, 141-149.

Centi, G., Nigro, C., Perathoner, S., and Stella, G. (1994). "*Reactivity of Cu-Based Zeolites and Oxides in the Conversion of NO in the Presence or Absence of O_2.*" ACS Symposium Series 552: Environmental Catalysis, Ed. J. N. Armor, American Chemical Society, Washington, DC, Chapter 3.

Curtin, T., Grange, P., and Delmon, B. (1997). "The Direct Decomposition of Nitrogen Monoxide." *Catal. Today*, **35**, 121-127.

d'Itri, J. L., and Sachtler, M. H. (1992). "Reduction of NO over Impregnated Cu/ZSM-5 in the Presence of O_2." *Catal. Lett.*, **15**, 289-295.

Dai, F.-Y., Suzuki, M., Takahashi, H., and Saito, Y. (**1986**). *Proceeding of the 7th International Zeolite Conference: New Developments in Zeolite Science and Technology.*, Ed. Y. Murakami, A. Lijima, and J.W. Ward, Tokyo, 223-230.

Danielson, J. (1967). "Air Pollution Engineering Manual." , US Department of Health, Education and Welfare, National Center for Air Pollution Control, OH.

De Jong, B. (1993). "Emission Characteristics of the Shell Low-NO_x Burner." *Comb. Sci. T.*, **93**, 129-151.

Dedecek, J., Sobalik, Z., Tvaruzkova, Z., Kaucky, D., and Wichterlova, B. (1995). "Coordination of Cu Ions in High-Silica Zeolite Materials. Cu^+ Photoluminescence, IR of NO Adsorbed on Cu^{2+}, and Cu^{2+} ESR Study." *J. Phys. Chem.*, **99**, 16327-16337.

Dyer, A. (1988). "*Zeolite as Ion Exchangers.*" An Introduction to Zeolite Molecular Sieves, John Wiley and Sons, Chapter 6.

Elvins, C., Jones, D., Lukins, N., Miskin, J., Ross, B., and Sanders. (1991). *Chemistry One, Materials, Chemistry in Every Life*, Rigby Heinemann, Melbourne.

Emmett, P. H. (1948). "Adsoption and Pore-Size Measurments on Charcoals and Whetlerites." *Chem. Rev.*, **43**, 69-148.

Emmett, P. H. (1954). "*Catalysis.*" Chatalysis, Vol. 1, Ed. Emmett, P. H., Reinhold Pub. Corp., New York.

Esch, G. J. V., and Menzel, D. B. (1982). "Health Effects Associated with Nitrogen Oxides." *The US-Dutch International Symposium.*, Maastricht, The Netherlands, Maastricht, The Netherlands, 79-88.

Forbes, N. R., and Rees, L. V. C. (1995). "The Synthesis of Ferrierite, ZSM-5, and Theta-1 in the Presence of Diethanolamine: Experimental." *Zeolites*, **15**, 444-451.

Freestone, N. (1998). "Highlights." *Chem. Indus.*, 2 November, 891-891.

Gabelica, Z., Blom, N., and Derouane, E. G. (1983). "Synthesis and Characterization of ZSM-5 Type Zeolites, III. A Critical Evaluation of the Role of Alkali and Ammonium Cations." *Appl. Catal*, **5**, 227-248.

Ganemi, B., Bjornbom, E., and Paul, J. (1998). "Conversion and in Situ FTIR Studies of Direct NO Decomposition over Cu-ZSM-5." *Appl. Catal. B*, **17**, 293-311.

Gibson, J. H., and Linthurst, R. A. (1982). "Effects of Acidic Precipitation on the American Continent." *The US-Dutch International Symposium.*, Studies in Environmental Science 21, Air Pollution By Nitrogen Oxides, Maastricht, The Netherlands, 577-593.

Gopalakrishnan, R., Davidson, J., Stafford, P., Hecker, W. C., and Bartholomew, C. H. (1994). "*Catalysts for Cleanup of NH_3, NO_x, and CO form a Nuclear Waste Processing Facility.*" ACS Symposium Series 552: Environmental Catalysis, Ed. J. N. Armor, American Chemical Society, Chapter 7.

Griffith, W. P. (1973). *Comprehensive Inorganic Chemistry*, Pergamon Press, .

Haag, W. O., Lago, R. M., and Weisz, P. B. (1984). "The Active Site of Acidic Aluminosilicate Catalysts." *Nature*, **309**, 589-591.

Hall, W. K., and Valyon, J. (1992). "Mechanism of NO Decomposition over Cu-ZSM-5." *Cat. Lett.*, **15**, 311-315.

Hamada, H. (1994). "Selective Reduction of NO by Hydrocarbons and Oxygenated Hydrocarbons over Metal Oxide Catalysts." *Catal. Today*, **22**, 21-40.

Harrison, B., Wyatt, M., and Gough, K. G. (1982). "*Catalysis of Reactions Involving the Reduction or Decomposition of Nitrogen Oxides.*" A Review of the Recent Literature Published up to Mid 1981, Catalysis, Vol. 5, The Royal Society of Chemistry, Chapter 4.

Headon, K. A., and Zhang, D. K. (1997). "Performance of Zeolite Supported Catalysts for Selective Catalytic Reduction of Nitric Oxide and Oxidation of Methane." *Ind. Eng. Chem. Res.*, **36**(11), 4595-4599.

Held, W., Konig, A., Richter, T., and Puppe, L. (1990). "Catalytic NO_x Reduction in Net Oxidizing Exhaust Gas." *Soc. Aut. Eng. International Congress and Exposition.*, MI, USA, Paper 900496, 13-20.

Hirabayashi, H., Yahiro, H., Mizuno, N., and Iwamoto, M. (1992). "High Catalytic Activity of Platinum-ZSM-5 Zeolite below 500 K in Water Vapour for Reduction of Nitrogen Monoxide." *Chem. Lett.*, 2235-2236.

Hoost, T. E., Laframboise, K. A., and Otto, K. (1995). "Co-adsorption of Propene and Nitrogen Oxides on Cu-ZSM-5: An FTIR Study." *Appl. Catal. B*, **7**, 79-93.

Hughes, R. (1984). "Diffusion and Deactivation of Catalysts." *Deactivation of Catalysts*, Academic Press, London, 29-54.

Iwamoto, M., Furukawa, H., Mine, Y., Uemura, F., Mikuriya, S., and Kagawa, S. (1986a). "Copper(II) Ion-exchanged ZSM-5 Zeolites as Highly Active Catalysts for Direct and Continuous Decomposition of Nitrogen Monoxide." *J. Chem. Soc. Chem. Commun.*, **15**, 1272-1273.

Iwamoto, M., Furukawa, H., and Kagawa, S. (1986b). "Catalytic Decomposition of Nitric Monoxide over Copper Ion-Exchanged Zeolites." *New Developments in Zeolite Science Technology.*, Studies in Surface Science and Catalysis 28, Ed. Y. Murikami, Elsevier Publishers, New York, 943-949.

Iwamoto, M., Yahiro, H., Mine, Y., and Kagawa, S. (1989). "Excessively Copper Ion-exchanged ZSM-5 Zeolites as Highly Active Catalysts for Direct Decomposition of Nitrogen Monoxide." *Chem. Lett.*, 213-216.

Iwamoto, M. (1990). "Decomposition of NO on Copper Ion-Exchanged Catalysts." *Proceedings of Meeting on Catalytic Technology for Removal of Nitrogen Monoxide.*, Tokyo, 7.

Iwamoto, M., Yahiro, H., Torikai, Y., Yoshioka, T., and Mizuno, N. (1990). "Novel Preparation Method of Highly Copper Ion-exchanged ZSM-5 Zeolites and Their Catalytic Activities for NO Decomposition." *Chem. Lett.*, 1967-1970.

Iwamoto, M., and Hamada, H. (1991). "Removal of Nitrogen Monoxide from Exhaust Gases through Novel Catalytic Processes." *Catal. Today*, **10**, 57-71.

Iwamoto, M., Yahiro, H., Tanda, K., Mizuno, N., and Mine, Y. (1991a). "Removal of Nitrogen Monoxide through a Navel Catalytic Process. 1. Decomposition on Copper Ion Exchanged ZSM-5 Zeolites." *J. Phys. Chem.*, **95**(9), 3727-3730.

Iwamoto, M., Yahiro, H., Shundo, S., Yu-uu, Y., and Mizuno, N. (1991b). "Influence of Sulfur Dioxide on Catalytic Removal of Nitric Oxide over Copper Ion-Exchanged ZSM-5 Zeolite." *Appl. Catal.*, **69**, L15-L19.

Iwamoto, M., and Mizuno, N. (1993). "NO_x Emission Control in Oxygen-Rich Exhaust Through Selective Catalytic Reduction by Hydrocarbon." *Proc. Instn. Mech. Engrs*, **207**, 23-33.

Jen, H. W., and Gandhi, H. S. (1994). "*Catalytic Reduction of NO by Hydrocarbon in Oxidizing Atmosphere.*" ACS Symposium Series 552: Environmental Catalysis, Ed. J. N. Armor, American Chemical Society, Chapter 5.

Kagawa, S., Ogawa, H., Furukawa, H., and Teraoka, Y. (1991). "Cocation Effect in Catalytic of Copper Ion-Exchanged ZSM-5 Zeolites for the Direct Decomposition of Nitrogen Monoxide." *Chem. Lett.*, 407-410.

Kharas, K. C. C. (1993). "Performance, Selectivity, and Mechanism in Cu-ZSM-5 Lean-Burn Catalysts." *Appl. Catal. B*, **2**, 207-224.

Kharas, K. C. C., Robota, H. J., and Datye, A. (1994). "*Deactivation of Cu-ZSM-5.*" ACS Symposium Series 552: Environmental Catalysis, Ed. J. N. Armor, American Chemical Society, 39-52.

Kulkarni, S. B., Shiralkar, V. P., Kootasthane, A. N., and Borade, R. B. (1982). "Studies in the Synthesis of ZSM-5 Zeolites." *Zeolites*, **2**, 313-318.

Lahaye, J., and Prado, G. (1986). *Proceeding of the NATO Advanced Research Workshop on Fundamentals of the Physical-Chemistry of Pulverised Coal*

Combustion., NATO ASI Series, Series E, Applied Science, Kluwer Academic Publishers, Boston, USA.

Lambert, D., and McGowan, T. P. E. (1996). "NO_x Control Techniques for the CPI." *Chem Eng.*, June 1996, 98-101.

Larsen, S. C., Aylor, A., Bell, A. T., and Reimer, J. A. (1994). "Electron Paramagnetic Resonance Studies of Copper Ion-Exchanged ZSM-5." *J. Phys. Chem.*, **98**, 11533-11540.

Li, Y., and Hall, K. (1990). "Stoichiometric Catalytic Decomposition of Nitric Oxide over Cu-ZSM-5 Catalysts." *J. Phys. Chem.*, **94**(16), 6145-6148.

Li, Y., and Hall, K. (1991). "Catalytic Decomposition of Nitric Oxide over Cu-Zeolites." *J. Catal.*, **129**, 202-215.

Li, Y., and Armor, J. N. (1992). "Catalytic Reduction of Nitrogen Oxides with Methane in the Presence of Excess Oxygen." *Appl. Catal. B*, **1**, L31-L40.

Li, Y., and Armor, J. N. (1993). "Selective Catalytic Reduction of NO_x with Methane over Metal Exchanged Zeolites." *Appl. Catal. B*, **2**, 239-256.

Li, Y., and Armor, J. N. (1994). "Selective Reduction of NO_x by Methane on Co-Ferrierites." *J. Catal.*, **150**, 376-387.

Li, Y., and Armor, J. N. (1995). "The Effect of SO_2 on the Catalytic Performance of Co-ZSM-5 and Co-Ferrierite for Selective Reduction of NO by CH_4 in the Presence of O_2." *Appl. Catal. B*, **5**, L257-L270.

Lindau, L. (1982). "NO_x Policy in Sweden." *The US-Dutch International Symposium.*, Studies in Environmental Science 21, Air Pollution By Nitrogen Oxides, Maastricht, The Netherlands, 1009-1012.

Lionta, G. D., Christoforou, S. C., Efthimiadis, E. A., and Vasalos, I. A. (1996). "Selective Catalytic Reduction of NO with Hydrocarbons: Experimental and Simulation Results." *Ind. Eng. Chem. Res.*, **35**, 2508-2515.

Lu, M., and Zhao, X. S. (1996). The University of Queensland, Brisbane, Qld 4073.

Martinez, A., Gomez, S. A., and Fuentes, G. A. (1997). "Deactivation of Cu-ZSM-5 during Selective Catalytic Reduction of NO by Propane under Wet Conditions." *Catalyst Deactivation 1997*, 225-230.

Mason, H. B., and Herther, M. A. (1982). "Emission Inventory for Stationary NO_x Sources (USA)." *The US-Dutch International Symposium.*, Studies in Environmental Science 21, Air Pollution By Nitrogen Oxides, Maastricht, The Netherlands, 131-141.

Montreuil, C. N., and Shelef, M. (1992). "Selective Reduction of Nitric Oxide over Cu-ZSM-5 Zeolite by Water-Soluble Oxygen-Containing Organic Compounds." *Appl. Catal. B*, **1**, L1-L8.

Moretti, G. (1994). "Effects of the Si/Al Atomic Ratio on the Activity of Cu-ZSM-5 Catalysts for Nitric Oxide Decomposition." *Catal. Lett.*, **23**, 135-140.

Nakatsuji, T., Yasukawa, K., Tabata, K., Ueda, K., and Niwa, M. (1998). "Catalytic Reduction System of NO_x in Exhaust Gases from Diesel Engines with Secondary Fuel Injection." *Appl. Catal. B*, **17**, 333-345.

Narita, E., Sato, K., and Okabe, T. (1984). "A Convenient Method for Crystallization of Zeolite ZSM-5 by using Seed Crystals in Acetone/Water Mixture System." *Chem. Lett.*, 1055-1058.

Narita, E., Sato, K., Yatabe, N., and Okabe, T. (1985). "Synthesis and Crystal Growth of Zeolite ZSM-5 from Sodium Aluminosilicate Systems free of Organic Templates." *Ind. Eng. Chem. Prod. Res. Dev.*, **24**(4), 507-512.

Nishizaka, Y., and Misono, M. (1993). "Catalytic Reduction of Nitrogen Monoxide by Methane over Palladium-Loading Zeolites in the Presence of Oxygen." *Chem. Lett.*, 1295-1298.

Sano, T., Kiyozumi, M., Mizukami, F., Takaya, H., Mouri, T., Inaoka, W., Toida, Y., Watanabe, M., and Toyoda, K. (1991). "Preparation and Characterization of ZSM-5 Zeolite film." *Zeolites*, **11**, 842-845.

Sano, T., Kasuno, T., Arazaki, S., and Kawakami, Y. (1997). "Sorption of Water Vapour on H-ZSM-5 Type Zeolites." *Progress in Zeolite and Microporous Materials Studies in Surface Science and Catalysis*, **105**, 1771-1778.

Sasaki, M., Hamada, H., Kintaichi, and Ito, T. (1992). "Role of Oxygen in Selective Reduction of Nitrogen Monoxide by Propane over Zeolite and Alumina-based Catalysts." *Catal. Lett.*, **15**, 297-304.

Sass, C. E., and Kevan, L. (1988). "Electron Spin Echo Modulation and Electron Spin Resonance Studies of Cupric Ions in H-ZSM-5, Na-ZSM-5, K-ZSM-5 and Ca-ZSM-5 Zeolites: Analysis of ^{13}C Electron Spin Echo Modulation." *J. Phys. Chem.*, **92**, 5192-5196.

Sato, S., YU-u, Y., Yahiro, H., Minzuno, N., and Iwamoto, M. (1991). "Cu-ZSM-5 Zeolite as Highly Active Catalyst for Removal of Nitrogen Monoxide from Emission of Diesel Engines." *Appl. Catal.*, **70**, L1-L5.

Sato, S., Hirabashi, H., Yahiro, H., Mizuno, N., and Iwamoto, M. (1992). "Iron Ion-Exchanged Zeolite: the Most Active Catalyst at 473 K for Selective Reduction of Nitrogen Monoxide by Ethane in Oxidizing Atmosphere." *Catal. Lett.*, **12**, 193-200.

Satterfield, C. N. (1991). "*Physical Characterization and Examination.*" Heterogeneous Catalysis in Industrial Practice, eds. 2, McGraw-Hill, Inc., New York, Chapter 5.

Schlatter, J. C., Sinkevitch, R. M., and Mitchell, P. J. (1983). "Laboratory Reactor System for 3-Way Automotive Catalyst Evaluation." *Ind. Eng. Chem. Prod. Res. Dev.*, **22**(1), 51-56.

Schoonheydt, R. A., Vandamme, L. J., Jacobs, P. A., and Uytterhoeven, J. B. (1976). "Chemical, Surface and Catalytic of Nonstoichiometrically Exchanged Zeolites." *J. Catal.*, **43**, 292-303.

Shelef, M. (1992). "On the Mechanism of Nitric oxide Decomposition over Cu-ZSM-5." *Catal. Lett.*, **15**, 305-310.

Shelef, M., and Graham, G. W. (1994). "Why Rhodium in Automotive Three-Way Catalyst?" *Catal. Rev.- Sci. Eng.*, **35(4)**, 457-481.

Shelef, M. (1995). "Selective Catalytic Reduction of NO_x with N-Free Reductants." *Chem. Rev.*, **95**(1), 209-225.

Shiralkar, V. P., and Clearfielld, A. (1989). "Synthesis of the Molecular Sieve ZSM-5 Without the Aid of Template." *Zeolites*, **9**, 363-370.

Sun, T., Trudeau, M. L., and Ying, J. Y. (1996). "The Nature of Cobalt Species in Co-ZSM-5 NO Emission Control Catalysts." *J. Phys. Chem.*, **100**, 13662-13666.

Syska, A. (1993). "Low NO_x Staged Air Recirculating Burner Undergoing Field Trials After Excellent Test Performance." *Industrial Heating*, 40-42.

Szostak, R. (1989). *Molecular Sieves Principles of Synthesis and Identification*, Van Nostrand Reinhold, New York.

Tanaka, T. (1997). "Selective Catalytic Reduction of NO over PtMo Catalysts with Alkaline or Alkaline Earth Metal under Lean Static Conditions." *Chem. Lett.*, 409-410.

Taylor, J. R. (1982). *An Introduction to Error Analysis*, Mill Valley, California.

Taylor, K. C. (1993). "Nitric Oxide Catalysis in Automotive Exhaust System." *Catal. Rev.-Sci. Eng*, **35**(4), 457-481.

Teraoka, Y., Fukuda, H., and Kagawa, S. (1990). "Catalytic Activity of Perovskite-Type Oxides for Direct Decomposition of Nitrogen Monoxide." *Chem. Lett.*, 1-4.

Torre-Abreu, C., Ribeiro, M. F., Henriques, C., and Ribeiro, F. R. (1997a). "Selective Catalytic Reduction of NO with Propene over CuMFI Zeolites: Dependence on Si/Al Ratio and Copper Loading." *Appl. Catal. B*, **11**, 383-401.

Torre-Abreu, Ribeiro, M. F., Henriques, C., and Ribeiro, F. R. (1997b). "Copper-Exchanged Mordenites as Active Catalysts for NO Selective Catalytic Reduction by Propene under Oxidising Conditions: Effect of Si/Al ratio, Copper Content and Bronsted Acidity." *Appl. Catal. B*, **13**, 251-264.

Tronconi, E., Forzatti, P., Gomez Martin, J. P., and Malloggi, S. (1992). "Selective Catalytic Removal of NO_x: A Mathematical Model for Design of Catalyst and Reactor." *Chem. Eng. Sci.*, **47**(9-11), 2401-2406.

Trout, B. L., Chakraborty, A. K., and Bell, A. T. (1996). "Local Spin Density Functional Theory Study of Copper Ion-Exchanged ZSM-5." *J. Phys. Chem.*, **100**, 4173-4179.

Tynjala, P., and Pakkanen, T. T. (1996). "Acidic Properties of ZSM-5 Zeolite Modified with Ba^{2+}, Al^{3+} and La^{3+} Ion-Exchange." *J. Mol. Catal. A Chem.*, **110**, 153-161.

Uguina, M.-A., Lucas, A., Ruiz, F., and Serrano, D.-P. (1995). "Synthesis of ZSM-5 from Ethanol-Containing Systems. Influence of the Gel Composition." *Ind. Eng. Chem. Res.*, **34**, 451-456.

Valyocsik, E. W., and Rollmann, L. D. (1985). "Diamines as Templates in Zeolite Crystallization." *Zeolites*, **5**, 123-125.

Valyon, J., and Hall, K. (1993). "Studies of the Surface Species Formed from NO on Copper Zeolites." *J. Phys. Chem.*, **97**, 1204-1212.

Vassallo, J., Miro, E., and Petunchi, J. (1995). "On the Role of Gas-Phase Reactions in the Mechanism of the Selective Reduction of NO_x." *Appl. Catal. B*, **6**, 65-78.

Wallman, P. H., and Carlsson, R. C. J. (1993). "NO_x Reduction by Ammonia." *Fuel*, **72**, 187-192.

Ward, J. W. (1984). "Molecular Sieve Catalysts." *Applied Industrial Catalysis*, B. E. Leach,. eds., Academic Press, Orlando, Chapter 9.

Weast, R. C., Astle, M. J., and Beyer, W. H. (1983-1984)."CRC Handbook of Chemistry and Physics." , CRC Press, Inc., Boca Raton, Florida.

Wendlandt, K. P., Reschetilowski, W., Unger, B., Weber, M., Forkmann, E., Kanazirev, V., and Penchev, V. (1987). "Effect of Pretreatment and Preparation Conditions on the Catalyst Properties of Modified ZSM-5 Zeolites." *VIth Int. Symp. Heterogeneous Catalysts.*, Part 2, Sofia, 107-111.

Whittingham, M. S. (1995). "In Chemistry 445 Laboratory Manual." , Binghamton University, New York.

Wichterlova, B., Dedecek, J., and Vondrova, A. (1995). "Identification of Cu Sites in ZSM-5 Active in NO Decomposition." *J. Phys. Chem.*, **99**(4), 1065-1067.

Wilkosz, J., Stobiecka, E., and Dudek, B. (1993). "The Investigations on the Synthesis of Zeolite ZSM-5 with the Use of Ethylendiamine as a Templating Agent." *Zeolites*, (13), 581-586.

Witzel, F., Sill, G. A., and Hall, W. K. (1994). "Reaction Studies of the Selective Reduction of NO by Various Hydrocarbons." *J. Catal*, **149**, 229-237.

Wojtowicz, M. A., Pels, J. R., and Moulijn, J. A. (1993). "Combustion of Coal as a Source of N_2O Emission." *Fuel Processing Technology*, **34**, 1-71.

Yang, R. T., and Li, W. (1995). "Note: Ion-exchanged Pillared Clays: A New Class of Catalysis for Selective Catalytic Reduction of NO by Hydrocarbons and Ammonia." *J. Catal.*, **155**, 414-417.

Yogo, K., Tanaka, S., Ihara, M., Hishiki, T., and Kikuchi, E. (1992). "Selective Reduction of NO with Propane on Gallium Ion-Exchanged Zeolites." *Chem. Lett.*, 1025-1028.

Yogo, K., Ihara, M., Teraasaki, I., and Kikuchi, E. (1993). "Selective Reduction of Nitrogen Monoxide with Methane or Ethane on Gallium Ion-Exchanged ZSM-5 in Oxygen-Rich Atmosphere." *Chem. Lett.*, 229-232.

Zeldovich, Y. B. (1946). *Acta Physicochimica USSR*, **21**, 577-628.

Zhang, Y., and Flytzani-Stephanopoulos, M. (1994). "*Catalytic Decomposition of Nitric Oxide over Promoted Copper-Ion-Exchanged ZSM-5 Zeolites.*" ACS Symposium Series 552: Environmental Catalysis, Ed. J. N. Armor, American Chemical Society, Washington, DC, Chapter 2.

Zhang, D. K., and Agnew, J. B. (1995). "Catalytic Decomposition of Nitric Oxide over Zeolite-Supported Catalyst." *Chemeca '95.*, Adelaide, Australia, .

Zhang, W., Yahiro, H., and Iwamoto, M. (1995a). "Reversible and Irreversible Adsorption of Nitrogen Monoxide on Cobalt Ion-Exchanged ZSM-5 and Mordenite Zeolites at 273-523 K." *J. Chem. Soc. Faraday Trans.*, **91**(4), 767-771.

Zhang, Y., Leo, K. M., Sarofim, A. F., Hu, Z., and Flytzani-Stephanopoulos, M. (1995b). "Preparation Effects on the Activity of Cu-ZSM-5 Catalysts for NO Decomposition." *Catal. Lett.*, **31**, 75-89.

Zhang, Y., and Flytzani-Stephanopoulos, M. (1996). "Hydrothermal Stability of Cerium Modified Cu-ZSM Catalyst for Nitric Oxide Decomposition." *J. Catal.*, **164**, 131-145.

Zhao, X. S., Lu, G. Q., and Zhang, D. K. (1995). "Zeolite-Based Catalysts for NO_x Decomposition." *The Australian Symposium on Combustion and the Forth Australian Flame Days.*, South Australia, .

Zhao, X., Lu, G. Q., and Millar, G. J. (1996). "Synthesis and Characterization of Highly Ordered MCM-41 in an Alkali-Free System and Its Catalytic Activity." *Catal. Lett.*, **38**, 33-37.

Zumdahl, S. S. (1986). *Chemistry*, D. C. Heath and Company, Massachusetts.

APPENDICES

APPENDIX A: Drawings of three autoclaves used in this study.

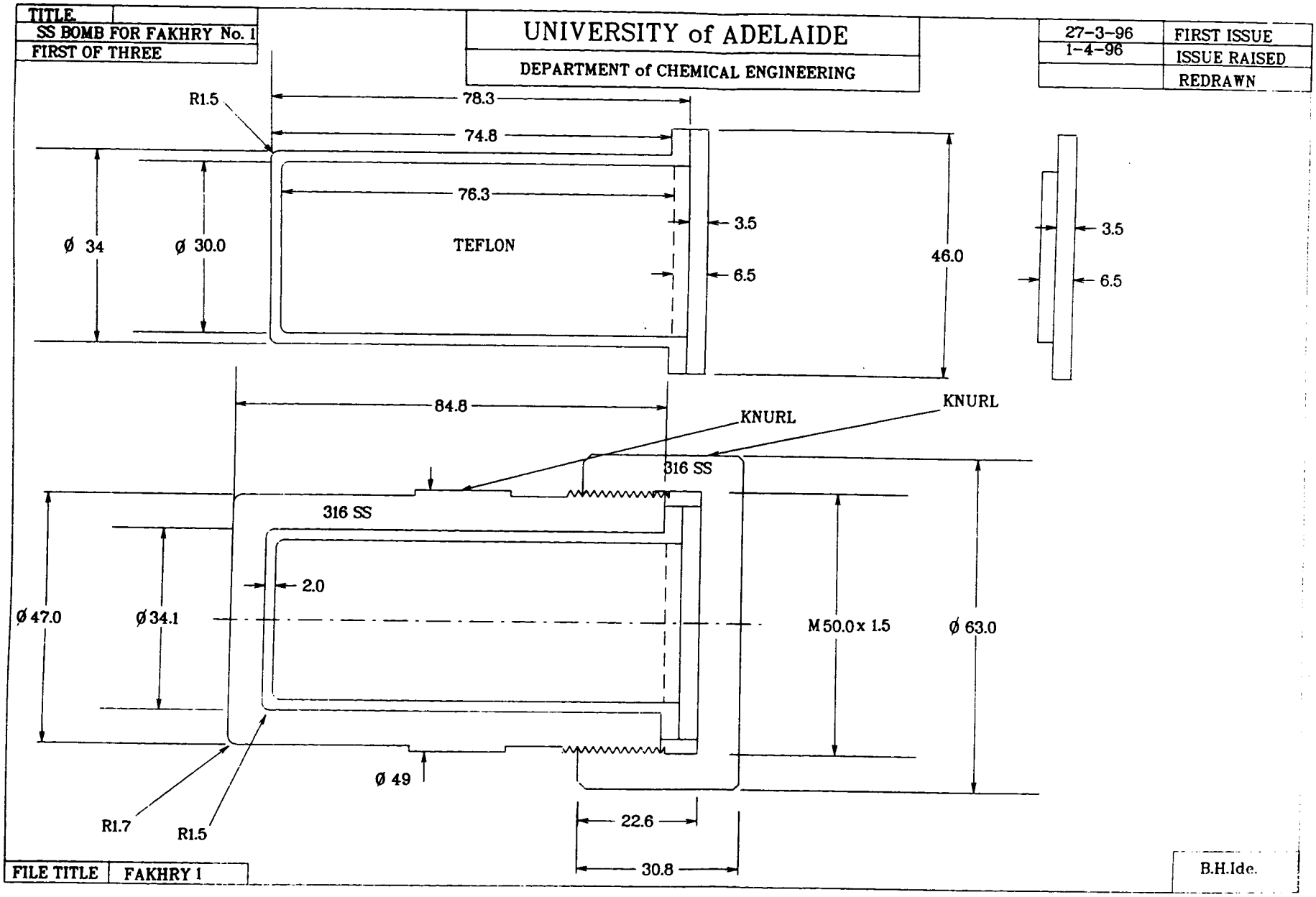
TITLE
SS BOMB FOR FAKHRY No. 1
FIRST OF THREE
UNIVERSITY of ADELAIDE
DEPARTMENT of CHEMICAL ENGINEERING
27-3-96 FIRST ISSUE
1-4-96 ISSUE RAISED
REDRAWN
R1.5
78.3
74.8
76.3
3.5
6.5
TEFLON
Ø 34
Ø 30.0
46.0
3.5
6.5
84.8
KNURL
KNURL
316 SS
316 SS
2.0
Ø 47.0
Ø 34.1
M 50.0 x 1.5
Ø 63.0
Ø 49
R1.7
R1.5
22.6
30.8
FILE TITLE FAKHRY 1
B.H.Ide.

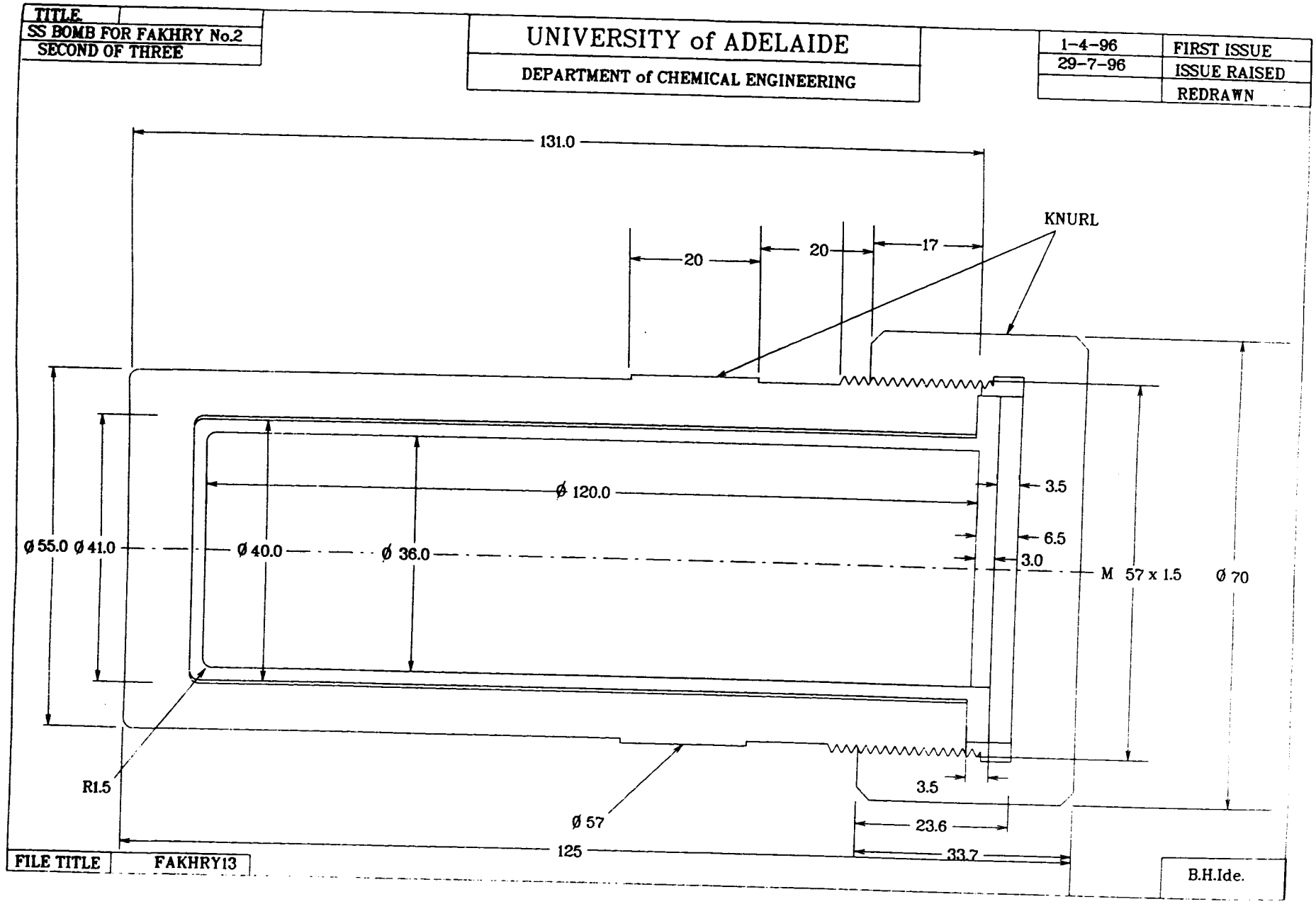
TITLE
SS BOMB FOR FAKHRY No.2
SECOND OF THREE
UNIVERSITY of ADELAIDE
DEPARTMENT of CHEMICAL ENGINEERING
1-4-96 FIRST ISSUE
29-7-96 ISSUE RAISED
REDRAWN
131.0
KNURL
20
20
17
Ø 120.0
3.5
6.5
3.0
Ø 55.0 Ø 41.0
Ø 40.0
Ø 36.0
M 57 x 1.5
Ø 70
R1.5
Ø 57
3.5
23.6
33.7
125
FILE TITLE
FAKHRY13
B.H.Ide.

TITLE.
SS BOMB FOR FAKHRY No 3
THIRD OF THREE

UNIVERSITY of ADELAIDE

DEPARTMENT of CHEMICAL ENGINEERING

1-4-96	FIRST ISSUE
	ISSUE RAISED
	REDRAWN

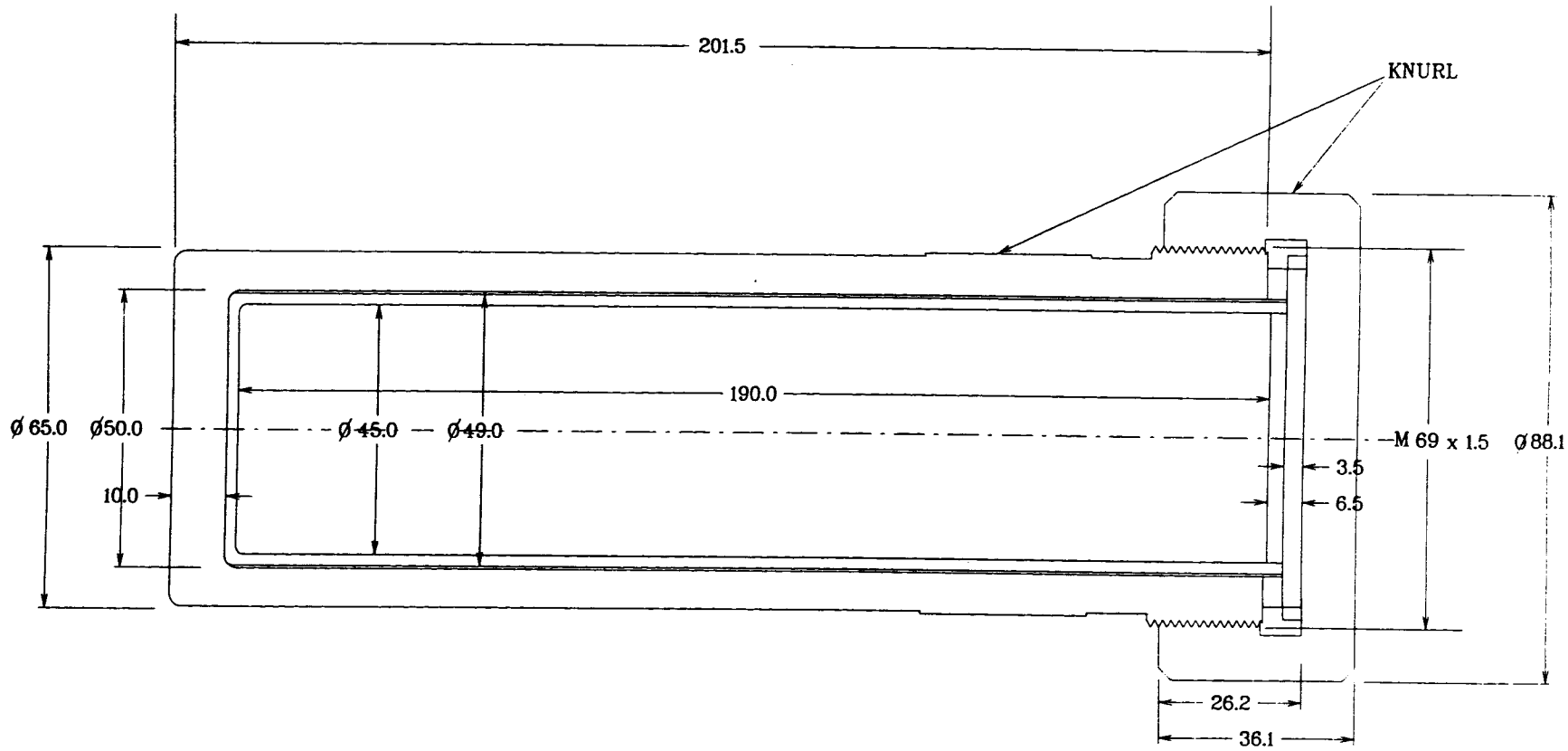

FILE TITLE	FAKHRY3

B.H.Ide.

APPENDIX B: XRD patterns of ZSM-5 zeolites synthesised in this study.

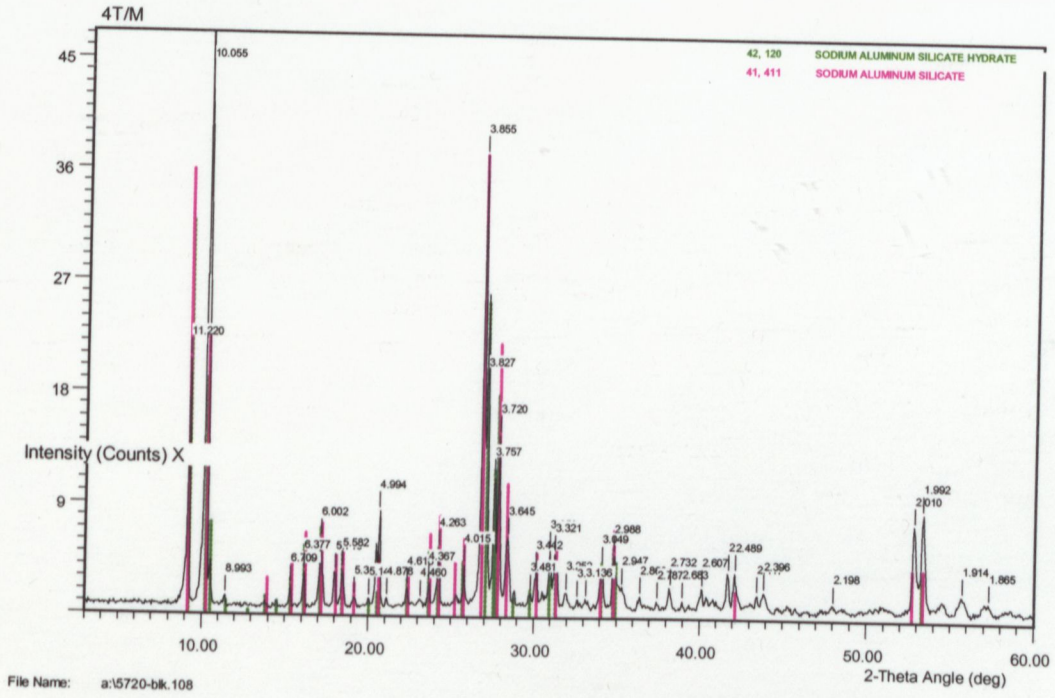

Figure B1: XRA pattern of Sample 4tm synthesised using Method I with SiO_2/Al_2O_3 ratio of 176, OH^-/SiO_2 ratio of 0.1, and 90% crystallinity.

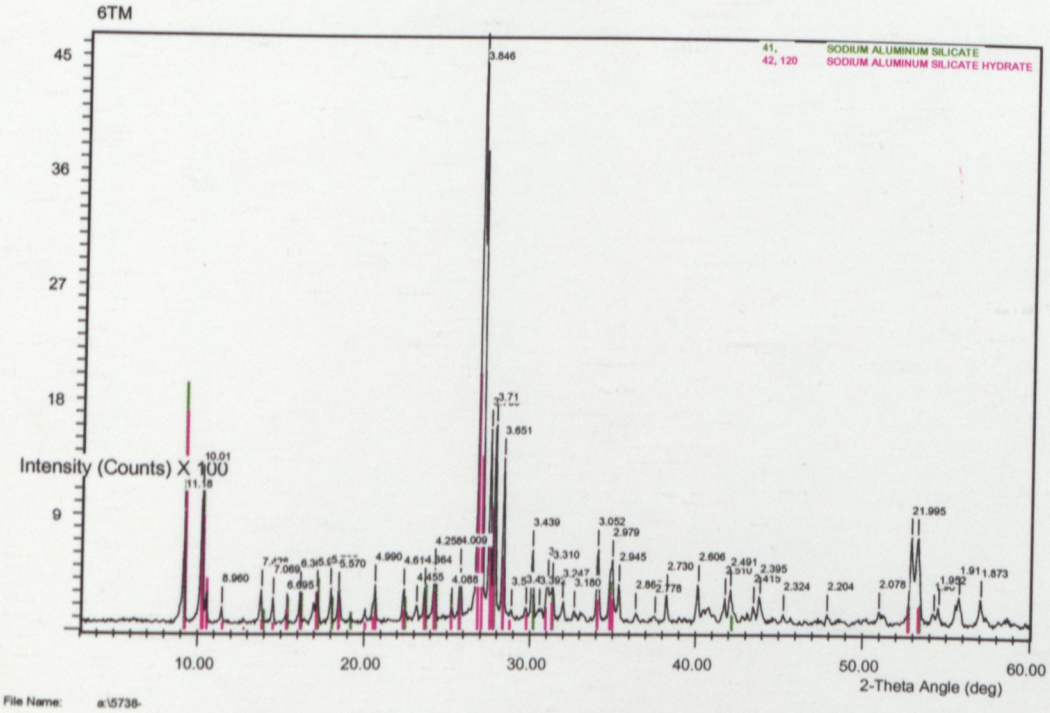

Figure B2: XRA pattern of Sample 6tm synthesised using Method I with SiO_2/Al_2O_3 ratio of 176, OH^-/SiO_2 ratio of 0.1, and 106% crystallinity.

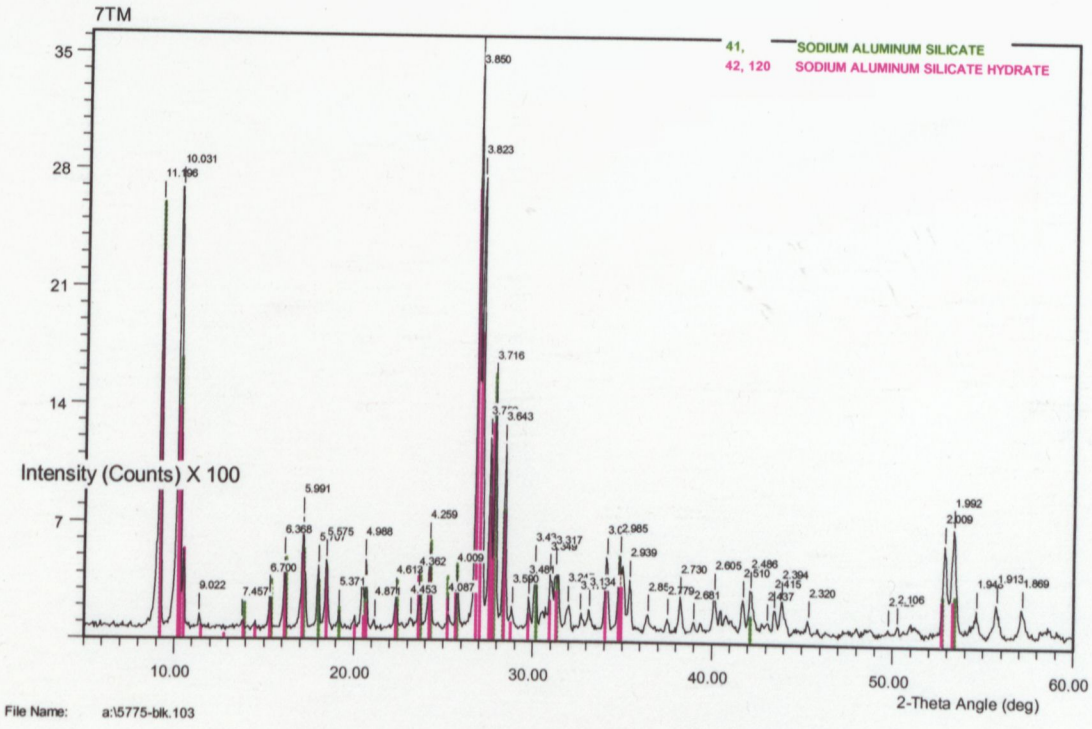

Figure B3: XRA pattern of Sample 7tm synthesised using Method I with SiO_2/Al_2O_3 ratio of 176, OH^-/SiO_2 ratio of 0.1, and 94% crystallinity.

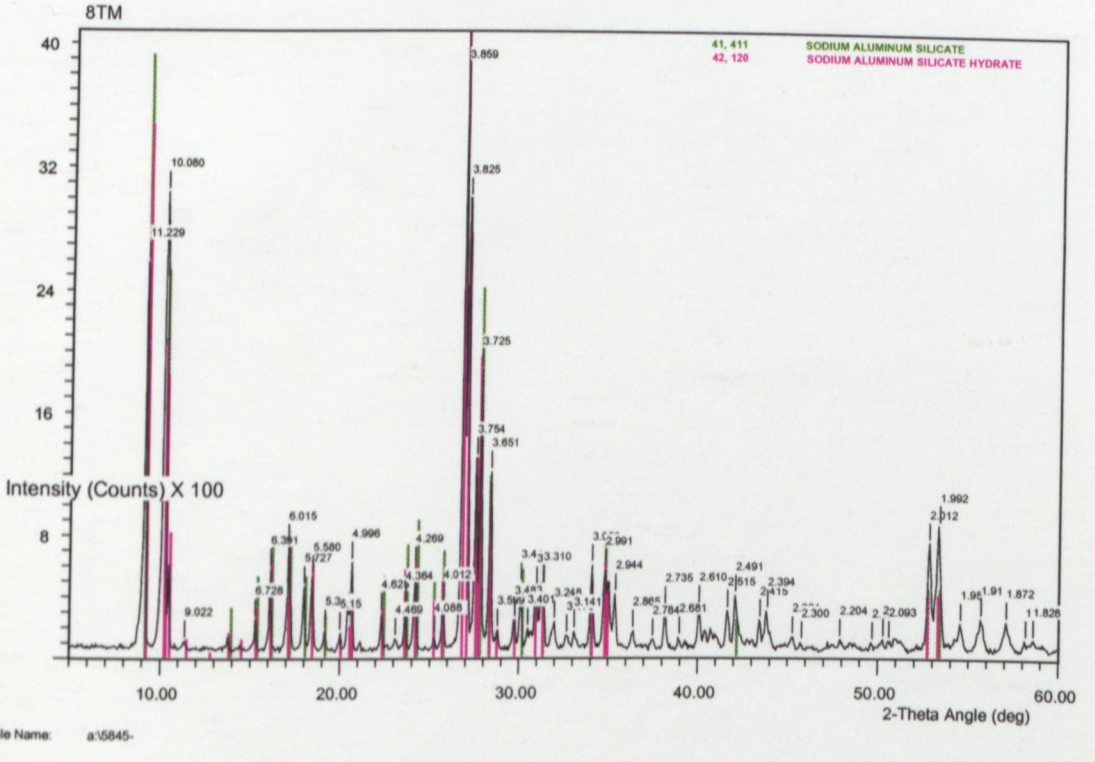

Figure B4: XRA pattern of Sample 8tm synthesised using Method I with SiO_2/Al_2O_3 ratio of 176, OH^-/SiO_2 ratio of 0.1, and 105% crystallinity.

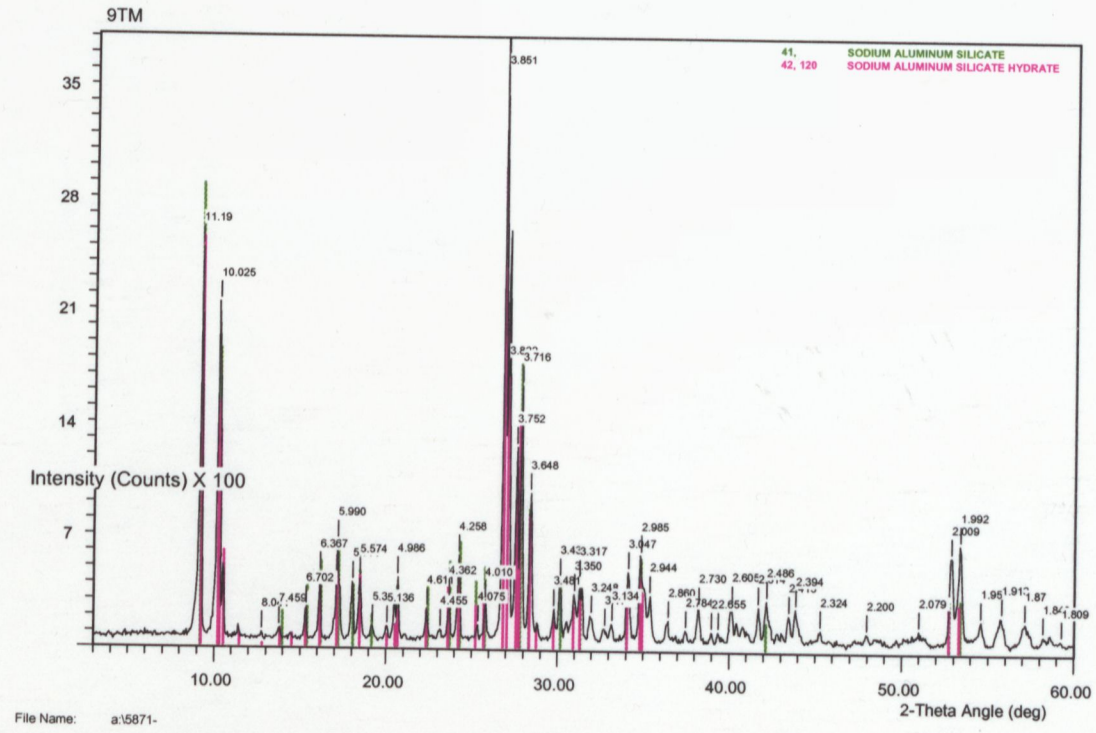

Figure B5: XRA pattern of Sample 9tm synthesised using Method I with SiO_2/Al_2O_3 ratio of 176, OH^-/SiO_2 ratio of 0.1, and 96% crystallinity.

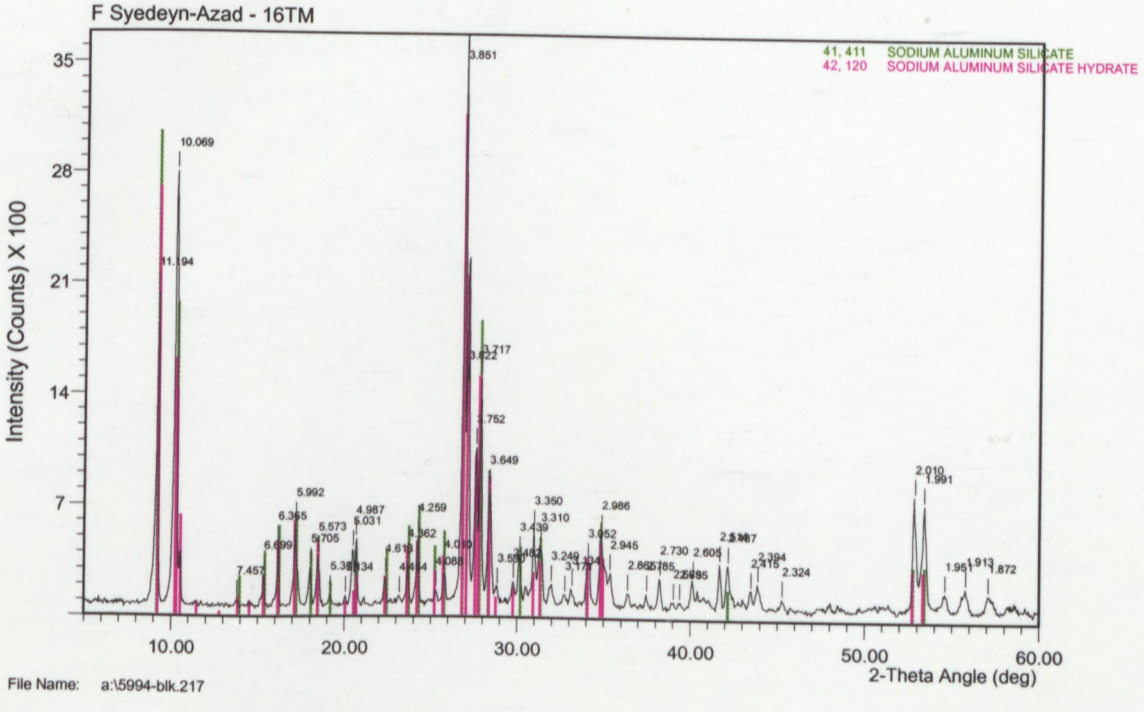

Figure B6: XRA pattern of Sample 16tm synthesised using Method I with SiO_2/Al_2O_3 ratio of 100, OH^-/SiO_2 ratio of 0.15, and 90% crystallinity.

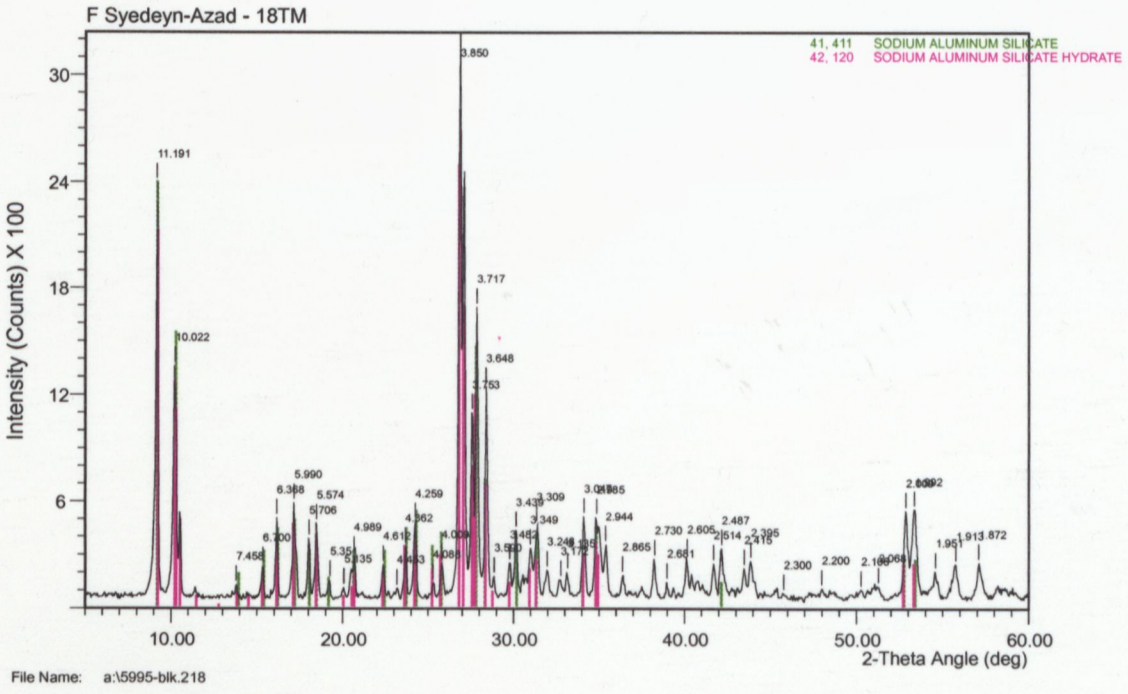

Figure B7: XRA pattern of Sample 18tm synthesised using Method I with SiO_2/Al_2O_3 ratio of 70, OH^-/SiO_2 ratio of 0.2, and 94% crystallinity.

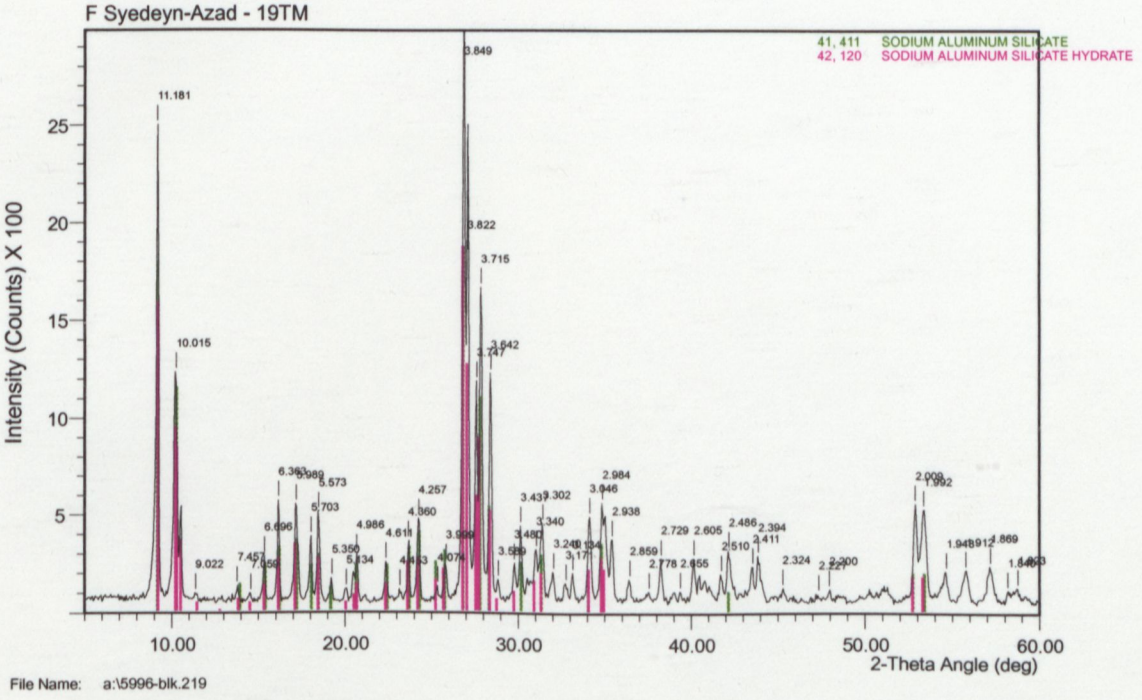

Figure B8: XRA pattern of Sample 19tm synthesised using Method I with SiO_2/Al_2O_3 ratio of 100, OH^-/SiO_2 ratio of 0.2, and 94% crystallinity.

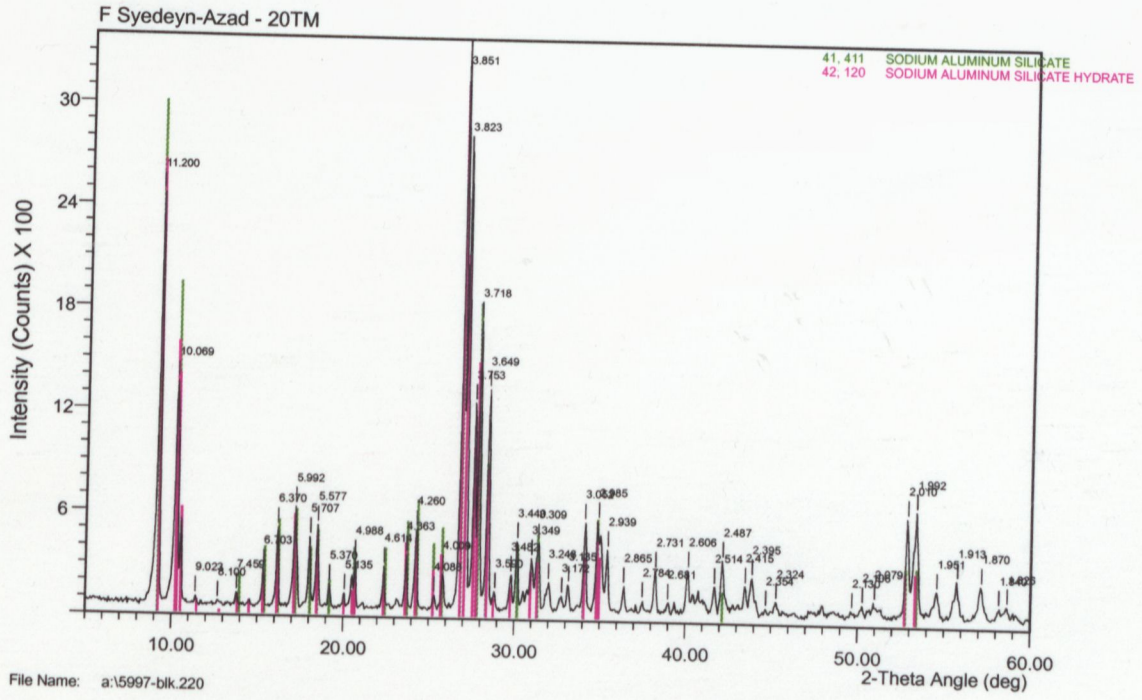

Figure B9: XRA pattern of Sample 20tm synthesised using Method I with SiO_2/Al_2O_3 ratio of 70, OH^-/SiO_2 ratio of 0.15, and 100% crystallinity.

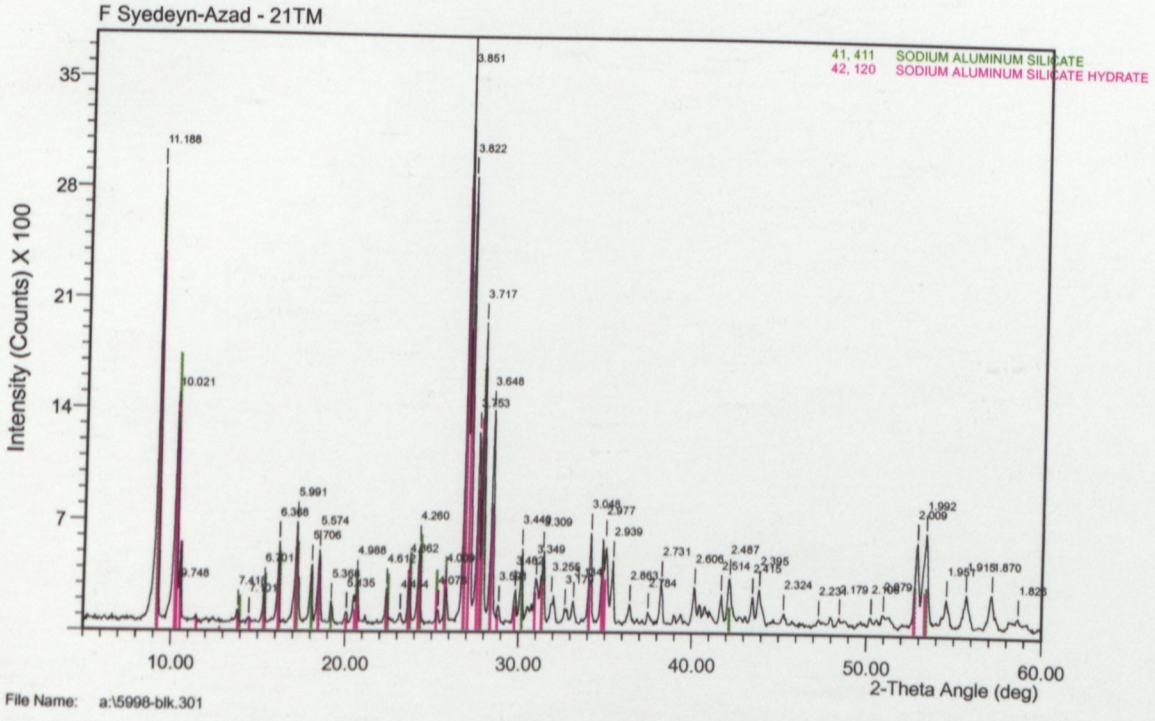

Figure B10: XRA pattern of Sample 21tm synthesised using Method I with SiO_2/Al_2O_3 ratio of 100, OH^-/SiO_2 ratio of 0.15, and 101% crystallinity.

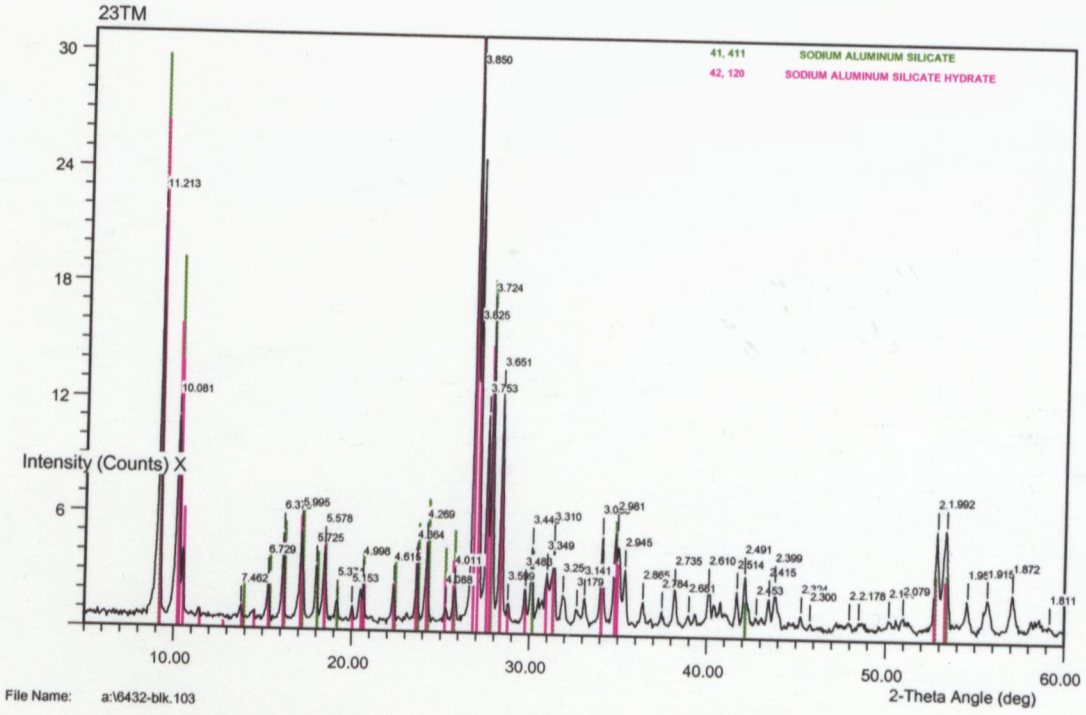

Figure B11: XRA pattern of Sample 23tm synthesised using Method I with SiO_2/Al_2O_3 ratio of 70, OH^-/SiO_2 ratio of 0.2, and 100% crystallinity.

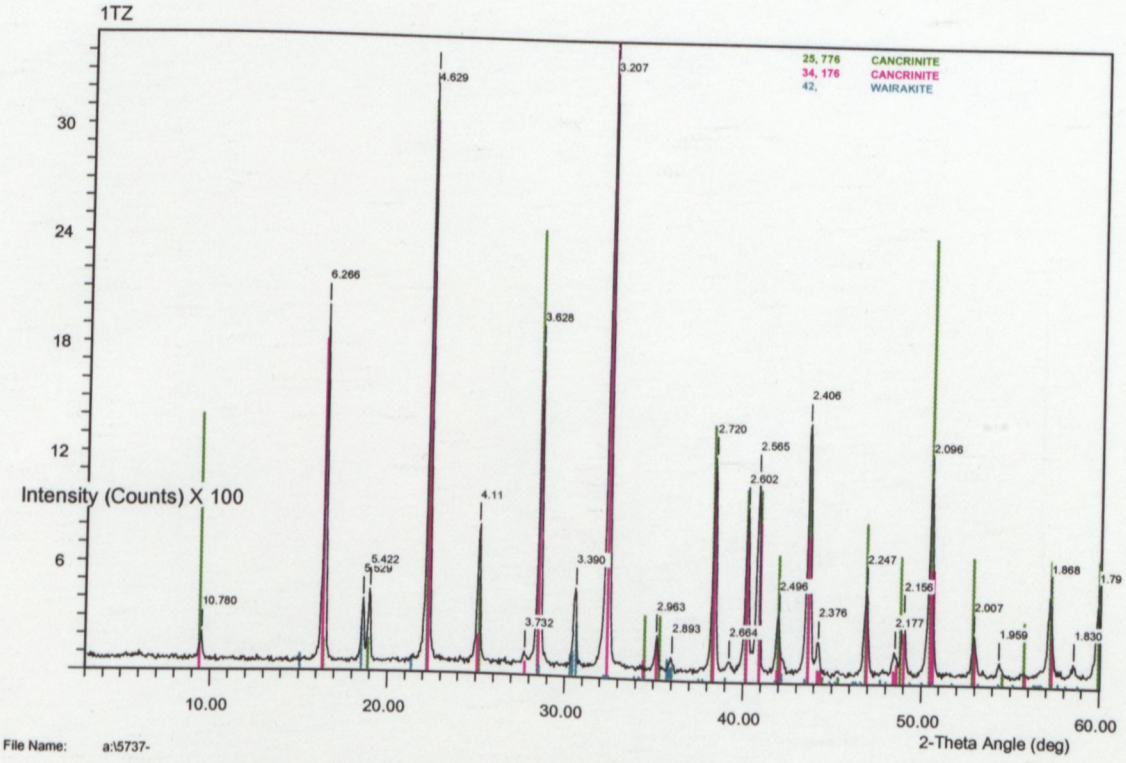

Figure B12: XRA pattern of Sample 1TZ synthesised using Method II with SiO_2/Al_2O_3 ratio of 96.5, OH^-/SiO_2 ratio of 0.2, and 0% crystallinity.

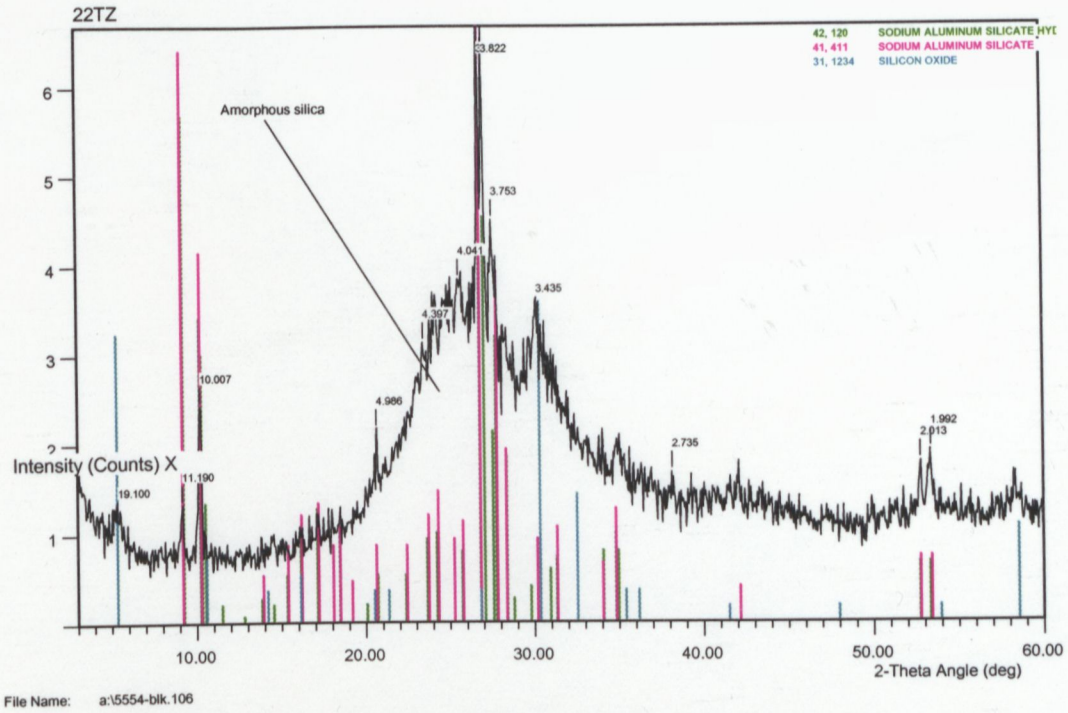

Figure B13: XRA pattern of Sample 22TZ synthesised using Method II with SiO_2/Al_2O_3 ratio of 96.5, OH^-/SiO_2 ratio of 0.2, and 12% crystallinity.

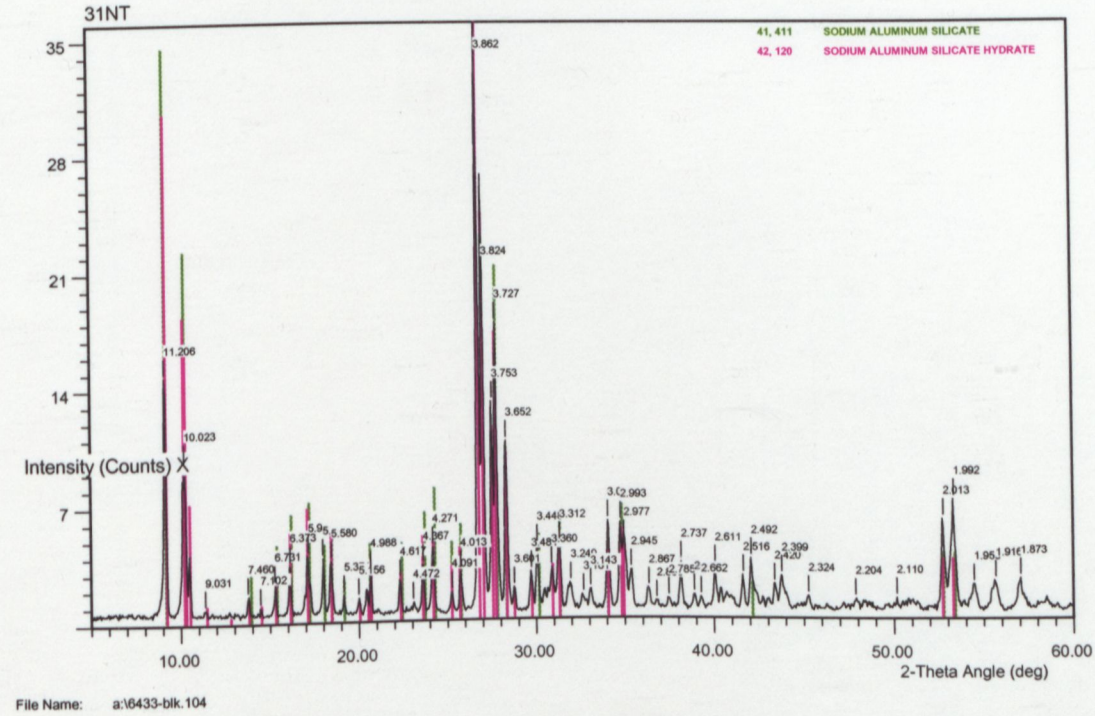

Figure B14: XRA pattern of Sample 31NT synthesised using Method III with SiO_2/Al_2O_3 ratio of 40, OH^-/SiO_2 ratio of 0.2, and 100% crystallinity.

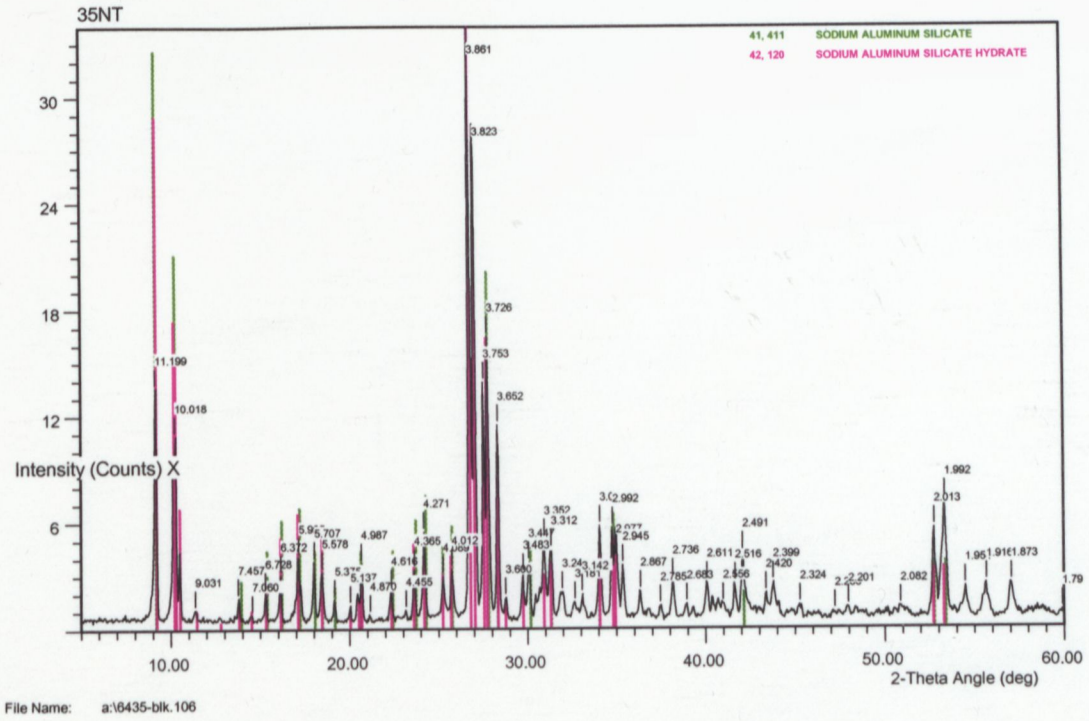

Figure B15: XRA pattern of Sample 35NT synthesised using Method III with SiO_2/Al_2O_3 ratio of 40, OH^-/SiO_2 ratio of 0.2, and 100% crystallinity.

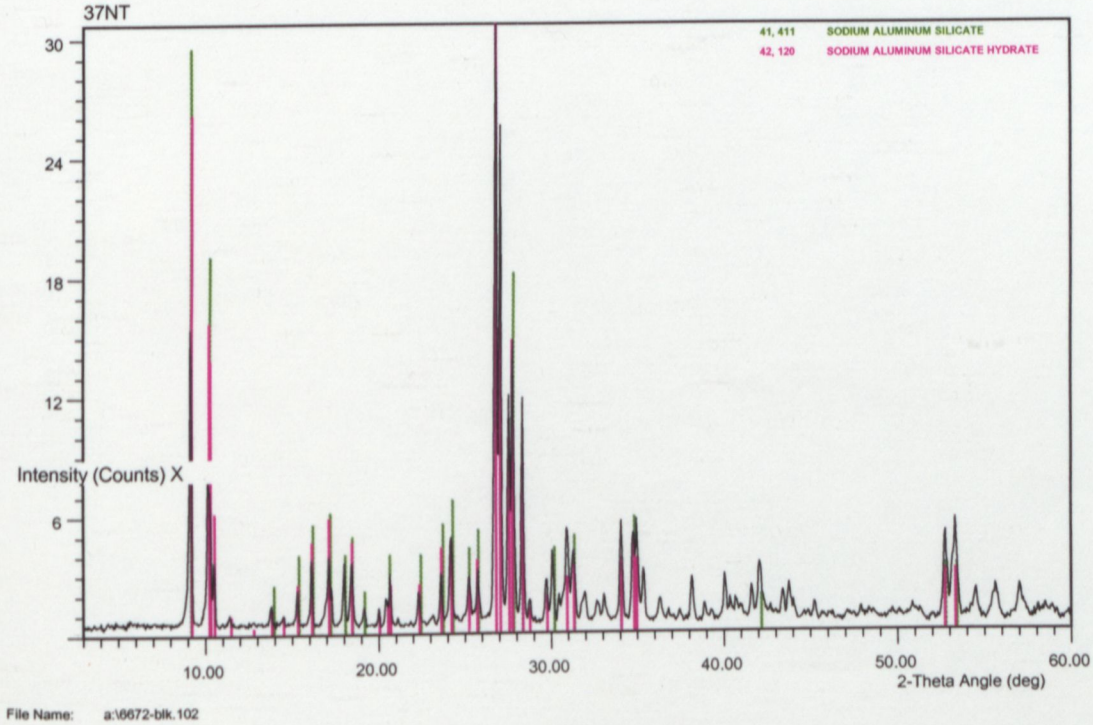

Figure B16: XRA pattern of Sample 37NT synthesised using Method III with SiO_2/Al_2O_3 ratio of 40, OH^-/SiO_2 ratio of 0.2, and 100% crystallinity.

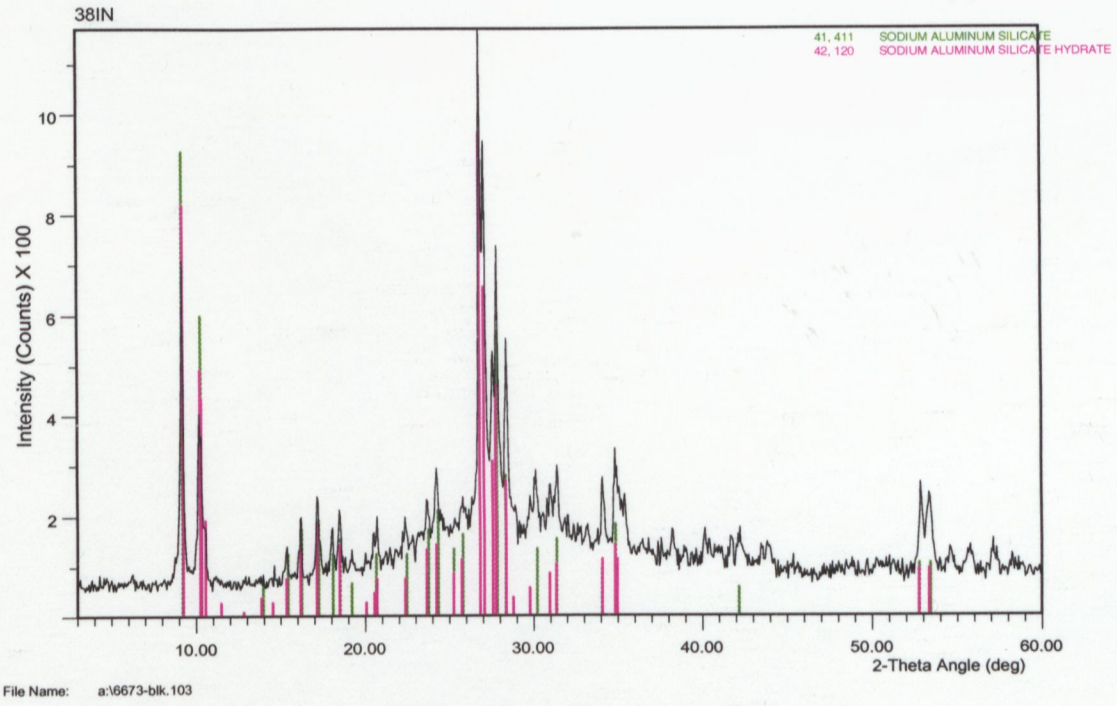

Figure B17: XRA pattern of Sample 38IN synthesised using Method IV with SiO_2/Al_2O_3 ratio of 26, OH^-/SiO_2 ratio of 9, and 59% crystallinity.

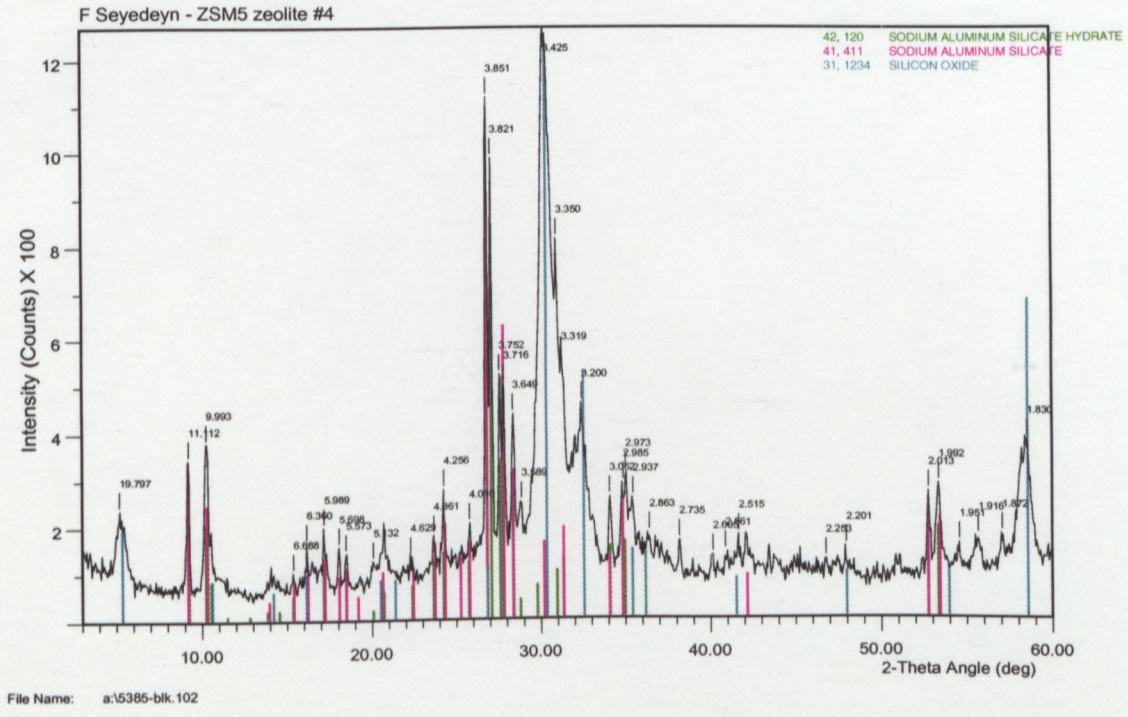

Figure B18: XRA pattern of Sample run 4 synthesied using Method III with the composition of 90 SiO_2: Al_2O_3: $7.7Na_2O$: $3000H_2O$, and 27% crystallinity.

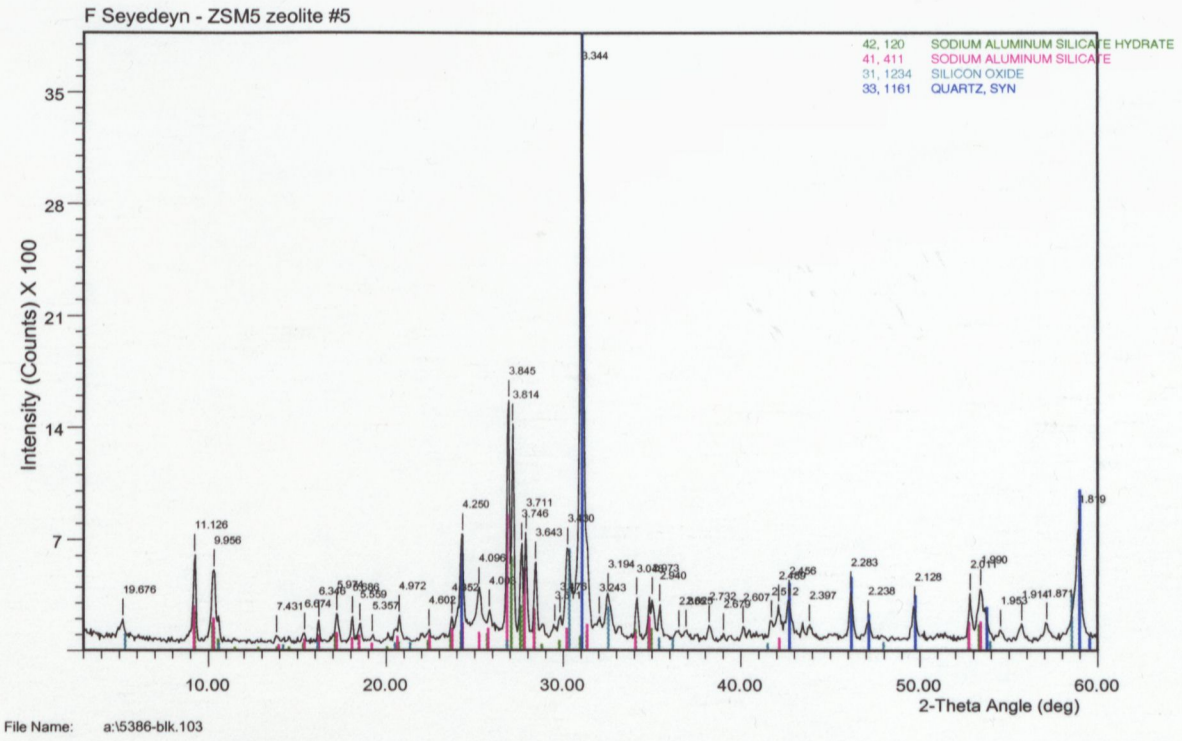

Figure B19: XRA pattern of Sample run 5 synthesised using Method III with the composition of 90 SiO_2: Al_2O_3: $7.7Na_2O$: $3000H_2O$, and 45% crystallinity.

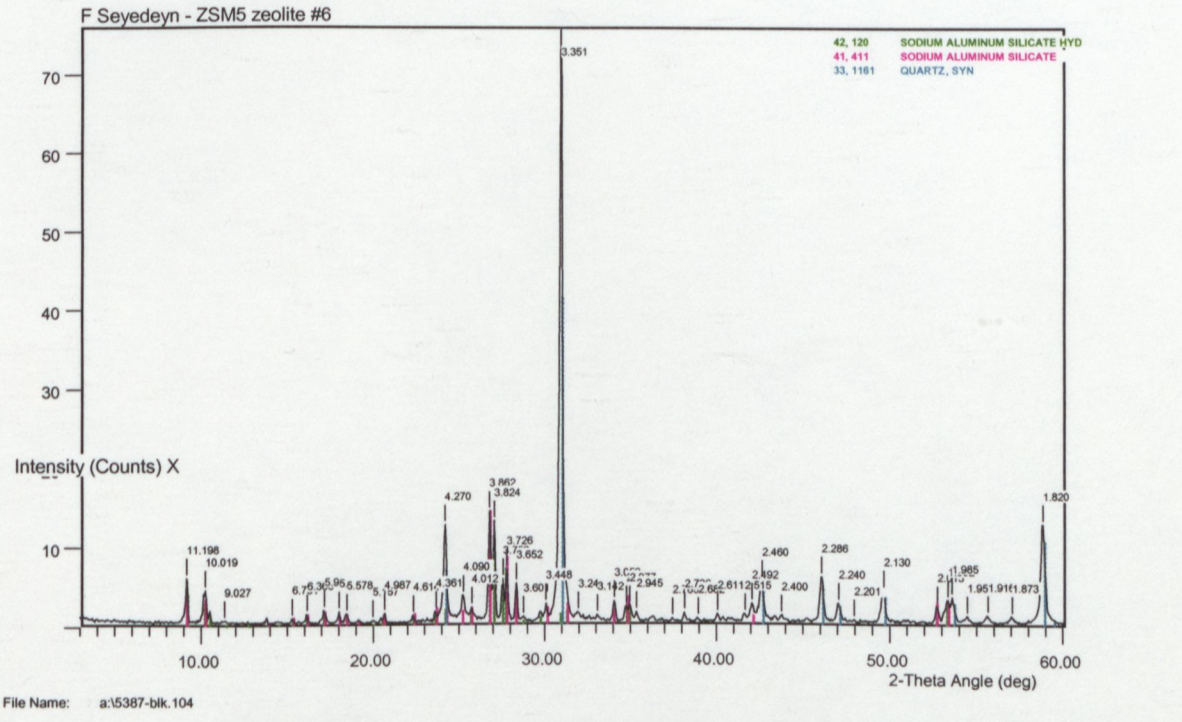

Figure B20: XRA pattern of Sample run 6 synthesised using Method III with the composition of 90 SiO_2: Al_2O_3: $7.7Na_2O$: $3000H_2O$, and 40% crystallinity.

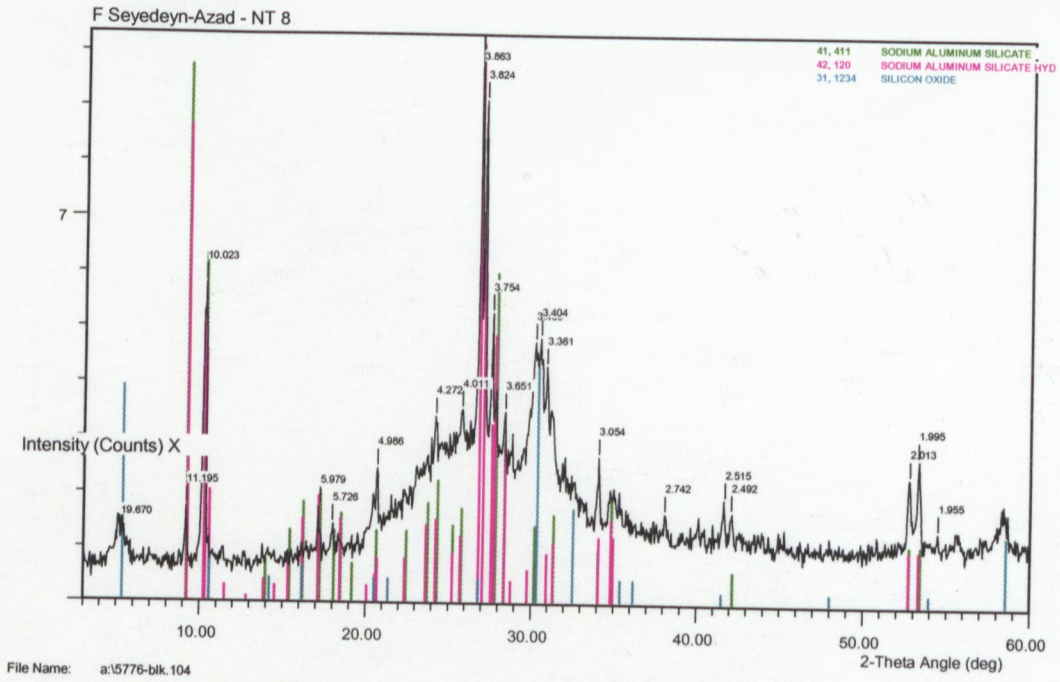

Figure B21: XRA pattern of Sample run 7 synthesised using Method III with the composition of 90 SiO_2: Al_2O_3: 7.7Na_2O: 3000H_2O, and 16% crystallinity.

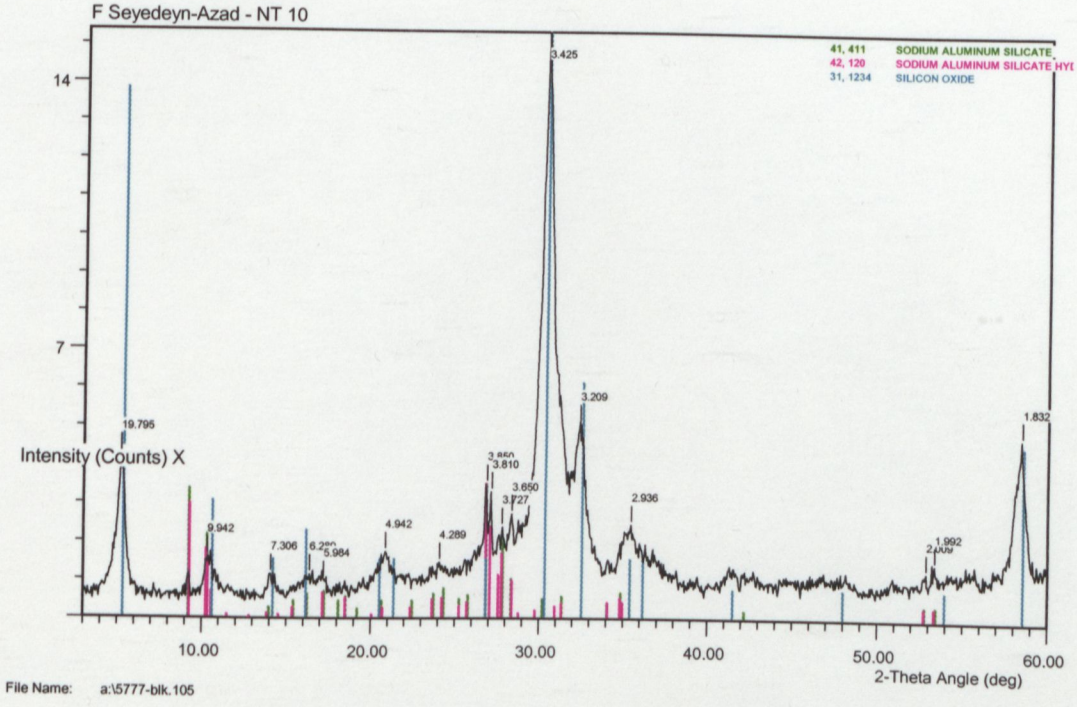

Figure B22: XRA pattern of Sample run 8 synthesised using Method III with the composition of 90 SiO_2: Al_2O_3: 7.7Na_2O: 3000H_2O, and 5% crystallinity.

APPENDIX C: Detailed analysis of the catalysts used in this study, analysed by Amdel Laboratories Ltd., South Australia.

Table C1. Detailed analysis of the copper ion-exchanged zeolites used in this study.

Sample code	Sample Name	Al_2O_3 %	CaO %	Fe_2O_3 %	K_2O %	MgO %	MnO %	Na_2O %	P_2O_5 %	SiO_2 %	TiO_2 %	Co ppm	Cu %
Cu-25-1	Cu-ZSM-5-50-58.0	2.97	0.02	0.09	0.03	0.02	<0.01	0.02	<0.01	89.6	0.01	30	1.08
Cu-25-2	Cu-ZSM-5-50-77.3	2.94	0.02	0.13	0.02	0.01	<0.01	<0.01	<0.01	89.6	0.01	<20	1.44
Cu-25-3	Cu-ZSM-5-50-99.3	2.91	0.01	0.16	0.02	0.02	<0.01	<0.01	<0.01	86.9	0.01	40	1.85
Cu-45-1	Cu-ZSM-5-50-62.3	2.94	0.04	0.06	0.03	0.03	<0.01	0.11	<0.01	88.6	0.01	40	1.15
Cu-45-2	Cu-ZSM-5-50-106.7	2.91	0.06	0.07	0.03	0.02	<0.01	0.03	0.02	86.9	0.01	50	1.97
Cu-45-3	Cu-ZSM-5-50-139.3	2.92	0.04	0.08	0.02	0.02	<0.01	<0.01	<0.01	86.0	0.01	<20	2.57
Cu-80-1	Cu-ZSM-5-50-132.6	2.92	0.02	0.05	<0.01	0.01	<0.01	<0.01	0.01	88.1	0.01	30	2.43
Cu-80-2	Cu-ZSM-5-50-111.1	2.86	0.04	0.05	0.02	0.02	<0.01	0.02	<0.01	85.7	0.01	50	2.07
Cu-H-NT	H-Cu-ZSM-5-40-101.7	4.06	0.02	0.07	<0.01	<0.01	<0.01	0.11	0.02	82.1	0.01	260	2.59
Sample 5	Cu-ZSM-5-176-199.2	1.04	-	-	-	-	-	-	-	88.6	-	<20	1.30
Sample 9b	Cu-ZSM-5-140-160.7	1.23	-	-	-	-	-	-	-	88.7	-	<20	1.24
3Cu24-100	Cu-ZSM-5-100-127.5	1.55	0.04	0.13	0.01	0.01	<0.01	0.09	0.02	88.5	<0.01	<20	1.24
Sample 7b	Cu-ZSM-5-100-168.6	1.62	-	-	-	-	-	-	-	87.7	-	<20	1.58

Table C1. Detailed analysis of the copper ion-exchanged zeolites used in this study (continued).

Sample code	Sample Name	Al_2O_3 %	CaO %	Fe_2O_3 %	K_2O %	MgO %	MnO %	Na_2O %	P_2O_5 %	SiO_2 %	TiO_2 %	Co ppm	Cu %
3Cu 8-100	Cu-ZSM-5-100-108.3	1.56	0.02	0.08	0.01	0.01	<0.01	0.14	0.02	88.6	0.01	<20	1.06
Sample 7a	Cu-ZSM-5-100-99	1.62	-	-	-	-	-	-	-	84.1	-	<20	1.29
Cu-25-3	H-Cu-ZSM-5-50-99.3	2.91	0.01	0.16	0.02	0.02	<0.01	<0.01	<0.01	86.9	0.01	40	1.85
Cu-25-2	H-Cu-ZSM-5-50-77.3	2.94	0.02	0.13	0.02	0.01	<0.01	<0.01	<0.01	89.6	0.01	<20	1.44

Table C2. Detailed analysis of the cobalt ion-exchanged zeolites used in this study.

Sample code	Sample Name	Al_2O_3 %	CaO %	Fe_2O_3 %	K_2O %	MgO %	MnO %	Na_2O %	P_2O_5 %	SiO_2 %	TiO_2 %	Co %	Cu ppm
6a	H-Co-ZSM-5-80-71	1.85	-	-	-	-	-	-	-	87.2	-	0.76	300
Co-H-80	H-Co-ZSM-5-80-77.9	1.93	0.05	0.06	0.06	0.03	<0.01	0.15	0.02	90.9	-	0.87	100
6b	H-Co-ZSM-5-80-96.6	1.86	-	-	-	-	-	-	-	1.86	-	1.04	400
CoH-NTB	H-Co-ZSM-5-40-45	4.03	-	-	-	-	-	-	-	80.9	-	1.05	200
HCo-80	H-Co-ZSM-5-80-428	1.84	0.01	0.09	0.04	0.02	<0.01	<0.01	0.02	81.1	0.01	4.45	<50

LIST OF PUBLICATIONS

1. **Fakhry Seyedeyn-Azad**, Dong-ke Zhang, A Study on ZSM-5 Zeolites Synthesised With and Without the Aid of Template, 3rd Conference of the Asian Crystallographic Association, 13-15 October 1998, Bangi, Malaysia.

2. **Fakhry Seyedeyn-Azad**, Kylie Headon, Weiping Mao, Dong-ke Zhang, X. S. Zhao and Max Lu, Nitrogen Oxides Decomposition over Synthesised Zeolite-Supported Catalysts, 2nd Asia Pacific Conference on Sustainable Energy and Environmental Technology, 14-17 June 1998, Gold Coast, Australia.

3. **F. Seyedeyn-Azad**, Kylie Headon, Weiping Mao, Dong-ke Zhang, X.S. Zhao and Max Lu, Decomposition of Nitrogen Oxides over Synthesised Zeolites and the Effect of Oxygen and Methane on the Reactions, Proceeding of the Second Iranian Congress of Chemical Engineering, pp. 27, 24-26 February 1997, Tehran, Iran.

4. Kylie Headon, **Fakhry Seyedeyn-Azad**, Dong-ke Zhang , X.S. Zhao and Max Lu, The direct Decomposition and Selective Catalytic Reduction of NO using Methane over Copper Ion-Exchanged Zeolites, Chemeca'96, Volume 1: 89-94, Sydney, 1996.

5. Kylie Headon, Sophia van der Linden-Dhont, **Fakhry Seyedeyn-Azad**, Weiping Mao and Dong-ke Zhang, Decomposition of Nitric Oxides over Zeolite-Supported Catalysts: Effect of Oxygen and Methane, Proceeding of the Asia-Pacific Conference on Sustainable Energy and Environmental Technology, pp. 201-208, 19-21 June 1996, Singapore.